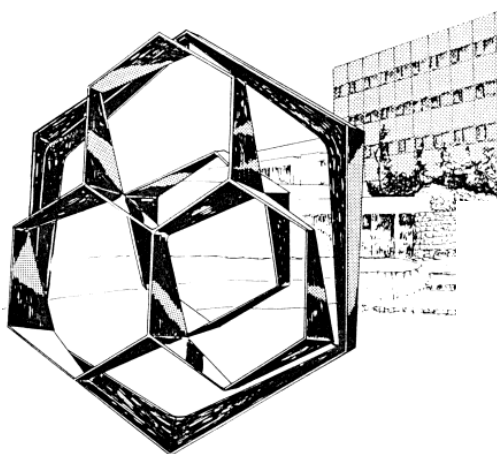FACULTE DES SCIENCES – DEPARTEMENT DE CHIMIE

CENTRE DE RECHERCHES DU CYCLOTRON

LIÈGE université

Synthesis of stable and radioactive isotope-containing peptidoglycan fragments

Directeur: **Professeur André LUXEN**

Dissertation présentée par

Nicolas Lamborelle

Pour l'obtention du grade de

Docteur en Sciences

Année Académique 2017-2018

Committee

Promoter: Professor André Luxen (*Université de Liège*)

President: Professor Christian Damblon (*Université de Liège*)

Members: Doctor Christophe Dugave (*Institut Frédéric-Joliot*)

             Doctor Simon Lacroix (*Université Libre de Bruxelles*)

             Professor Lionel Delaude (*Université de Liège*)

             Professor Bernard Joris (*Université de Liège*)

             Doctor Christian Lemaire (*Université de Liège*)

Abstract

In this work, a method for the total synthesis of different isotope-containing *meso*-diaminopimelic acids (*m*-A$_2$pm or (2*S*,6*R*)-A$_2$pm) is presented. This compound, specific of bacterial cell wall, allows for the reticulation of peptidoglycan in most Gram-negative and some Gram-positive bacteria. A preparation of new isotope-containing compounds (1-^{13}C)(2*S*,6*R*)-A$_2$pm and (4,5-^{2}H$_2$)(2*S*,6*R*)-A$_2$pm is hereby presented. These compounds can be used as chromatography and quantitative mass spectrometry references for the study of peptidoglycan dynamics. The first total stereoselective synthesis of high specific activity (30 Ci/mmol) tritiated [4,5-^{3}H](2*S*,6*R*)-A$_2$pm is also described. Furthermore, the synthesis of differentially protected (2*S*,6*R*)-A$_2$pm and (4,5-^{2}H$_2$)(2*S*,6*R*)-A$_2$pm allowed the preparation of peptidoglycan peptide fragments, which broaden the scope of applications to studies of β-lactamase induction phenomenon in penicillin resistant bacteria as well as to studies in the field of human innate immune system.

Résumé

Ce travail décrit une méthode de synthèse totale d'acides *méso*-diaminopimélique (m-A$_2$pm ou (2S,6R)-A$_2$pm) marqués. Ce composé, spécifique de la paroi bactérienne, permet la réticulation du peptidoglycane de la plupart des bactéries à Gram-négatif et de quelques bactéries à Gram-positif. La synthèse de nouveaux composés marqués, (1-^{13}C)(2S,6R)-A$_2$pm et (4,5-^{2}H$_2$)(2S,6R)-A$_2$pm, pouvant servir de références en chromatographie et en spectrométrie de masse quantitative pour l'étude du métabolisme du peptidoglycane est décrite. La première synthèse totale stéréoselective d'acide *méso*-diaminopimélique tritié [4,5-^{3}H](2S,6R)-A$_2$pm à haute activité spécifique (30 Ci/mmol) est également décrite. Enfin, la préparation de (2S,6R)-A$_2$pm et (4,5-^{2}H$_2$)(2S,6R)-A$_2$pm différemment protégés est présentée. Ces composés permettent la synthèse de fragments peptidiques de peptidoglycane, ce qui élargit le champ des applications aux études du phénomène d'induction de β-lactamases chez les bactéries résistantes aux pénicillines ainsi qu'à des études dans le domaine du système immunitaire inné chez l'humain.

Acknowledgements

First and foremost, I would like to express my gratitude to my promoter Professor André Luxen for giving me the opportunity to be a part of his laboratory, the Cyclotron Research Center, during these years. I'm thankful for his guidance and support all along my work.

I also thank the jury members, Doctor Christophe Dugave, Doctor Simon Lacroix, Professor Lionel Delaude, Professor Bernard Joris, Doctor Christian Lemaire and the president Professor Christian Damblon for the approval to examine this work.

I thank the Chemistry Department at the University of Liège for giving me the privilege to be a teaching assistant and for the funding of my PhD research.

I thank the members of the Laboratoire de Marquage par le Tritium of the Commissariat à l'Énergie Atomique of Paris-Saclay for welcoming me in their laboratory. I would like to specially thank Doctor Sophie Feuillastre, Olivia Carvalho and Sebastien Garcia-Argote who performed the synthesis of tritiated meso-diaminopimelic acid. I also thank Doctor Bernard Rousseau for saving me from the snow storm which paralyzed Paris during my time there.

I thank Doctor Jean-Christophe Monbaliu for his precious collaboration for the development of the preparation of vinylglycine derivatives by flow chemistry and for what he brings to the Chemistry Department. I thank Professor Christian Damblon for our collaboration in the structural analyses classes, for the liberty he offered me in this context and for all our passionate discussions around and away from the NMR instruments. I thank Professor Lionel Delaude for his help during the first cross-metathesis test. I thank Doctor Astrid Zervosen for her support and advice in the laboratory and on the agrégation benches. I thank Doctor Justine Simon for all

List of abbreviations

AG	allylglycine
Ala	alanine
APT	attached proton test
ATP	adenosine triphosphate
B.	*Bacillus*
BAIB	bis(acetoxy)iodobenzene
BPR	back pressure regulator
Boc	*tert*-butoxycarbonyl
br	broad
Cbz	carboxybenzyl
CEA	Commissariat à l'énergie atomique et aux énergies alternatives
CiTOS	Center for Integrated Technology and Organic Synthesis
CRC	Cycloton Research Center
COD	cycloocta-1,5-diene
COSY	correlation spectroscopy
d	doublet
DBU	diazabicycloundecene
DCC	dicyclohexylcarbodiimide
DCU	dicyclohexylurea
DET	diethyl tartrate
DHB	dehydrobutyrine
DIBAL	diisobutylaluminium hydride
DMA	*N,N*-dimethylacetamide
DMAC	dimethyl acetylenedicarboxylate
DMAP	4-dimethylaminopyridine
DMF	*N,N*-dimethylformamide
DNA	deoxyribonucleic acid
DOPA	3,4-dihydroxyphenylalanine
dr	diastereomeric ratio
E.	*Escherichia*
EDCI	1-ethyl-3-(3-dimethylaminopropyl)carbodiimide
ee	enantiomeric excess
equiv.	equivalent
ESI	electrospray ionization

FADH	flavin adenine dinucleotide
Fmoc	fluorenylmethyloxycarbonyl
GlcNAc	N-acetylglucosamine
Glu	glutamic acid
HBTU	hexafluorophosphate benzotriazole tetramethyl uronium
HMBC	heteronuclear multiple bond correlation
HMDS	bis(trimethylsilyl)amide
HMM	high molecular mass
HPLC	high performance liquid chromatography
HRMS	high resolution mass spectrometry
HSQC	heteronuclear single quantum coherence
J	coupling constant
LMT	Laboratoire de Marquage par le Tritium
LMM	low molecular mass
Lys	lysine
m	multiplet
m-A$_2$pm	meso-diaminopimelic acid
mp	melting point
mRNA	messenger RNA
MurNAc	N-acetylmuramic acid
NAC	N-acetyl-L-cysteine
NADP	nicotinamide adenine dinucleotide phosphate
NBD	nobornadiene
NMM	N-methylmorpholine
NMR	nuclear magnetic resonance
NOD	nucleotide-binding oligomerization domain
OP	operator
OPA	o-phthaldehyde
PBP	penicillin-binding protein
PCC	pyridinium chlorochromate
PDC	pyridinium dichromate
PHA	polyhydroxyalkanoate
PPTS	pyridinium p-toluenesulfonate
PTC	phase-transfer catalysis
PyBOP	benzotriazol-1-yl-oxytripyrrolidinophosphonium hexafluorophosphate
q	quadruplet
RCM	ring closing metathesis

RNA	ribonucleic acid
rt	room temperature
s	singlet
SCBM	Service de Chimie Bio-organique et de Marquage
SPPS	solid-phase peptide synthesis
t	triplet
TBHP	*tert*-butyl hydroperoxide
TEMPO	2,2,6,6-tetramethylpiperidine-1-oxyl
TFA	trifluoroacetic acid
THF	tetrahydrofuran
TMS	trimethylsilyl
tRNA	transfer RNA
UDP	uridine diphosphate
UMP	uridine monophosphate
VG	vinylglycine

Contents

Chapter I

Introduction

I.1. General Introduction

Humans have been intrigued by the sky and the far infinite since the dawn of times, but a whole other infinite became accessible when microscopes came up in the late 16th – early 17th centuries. Antoine van Leeuwenhoek brought some improvements to these early models and was the first to observe microorganisms using hand-crafted microscopes of his own in 1674. He called these microorganisms *animalcula*. Most of these *tiny animals* are now called *bacteria*[a] as a result from Ehrenberg's studies in 1828. This new world has been intensively studied since and results from these works changed our world. From Louis Pasteur (1822-1894) and his understanding of the fermentation process and his development of the pasteurization process to Robert Koch (1843-1910, Nobel Prize in medicine in 1905) who postulated that microorganisms are the cause of infectious diseases, the discoveries of these times still have a tremendous impact on our current way of life.

Bacteria appeared on Earth about 3.5 billion years ago during the Archean Eon. They were among the first living organisms on this planet. Bacteria are prokaryotic forms of life, most of the time unicellular, and display various shapes and sizes (0.5-5 µm). They can be found everywhere, even in the harshest conditions, where no other form of life can survive. Some can live in hot springs and around deep sea hydrothermal vents (thermophilic bacteria), some bacteria are found in extreme cold environment such as Antarctica (psychrophilic bacteria). Others are capable to cope with very acidic conditions (acidophilic bacteria) and some can even survive in highly radioactive environments.

Though many bacteria are known because of the illnesses they cause, the vast majority of them are harmless and many are even beneficial to humans. As an example, *Escherichia Coli*, a symbiont in the human intestine, fulfills an important role in the digestion and in the secretion of vitamins. Bacteria are also essential to

---

[a] from the Greek *bakterion*, "small staff"

the cheese production, turning sugars found in milk into lactic acid. Some bacteria are used as depolluting agents to convert organic matter found in sewage into fertilizer. Some biodegradable plastics such as PHA (polyhydroxyalkanoate), are produced by bacteria from sugars derived from corn[1].

But it is obvious why bacteria got their negative reputation. It is estimated that they cause about half of all the human diseases. Tuberculosis, caused by *Mycobacterium tuberculosis*, kills 2 million people a year and about 2 more million people die each year from diarrheal diseases caused by various bacteria[1]. Among the most common bacterial infections, we may also cite the Lyme disease caused by bacterium *Borrelia burgdorferi* carried by ticks, tetanus caused by *Clostridium tetani* found in soil, cholera, botulism and typhoid fever.

Bacterial diseases were very often lethal before the development of antibiotics. In the late 19th century, the German chemical industry had provided dyes able to selectively stain tissues or pathogens. This permitted Paul Ehrlich to propose his concept of selective chemotherapy. He reasoned that if it is possible to selectively stain a pathogen, it should also be possible to kill it using what he called a "magic bullet" without harming the surrounding cells[2]. However, it is Alexander Fleming who made the famous, though fortuitous, discovery of penicillin in 1929 as the first antibiotic[3]. Many more antibiotics are now available but their overuse and misuse led to a new issue: bacteria are developing resistance mechanisms.

I.2. The bacterial cell

Selective chemotherapy can only be achieved because the bacterial cell is different from ours. Bacteria are prokaryotes in opposition to the eukaryotes cells we are made of[1]. The most noticeable difference lies in the absence of a membrane-bound nucleus in prokaryotic cells[b] (**Figure 1**).
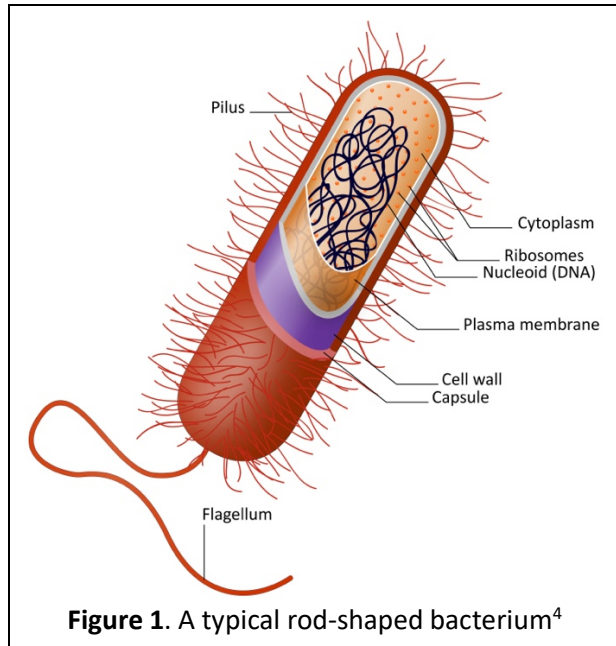
The prokaryotic genome,

Figure 1. A typical rod-shaped bacterium[4]

usually a single circular chromosome, is therefore floating in the cytoplasm and folded into a compact structure called the nucleoid. A typical prokaryotic cell also has smaller circular DNA molecules called plasmids independent from the single chromosome. The cytoplasm contains ribosomes (slightly smaller than their eukaryotic counterparts and different in their protein and RNA content), which read mRNA and use tRNA to synthesize proteins. The slight differences between prokaryotic and eukaryotic ribosomes can be exploited to design antibiotics that do not harm prokaryotic cells such as ours[1]. Some vesicles or inclusion bodies may be observed in the bacterial cytoplasm as nutrients stocks.

The outer structure, called bacterial cell wall, contains a layer of peptidoglycan, a rigid macromolecule. This component is essential to the bacteria to withstand its internal osmotic pressure as its cytoplasm is highly hypertonic[5]. Therefore, peptidoglycan metabolism represents a perfect target for a "magic bullet".

---

[b] from Greek *pro* "before" and *karyon* "nut, kernel" here referring to the nucleus.

I.3. The bacterial cell wall

Bacterial cell wall represents a very active research topic. This barrier allows bacteria to withstand their high internal osmotic pressure due to the highly concentrated cytosol compared to their outer environment[1,5]. It is also the theater of exchanges with the exterior and the target of many antibiotics. Bacteria can be categorized in two groups: Gram-positive and Gram-negative, depending on their ability to retain Gram stain[c]. This is due to a structural difference between their walls. Both have a layer of peptidoglycan but the one found in Gram-positive bacteria is much thicker (20-80 nm vs 1-3 nm). Additionally, Gram-negative bacteria peptidoglycan is surrounded by an external asymmetric membrane made of phospholipids and lipopolysaccharides[5] (**Figure 2**).
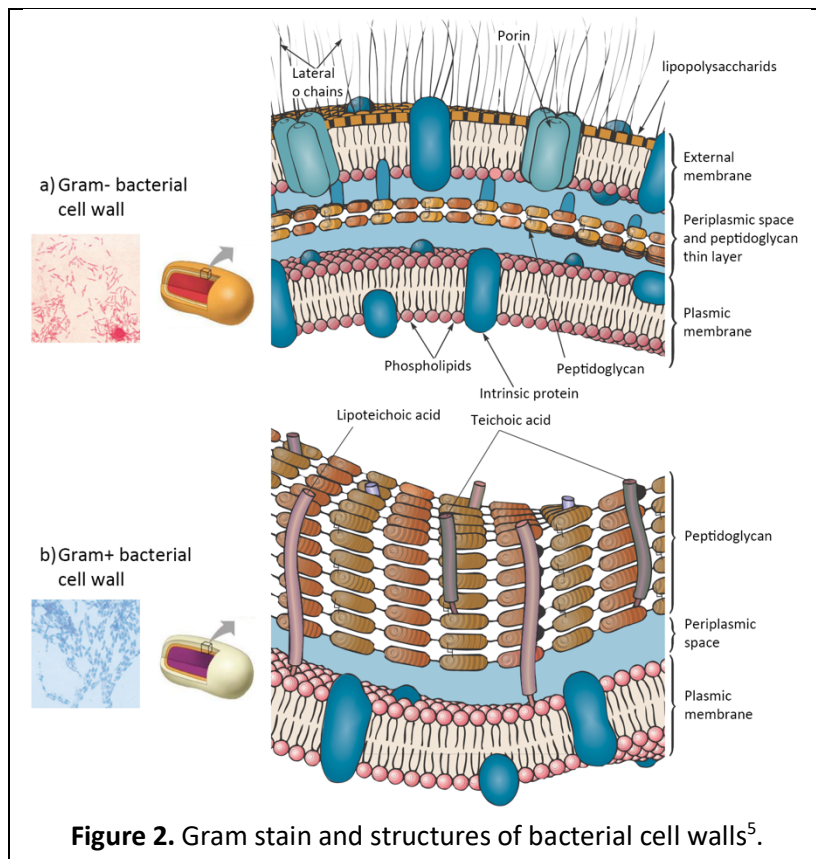

Figure 2. Gram stain and structures of bacterial cell walls[5].

---

[c] Named after Hans Christian Gram who developed it in 1884[5].
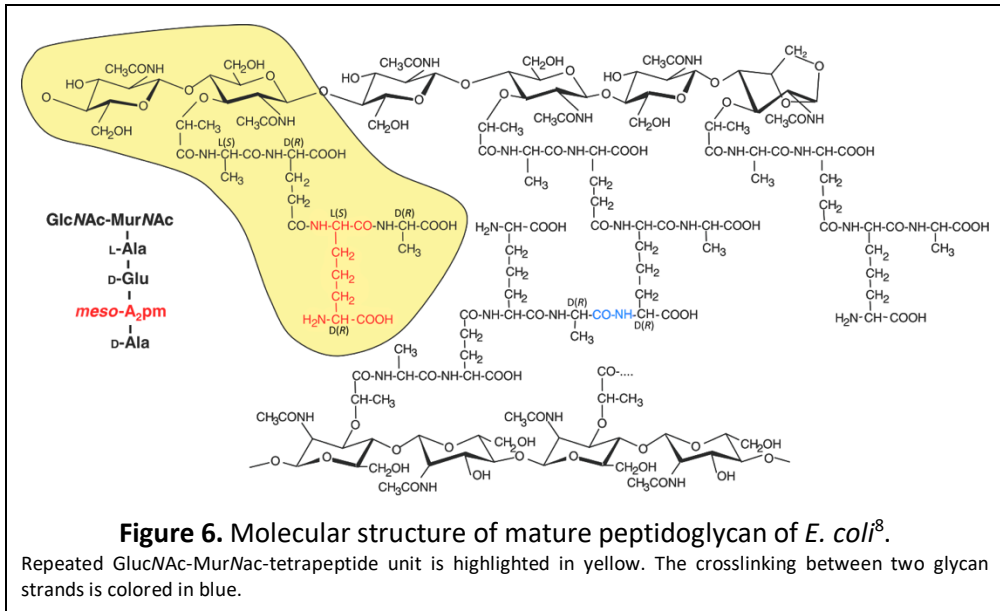
I.4. Peptidoglycan

Peptidoglycan is a giant macromolecule made of glycan strands reticulated by short peptides, that envelops the plasma membrane as a mesh net called *sacculus*[6,7] (**Figure 3**). This impressive structure is responsible for stabilizing and shape-maintaining the cell wall. Glycan strands are made of alternating units of

Figure 3. Model of a *sacculus*[6]. Lines represent glycan strands and arrows represent peptide reticulations
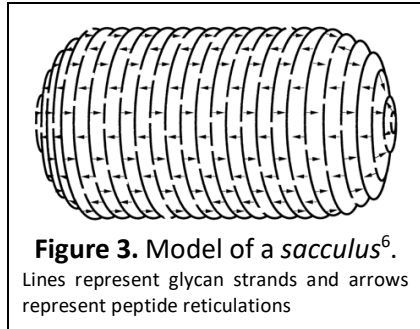
N-acetylglucosamine (Glc*N*Ac) and *N*-acetylmuramic acid (Mur*N*Ac) linked together by β-(1→4) glycosidic bonds (**Figure 4**). Each Mur*N*Ac unit is substituted by a short peptide; most of them with the following structure: L-Ala-γ-D-Glu-L-diamino acid-D-Ala-OH. These tetrapeptides are at the origin of the peptidoglycan reticulation. The nature of the diamino acid varies from species to species. In most Gram-negative bacteria and in *Bacilli* (a genus of Gram-positive, rod shaped bacteria), it is *meso*-diaminopimelic acid (*m*-A$_2$pm, an amino acid specific to bacterial peptidoglycan, **Figure 5**) and for the majority of Gram-positive bacteria, *m*-A$_2$pm is replaced by L-Lysine[7].

Figure 4. General structure of peptidoglycan.

Figure 5. *meso*-Diaminopimelic acid and L-lysine
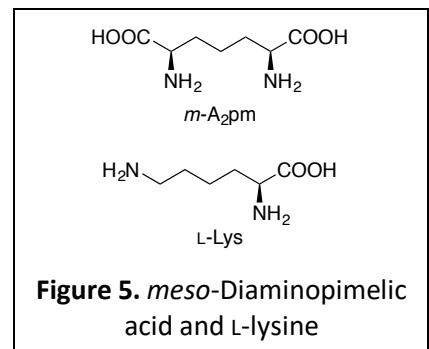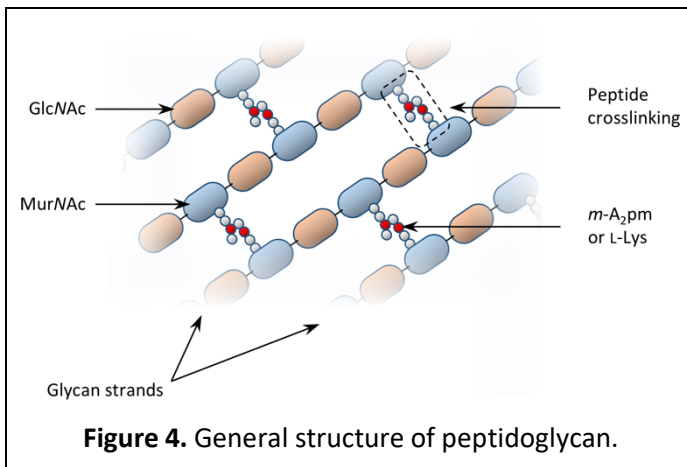
The reticulation of peptidoglycan is generally due to a link between the free amino group of the amino acid in position-3 of a tetrapeptide (*m*-A$_2$pm or L-Lys) of one glycan strand and the carboxylic moiety of D-Ala in position-4 of another tetrapeptide attached to a second glycan strand[7]. The detailed structure of mature peptidoglycan of *E. coli* is given in **Figure 6** as an example.

Figure 6. Molecular structure of mature peptidoglycan of *E. coli*[8].
Repeated Glc*N*Ac-Mur*N*ac-tetrapeptide unit is highlighted in yellow. The crosslinking between two glycan strands is colored in blue.
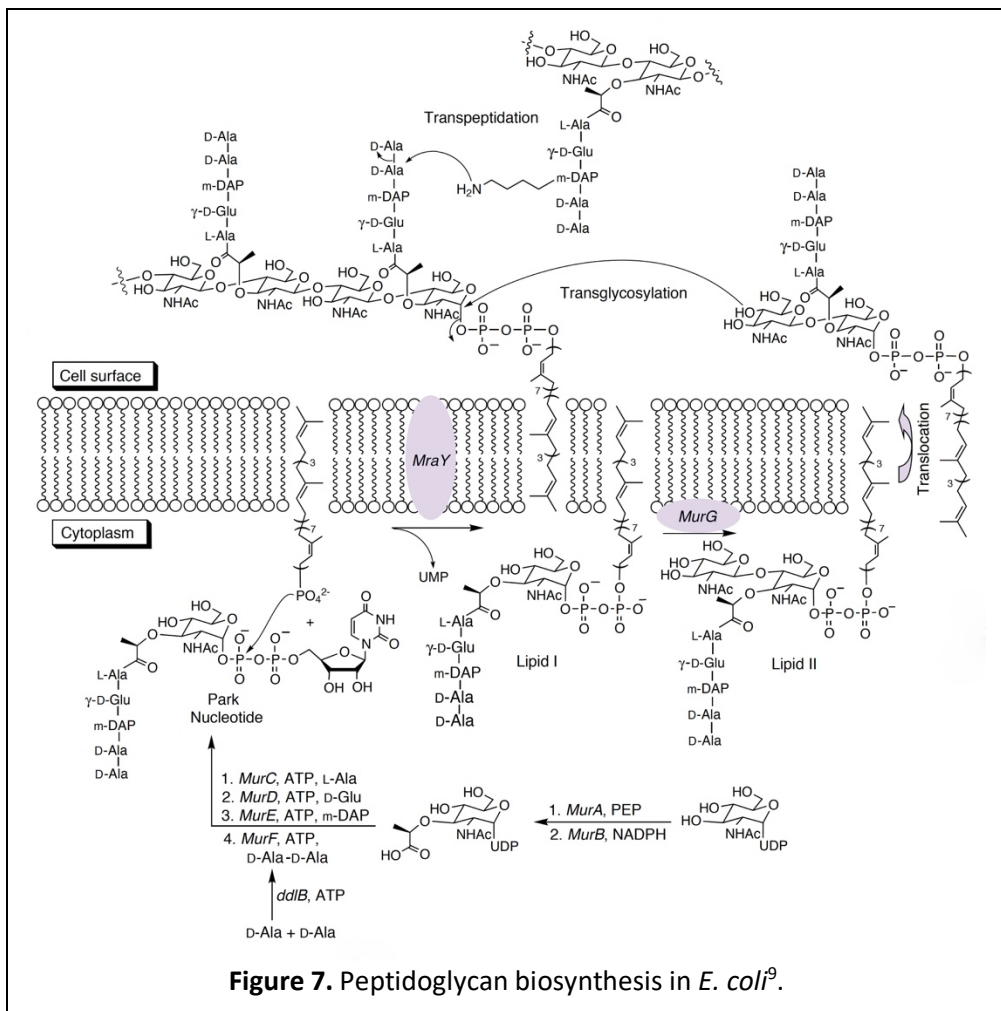
I.5. Peptidoglycan metabolism

I.5.a) Peptidoglycan biosynthesis

The peptidoglycan biosynthesis is a complex multistep process occurring in three different bacterial compartments (**Figure 7**):

1. In the cytoplasm;

2. In the cytoplasmic membrane;

3. Outside the cell (in the periplasm in case of Gram-negative bacteria).

Figure 7. Peptidoglycan biosynthesis in *E. coli*[9].

1. The cytoplasmic phase[10,11] starts with the addition of enolpyruvate to uridine diphosphate-*N*-glucosamine (UDP-Glc*N*Ac) by enolpyruvyl transferase MurA. Reductase MurB then catalyzes the reduction of the previously introduced alkene to form UDP-Mur*N*Ac. Then MurC, MurD, MurE and MurF ligases, grow a L-Ala-γ-D-Glu-*m*-A$_2$pm-D-Ala-D-Ala-OH fragment to afford an UDP-MurNAc-pentapeptide often referred to as the Park nucleotide[9].

2. The phospho-Mur*N*Ac-pentapeptide fragment of this molecule is then transferred to an undecaprenyl-phosphate anchored in the membrane under the action of MraY[12], a membrane enzyme to yield Lipid I. The membrane phase continues as MurG glycosyltransferase adds a Glc*N*Ac moiety to form Lipid II. This building bloc of the peptidoglycan needs to be translocated by the flippase MurJ[13,14] to allow next steps.

3. Once flipped, a glycosyltransferase outside the membrane assembles lipid II blocs through polymerization to form glycan strands. Reticulation of peptidoglycan is finally performed by the action of a DD-transpeptidase[15]. During the crosslinking process, the active serine of this enzyme is acylated by the penultimate D-alanine of a pentapeptide from a first glycan strand (the donor strand). This binding provokes the concomitant release of the terminal D-alanine. The resulting DD-transpeptidase-tetrapeptide adduct then undergoes a nucleophilic attack from the D-side amino group of a *m*-A$_2$pm of second pentapeptide from a second glycan strand (the acceptor strand)[11,16,17]. Maturation of peptidoglycan consists in the cleavage of ultimate D-Ala from the remaining D-Ala-D-Ala residues thanks to a DD-carboxypeptidase[18–20].

All these enzymes (MurA, MurB, MurC, MurD, MurE, MurF, MraY, MurG, MurJ, glycosyltransferase, DD-transpeptidase, DD-carboxypeptidase) have important roles in the peptidoglycan biosynthesis. Therefore, if any of these were to be inhibited, growth and life of a bacteria population could be seriously compromised.

I.5.b) Peptidoglycan turnover and recycling

Peptidoglycan being a crucial element of the bacterial structure, its metabolism is intimately bound to bacterial growth and division. In view of its function of shape-maintaining the cell wall, one might think that peptidoglycan is a static structure. But it is actually highly dynamic in the sense that it is constantly renewed[21]. It is estimated that in some Gram-negative and Gram-positive species, up to 50% of the preexisting peptidoglycan is degraded and replaced during a single cellular cycle[22]. Some enzymes keep on breaking down the peptidoglycan so that others can insert new fragments during cell growth. This process is called peptidoglycan turnover.

Because such a loss of material would be unbearable for these organisms, biochemists hypothesized that fragments resulting from the peptidoglycan turnover are taken up and recovered by bacteria[23]. This was actually observed in Gram-negative bacteria such as *E. coli*, in which peptidoglycan fragments are reimported from the periplasmic region where they accumulate. The current model explaining peptidoglycan recycling shows a complex pathway catalyzed by a dozen of dedicated enzymes breaking down bigger fragments into smaller ones ready to be incorporated in the peptidoglycan biosynthesis[21,24].

Peptidoglycan recycling would be even more beneficial to Gram-positive bacteria given their much larger peptidoglycan layer. Indeed, it has recently been observed that Gram-positive model bacteria *Staphylococcus aureus*, *Bacillus subtilis*, and *Streptomyces coelicolor* all recycle the sugar *N*-acetylmuramic acid (Mur*N*Ac)[25]. Whether or not Gram-positive organisms recycle other peptidoglycan fragments remains unclear. One might say that peptidoglycan metabolism is a clever dynamic equilibrium of biosynthesis, catabolism and recycling (**Figure 8**).

Figure 8. Cell wall recycling in Gram-negative bacteria[23].
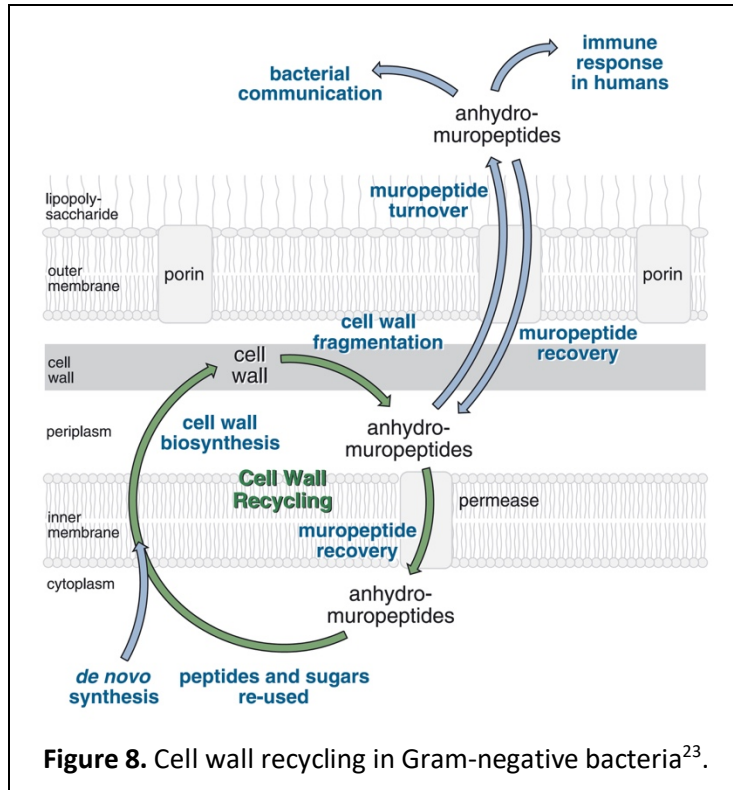
Several models[6,17] describe peptidoglycan turnover in different organisms but some similarities appear:

- Sacculus meshes have to be cleaved to insert new peptidoglycan fragments
- Catabolism and anabolism of peptidoglycan have to be concerted to avoid the bacteria lysis.

Models can be categorized among two different insertion strategies. In the first one, hydrolases act first to cut the mesh and then, synthases come into play to polymerize glycan strands. The second main strategy is known as "make-before-break": first, synthases polymerize glycan strands and then, hydrolases make incision to blend new strands in the existing sacculus. The key point of these mechanisms is that the cell wall must never be weakened to avoid the bacteria lysis. This is especially true in Gram-negative bacteria since their peptidoglycan layer is thinner[6].

Peptidoglycan fragments not reintroduced into the bacterial cell through recycling can trigger a response from the human innate immune system in case of an infection (**Figure 8**). These danger-associated molecular patterns are recognized by pattern recognition receptors NOD1 and NOD2 (for nucleotide-binding oligomerization domain)[26]. Once activated NOD1 and NOD2 containing proteins (or peptidoglycan recognition proteins PGRP) trigger an inflammatory response trough signaling cascades[27]. These cytosolic proteins are associated with several inflammatory diseases such as asthma[28] or Crohn's disease[29,30] upon mutation of *NOD1* and *NOD2* genes.

I.5.c) Penicillin-Binding Proteins

Many essential enzymatic activities related to peptidoglycan metabolism are assured by "Penicillin-Binding Proteins" or PBPs[17]. As suggested by their name, PBPs are able to covalently bond penicillin, which affects their activities. PBPs have several activities:

- Transglycosylation (polymerization of glycan strands)
- DD-transpeptidation (peptidoglycan cross-linking)
- DD-carboxypeptidation (cleavage of the last D-alanine of pentapeptides)
- DD-Endopeptidation (reticulation hydrolysis)

PBPs can be categorized in two main groups: high molecular mass (HMM) PBPs and low molecular mass (LMM) PBPs. HMM PBPs are multimodular enzymes. Their C-terminal penicillin-binding domain has a DD-transpeptidase activity. HMM PBPs can be divided in class A PBPs and class B PBPs depending on their N-terminal domain activity. Class A PBPs N-terminal domains are responsible for glycan strand elongation (glycosyltransferase activity) and class B PBPs N-terminal domains are believed to be active in cell morphogenesis.

LMM PBPs are sometimes referred to as class C PBPs. They can be divided in four subcategories depending on their primary structure homology with *E. coli* Class C main PBPs (PBP4, PBP5, PBP7, AmpH), which are involved in cell separation, peptidoglycan maturation and recycling.

All PBPs display some kind of DD-peptidase activity (DD-transpeptidase, DD-carboxypeptidase or DD-endopeptidase). The terminal D-Ala-D-Ala bond is necessary for these enzymes to form a Henri-Michaelis complex with their substrate.

While the L-Ala-γ-D-Glu-*m*-A$_2$pm (or L-Lys)-D-Ala-D-Ala-OH pentapeptide stem forms a short-lived complex with PBPs before hydrolysis of the D-Ala-D-Ala peptide bond (DD-carboxypeptidase activity) or before substitution of the last D-Ala by the amino group of *m*-A$_2$pm or L-Lys of another peptide (DD-transpeptidase activity), the structurally similar penicillin (**Figure 9**) durably binds with PBPs and therefore disables their activities[17]. Bacteria cannot survive as PBP-penicillin complex half-life exceeds bacteria generation time.

Figure 9. Penicillin structure (a) compared to D-Ala-D-Ala pentapeptide moiety (b).
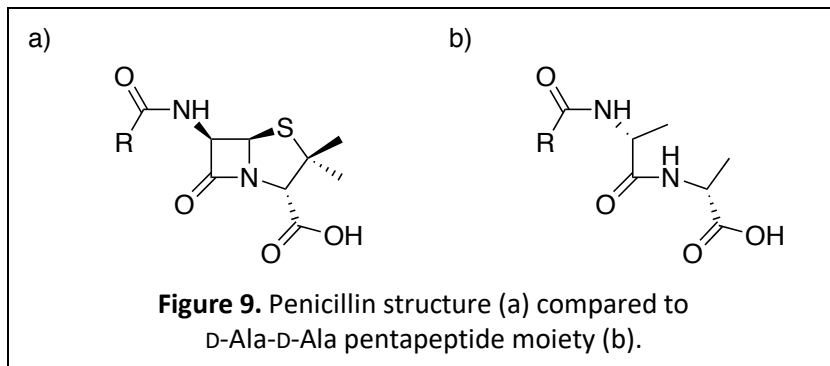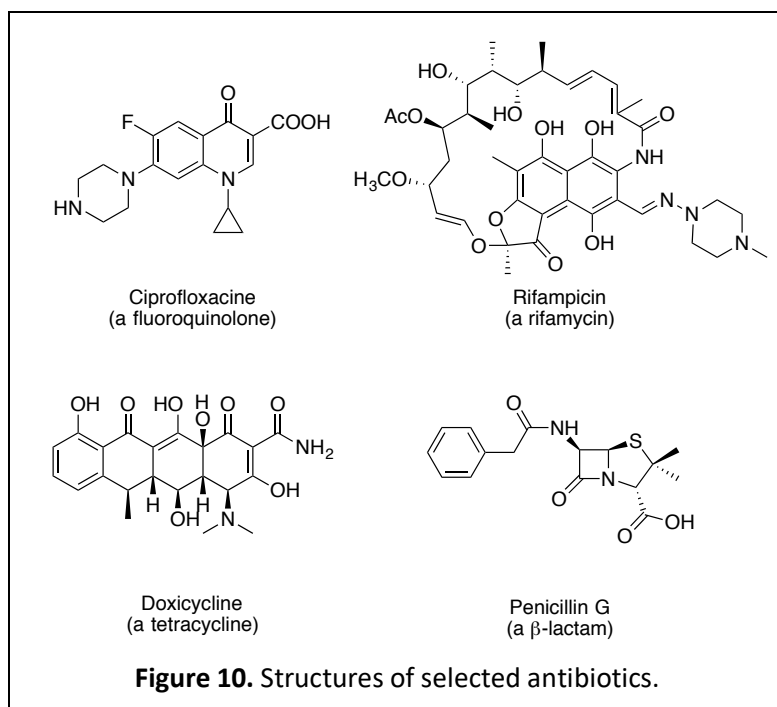
I.6. Antibiotics

Many antibiotics have been discovered and developed since Alexander Fleming published his work on penicillin in 1929[3]. Some of them induce cell death (bactericidal drugs) and others only inhibit cell growth (bacteriostatic drugs)[31]. Most of antibiotics used nowadays are natural or semi-synthetic products but some fully synthetic molecules are also available. These drugs can be classified following their bacterial target (**Table 1**).

Table 1. Main classes of antibiotics and their targets[31].

DNA Synthesis inhibitors	RNA synthesis inhibitors	Protein synthesis inhibitors	Cell wall synthesis inhibitors
• Fluoroquinolones • Trimethoprim – sulfamethoxazole	• Rifamycins	• Tetracyclines • Aminoglycosides • Macrolides • Streptogramins • Phenicols	• β-lactams • Glycopeptides • Glycolipopeptides • Lipopeptides

Ciprofloxacine
(a fluoroquinolone)

Rifampicin
(a rifamycin)

Doxicycline
(a tetracycline)

Penicillin G
(a β-lactam)

Figure 10. Structures of selected antibiotics.

Some antibiotics such as fluoroquinolones inhibit bacterial DNA replication by interfering with the maintenance of chromosomal topology. This class of antibiotics targets topoisomerases II and IV at the DNA cleavage stage preventing them from joining DNA strands back. Others like rifamycins inhibit RNA synthesis by stopping DNA transcription. These drugs prevent RNA strand from emerging out of RNA polymerases by blocking their β-subunit. Tetracyclines inhibit proteins synthesis by targeting ribosomes. These compounds block the access of aminoacyl tRNAs to the 30S ribosomal subunit. β-lactams such as penicillin interfere with PBPs and inhibit the cell wall synthesis leading to the lysis of the bacteria[31]. Notable drugs from these classes of antibiotics are depicted in **Figure 10**.

As previously mentioned, the bacterial cell wall metabolism is a key target for antibiotics. A few of these and their mode of actions over the peptidoglycan synthesis are shown in **Figure 11**.
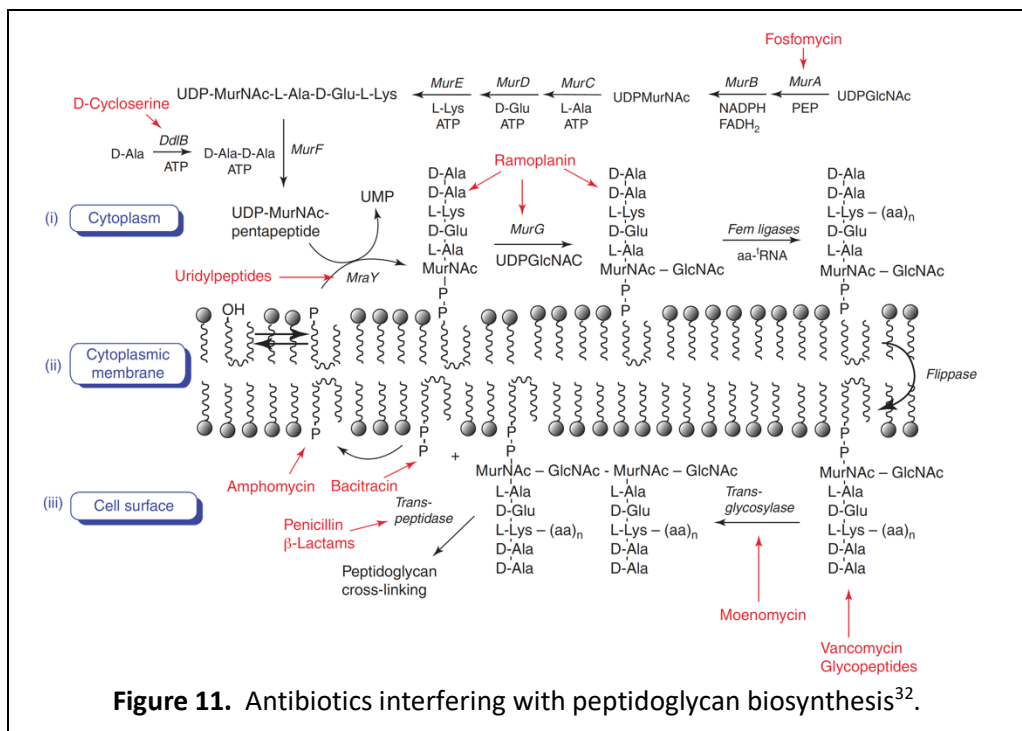

Figure 11. Antibiotics interfering with peptidoglycan biosynthesis[32].

16

The Golden Years of antibiotic discovery and development have passed. Arrivals of these "wonder drugs" permitted the rise of the pharmaceutical industry and the antibiotic market is still a very lucrative business today, but as years went by, drug resistant bacteria appeared and the number of treatment options went down. Paradoxically, there is less effort today to find new drugs when the medical need keeps on increasing.
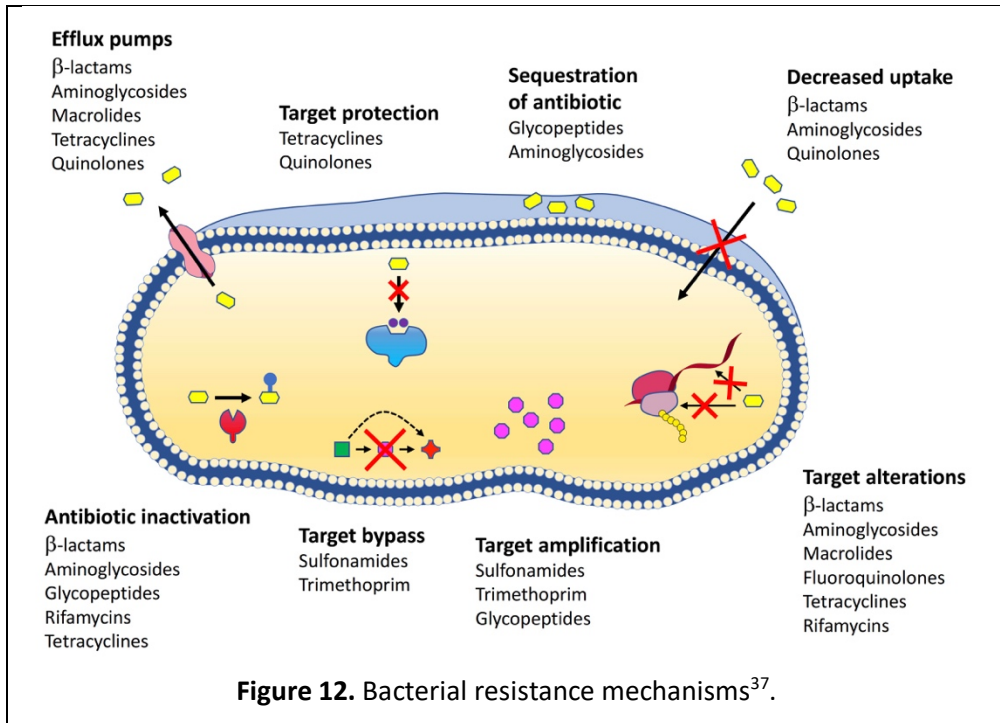
I.7. Resistance

I.7.a) The phenomenon

Bacteria may be seen as primitive or inferior organisms to a human eye but they are actually highly evolved species. They responded to 3.5 billion years of environmental challenges. Bacteria have short generation times and reproduce by binary fission. This explains why they evolve so quickly. Each division may induce mutations in genes of the newly formed cells. This allows large amounts of genetic variation in a population. An example with an average population of *E. coli* in a human intestine might help the reader to have a better grasp on this concept. The probability to have a mutation of a given gene during a cell division is about one in 10 million (10^{-7}). About 2×10^{10} new *E. coli* cells arise each day in a person's intestine. This translate to approximately 2000 bacteria with a mutation in that gene per day ($10^{-7} \times 2 \times 10^{10}$ = 2000). If one take into account that *E. coli* has around 4300 genes, it is estimated that the total number of mutations among the *E. coli* population in a human host is roughly 9 million per day[1].

In addition to these random mutations, genotype and possibly phenotypes of a bacteria can be altered by different mechanisms[1]:

- Transformation: exchange of homologous DNA segments with the surroundings (they might be from broken-open cells)
- Transduction: exchange of bacterial DNA with bacteriophage homologous DNA segments
- Conjugation: transfer of DNA material between two different cells that are temporarily joined (they may be from different species).

Antibiotic drugs are just another challenge to bacteria: each time antibiotics are used, a selective pressure is applied and some survivors among the targeted pathogens might engender new populations of resistant bacteria. This became a serious issue since antibiotics are everywhere, especially in farming and healthcare

facilities. And now, resistant bacteria are escaping the hospitals. Some even say that we are now in a post-antibiotic era[33–35]. It is estimated that antibiotic resistance causes over 25 000 deaths each year in the European Union, with an estimated cost of 1.5 billion € per year[36].

**Figure 12.** Bacterial resistance mechanisms[37].

A variety of resistance mechanisms have been reported so far (**Figure 12**): efflux of antibiotics by efflux pumps; decreased influx of antibiotics; sequestration of antibiotics; target modification to avoid binding with antibiotics; target protection to avoid binding with antibiotics; target bypass (new metabolic pathways not requiring the target intermediary); target amplification (synthesis of more targets than usual so the bacteria can survive even if a portion of these is affected); antibiotic inactivation by specific enzymes.

The next section will detail one of these resistance mechanisms: the penicillin inactivation by a β-lactamase in *Bacillus licheniformis* (a Gram-positive bacteria).

I.7.b) Induction of a β-lactamase in *B. licheniformis*

β-lactamases are enzymes capable of deactivating β-lactam antibiotics such as penicillin by hydrolyzing their β-lactam ring. The first of this kind to be identified was penicillinase in 1940 (isolated from *E. coli*), even before penicillin entered clinical use[33,38].

Bacillus licheniformis strain 749/I is also able to produce a β-lactamase (BlaP) coded by *blaP* gene. When there is no penicillin, BlaP is only produced at a very low level. The current model[39] shows that in the absence of penicillin the *bla* divergon coding for BlaP, BlaR1 and BlaI is expressed at a low level (**Figure 13a**). BlaR1 is a membrane-bound penicillin-binding receptor and BlaI acts as a cytoplasmic repressor of *bla* divergon when dimerized. In this case, PBP1 (a membrane bound PBP with a transpeptidase activity) is active and peptidoglycan reticulation occurs normally.

Figure 13a. In the absence of penicillin, gene *blaP* is repressed.
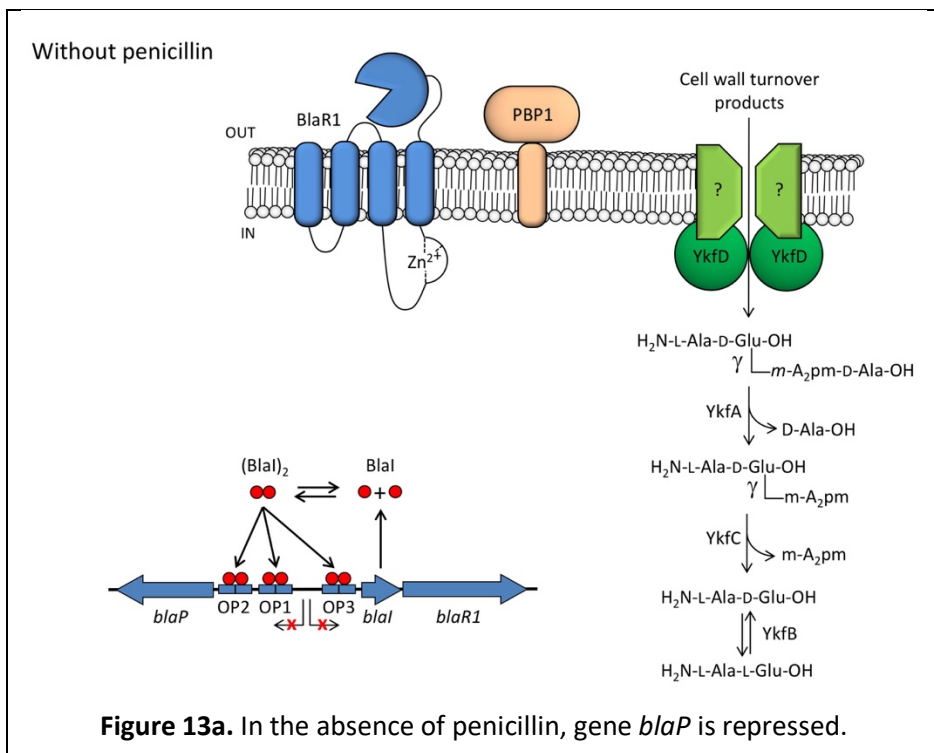
When a sub-lethal dose of penicillin is added into the medium, PBP1 is partially inactivated by penicillin and reticulation of peptidoglycan is compromised. Because of this, the anabolism-catabolism equilibrium of peptidoglycan gets dubious and quantities of cell wall turnover products is on the rise (a penicillin stress is generated by the partial deactivation of PBP1, **Figure 13b**).

Penicillin also binds to receptor BlaR1. This opens a new path for cell wall turnover products: H_2N-L-Ala-γ-D-Glu-m-A$_2$pm tripeptide resulting from the activity of YkfA is hydrolyzed into γ-D-Glu-m-A$_2$pm dipeptide by activated BlaR1. This dipeptide inactivates BlaI dimer repressor so the divergon *bla* is expressed and production of β-lactamase BlaP is triggered.

**Figure 13b.** In the presence of penicillin, gene *blaP* is expressed.
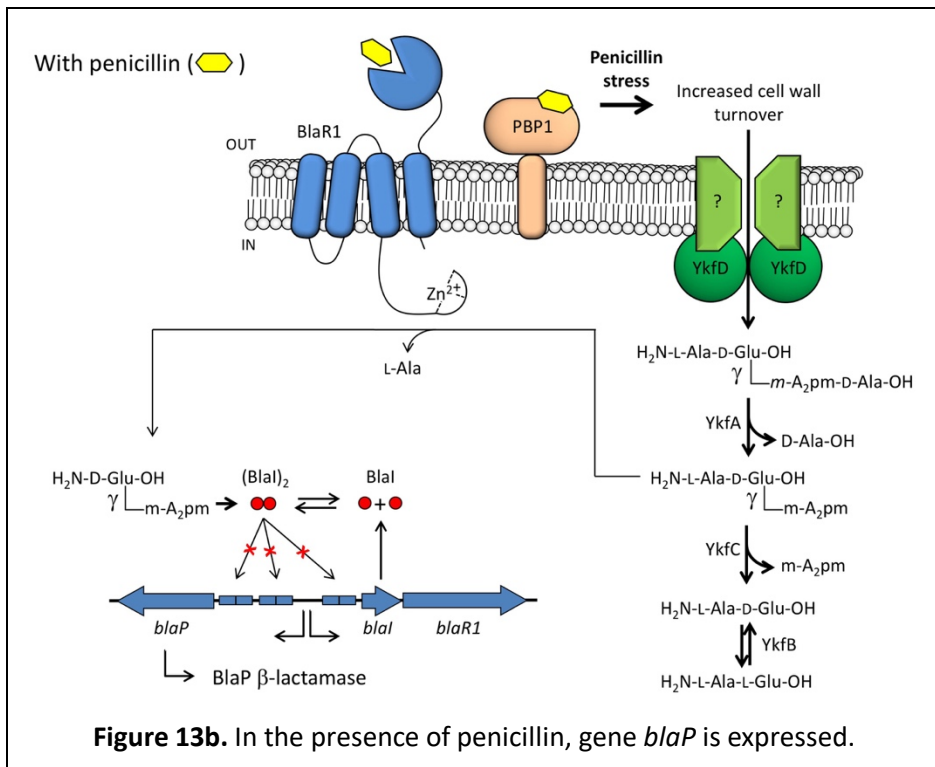
I.8. Objectives

As pharmaceutical companies neglect the development of new antibiotics in the era of resistance, fundamental research in this area becomes increasingly essential. Biochemists face huge challenges when they strive to study such complex biochemical mechanisms. These studies require chemical tools. Some can be prepared by enzymatic synthesis, but others are more challenging. The goal of this work is to broaden the biochemist toolbox to study peptidoglycan metabolism and antibiotics resistance mechanisms.

Enzymatic *in vitro* studies require substrates. NMR experiments designed to study the tridimensional structure of peptidoglycan could benefit from ^{13}C or ^{15}N labelled compounds. Quantitative analyses to study peptidoglycan dynamics require chromatography references as well as isotopologues for mass spectrometry. Non-radioactive and radioactive probes allow for peptidoglycan recycling analyses. Peptide fragments of peptidoglycan are also useful in order to study the innate immune system as they are sensed as danger associated patterns by receptors like NOD containing proteins. Due to its specificity to the bacterial cell wall, *meso*-diaminopimelic acid (**Figure 14**) seems to be a perfect probe to study peptidoglycan metabolism. This particular amino acid is also implicated in each of the peptides intervening in the current model for the induction of β-lactamase BlaP in *B. licheniformis*[39].

Figure 14. *meso*-diaminopimelic acid and foreseen substitution and labelling positions.
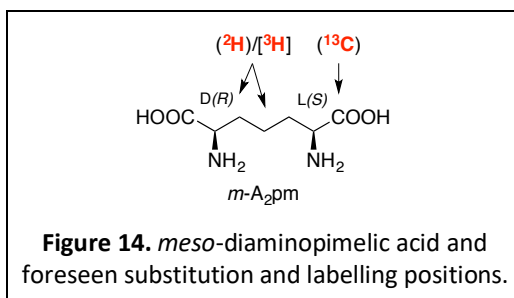
Chemistry is the only viable way to prepare these tools as enzymatic syntheses produce very low amounts of products and require multiple purification steps. In addition, these methods do not allow for selective labelling. Therefore, we will in this work synthesize different radioactive and non-radioactive isotope-containing m-A$_2$pm and m-A$_2$pm containing peptides.

Although m-A$_2$pm appears as a very simple compound at a first glance, the organic chemist will face some challenges in the syntheses of its isotope-containing analogues and its incorporation in peptides. Indeed, we will have to find a way to prepare a symmetric compound with two chiral centers of opposite configuration. Moreover, several differentially protected m-A$_2$pm will have to be prepared in anticipation of their insertion in peptide synthesis (**Figure 15**). Indeed, the biochemist toolbox remains incomplete as enzymatic digestions cannot provide every possible fragment of the peptidoglycan cross-link. **PEP2** and a deuterated analogue of it will be useful as chromatography and mass spectrometry references for the study of dynamics of the induction of β-lactamase in *B. licheniformis* as it appears in the current model. **PEP1** and **PEP3** contain the peptide bond responsible of the cross-linking between glycan strands in peptidoglycan and therefore will be useful to study the enzymatic activity of DD-transpeptidases. All these compounds could also be used in studies of the human innate immune system. The next chapter will focus on the different strategies reported so far for the preparation of such compounds.

Figure 15. target peptides
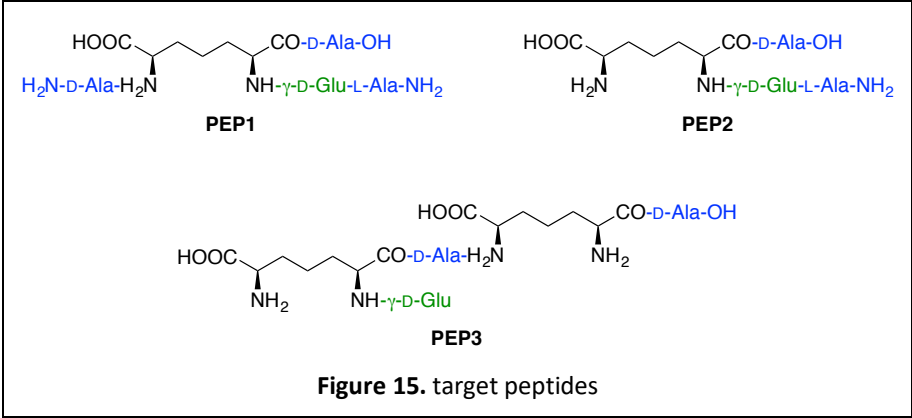
Chapter II

Bibliography

It is not surprising that several groups investigated the preparation of *meso*-diaminopimelic acid, this compound being such an important link of peptidoglycan, both figuratively and literally. Efforts toward the chemical synthesis of isotope-containing *m*-A$_2$pm (^{2}H, ^{3}H, ^{14}C) were reported from as early as the 1960's[40–45]. The first total syntheses did not display any selectivity toward the *meso* diastereoisomer. However, a notable preparation of tritiated *m*-A$_2$pm was reported in 1985 by Schott *et al.*[46] (**Scheme 1**). It begins with a photochemically induced radical chlorination of an existing *m*-A$_2$pm, probably isolated from peptidoglycan. Chloro-*m*-A$_2$pm derivatives were then converted into [^{3}H]*m*-A$_2$pm by catalytic dehydrohalogenation and reduction using tritium gas.

Scheme 1. Tritiation of an existing *m*-A$_2$pm (Schott *et al.*)[46].
(a) conc. HCl, Cl$_2$, hν, 70-80 °C; (b) T$_2$ (1 atm), Pd/C (10 % wt).
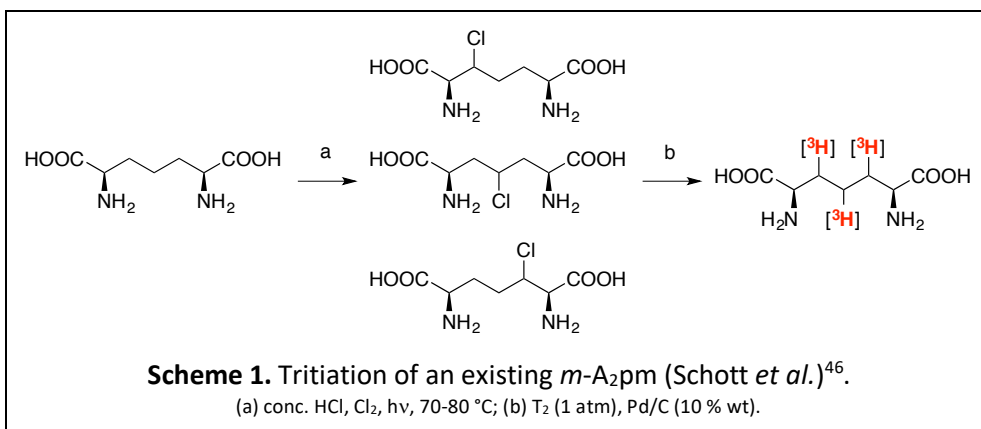
Alongside, some efforts have also been made to isolate *m*-A$_2$pm from the peptidoglycan of bacteria grown in ^{14}C or ^{3}H enriched media[47]. But these methods did not offer the aimed flexibility required for the variety of target molecules of this work.

Many groups have investigated the chemical synthesis of peptidoglycan fragments during the last 25 years and several stereoselective syntheses of m-A$_2$pm and m-A$_2$pm containing peptides were reported. A few notable syntheses will be discussed in the following paragraphs and ultimately, we will choose one to base our strategy on. A few factors helped us to decide which strategy to opt for:

- Stereoselectivity;
- Carbon-13 compatibility;
- Deuterium and tritium compatibility;
- Peptide synthesis possibility.

As its name suggest, m-A$_2$pm or (2S,6R)-A$_2$pm includes two stereogenic carbons of opposite configurations. This represents one of the challenges that we will face in this work, and of course high optical purity is a decisive factor in the strategic choices we will have to make.

Since we want to obtain a carbon-13 substituted m-A$_2$pm, the synthetic pathway that we will choose has to start with a carbon-13 substituted synthon. The commercial availability of a such starting material is therefore a necessity. This compound should not be used in excess at any point during the synthesis as for obvisou cost reasons. Only syntheses respecting this last criterion will be mentioned.

We also intend to prepare deuterium-substituted and tritium-labelled m-A$_2$pm, so an easy to label intermediate is needed (e.g. by alkene reduction). If we want to perform a tritium labelling, this should be done during the last chemical step.

Finally, we would like to prepare some peptides using solid-phase peptide synthesis and depending on the target molecule, there should be a high flexibility over the protecting groups we may have to use.

II.1. Jurgens and Chen syntheses

Jurgens was the first to publish a total enantioselective synthesis of a differentially protected *meso*-diaminopimelic acid in 1992[48]. His starting material was Garner's aldehyde, already containing the first chiral center of *m*-A$_2$pm (**Scheme 2**). The key step of this strategy is the introduction of the second chiral center by alkylation of a Schollkopf reagent, a chiral auxiliary (step d). The alkene function in this product is later reduced by hydrogen making it a good substrate for an eventual deuterium labelling. However, a tritium reduction is not conceivable since a few more steps are required to produce free *m*-A$_2$pm.

It should also be noted that no carbon-13 substituted Garner's aldehyde is commercially available, although, such compounds could be prepared from (^{13}C)serine[49]. All carbon-13 substituted analogues of serine are available in L-configuration but none in D-configuration, meaning that a (*R*)-configured Schollkopf reagent would be necessary to prepare *m*-A$_2$pm.

Chen *et al.* followed a very similar approach in 2014[50]. Yet, they used a different starting material and their *meso*-diaminopimelic acid skeleton did not feature an alkene anymore (**Scheme 2**). In this case, the oxazolidine precursor could be prepared from L-glutamic acid (available in a variety of stable isotopomers)[50].

These two syntheses will be disregarded as the deuterium/tritium introduction opportunity happens at a too early stage of the strategy.
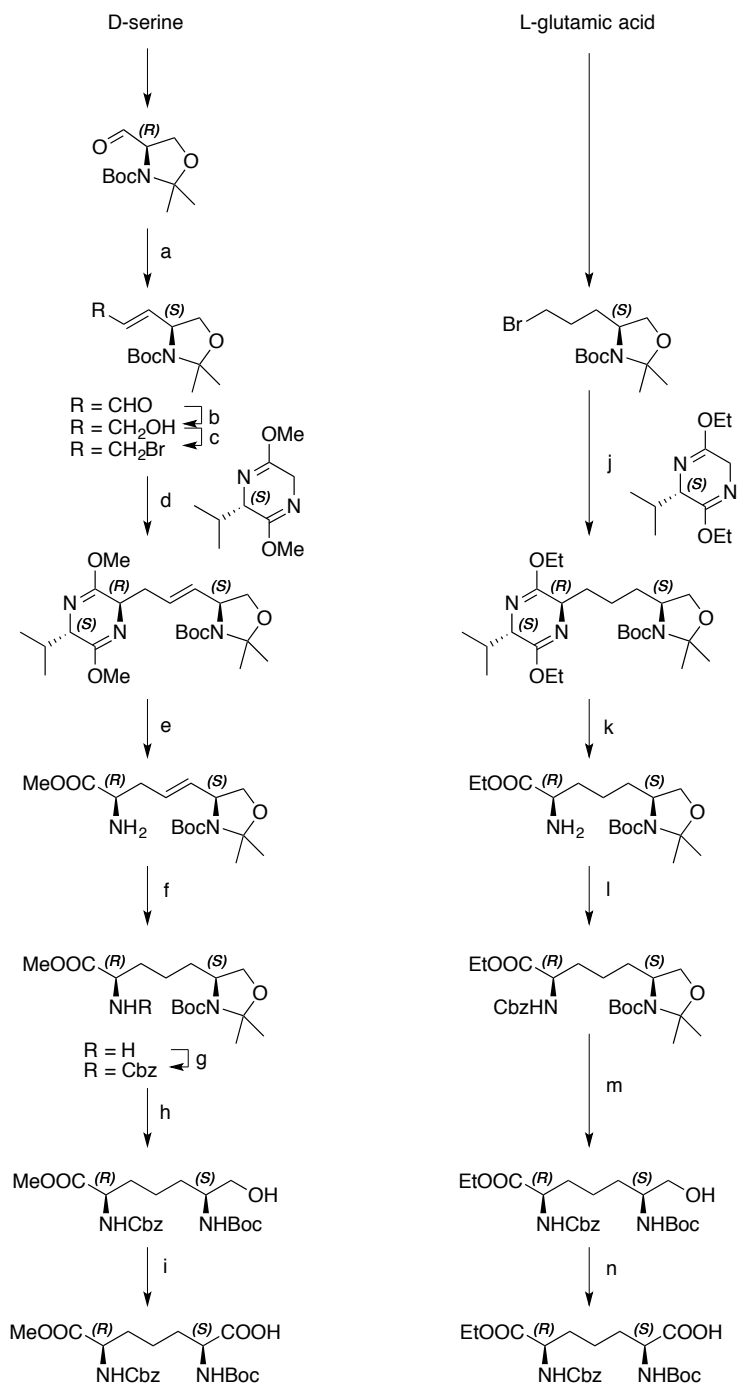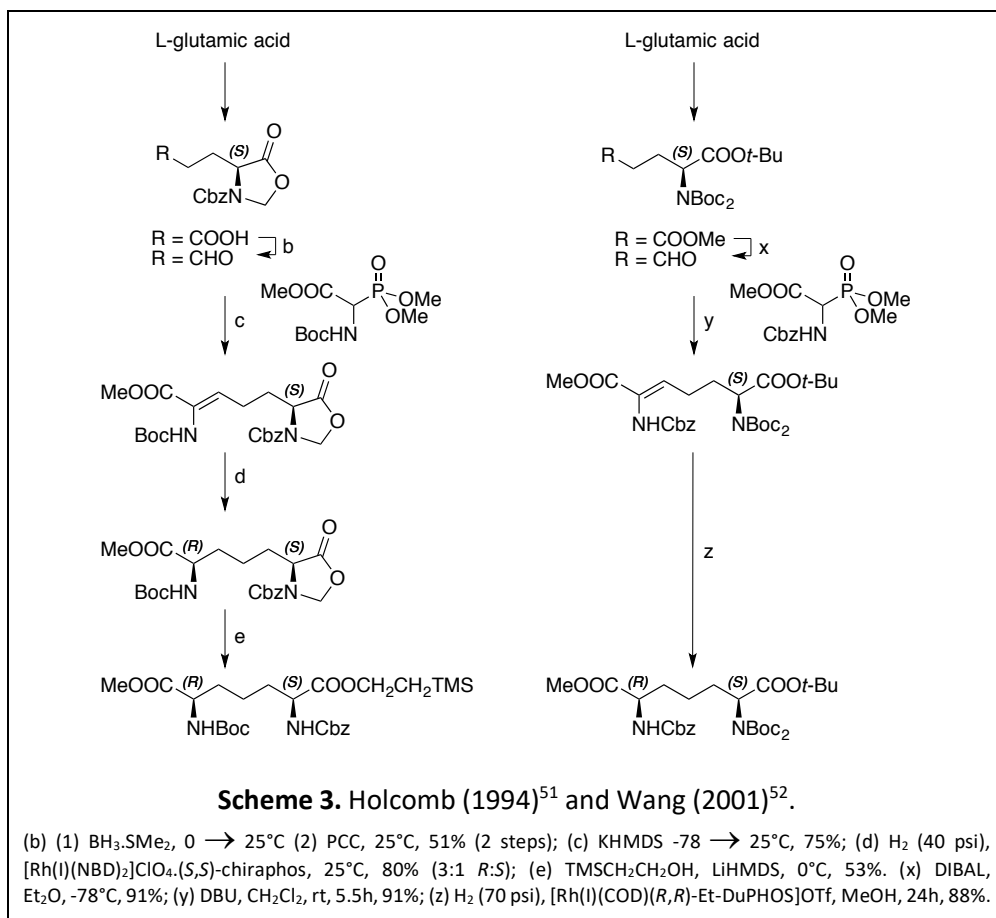
Scheme 2. Jurgens (1992)[48] and Chen (2014)[50].

(a) Ph₃P=CHCHO, toluene, Δ, 80%; (b) DIBAL, CH₂Cl₂, 0°C, 60%; (c) Ph₃P, CBr₄, CH₂Cl₂, 0°C, 95%; (d) *n*-BuLi, THF, -78°C, 95%; (e) 0.1M HCl, THF, H₂O, 48%; (f) H₂, Pd/C, EtOAc, quant.; (g) Cbz-Cl, Et₂O, NaHCO₃, 84%; (h) *p*-TsOH, H₂O, CH₃OH, 91%; (i) PDC, DMF, 75%. (j) *n*-BuLi, THF, -78°C, 3h, 65%; (k) 0.5M HCl, THF, 0°C, 2h; (l) CbzCl, Et₃N, CH₂Cl₂, rt, 2h, 70% (2 steps); (m) *p*-TsOH , H₂O, MeOH, rt, 36h, 80%; (n) TEMPO, BAIB, CH₂Cl₂, H₂O, rt, 1h, 72%.
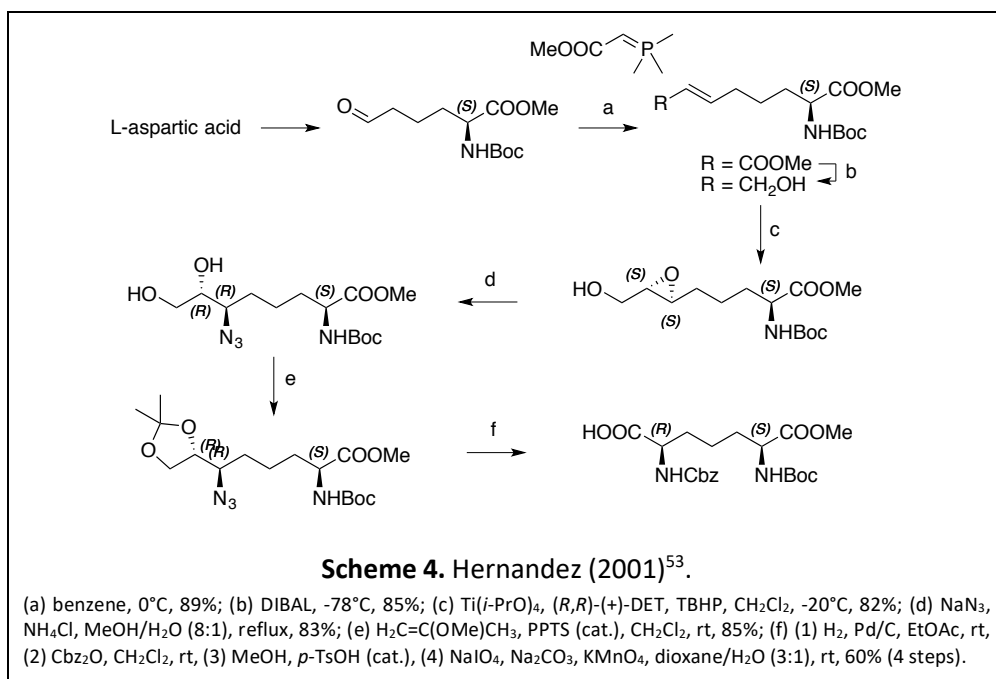
II.2. Holcomb and Wang syntheses

Holcomb *et al.* (1994) started their chemical pathway from L-glutamic acid (readily available in any stable isotopomer)[51]. The second chiral center is introduced via an asymmetrical hydrogenation of an alkene obtained by a Wittig reaction (**Scheme 3**). Wang *et al.* adopted an identical strategy in 2001, which differed only in the choice of protecting groups[52]. It should be noted that the chiral selectivity of the Wang synthesis is vastly superior to the one reported by Holcomb, which requires a chromatography separation of the diastereoisomers. The reduction step represents an easy way to introduce deuterium atoms but the protecting groups would have to be changed to afford free tritiated *m*-A$_2$pm in a single reduction step. As mentioned in the previous section, L-glutamic acid is available as a variety of stable isotopomers.
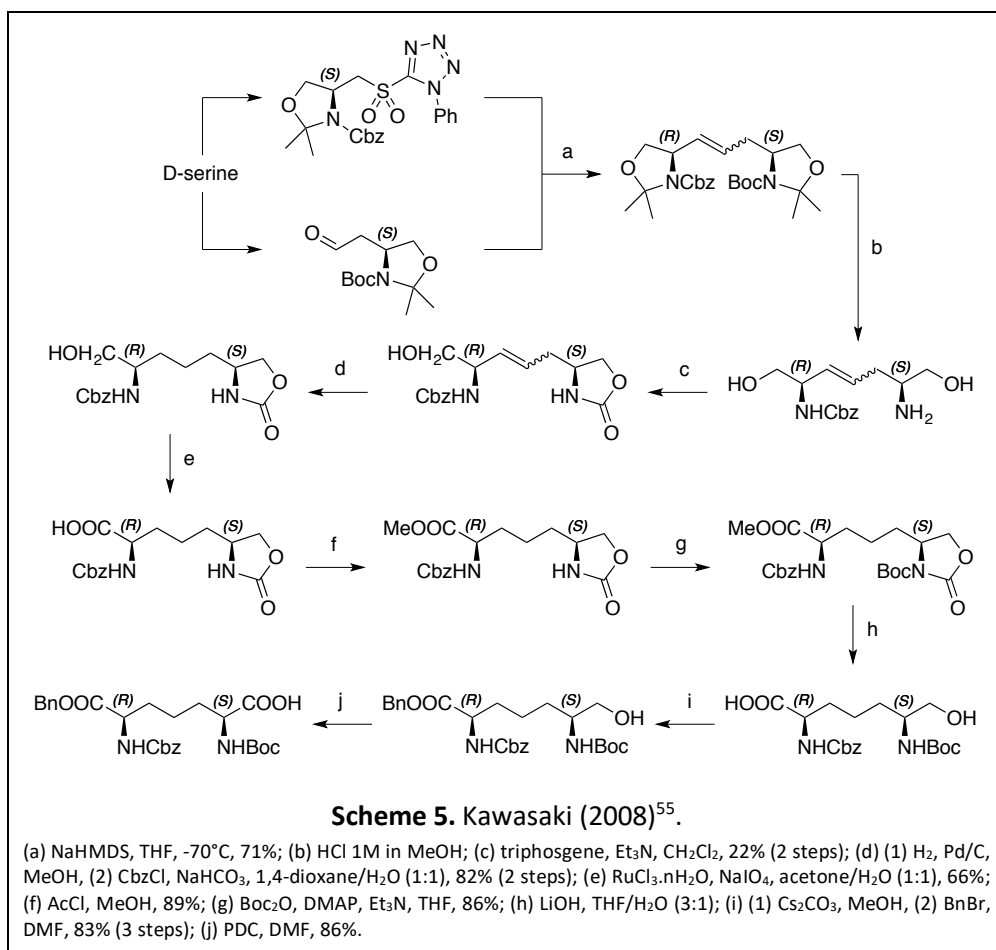

Scheme 3. Holcomb (1994)[51] and Wang (2001)[52].

(b) (1) BH$_3$.SMe$_2$, 0 ⟶ 25°C (2) PCC, 25°C, 51% (2 steps); (c) KHMDS -78 ⟶ 25°C, 75%; (d) H$_2$ (40 psi), [Rh(I)(NBD)$_2$]ClO$_4$.(*S,S*)-chiraphos, 25°C, 80% (3:1 *R:S*); (e) TMSCH$_2$CH$_2$OH, LiHMDS, 0°C, 53%. (x) DIBAL, Et$_2$O, -78°C, 91%; (y) DBU, CH$_2$Cl$_2$, rt, 5.5h, 91%; (z) H$_2$ (70 psi), [Rh(I)(COD)(*R,R*)-Et-DuPHOS]OTf, MeOH, 24h, 88%.

II.3. Hernandez synthesis

Hernandez and Martin reported a new preparation of *m*-A$_2$pm from L-aspartic acid in 2001[53]. The key step of this synthesis is the introduction of the second asymmetric carbon thanks to an Katsuki-Sharpless asymmetric epoxidation[54] of an alkene obtained by a Wittig reaction (**Scheme 4**). The final differentially protected molecule is obtained after the epoxide opening, several protection/deprotection and reduction/oxidation steps. Although carbon-13 labelled L-aspartic acid are available, there is no satisfying opportunity for a deuterium or tritium introduction.

Scheme 4. Hernandez (2001)[53].

(a) benzene, 0°C, 89%; (b) DIBAL, -78°C, 85%; (c) Ti(*i*-PrO)$_4$, (*R*,*R*)-(+)-DET, TBHP, CH$_2$Cl$_2$, -20°C, 82%; (d) NaN$_3$, NH$_4$Cl, MeOH/H$_2$O (8:1), reflux, 83%; (e) H$_2$C=C(OMe)CH$_3$, PPTS (cat.), CH$_2$Cl$_2$, rt, 85%; (f) (1) H$_2$, Pd/C, EtOAc, rt, (2) Cbz$_2$O, CH$_2$Cl$_2$, rt, (3) MeOH, *p*-TsOH (cat.), (4) NaIO$_4$, Na$_2$CO$_3$, KMnO$_4$, dioxane/H$_2$O (3:1), rt, 60% (4 steps).

II.4. Kawasaki synthesis

The synthesis reported by Kawasaki *et al.*[55] in 2008 enforces a Julia-Kocienski olefination[56] reaction as the key step (step a, **Scheme 5**). The two chiral centers are already present in the aldehyde and sulfone precursors. Both of these are derived from D-serine, which is available as ^{13}C-substituted isotopomers. This chemical pathway features an alkene reduction making it suitable for a deuterium labelling. However, this reduction step occurs at an early stage of the synthesis compromising the possibility of a tritium labelling.

Scheme 5. Kawasaki (2008)[55].

(a) NaHMDS, THF, -70°C, 71%; (b) HCl 1M in MeOH; (c) triphosgene, Et$_3$N, CH$_2$Cl$_2$, 22% (2 steps); (d) (1) H$_2$, Pd/C, MeOH, (2) CbzCl, NaHCO$_3$, 1,4-dioxane/H$_2$O (1:1), 82% (2 steps); (e) RuCl$_3$.nH$_2$O, NaIO$_4$, acetone/H$_2$O (1:1), 66%; (f) AcCl, MeOH, 89%; (g) Boc$_2$O, DMAP, Et$_3$N, THF, 86%; (h) LiOH, THF/H$_2$O (3:1); (i) (1) Cs$_2$CO$_3$, MeOH, (2) BnBr, DMF, 83% (3 steps); (j) PDC, DMF, 86%.

II.5. Del Valle, Chowdhury and Saito syntheses

These three syntheses have a common key step: an olefin metathesis (steps c, g and I, **Scheme 6**). All three groups opted for olefinic synthons already containing the chiral centers present in m-A$_2$pm.

Del Valle and Goodman chose a ring closing metathesis (RCM) ensuring almost quantitative yields in their 2004 publication[57] (**Scheme 6**, left). However, this strategy requires more steps to prepare the diene substrate needed for RCM and to open the resulting ring. Alkene is then reduced and alcohol oxidized to afford the target molecule.

Saito *et al.* performed a cross-metathesis between a protected allylglycine and an oxazolidine derived from D-serine[58] (**Scheme 6**, right). An excess of the oxazolidine synthon is necessary to limit the formation of homodimers of allylglycine. As for Del Valle synthesis, three more steps are required to reach the target molecule: alkene reduction, oxazolidine opening and alcohol oxidation.

Chowdhury and Boons presented a very straightforward approach in 2005[59] (**Scheme 6**, middle). The m-A$_2$pm framework is formed in a single step from protected (*R*)-allylglycine and (*S*)-vinylglycine. The remaining step being a reduction of the alkene function. As for Saito's synthesis, an excess of vinylglycine synthon is necessary to limit the formation of homodimers of allylglycine. Vinylglycine does not react with itself probably due to steric reasons.

These three strategies use precursors that can be prepared from amino acids available in a variety of ^{13}C-substitued isotopomers. But only Chowdhury's synthesis is worth considering since the reduction could be applied as a final step. This strategy is very appealing to us because, with the right choices of protecting groups, a variety may of m-A$_2$pm derivatives may be produced with different goals in mind (peptides, (^{13}C)m-A$_2$pm, (^{2}H)m-A$_2$pm and [^{3}H]m-A$_2$pm).

L-methionine   glycine

HO

HO   (S) NCbzBn

(R) NH₂

a

AcO

(R) NCbzBn

N
H

b

glycine   L-methionine   glycine   D-serine

AcO

(R) NCbzBn

N
Boc

t-BuOOC (R)   (S) COOBn   BnOOC (R)   (S)

NHBoc   NHFmoc   NHCbz   BocN

c   g   i

AcO   Boc

(R) (S)

NCbzBn

t-BuOOC (R)   (S) COOBn   BnOOC (R)   (S)

NHBoc   NHFmoc   CbzHN   BocN

d   j

HO   NHBoc
(R)   COOMe
(S)
NCbzBn

BnOOC (R)   (S)

CbzHN   BocN

e   h   k

HO (R)   (S) COOMe

NHBoc   NCbzBn

t-BuOOC (R)   (S) COOH   BnOOC (R)   (S) OH

NHBoc   NHFmoc   NHCbz   NHBoc

f   l

HOOC (R)   (S) COOMe   t-BuOOC (R)   (S) COOH   BnOOC (R)   (S) COOH

NHBoc   NCbzBn   NHBoc   NHFmoc   NHCbz   NHBoc

Scheme 6. Del Valle (2004)[57], Chowdhury (2005)[59] and Saito (2013)[58] strategies.

(a) (1) PyBOP, Et₃N, CH₂Cl₂, (2) Ac₂O, pyridine, CH₂Cl₂, 83% (2 steps); (b) Boc₂O, DMAP, THF, 77%; (c) 2 mol% Grubbs 2nd gen. cat., CH₂Cl₂, reflux, 2h, 99%; (d) (1) LiOH 2M, THF, (2) MeI, K₂CO₃, DMF; (e) H₂, 2mol% [Ir(COD)PyPCy₃]PF₆, CH₂Cl₂, 56% (3 steps); (f) NaClO, NaClO₂, TEMPO, MeCN, H₂O (92%). (g) Grubbs 2nd gen. cat., 64%; (h) H₂, 3% Pt/C, EtOH, CH₂Cl₂, H₂O, 98%. (i) 5mol% Grubbs 2nd gen. cat., 73%; (j) H₂, PtO₂, EtOAc, rt, 14h, 97%; (k) p-TsOH, H₂O, MeOH, 81%; (l) NaClO, NaClO₂, TEMPO, MeCN, H₂O.

II.6. Peptides

Several groups have reported syntheses of *m*-A$_2$pm containing peptides and muropeptides. Some prepared short peptides in solution[50,51,55,57–61] while others inserted differentially or orthogonally protected *m*-A$_2$pm in solid-phase peptide synthesis[59,62–64] (SPPS, concept illustration in **Scheme 7**). The former strategies will be dismissed as they require extensive purification after each coupling whereas the latter only require a single purification step after cleaving the peptide from resin.

Recently, Dr J. Simon *et al.* proposed a new methodology for the synthesis of *m*-A$_2$pm containing peptides inspired by Chowdhury cross-metathesis[65]. Rather than inserting an adequately protected *m*-A$_2$pm directly into SPPS, they grew a peptide containing an allylglycine and then, performed an on-resin cross-metathesis with a vinylglycine synthon to turn the

Scheme 7. SPPS of a *m*-A$_2$pm containing peptide (classical approach).
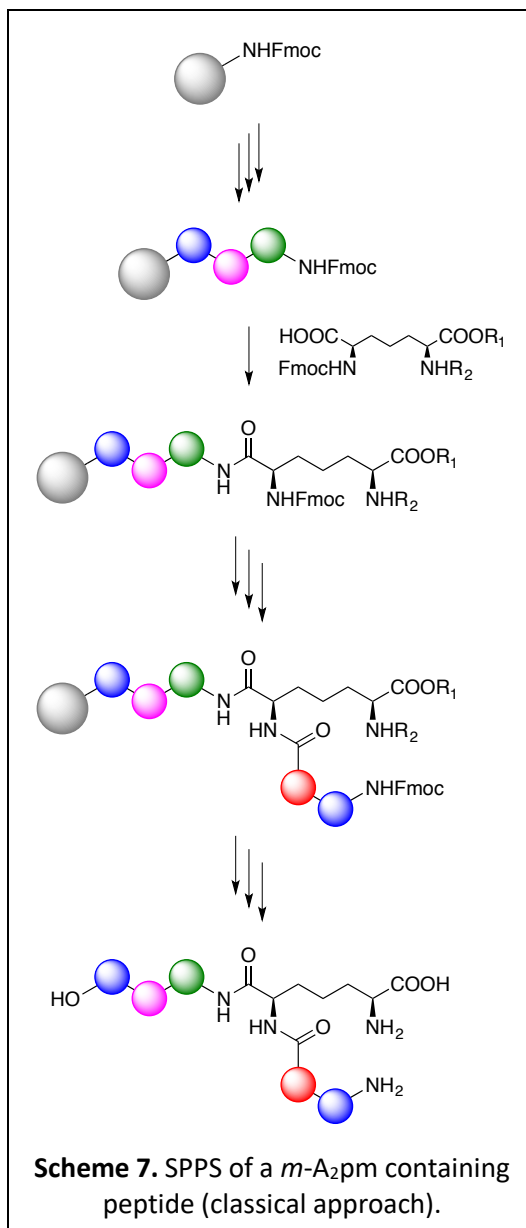
allylglycine into an *m*-A$_2$pm (concept illustration in **Scheme 8**).

Scheme 8. SPPS of a *m*-A$_2$pm containing peptide via on-resin cross-metathesis.
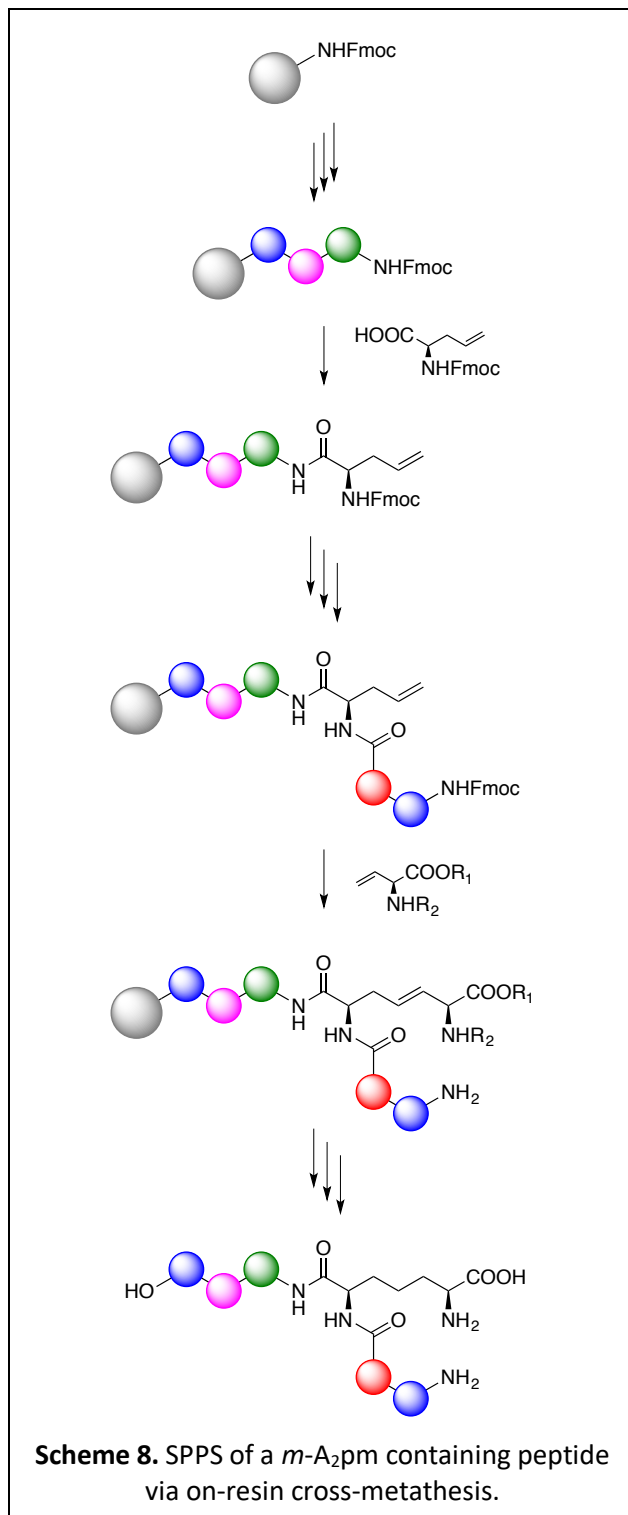
Chapter III

Results and discussion

Scheme 1. General strategy for the preparation of free m-A$_2$pm, (^{2}H$_2$)m-A$_2$pm, [^{3}H]m-A$_2$pm and peptide fragments of peptidoglycan.

40
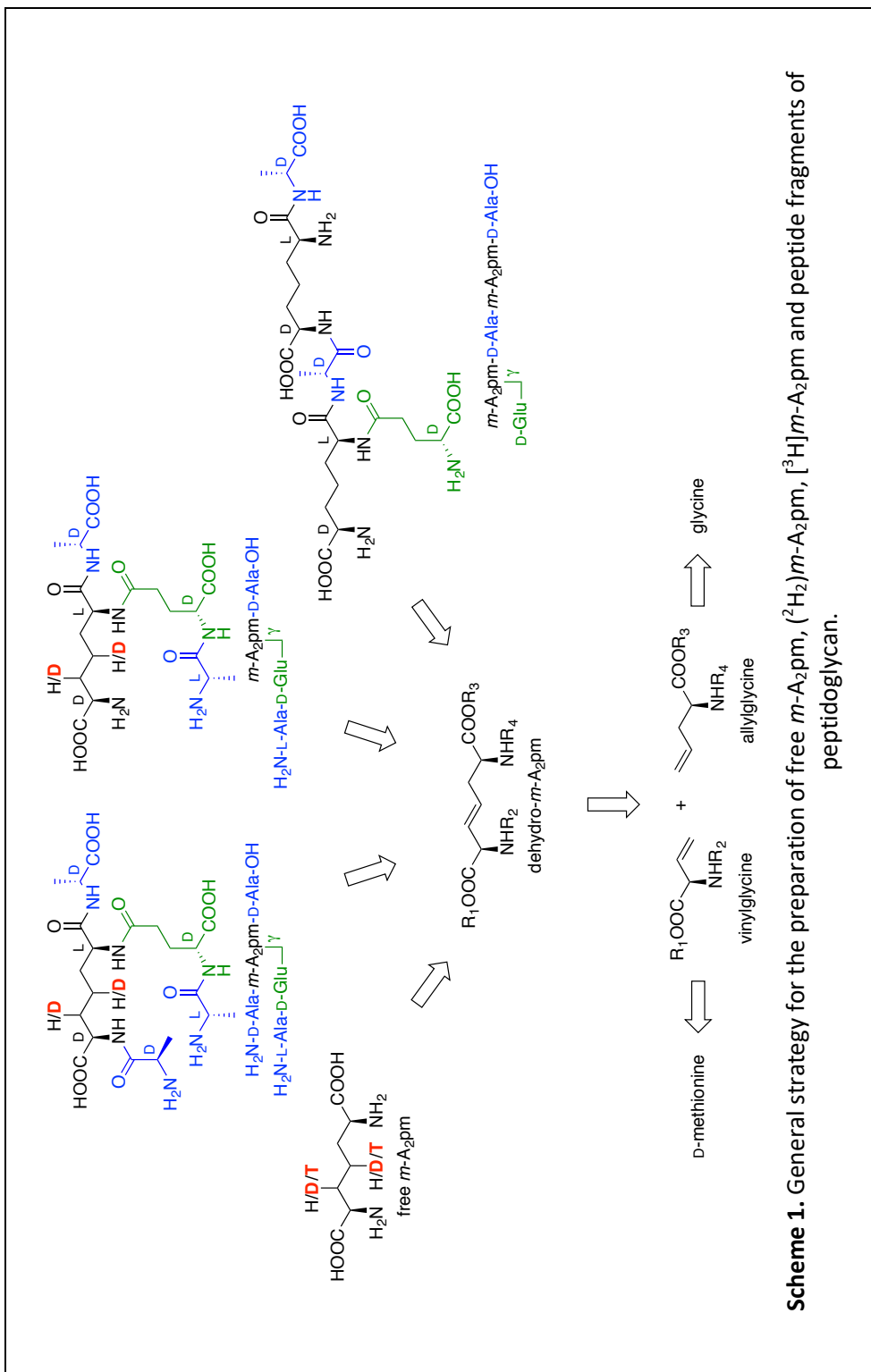
III.1. Strategy

As a reminder, the first goal of this work is the preparation of non-radioactive and radioactive isotope-containing *meso*-diaminopimelic acid: *m*-A$_2$pm, (^{2}H$_2$)*m*-A$_2$pm, [^{3}H]-*m*-A$_2$pm and (^{13}C)*m*-A$_2$pm.

The second goal is the synthesis of *m*-A$_2$pm and (^{2}H$_2$)*m*-A$_2$pm containing peptides. Because of the variety of target molecules (**Scheme 1**), The most versatile and straightforward strategy found so far will be enforced. Chowdhury's approach allows to mix and match couples of differently protected allylglycine (AG) and vinylglycine (VG) synthons to afford *m*-A$_2$pm with several sets of protecting groups.

Protecting groups and absolute configurations of AG and VG synthons must be chosen wisely depending on the anticipated fate of the dehydro-*m*-A$_2$pm derivatives obtained by cross metathesis, especially for peptide synthesis purposes. Depending on the targeted peptide, either orthogonally or differentially protected *m*-A$_2$pm will be needed. To avoid any information overdose to the reader at this early stage, actual protecting groups choices are argued in the following subchapters depending on the target molecule discussed (see **paragraph III.5.b** protecting groups choice).

Syntheses of free *m*-A$_2$pm, (^{2}H$_2$)*m*-A$_2$pm and [^{3}H]*m*-A$_2$pm will only differ in the catalytic reduction conditions of a common cross-metathesis dehydro-*m*-A$_2$pm key intermediate, but in contrast to deuterium and tritium, carbon-13 has to be introduced at the beginning of the synthetic pathway (**Scheme 2**). Although D-methionine and glycine are commercially available as several carbon-13 isotopomers, (1-^{13}C)glycine is the cheapest option available (172 €/g). In addition, in order to avoid large amounts of homodimers of allylglycine synthons during the cross metathesis key step, Chowdhury uses an excess of vinylglycine synthon, making it a poor choice as a carbon-13 substituted synthon for cost reasons. Consequently, it

was decided to produce (^{13}C)allylglycine from (1-^{13}C)glycine. We opted for (*R*)-VG and (^{13}C)(*S*)-AG synthons.

Scheme 2. General strategy for the preparation of (^{13}C)*m*-A$_2$pm.
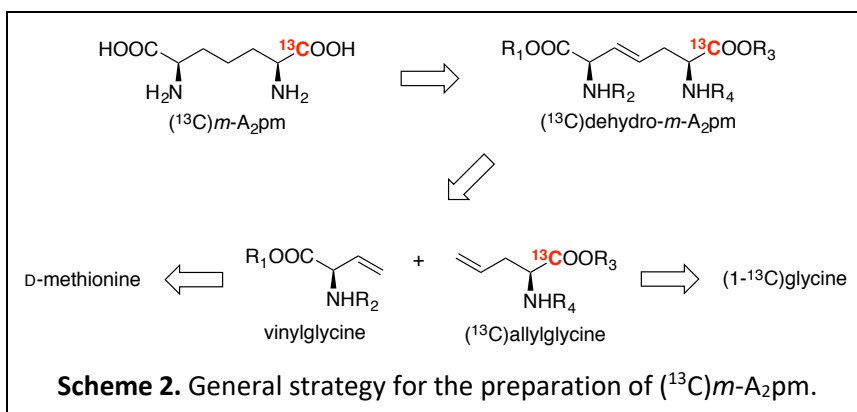
The first part of this chapter will focus on the preparation of AG and (^{13}C)AG synthons. The second part will describe the synthesis of the VG synthons. Then, syntheses of free and protected *m*-A$_2$pm will be discussed. The last subchapter will discuss peptides syntheses.

III.2. Allylglycine and (^{13}C)allylglycine preparation

III.2.a) Strategy

Allylglycine derivatives can be enantioselectively produced by phase-transfer catalysis (PTC) of a Schiff base using a chiral quaternary ammonium salt as a catalyst[66] (see retrosynthetic path described in **Scheme 3**). Such Schiff bases can be prepared from glycine. A benzophenone imine Schiff base was chosen since it is known to ensure monoalkylation in opposition to benzaldimine Schiff bases which are prone to dialkylation[67,68]. Due to the relatively high price tag of (1-^{13}C)glycine (172 €/g), all chemical steps were optimized on the cheap natural isotopic abundance glycine (0.1 €/g).

Scheme 3. Retrosynthetic path for the preparation of allylglycine derivatives.
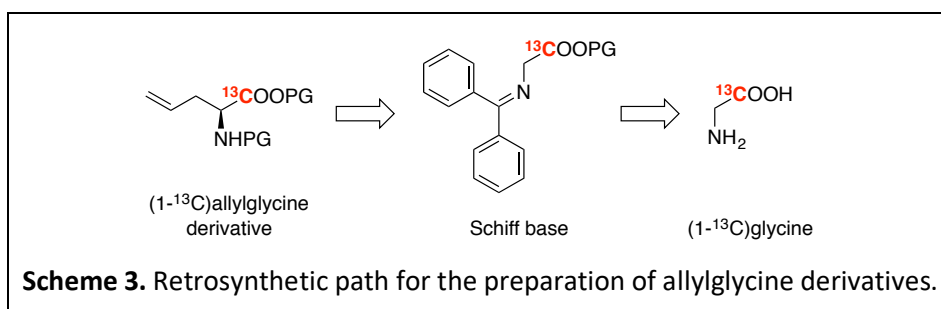
III.2.b) Preparation of Schiff bases

In order to prepare the desired natural isotopic abundance and carbon-13 substituted Schiff bases **5** and (^{13}C)**5**, glycine *tert*-butyl esters **4** and (^{13}C)**4** (**Scheme 4**) had to be prepared first. This particular type of ester can be tricky to prepare and requires a protection of glycine's amino group. So, glycine **1** was first converted into a carboxybenzyl carbamate **2**. This protecting group was chosen because its catalytic reduction removal conditions are compatible with a *tert*-butyl ester. The protection went smoothly on glycine **1** and was repeated on (1-^{13}C)glycine (^{13}C)**1** with similar yields (96%).

Scheme 4. Preparation of Schiff bases **5** and (^{13}C)**5**.
(a) Cbz-Cl, NaOH, toluene, 0 °C to rt, 96%; (b) t-BuOH, DCC, DMAP, CH$_2$Cl$_2$, 93%; (c) H$_2$ (5 bar), Pd/C, HCl, MeOH; (d) Ph$_2$C=NH, CH$_2$Cl$_2$, anh. MgSO$_4$, 94% (2 steps).
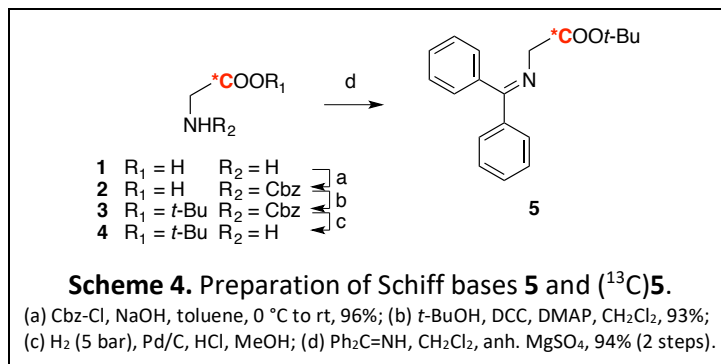
This first step was the occasion to witness analytical particularities of carbon-13 substituted compounds in mass spectrometry and NMR spectroscopy. Obviously, mass spectra were shifted one unit to the right but more interestingly, some carbon-hydrogen couplings were observed on ^{1}H NMR as well as carbon-carbon couplings on ^{13}C NMR (in addition to a hundred times more intense than usual peak for the carbon-13 substituted atom). NMR couplings observed on (^{13}C)**2** are displayed in **Figure 1**. Similar behaviors were observed in every carbon-13 substituted compounds synthesized from this point (see **Chapter VI**: Supplementary Data).

Figure 1. Comparison of NMR signals of CH$_{2\alpha}$ in **2** and (^{13}C)**2**.
H$_\alpha$ of (^{13}C)**2** appears as a triplet due to similar J_{HH} and J_{HC} in ^{1}H NMR. C$_\alpha$ appears as a doublet in ^{13}C NMR. Spectra taken in DMSO-d$_6$ on a 400MHz Bruker instrument.
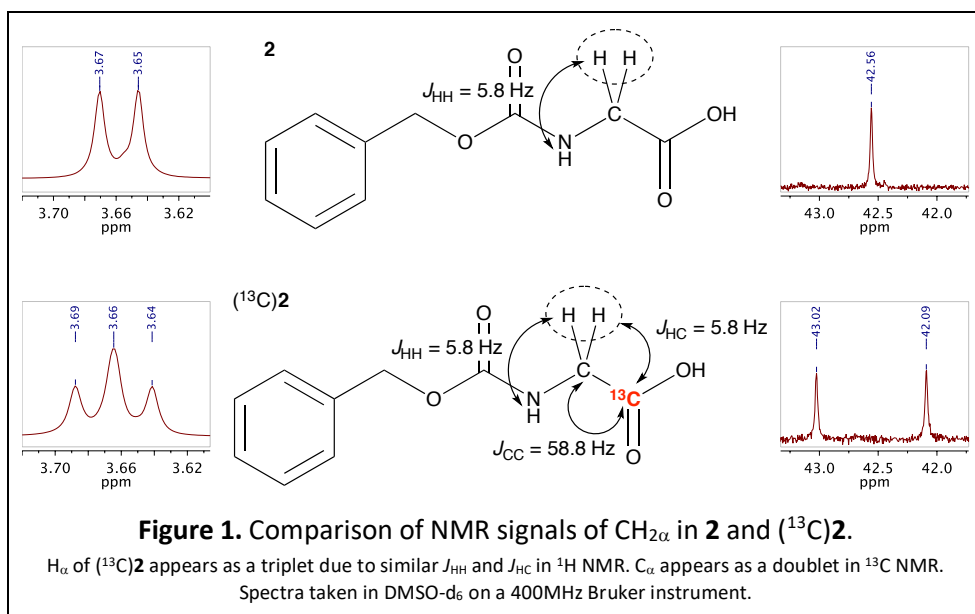
Tert-butyl protection of the carboxylic group was tested using Steglich's esterification[69]. Two carbodiimides were considered for this reaction: EDCI and DCC. The former has the advantage of being converted into a water soluble, easy to extract, corresponding urea. However, DCC gave better yields (93% vs 72%) and we had to cope with DCU elimination by multiple precipitations in ether. (^{13}C)**3** was obtained using these last conditions with a 93% yield.

Removal of the amino protecting group through catalytic hydrogenation surprisingly proved to be more difficult than expected (**Table 1**). Two different catalysts (Pd/C 5% wet and Pd/C 10% dry) were tested but none of them afforded satisfying results using THF as the solvent (entries 1, 2). Quantities of crude product **4** obtained after work-ups were very low. Our first hypothesis was a poor washing of the filtered catalyst. So, methanol was used and higher amounts of **4** although still lower than expected were obtained (entry 3). Using methanol as the reaction solvent improved a bit but still not in a satisfactory manner (entry 4). Our hypothesis then evolved: the free amino group might act as a poison to the catalyst. To avoid this issue, it was decided to add some acid to the medium. The acid choice and its quantity are crucial in order to avoid a cleavage of the *tert*-butyl ester. We first settled on using 1 equivalent of acetic acid (entry 5). Conversion improved a lot, comforting our hypothesis. Finally, using 0.48 equivalent of sulfuric acid or 0.95 equivalent of hydrochloric acid led to yields around 95% (entries 6, 7). These last conditions were then repeated on (^{13}C)**3**.

Table 1. Optimization of Cbz carbamate cleavage (step c, **Scheme 4**).

#	P(H$_2$)	Solvent	Washing solvent	Catalyst (quantity)	Duration	Yield
1	1-3 bar	THF	THF	Pd/C 5% wet (1%)	5 h	<1%
2	3 bar	THF	THF	Pd/C 10% dry (1%)	18 h	4%
3	5 bar	THF	MeOH	Pd/C 10% dry (1%)	120 h	23%
4	5 bar	MeOH	MeOH	Pd/C 10% dry (1%)	120 h	37%
5	5 bar	MeOH + 1.0 equiv. HOAc	MeOH	Pd/C 10% dry (1%)	120 h	56%
6	5 bar	MeOH + 0.48 equiv. H$_2$SO$_4$	MeOH	Pd/C 10% dry (2%)	2h	95%
7	5 bar	MeOH + 0.95 equiv. HCl	MeOH	Pd/C 10% dry (2%)	2h	97%

The last step toward the formation of the desired Schiff base can be accomplished using different reactants: dichlorodiphenylmethane, benzophenone or benzophenone imine[70–72]. The best results were obtained using the latter. The driving force of this reaction is the precipitation of by-product NH_4Cl. Addition of anhydrous $MgSO_4$ to the medium ensured precipitation of the salt and allowed total conversion of glycine *tert*-butyl ester **4** into Schiff base **5**. These optimized conditions were repeated on crude (^{13}C)**4** and allowed the formation of (^{13}C)**5** with a satisfying 94% yield over two steps. Carbon-13 substituted Schiff base (^{13}C)**5** was prepared on an over 10 g scale from (1-^{13}C)glycine (^{13}C)**1** with an overall yield of 84% over four steps.

III.2.c) Chiral alkylations and protections

The Cyclotron Research Center (CRC) is familiar with chiral phase transfer catalysis, for instance in the synthesis of α-benzylated lanthionine (an analogue of *m*-A$_2$pm)[73] or [18F]fluoro-L-DOPA[74–76], 6-[18F]fluoro-L-tyrosine[75] and 6-[18F]fluoro-L-m-tyrosine[76], for PET applications. Among the chiral quaternary ammonium salts already tested at the CRC, we may cite cinchonine and cinchonidine derived quaternary ammoniums and Maruoka's catalysts[66] (**Figure 2**).
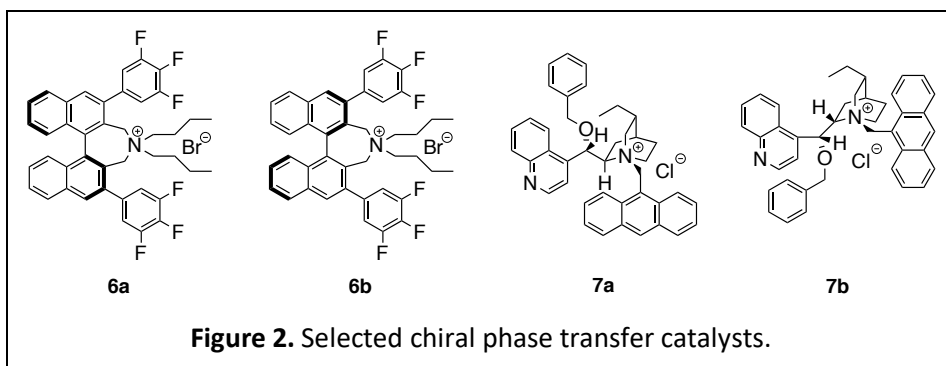
Figure 2. Selected chiral phase transfer catalysts.

Maruoka's phase transfer catalysts **6a** and **6b** are exceptionally active (only 0.5 mol% is usually needed) and stereoselective (enantiomeric excesses over 95%). They even

can afford high enantioselectivity at high temperatures. They are now commercially available (50 mg = 261 €), but it was not the case at the beginning of this work. The very long multistep preparation of these catalysts led us to consider cinchonine and cinchonidine derivatives **7a** and **7b**. These compounds, although less efficient than **6a** and **6b**, stand out as easy to prepare catalysts from cheap cinchonine (100 g = 110 €) and cinchonidine (100 g = 167 €) while remaining sufficiently active and selective. They were synthesized following Lygo's procedure[77] depicted in **Scheme 5**. Cinchonidine derivative **7b** was used to prepare (*S*)-AG derivatives and cinchonine derivative **7a** for the preparation of (*R*)-AG as chiral HPLC references.

Scheme 5. Preparation of catalyst **7b**.

(a) H₂ (5 bar), Pd/C (10%, dry), rt, 97%; (b) 9-chloromethylanthracene, toluene, N₂, 95 °C, 72%; (c) BnBr, NaOH 50%, CH₂Cl₂, 0 °C, 72%.

Scheme 6. Preparation of AG derivatives **10**, (¹³C)**10** and **11**.

(a) CH₂=CH-CH₂-Br, **7b**, KOH 50%, toluene/CH₂Cl₂ 10:1, -20°C, 95%; (b) citric acid, H₂O/THF; (c) Fmoc-OSu, THF/H₂O 65% (2 steps); (d) Cbz-Cl, Na₂CO₃, toluene, 0°C to rt, % (55%, 2 steps).
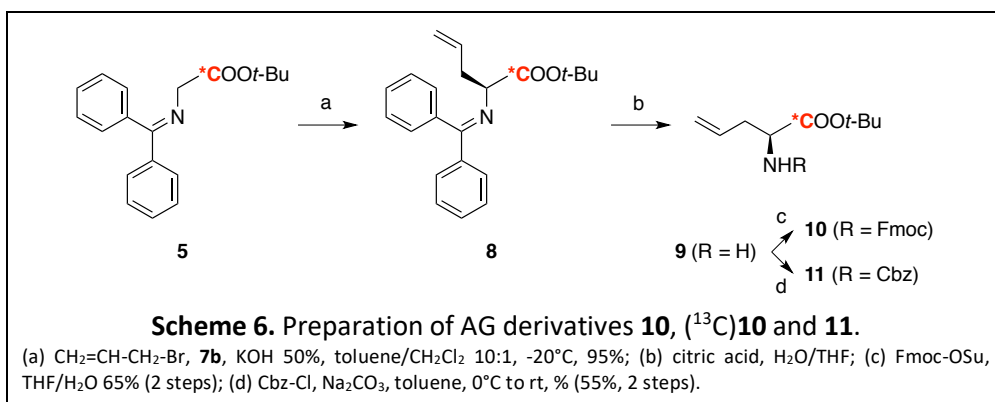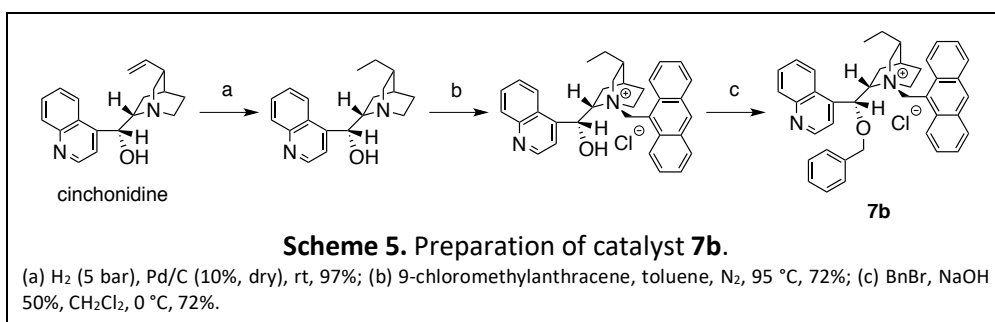
PTC alkylations of Schiff bases **5** and (¹³C)**5** were performed using a mixture of toluene and dichloromethane (10:1) as the organic phase and 50% aqueous KOH as a base (step a, **Scheme 6**). Toluene usually helps achieving better enantioselectivity but a fraction of dichloromethane was necessary to solubilize the catalyst. As with

all PTC, a vigorous agitation was required to maximize the interface area between the two phases. A low temperature (-20 °C) also ensures a high enantioselectivity. Although as much as 10 mol% of catalyst **7b** were necessary, this compound can be recovered by precipitation in ether. Carbon-12 chemistry was tested and scaled-up on commercial Schiff base **5** to prepare **8** (up to 20 g) before being repeated on synthesized (^{13}C)**5** at a 10 g scale with a 95% yield.

In the following step, benzophenone imine had to be cleaved in order to introduce adequate protecting groups. A weak acid (citric acid) was employed to selectively cleave the imine function. These experiments were monitored by HPLC to avoid any over exposure to acidic conditions which would lead to the *tert*-butyl ester hydrolysis. Crude **9** was directly converted into (*S*)-FmocNH-AG-O*t*-Bu **10** (yield = 66% from **8** to **10**, 3 g scale) and (*S*)-CbzNH-AG-O*t*-Bu **11** (yield = 55% from **8** to **11**, 2 g scale). Crude (^{13}C)**9** was directly converted into (^{13}C)(*S*)-FmocNH-AG-O*t*-Bu (^{13}C)**10** on a 5 g scale (yield = 65% from (^{13}C)**8** to (^{13}C)**10**). (*R*)-enantiomers of **10** and **11** were also prepared as references for chiral HPLC.

Optical purities of the three AG derivatives were determined by HPLC using a Daicel Chiralcel® OD-H chiral column (chromatograms and enantiomeric excesses are compiled in **Figure 3**). An additional treatment by TFA was necessary to separate enantiomers of **11**.
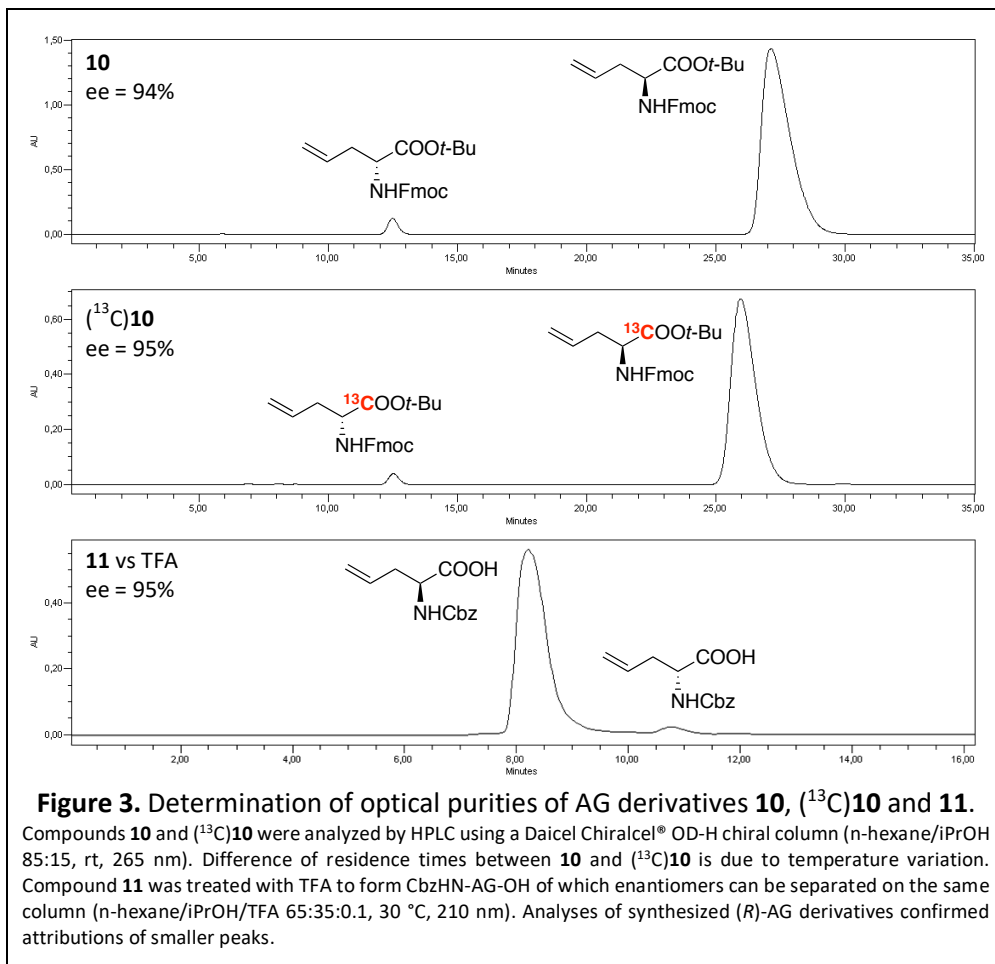
Figure 3. Determination of optical purities of AG derivatives **10**, (^{13}C)**10** and **11**.
Compounds **10** and (^{13}C)**10** were analyzed by HPLC using a Daicel Chiralcel® OD-H chiral column (n-hexane/iPrOH 85:15, rt, 265 nm). Difference of residence times between **10** and (^{13}C)**10** is due to temperature variation. Compound **11** was treated with TFA to form CbzHN-AG-OH of which enantiomers can be separated on the same column (n-hexane/iPrOH/TFA 65:35:0.1, 30 °C, 210 nm). Analyses of synthesized (*R*)-AG derivatives confirmed attributions of smaller peaks.

III.3. Vinylglycine preparation

The vinylglycine synthon **16** needed for cross-metathesis experiments is commercially available but due to the ever-raising prices of this compound ($998 for 5 g at the time of writing), it was prepared in our laboratory. A plethora of preparations of VG derivatives have been reported[78–94] but the most straightforward strategy uses methionine **12** as a starting material. Once fully protected and converted into a methionine sulfoxide derivative (MetO) **15**, protected VG derivative **16** can be obtained by *syn* sylfoxide elimination through thermolysis (**Scheme 7**).[79–81]

Scheme 7. Synthesis of vinylglycine precursor **15**.
(a) CbzCl, NaOH 1M, toluene, 0 °C to rt, 97%; (b) TMSCl, MeOH, rt, 94%; (c) NaIO₄, MeOH, rt, 99%.
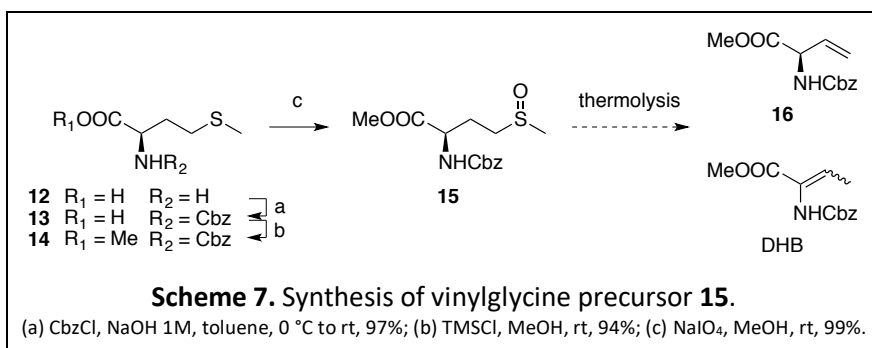
Unfortunately, previously reported thermolysis methods tested during the course of this work were hampered by extensive isomerization. Batch thermolysis in a high boiling point solvent such as 2,4-dichlorotoluene required long reaction times causing the formation of a dehydrobutyrine derivative (DHB) side-product that is impossible to separate from our desired vinylglycine derivative[82]. A promising alternative to batch methods was to avoid using any solvent by performing the thermolysis in a Kugelrohr distillation apparatus as reported by Rapoport *et al*.[79] Small scale tests were encouraging but all attempts to reproduce these results at larger scales failed, as the crude products were also contaminated with large amounts of DHB. Whichever method employed, large amounts of DHB formed were always accompanied by poor enantiomeric excesses.

These observations led us to consider a continuous-flow alternative in order to minimize reaction times in hope to avoid isomerization and to improve enantioselectivity. Continuous-flow chemical processing enables the continuous production of chemicals with high flexibility and stability over parameters such as pressure, temperature, homogeneity of the medium and reaction times. In the present case, the temperature is a key factor and using a high pressure mesofluidic reactor as the one depicted in **Scheme 8** allows to use toluene as a solvent at temperatures well above its atmospheric boiling point (250 – 290 °C vs 110.6 °C). Control over the flow-rate via an HPLC pump allows for precise tuning of residence times. While batch methods require hours long refluxes in high boiling point solvents, continuous-flow thermolysis residence times in superheated toluene ranged from 20 to 102 seconds. Computational studies performed by Doctor Monbaliu (CiTOS, University of Liège) showed that the methylsulfenic acid by-product (MeSOH) was responsible for the isomerization of desired the VG **16** into DHB. The addition of 1.0 equiv. of dimethyl acetylenedicarboxylate (DMAC) as a scavenger of MeSOH to the MetO **15** solution contributed to avoid the formation of DHB. This innovative method of preparation of VG derivatives allowed us to prepare VG synthons **16** on a 10 g scale from MetO **15**, and **18** on a 5 g scale from MetO **17** with optical purities of 97%.

Results of this work were published in *Organic & Biomolecular Chemistry* in 2015[95] (publication attached in **Chapter VII**).

Scheme 8. Syntheses of vinylglycine derivatives **15** and **16** using continuous-flow thermolysis of methionine oxide derivatives.
(a) methionine sulfoxide derivative solution in toluene (10 g.L^{-1}), flow rate = 1 mL.min^{-1}, 1.0 equiv. DMAC. Back Pressure Regulator (BPR) ensures that superheated toluene remains liquid.
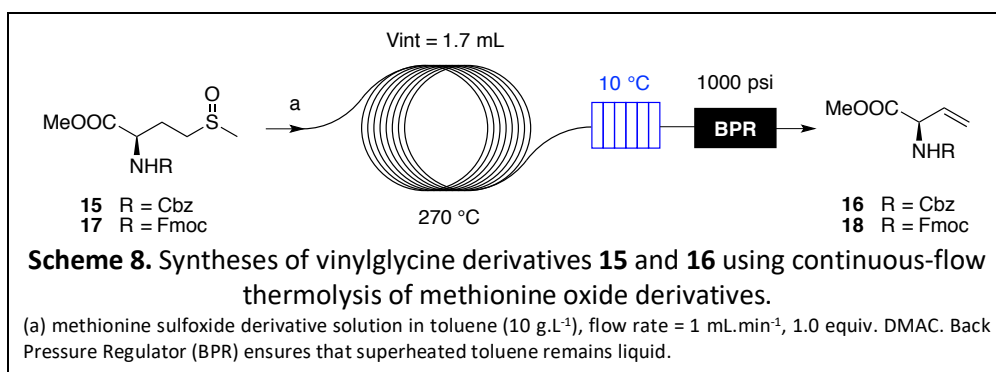
III.4. *m*-A$_2$pm syntheses

III.4.a) Differentially protected *m*-A$_2$pm syntheses

With these three allylglycine (AG) (**10**, (¹³C)**10** and **11**) and two vinylglycine (VG) (**16** and **18**) synthons in hand, we were ready to perform cross-metatheses to get dehydro-*m*-A$_2$pm derivatives with different substitution patterns. We first considered a coupling between (*S*)-FmocNH-AG-O*t*-Bu **10** and (*R*)-CbzNH-VG-OMe **16** (**Scheme 9**). This set of protecting groups (Fmoc carbamate, *t*-Bu ester, Cbz carbamate and Me ester) is very versatile to build *m*-A$_2$pm containing peptides **PEP1** and **PEP2** using solid phase supported peptide synthesis (SPPS) with the Fmoc strategy (see **subchapter III.5.b**).

Scheme 9. Preparation of differentially protected *m*-A$_2$pm **22**, (²H$_2$)**22**, **23** and (²H$_2$)**23**.
(a) 1 equiv. **10**, 3 equiv. **16**, 20 mol% Grubbs 2nd gen. cat., CH$_2$Cl$_2$, reflux, N$_2$, 75%; (b) **20**: H$_2$ (1 bar), Pd/C (10% wt, dry), HCl, H$_2$O/THF 1:5, rt; (²H$_2$)**20**: D$_2$ (1 bar), Pd/C (10% wt, dry), DCl, D$_2$O/THF 1:5, rt; (c) TFA, 93% (2 steps); (d) CbzCl, NaHCO$_3$, THF, 49%; (e) Boc$_2$O, NaHCO$_3$, THF, 98%.
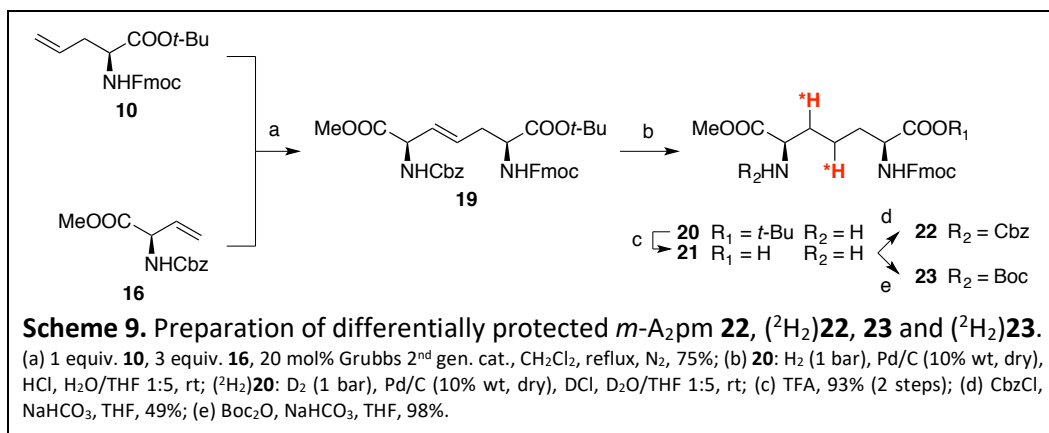
These cross-metatheses were performed using Grubbs' second-generation catalyst as Chowdhury reported that there was no cross-coupling occurring when Grubbs' first-generation catalyst is employed. Following another Chowdhury's suggestion, 2 equivalents of VG **16** were used to avoid homodimerization of AG **10**. However, some homodimerization was still observed (**Scheme 10** and **Table 2**, entry 1). Raising the number of equivalents of VG **16** to three was still not sufficient to completely avoid the formation of AG homodimer but led to very good yields for olefin cross-metatheses ranging from 73% to 78% (entries 2 – 4). No homodimerization of VG **16** was observed in these conditions. This cross-metathesis was scaled to produce up to 2.75 g of dehydro-*m*-A$_2$pm **19**.

Table 2. Optimization of the cross-metathesis step.

#	Reactants		Crude HPLC analysis (corrected)*			
	AG **10**	VG **16**	AG **10**	Homodimer AG-AG	Dehydro-*m*-A$_2$pm **19**	Yield
1	1 mmol	2 mmol (2.0 equiv.)	12%	8%	80%	58%
2	1 mmol	3 mmol (3.0 equiv.)	11%	4%	85%	75%
3	1.75 mmol	5.25 mmol (3.0 equiv.)	10%	4%	86%	78%
4	6.13 mmol	17.6 mmol (2.9 equiv.)	14%	4%	82%	73%

*The medium was analyzed by HPLC. Homodimer AG-AG peak surface was divided by 2 to take into account its double Fmoc protection. Chromatograms were analyzed at 265 nm, a wavelength almost not absorbed by Cbz but strongly absorbed by Fmoc.

Scheme 10. Cross-metathesis step and side-product homodimer AG-AG.
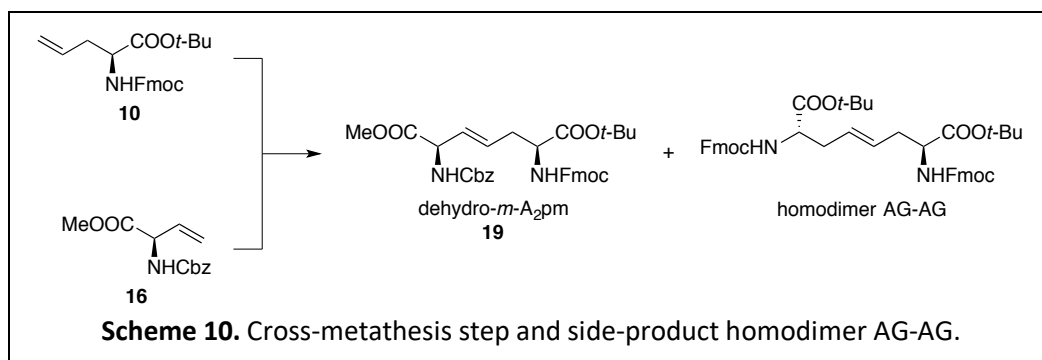
It should be noted that the alkene function of dehydro-*m*-A$_2$pm derivatives is very prone to isomerization in alkaline conditions such as the ones used in peptide synthesis[65] (see **Scheme 11**). This is why it had to be reduced prior to any utilization in SPPS, giving us an opportunity to introduce deuterium atoms. This reduction step inevitably caused the cleavage of the Cbz carbamate, forcing us to reprotect **21** and (^{2}H$_2$)**21** before using them in SPPS. This gave us an occasion to switch to another protecting group such as Boc carbamate to afford differentially protected *m*-A$_2$pm **23** and (^{2}H$_2$)**23** or to reprotect using Cbz-Cl to afford differentially protected *m*-A$_2$pm **22** and (^{2}H$_2$)**22**.

Scheme 11. Isomerization of dehydro-*m*-A$_2$pm derivatives in alkaline conditions
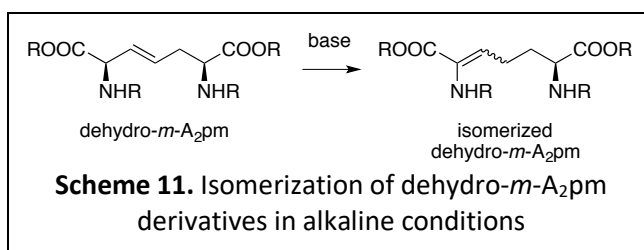
A second cross metathesis (depicted in **Scheme 12**) was performed between (*S*)-CbzNH-AG-O*t*-Bu **11** and (*R*)-FmocNH-VG-OMe **18** specifically to access cross-linked peptidoglycan fragments such as **PEP3** (see **subchapter III.5.b**).

Scheme 12. Preparation of differentially protected *m*-A$_2$pm **27**.
(a) 1 equiv. **11**, 2 equiv. **18**, 20 mol% Grubbs 2nd gen. cat., CH$_2$Cl$_2$, reflux, N$_2$, 49%; (b) H$_2$ (5 bar), Pd/C (10%, dry), THF, rt; (c) THF, rt; TFA, CH$_2$Cl$_2$, rt; (d) 1.2 equiv. Boc$_2$O, 3.0 equiv. Et$_3$N, CH$_2$Cl$_2$, 90% (3 steps).
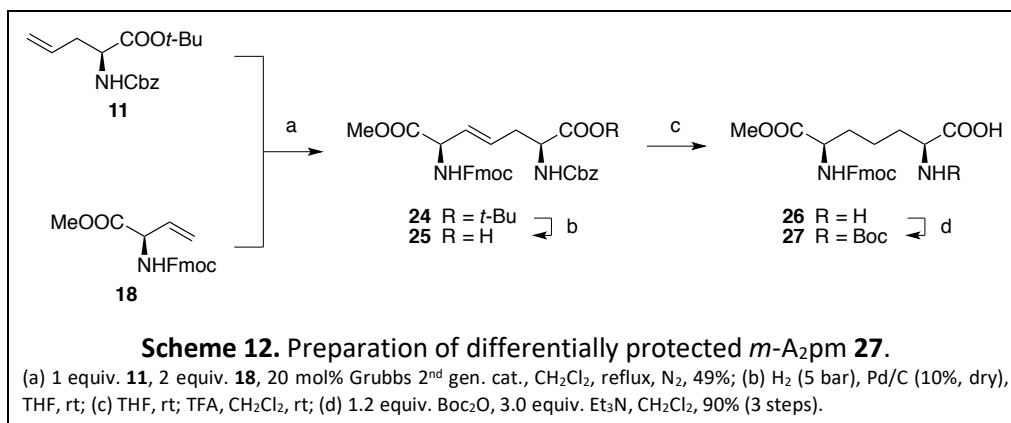
At first, dehydro-*m*-A$_2$pm **19** was foreseen as a free *m*-A$_2$pm, (^{2}H$_2$) *m*-A$_2$pm and [^{3}H]*m*-A$_2$pm precursor. Unfortunately, this cross-metathesis product was very difficult to totally deprotect. As mentioned above, the Fmoc protecting group cannot be removed in alkaline conditions with the alkene function still unreduced without leading to isomerization – which would cause the loss of chirality control. Although it is possible to cleave Fmoc carbamates and Cbz carbamate using a catalytic reduction, high hydrogen pressure and long reaction times are usually required to catalytically cleave the Fmoc protecting group (see **section III.4.d**) (^{13}C)*m*-A$_2$pm synthesis section). Such conditions are not conceivable for the preparation of tritiated [^{3}H]*m*-A$_2$pm. Hence, it was necessary to prepare another dehydro-*m*-A$_2$pm derivative with a better suited set of protecting groups to obtain to free *m*-A$_2$pm, (^{2}H$_2$)*m*-A$_2$pm and [^{3}H]*m*-A$_2$pm.

III.4.b) Free *m*-A$_2$pm and (^{2}H$_2$)*m*-A$_2$pm syntheses

In light of the reasons previously mentioned, It was decided to use (*S*)-CbzNH-AG-O*t*-Bu **11** and (*R*)-CbzNH-VG-OMe **16** to form a dehydro-*m*-A$_2$pm derivative easier to deprotect and to reduce in order to synthesize free *m*-A$_2$pm **30**, (^{2}H$_2$)*m*-A$_2$pm (^{2}H$_2$)**30** and [^{3}H]*m*-A$_2$pm [^{3}H]**30**. The choice of two carboxybenzyl carbamates protecting groups allowed us to kill three birds – two deprotections and an alkene reduction – with a single stone (**Scheme 13**).

Scheme 13. Preparation of free *m*-A$_2$pm and (^{2}H$_2$)*m*-A$_2$pm.
(a) 1 equiv. **11**, 2 equiv. **16**, 10 mol% Grubbs 2nd gen. cat., CH$_2$Cl$_2$, reflux, N$_2$, 40%; (b) HCl 2 mol/L, 1,4-dioxane, reflux, 100%; (c) H$_2$ (5 bar), Pd black, THF/H$_2$O 1:4, 100% (d) D$_2$ (5 bar), Pd black, THF/D$_2$O 1:4, 100%.
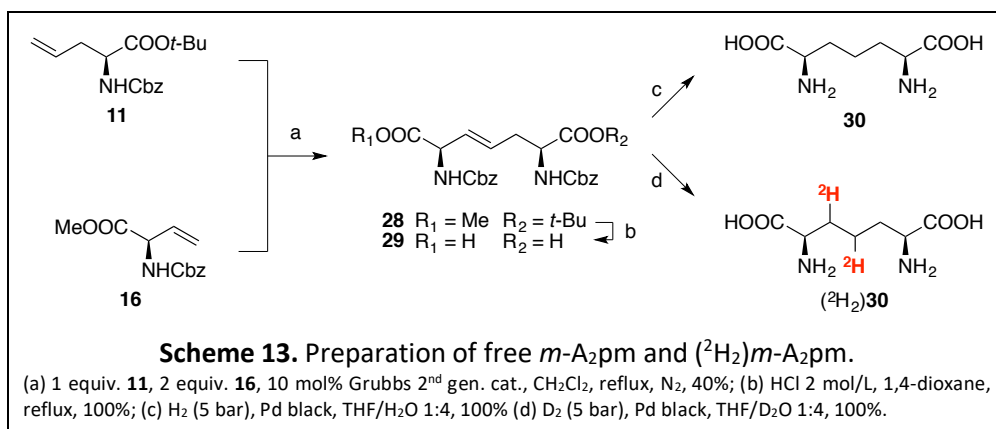
First, dehydro-*m*-A$_2$pm **28** was treated with hydrochloric acid to cleave both esters and to afford **29**, a compound ready to be reduced using hydrogen, deuterium or tritium gaz. We began with the production of *m*-A$_2$pm, **30**. H$_2$ reductions of dehydro-*m*-A$_2$pm derivative **29** were performed in several mixtures of THF and water in an autoclave under 5 bars of pressure. The organic solvent is required to solubilize the reactant and a minimum of water is necessary to solubilize the products and intermediates. Indeed, when the proportion of water is too low, intermediates precipitate and cannot undergo full reduction (see **Table 3** and **Scheme 14**). The best conditions (entry 4), only permit a partial solubilization of **29** but the solution quickly becomes limpid as the Cbz carbamates are cleaved. These last two steps displayed quantitative yields and allowed us to prepare **30** and (^{2}H$_2$)**30** on a 10 mg scale.

Table 3. Optimization of the hydrogen catalytic reduction (step c, **Scheme 13**).

#	P(H$_2$)	Solvent	V$_{solvent}$	Catalyst	Time	Cbz removal	Alkene reduction
1	5 bar	THF	5 mL	Pd black	2 h	0/2	none
2	5 bar	THF/H$_2$O 4:1	5 mL	Pd black	2 h	1/2	none
3	5 bar	THF/H$_2$O 1:1	5 mL	Pd black	2 h	1/2 – 2/2	partial
4	5 bar	THF/H$_2$O 1:4	5 mL	Pd black	2 h	2/2	total

Scheme 14. Precipitation of catalytic reduction intermediates in solvents with lesser proportions of water prevents total deprotection and reduction of dehydro-*m*-A$_2$pm derivative **29**.
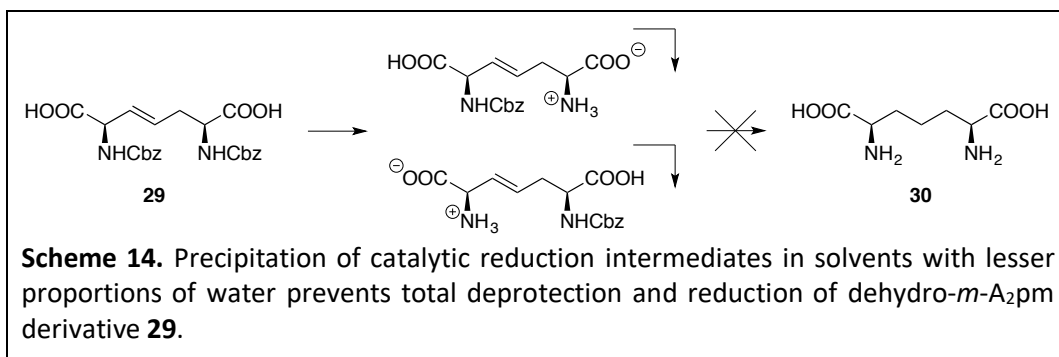
When trying to transpose these latter conditions (entry 4, **Table 3**) to a deuterium reduction by only switching gas, lower than expected labeling levels were observed (see isotopic profile of [^{2}H]**30**, **Figure 4**). This phenomenon was also reported and explained by Lee and Whitesides in the case of a platinum catalyst and protic solvents[96]. A rapid exchange between the D$_2$ gas and the surrounding H$_2$O molecules occurs at the catalyst surface resulting in HD and H$_2$ reductions. To avoid this issue, the experiment was simply conducted in D$_2$O instead of H$_2$O (step d, **Scheme 13**) and this afforded deuterium substituted (^{2}H$_2$)**30** as shown in **Figure 4**.

Figure 4. Isotopic profiles of **30**, [^{2}H]**30** and (^{2}H$_2$)**30** (ESI-MS, positive mode).
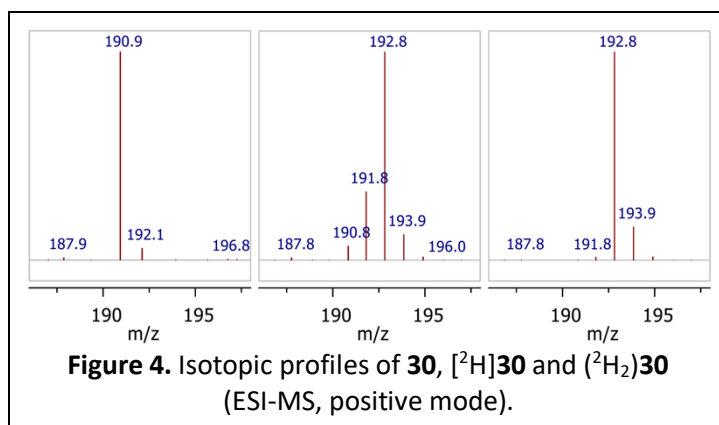
Several separation methods of m-A$_2$pm diastereoisomers for the determination of their diastereomeric ratio (dr) have been reported[97–102]. Among these methods, McKerrow's o-phthaldehyde/N-acetyl-L-cysteine (OPA/NAC) derivatization retained our attention as a simple method providing a good separation without the requirement of a chiral HPLC column[97]. This derivatization process (**Scheme 15**) also has the advantage of introducing chromophores in the structure, therefore easing the detection of the different stereoisomers of A$_2$pm: (S,S)-, (R,R)- and (R,S)-A$_2$pm or m-A$_2$pm. The chirality of the L-cysteine moiety allows for the separation of (S,S) and (R,R) enantiomers. The results of these analyses are shown in **Figure 5**. The higher amount of (S,S)-stereoisomer highlights a loss of stereoselectivity on the (R)-side of dehydro-m-A$_2$pm. However, NMR analysis of (^{2}H$_2$)**30** does not show a deuteration of C$_\alpha$(R), which would result from the reduction of an isomerized dehydro-m-A$_2$pm.

Scheme 15. OPA/NAC derivatization of m-A$_2$pm.

A solution prepared from K$_2$B$_4$O$_7$.4H$_2$O, OPA and NAC was added to solutions of **30** and (^{2}H$_2$)**30** following procedure described by McKerrow[97].

Figure 5. Chromatograms of OPA/NAC derivatized **30** and (^{2}H$_2$)**30**.
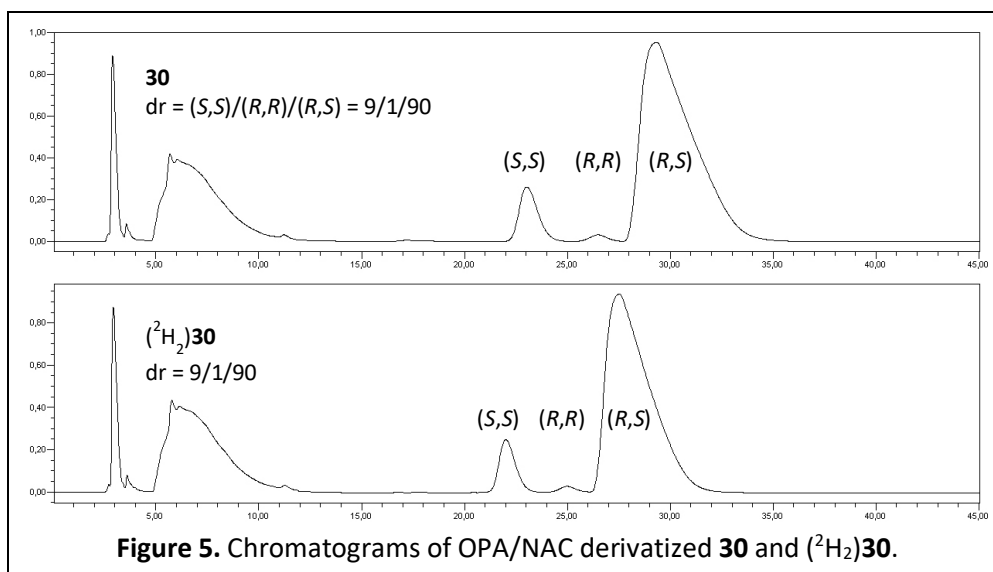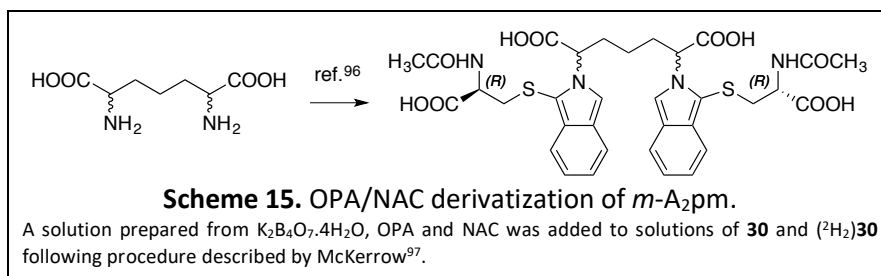
^{1}H NMR spectra integrations confirm the labelling and the small amount of (*S*,*S*) and (*R*,*R*) diastereoisomers found by HPLC (**Figure 6**). ^{13}C-APT NMR spectra display some particularities of deuterium substituted compounds such as carbon-13 – deuterium couplings in CHDs ($C_{4/5}$HD), orientation switch ($C_{4/5}H_2 \rightarrow C_{4/5}$HD) and chemical shift variation due to the introduction of deuterium atoms (C_2 and C_6, C_3 and C_5 have different chemical shifts in ($^2H_2$)**30**).
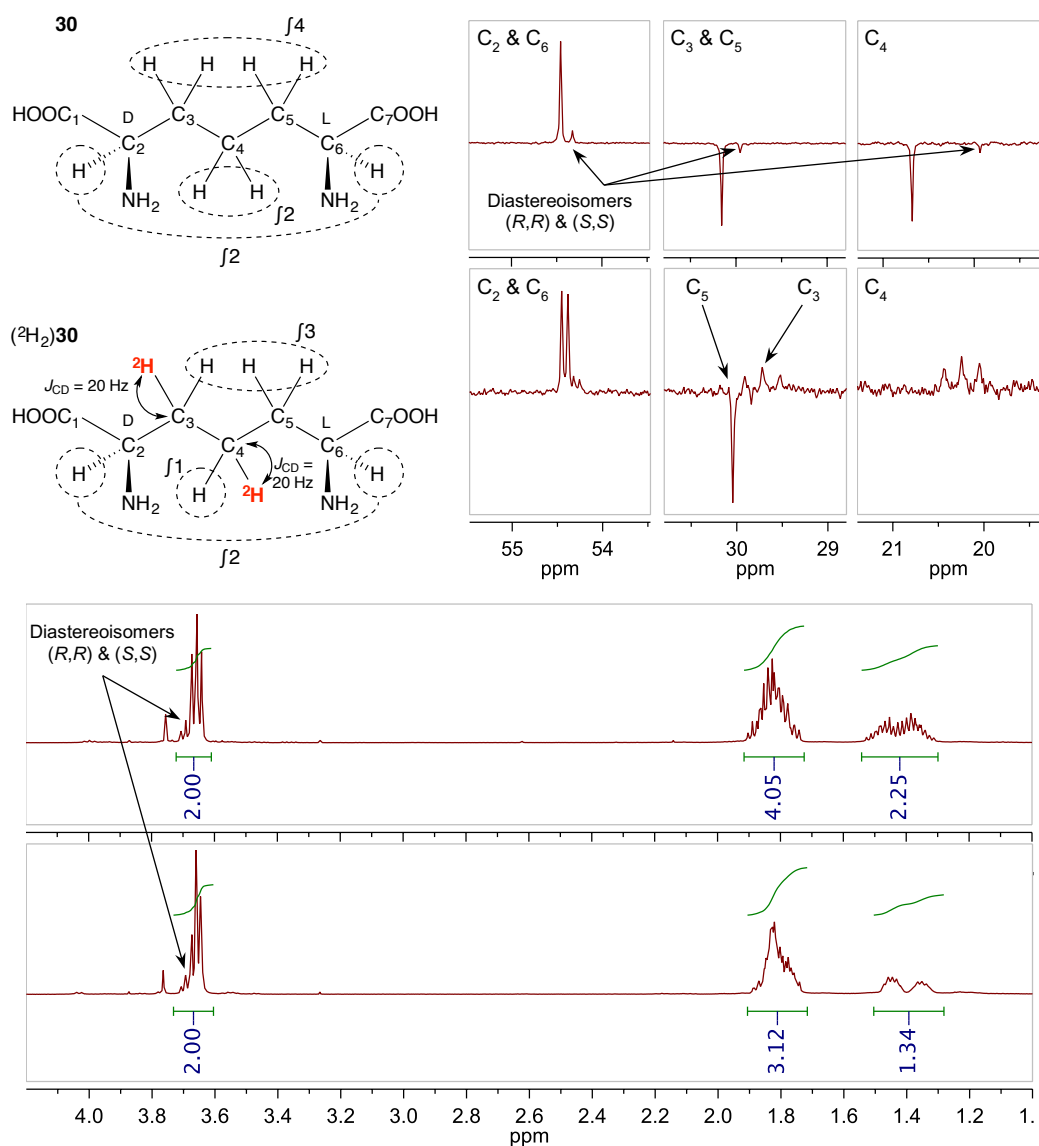
Figure 6. Highlights from NMR spectra of **30** and ($^2H_2$)**30**.

III.4.c) [^{3}H]m-A$_2$pm synthesis

The Cyclotron Research Center (CRC), lacks the equipment and authorizations required to perform tritium chemistry. Part of the following experiments were carried out at the *Commissariat à l'Énergie Atomique* (CEA) of Saclay, France in the *Laboratoire de Marquage par le Tritium* (LMT) of the *Service de Chimie Bio-organique et de Marquage* (SCBM). This research unit has a long history of synthesis of tritium and carbon-14 radiolabelled compounds. Experiments at the CEA were performed under the supervision of Doctor Sophie Feuillastre with the help of Olivia Carvalho and Sebastien Garcia-Argote.

Figure 7. Tritium reduction apparatus.
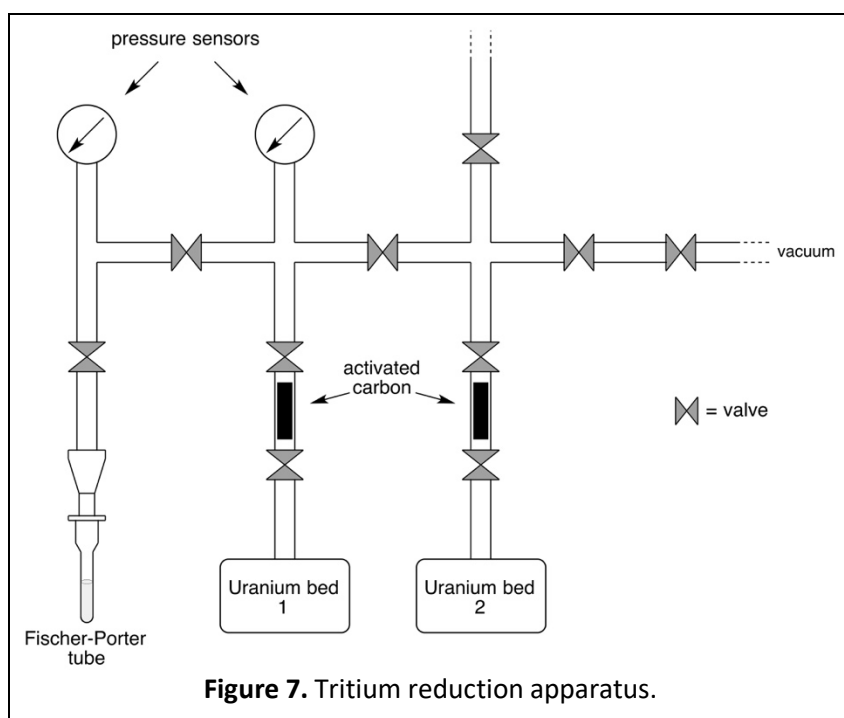
A tritium reduction obviously requires more precautions than hydrogen and deuterium ones. Whereas hydrogen and deuterium reduction were simply performed in an autoclave and gases rejected into the atmosphere, a precise control over tritium gas whereabouts is essential. **Figure 7** depicts the apparatus used for this purpose. Uranium beds are used as a source of tritium gas. When heated, they

release tritium gas but upon cooling they trap tritium as uranium tritide UT_3 to the point that a mild vacuum is generated. Bed 1 is the source of pure tritium gas while bed 2 is used to trap contaminated gas in case of a probable exchange between T_2 and protic solvents. A turbopump is used to put the whole system under vacuum before the introduction of tritium and to reject residual gases that could not be trapped on the uranium beds. The solution containing the substrate to reduce and catalyst in the Fischer-Porter tube has to be frozen in liquid N_2 before vacuum is made. Special care is applied to the pressure monitoring in the different sections of the system thanks to two pressure sensors.

Because of the exchange phenomenon mentioned earlier, water should be avoided if possible. Not so much because it would cause lower specific activities in our final product but because of the tritiated water waste it would generate. Of course, using T_2O as a solvent to maximize specific activities is not an option. High pressures of T_2 are also avoided: in a given volume of gas above the solution surface, the total activity is indeed proportional to the radioactive gas pressure.

Therefore, different conditions were tried to take into account these new parameters. First, test pressures had to be tuned down from 5 to 1 bar. Prior to having access to the installations of the CEA, reductions experiments with lower pressure of deuterium gas were investigated at the CRC with alternate solvents: DMA, DMF, MeOH and THF. Unfortunately, none of them gave satisfactory results (**Table 4**, entries 1 – 6). Tests in mixtures of THF and H_2O in various proportions comforted our feeling that the use water is a necessity for this experiment (entries 7 – 15). Some additional deuterium tests were performed at the CEA to fit most closely tritium limitations and conditions (pressure, glassware, variations in the operating procedure, …). In this context, some optimizations were conducted to achieve full deprotection and reduction, as well as satisfactory projected activities (entries 16 and 17). Lower volumes of solvents led to higher labelling levels (entries 18 – 20) but

long reaction times were still required to afford fully deprotected and reduced dehydro-*m*-A$_2$pm without the requirement of any further purification (entry 19). These last conditions were repeated with a slightly shorter reaction time due to schedule reasons with good results but showed that the 24 h were indeed necessary to achieve completion.

Table 4. Optimization of the deuterium reduction of **29** in view of its tritium reduction.

#	Solvent	V$_{solvent}$	Catalyst	Time	Cbz removal[a]	Alkene reduction[a]	Labelling level[b]
1	DMA	1.5 mL	Pd/C 10%	1 h	0/2	none	0
2	DMF	1.5 mL	Pd/C 10%	1 h	0/2	none	0
3	DMF	1.5 mL	Pd black[a]	1 h – 24h	0/2	none	0
4	MeOH[c]	1.5 mL	Pd/C 10%	1h	0/2	none	0
5	THF	1.5 mL	Pd/C 10%	1 h	0/2	none	0
6	THF	1.5 mL	Pd black[a]	1 h – 24h	0/2	none	0
7	THF/H$_2$O 4:1	1.5 mL	Pd/C 10%	1 h	0/2	none	0
8	THF/H$_2$O 4:1	1.5 mL	Pd black[a]	1 h – 24h	1/2	none	0
9	THF/H$_2$O 1:1	1.5 mL	Pd/C 10%	1 h	1/2	none	0
10	THF/H$_2$O 1:1	1.5 mL	Pd black[a]	1 h – 4h	1/2	none	0
11	THF/H$_2$O 1:1	1.5 mL	Pd black[a]	24 h	2/2	total	0.82 D
12	THF/H$_2$O 1:4	1.5 mL	Pd/C 10%	1 h	1/2	none	0
13	THF/H$_2$O 1:4	1.5 mL	Pd black[a]	1 h	1/2	none	0
14	THF/H$_2$O 1:4	1.5 mL	Pd black[a]	4 h	2/2	total	1.04 D
15	THF/H$_2$O 1:4	1.5 mL	Pd black[a]	24 h	2/2	total	1.04 D
16	THF/H$_2$O 1:4	1.5 mL	Pd black[a]	4 h	1/2 – 2/2	partial	0.54 D
17	THF/H$_2$O 1:4	1.5 mL	Pd black[b]	4 h	1/2 – 2/2	partial	0.82 D
18	THF/H$_2$O 1:4	0.75 mL	Pd black[b]	4 h	1/2 – 2/2	partial	1.00 D
19	THF/H$_2$O 1:4	0.75 mL	Pd black[b]	24 h	2/2	total	0.92 D
20	THF/H$_2$O 1:4	0.75 mL	Pd black[b]	22.5 h	(1/2) 2/2	total	1.10 D

[a]Due to an impossibility to separate intermediate by HPLC, we were not able to properly quantify the different intermediates. [b]Deuterium labelling level was determined by HPLC-ESI-MS (positive mode).

The best conditions (entry 19, **Table 4**) were successfully repeated using tritium gas (**Scheme 16**). Labile activity was removed by evaporation / dissolution in water cycles. HPLC-MS analysis showed a 95% radiochemical purity as well as a high specific activity of 30.2 Ci/mmol (**Table 5**), which corresponds to a 1.04 tritium/molecule labelling. The total activity (239 mCi) was measured by a liquid scintillation counter. This translates to a production of 8 μmol of [^{3}H]**30** from 11 μmol of **29**. This 73% yield, lower than expected, is due to a partial loss of product during th evaporation of solvents.

Scheme 16. Preparation of [^{3}H]*m*-A$_2$pm.
(a) T$_2$ (1 atm), Pd black, THF/H$_2$O 1:4, 24h, rt.
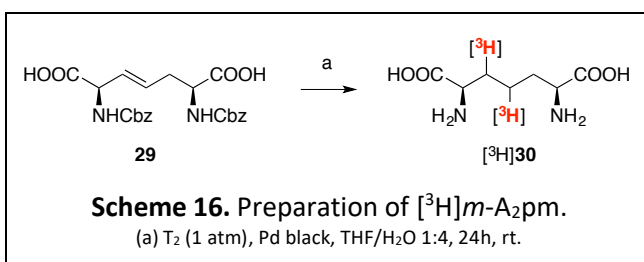
Table 5. Isotopic distribution of [^{3}H]**30** determined by HPLC-ESI-MS (positive mode).

	M+1	M+2	M+3 (1T)	M+4	M+5 (2T)	M+6
m/z	191	192	193	194	195	196
%area	0	1.5	45.9	-1.4	29.1	2.0
			1.04T/molecule		**30.2 Ci/mmol**	

III.4.d) Free (^{13}C)*m*-A$_2$pm synthesis

At an early stage of this work, a set of protecting groups (Fmoc carbamate, *t*-Bu ester, Cbz carbamate and Me ester) aiming to be the most versatile for the preparation of *m*-A$_2$pm-containing peptides and free *m*-A$_2$pm (see **section III.4.a**) was chosen. It is the reason why we settled on Fmoc carbamate and *tert*-butyl ester protecting groups for our AG synthons (both in ^{12}C and ^{13}C chemistry). Only two equivalents of VG were used for the cross-metathesis step whereas three were used in ^{12}C chemistry. Indeed, it was performed with commercial VG **10** prior to the development of our flow-chemistry synthesis as a cheap source of VG synthons.

Scheme 17. Preparation of free (^{13}C)*m*-A$_2$pm.

a) 1 equiv. (^{13}C)**16**, 2 equiv. **10**, 20 mol% Grubbs 2nd gen. cat., CH$_2$Cl$_2$, reflux, N$_2$, 66%; (b) HCl 2 mol/L, 1,4-dioxane, reflux, 86%; (c) H$_2$ (5 bars), Pd black, THF/H$_2$O 1:4, 41%.
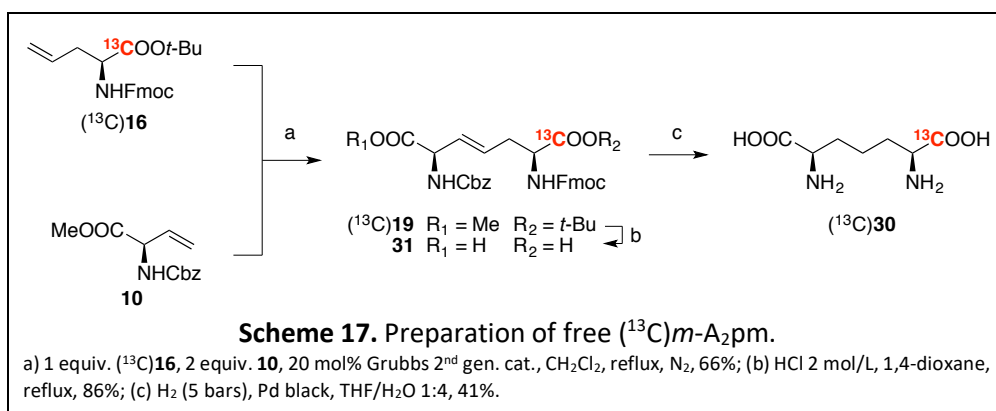
As mentioned earlier, this choice of protecting groups showed to be problematic for the preparation of tritiated free *m*-A$_2$pm. The last step required high pressures of hydrogen and long reaction times, both incompatible with a tritium catalytic reduction due to security policies, high amounts of radioactive waste and prohibitive cost. However, once both esters of (^{13}C)**19** cleaved using hydrochloric acid, we still managed to reduce and totally deprotect derivative (^{13}C)**31** in a single step under these conditions to afford (^{13}C)**30**. After a few hours, reduction doesn't evolve anymore. An extraction of the methylfluorene by-product (from Fmoc deprotection) in diethyl ether was necessary so this step could undergo completely. A loss of product during this extraction might explain the overall low 35% yield over the final two steps.

Mass spectrometry analysis of (^{13}C)**30** confirmed the carbon-13 substitution as expected (**Figure 7**). Some particularities of carbon-13 substituted compounds can be observed in ^{1}H NMR (^{13}C – H coupling) and ^{13}C-APT NMR (100 times more intense than usual peak for the substituted atom and C – C coupling provoking an inverted doublet for C_6 compared to the down oriented singlet for C_2).
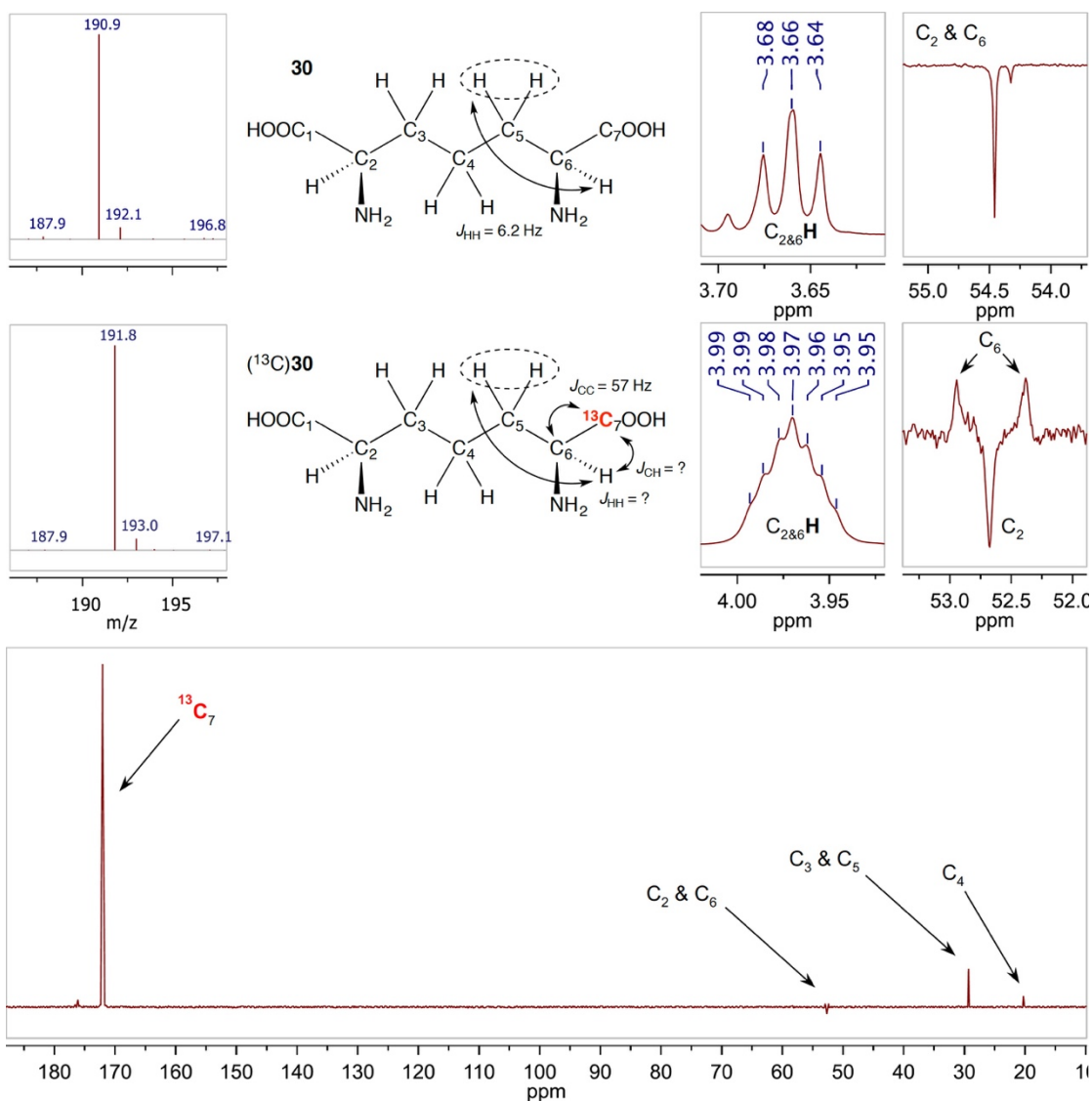
Figure 7. Comparison of **30** and (^{13}C)**30** NMR and mass spectra.

HPLC analysis of *o*-phthaldehyde/*N*-acetyl-L-cysteine derivatized (^{13}C)**30** showed similar diastereomeric ratio as those observed for **30** and (^{2}H$_2$)**30** (**Figure 8**). Here again, a higher proportion of (*S,S*) compound is observed even though chiral HPLC analysis of commercial (*R*)-VG **16** used in the cross metathesis step showed a 99% enantiomeric excess.

Figure 8. Chromatogram of OPA/NAC derivatized (^{13}C)**30**.
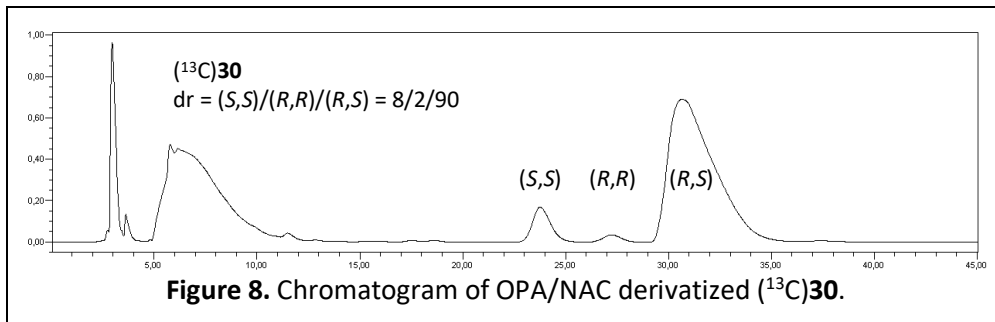
III.5. Peptide preparation

III.5.a) Solid-Phase Peptide Synthesis

To fully appreciate the complex chemical strategy of the present work, we will first remind the reader some basics of solid-phase peptide synthesis. Merrifield is considered as the father of this way of preparing peptides[103]. Before his groundbreaking work, chemists would have to couple amino acids in solution, usually with poor yields and extensive purifications after each coupling step. His idea is somewhat simple (and so most elegant): anchor the first amino acid onto a resin and grow it from there. This allows to use high excesses of reagent without any worries about purification as they are simply rinsed off the resin before the next step. Additions of new amino acids to the peptide chains consist of repeating the following sequence as many times as needed:

- Deprotect the anchored amino group of the resin or of the previous amino acid added onto the growing peptide;
- Rinse off deprotection agent;
- Add the next amino acid and coupling reagents;
- Rinse off excess of amino acid and coupling reagent.

Finally, the peptide is cleaved from the resin before a single purification step. Obviously, this sequence gets more complicated as complexity of the desired peptide arises.

Scheme 18. Peptide growth in SPPS.
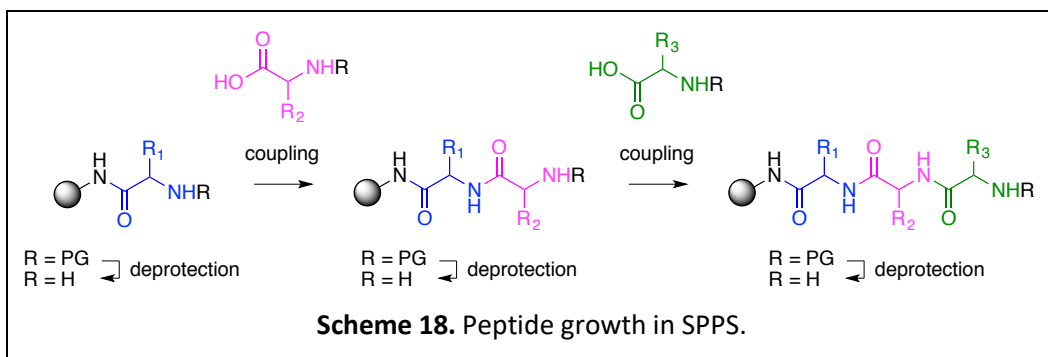
III.5.b) Protecting group choices

Fmoc SPPS strategy was chosen to prepare m-A$_2$pm and (^{2}H$_2$)m-A$_2$pm containing peptides as Fmoc carbamate provides a chromophore for HPLC monitoring. A nice perk of all the target peptides of this work is that they share a common stem: HO-D-Ala-m-A$_2$pm (**Scheme 19**). This means that a single common resin was needed. The Wang-D-Ala-NHFmoc resin was chosen based on Dr J. Simon's work[65]. In order to introduce m-A$_2$pm in the target peptides, this diamino diacid has to be fully protected except for the L side carboxylic acid function where the first coupling step with the functionalized resin should occur (R$_3$ = H). The second carboxylic acid is not implicated in any peptide bond and should stay protected during the whole synthesis. Thus, it was decided to protect it as a methyl ester in each differentially protected m-A$_2$pm synthesized (R$_1$ = Me). Remaining protecting groups differ depending on the target peptide and the substitution of the m-A$_2$pm they include.

Scheme 19. Target peptides.
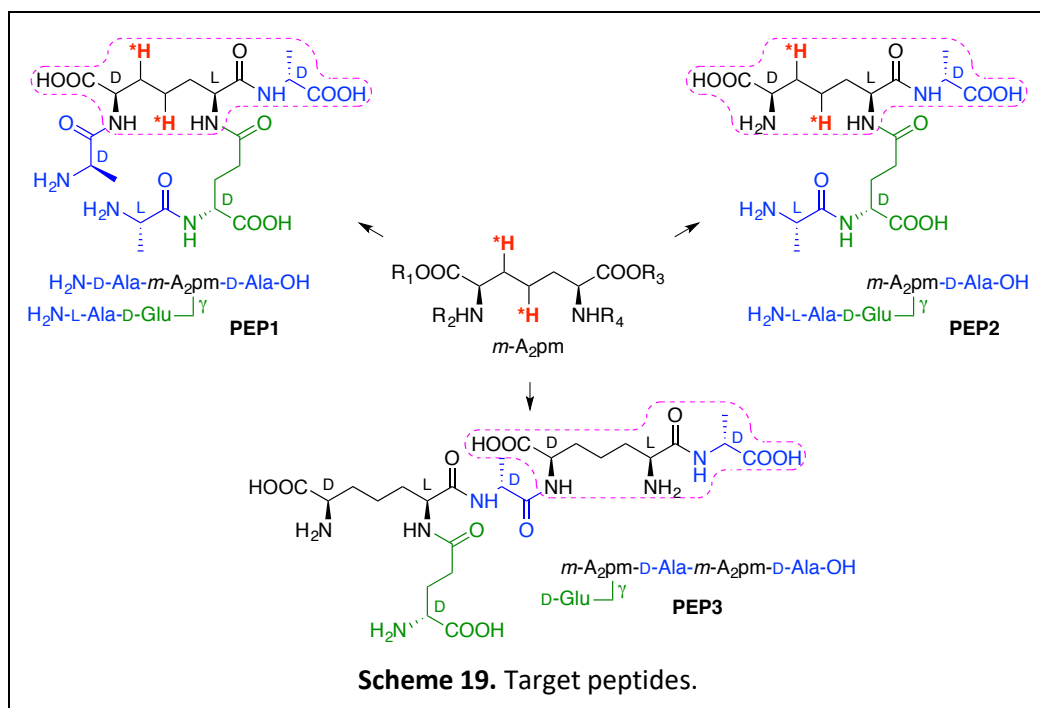
The most challenging target molecule is probably **PEP1** as its m-A$_2$pm is trisubstituted. In this case, the two amino groups should be independently deprotected to allow for the next couplings in SPPS (**Scheme 20**). One of these two amino groups has to be Fmoc protected for the first growth (R$_4$ = Fmoc). While the remaining amino protecting group has to withstand SPPS conditions and should be cleavable without releasing the growing peptide from the resin (R$_2$ = Cbz) before the addition of the final D-Ala.

Scheme 20. PEP1 and (^{2}H$_2$)**PEP1** m-A$_2$pm precursors **22** and (^{2}H$_2$)**22**.
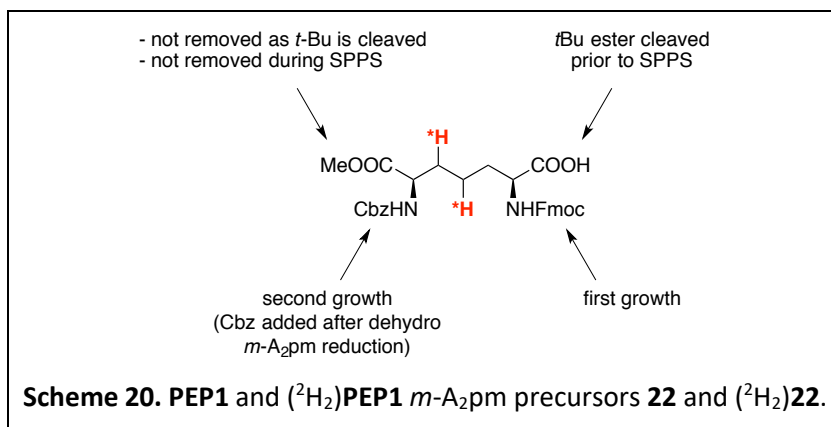
Although **PEP2** could be prepared using the same differentially protected m-A$_2$pm, it was decided to replace Cbz by Boc in order to avoid an additional step after deanchoring from the resin (**Scheme 21**).

Scheme 21. **PEP2**, (^{2}H$_2$)**PEP2** and **PEP3** m-A$_2$pm precursors **23** and (^{2}H$_2$)**23**.
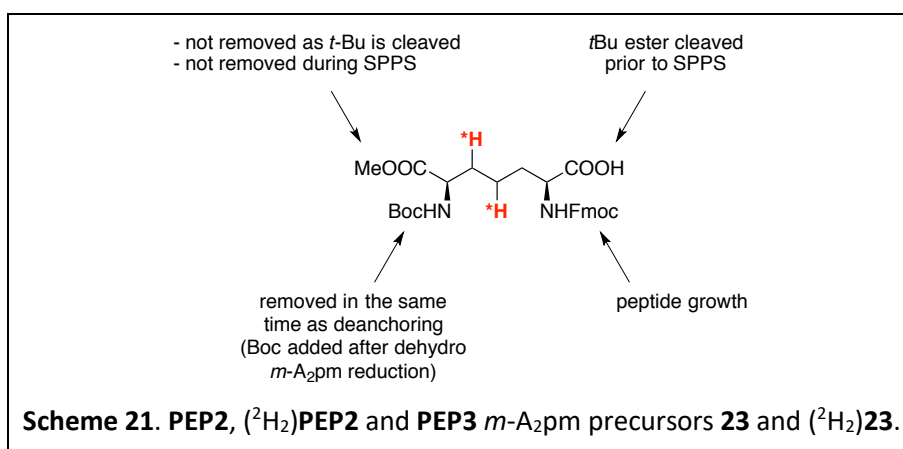
PEP3 is quite different from **PEP1** and **PEP2** as it contains two *m*-A$_2$pm. The first one had to be protected with a Fmoc on the D side amino group as it is from that function that the peptide has to grow (**Scheme 22**). The remaining amino group was Boc protected to be cleaved in the same time as deanchoring from the resin (R$_4$ = Boc). The second *m*-A$_2$pm is the same as the one used for **PEP2**.

- not removed as *t*-Bu is cleaved
- not removed during SPPS

*t*Bu ester cleaved
prior to SPPS

MeOOC, COOH

FmocHN   NHBoc

peptide growth

removed in the same
time as deanchoring
(Boc added after dehydro
m-A$_2$pm reduction)

Scheme 22. **PEP3** *m*-A$_2$pm precursor **27**.
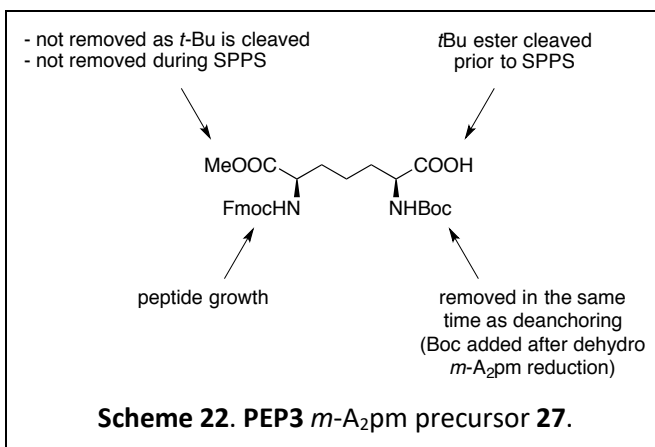
III.5.c) Peptides synthesis

Synthesis of **PEP1** and (^{2}H$_2$)**PEP1** started with the growth of Wang-D-Ala-*m*-A$_2$pm-γ-D-Glu-L-Ala and Wang-D-Ala-(^{2}H$_2$)*m*-A$_2$pm-γ-D-Glu-L-Ala moieties using protected *m*-A$_2$pm **22** and (^{2}H$_2$)**22** respectively (**Scheme 23**). Unfortunately, no way to cleave the Cbz carbamate while keeping the peptide anchored to the resin was found. So, it was decided to stop these syntheses at this point and to cleave **32** and (^{2}H$_2$)**32** from the resin for analysis. These compounds could be deprotected to afford **PEP2** and (^{2}H$_2$)**PEP2** by catalytic reduction (Cbz removal), LiOH treatment (methyl ester cleavage) and a final treatment using polystyrene-supported piperazine (Fmoc removal).

Scheme 23. Aborted synthesis of **PEP1** and (^{2}H$_2$)**PEP1**.
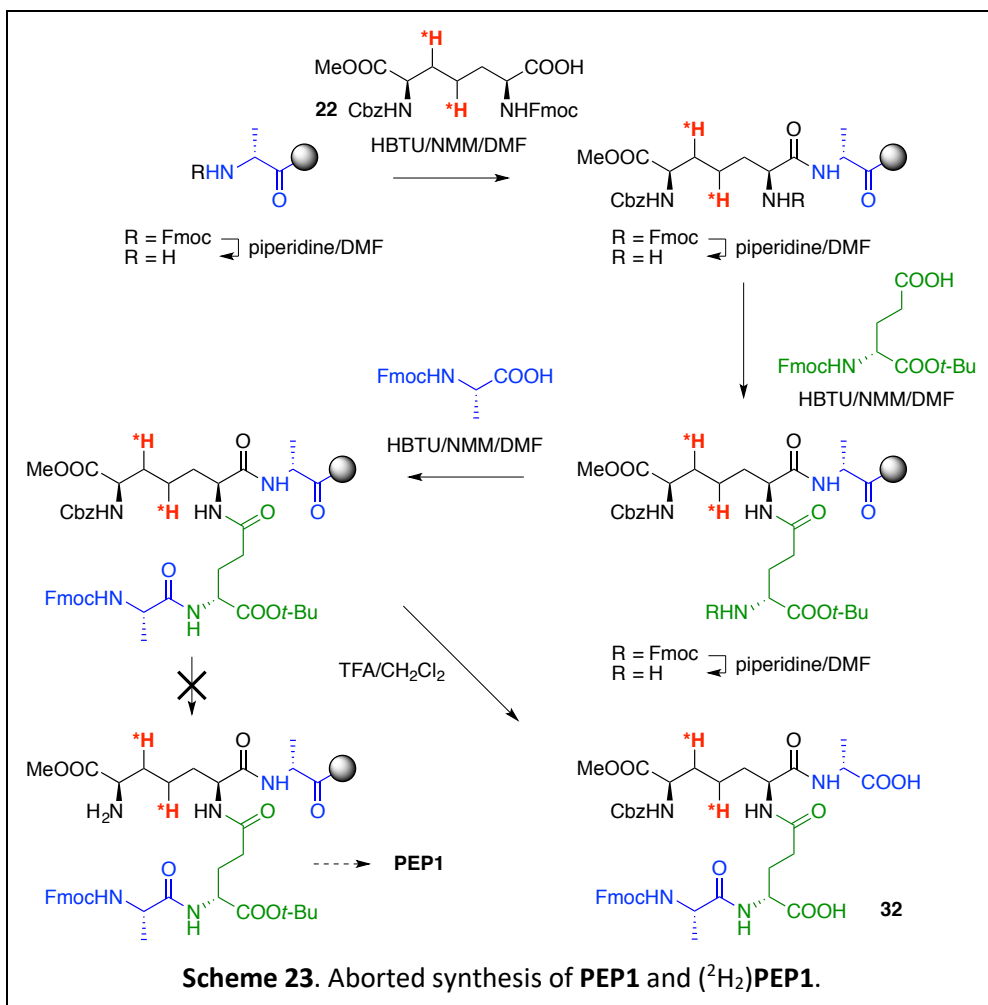
Mass spectrometry and NMR analyses of these two protected peptides confirmed their structures and the deuterium substitution of $(^2H_2)$**32**. **Figure 9** highlights the 2 unit shift in mass spectra and phase inversion between CH_2s and CHDs in HSQC spectra of **32** and $(^2H_2)$**32**. If the deuterium substitution of the dashed circled position of the m-A_2pm residue makes no doubt, the difference between chemical shifts of the two $CH_{2\beta}$s of the m-A_2pm residue (solid circle) is too weak to be absolutely sure of the second deuterium substitution position.

Figure 9. Comparison of **32** and $(^2H_2)$**32** mass and HSQC spectra.
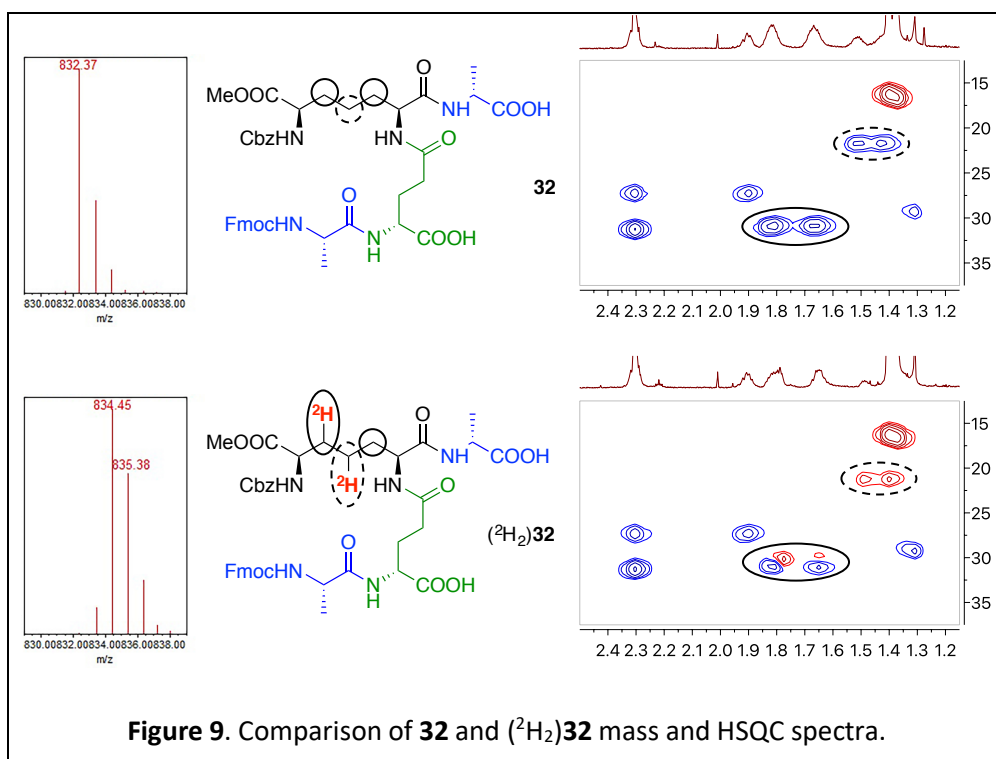
Rather than to deprotect **32** and $(^2H_2)$**32** to afford **PEP2** and $(^2H_2)$**PEP2**, new syntheses using protected m-A_2pm **23** and $(^2H_2)$**23** were performed to test their incorporation in SPPS.

PEP2 syntheses using protected *m*-A$_2$pm **23** and (^{2}H$_2$)**23** are nearly identical to the previous ones except that no catalytic reduction is required to cleave a Cbz carbamate thanks to its replacement by a Boc protection. A TFA treatment simultaneously deanchored the growing peptides from resin and cleaved Boc protecting group to afford **33** and (^{2}H$_2$)**33** (**Scheme 24**). Final deprotections depicted in **Scheme 24** remains to be investigated.

Scheme 24. Synthesis of **PEP2** and (^{2}H$_2$)**PEP2**.
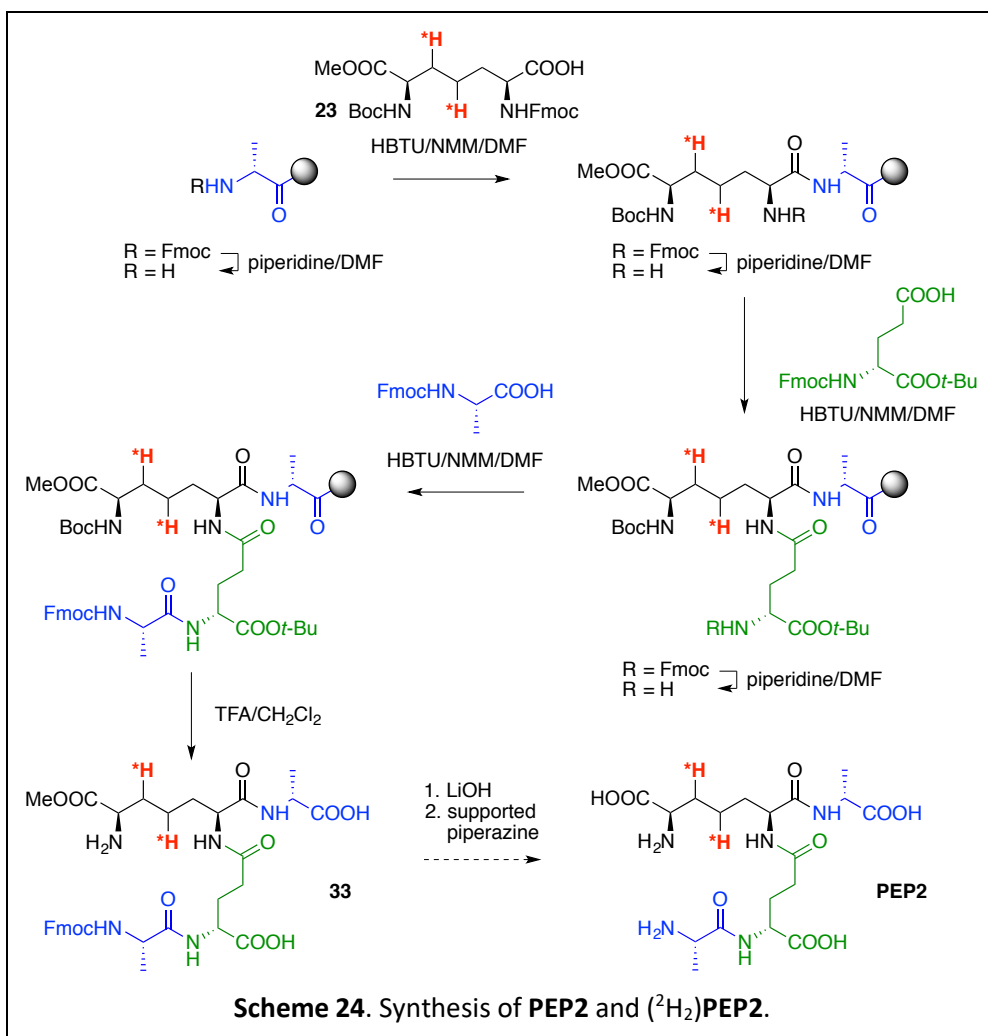
Mass spectrometry and NMR analyses confirmed the peptides structures and deuterium substitution of (^{2}H$_2$)**33**. **Figure 10** highlights the 2 units shift in mass spectra and the phase inversion between CH$_2$s and CHDs in HSQC spectra of **32** and (^{2}H$_2$)**32**. Contrary to the previous spectra, chemical shifts of the two CH$_{2\beta}$s of the *m*-A$_2$pm residue are now different enough to confirm positions of the two deuterium substitutions.

Figure 10. Comparison of **33** and (^{2}H$_2$)**33** mass and HSQC spectra.
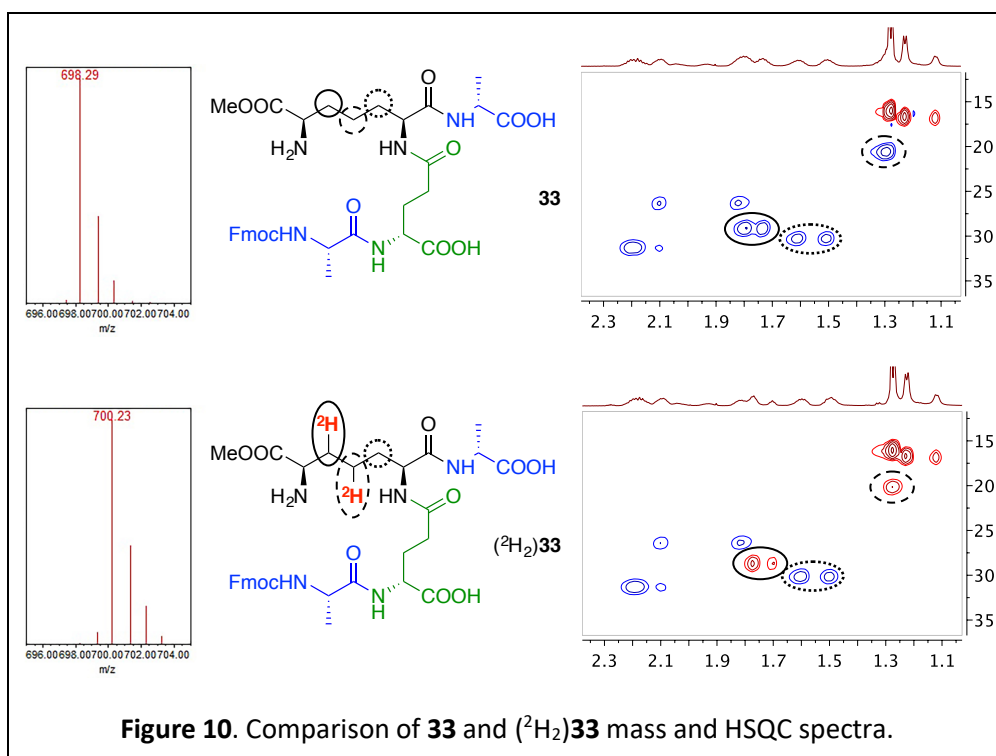
Unfortunately, shortage of time did not allow us to perform a **PEP3** SPPS test but the successful incorporations of **22** and **23** in SPPS are encouraging.

Chapter IV

Conclusion

The goal of our work was to develop a synthesis of several peptide fragments responsible for the reticulation between glycan strands in the bacterial peptidoglycan. The target fragments ranged from the *meso*-diaminopimelic acid (*m*-A$_2$pm) by itself to peptides containing this particular diamino diacid (**Scheme 1** and **2**).

Scheme 1. Target *meso*-diaminopimelic acids
30, (^{2}H$_2$)**30**, [^{3}H]**30** and (^{13}C)**30**.

Scheme 2. Target peptides **PEP1**, (^{2}H$_2$)**PEP1**, **PEP2**, (^{2}H$_2$)**PEP2** and **PEP3**.
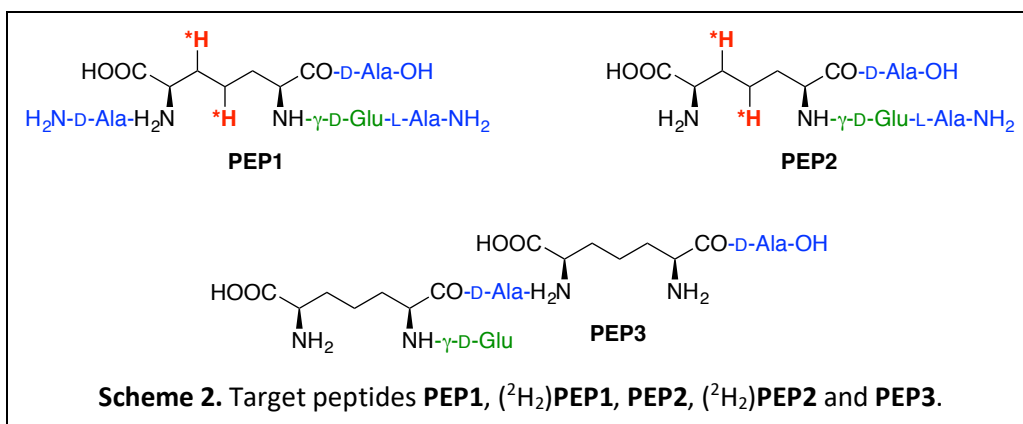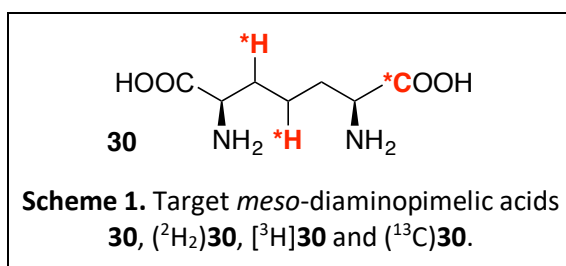
Being specific of the bacterial peptidoglycan, key compound *m*-A$_2$pm **30** is a perfect probe for the study of the different aspects of peptidoglycan metabolism such as its turnover and recycling. Deuterated and tritiated *m*-A$_2$pm, (^{2}H$_2$)**30** and [^{3}H]**30**, will be especially useful in this field. Carbon-13 substituted *m*-A$_2$pm (^{13}C)**30** will be used in solid NMR experiments aiming to establish the 3D structure of peptidoglycan *sacculi*.

Variety in the target molecules called for a versatile strategy. This is why Chowdhury's cross metathesis between a vinylglycine synthon and an allylglycine synthon was used as the key step of this work (**Scheme 3**). This gave us control over stereochemistry and the opportunity to independently protect each amino and carboxylic acid groups.

Scheme 3. Cross-metathesis key step.
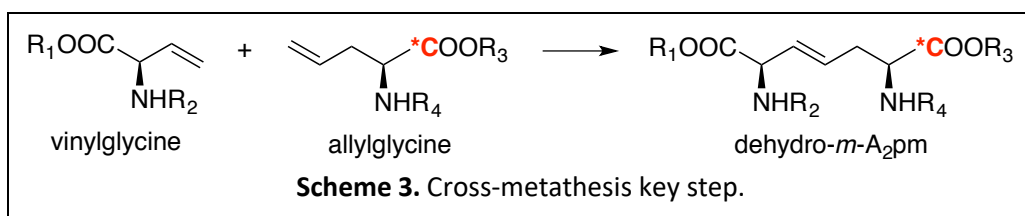
We developed an innovative scale-independent continuous-flow method of preparation of vinylglycine derivatives which allowed us to synthesize two protected vinylglycine synthons **16** and **18** (**Scheme 4**). This convenient method was used to provide large quantities (5 to 10 g scale) of these building blocks. The development of this method was published in *Organic & Biomolecular Chemistry* in 2015[95] and offers a scale-independent alternative to thermolyses performed in batch or Kugelrohr apparatus.

Scheme 4. Continuous flow synthesis of vinylglycine synthons **16** and **18**.
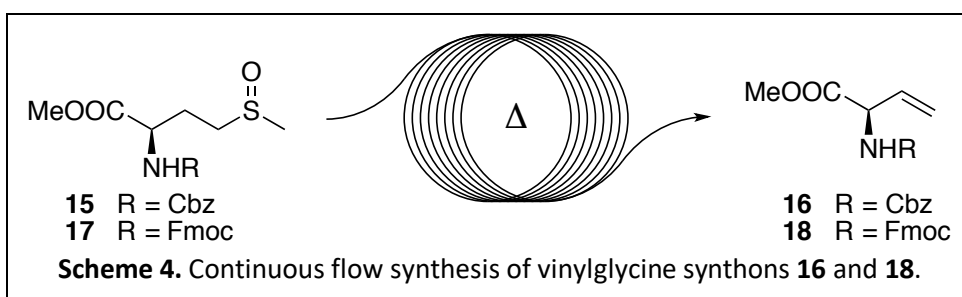
Three protected allylglycines **10**, (^{13}C)**10** and **11** were enantioselectively synthesized in large quantities using phase transfer catalyzed alkylation of a Schiff base **8**. Carbon-13 substituted Schiff base (^{13}C)**8** necessary to the synthesis of (^{13}C)**10** was prepared on a several grams scale from (1-^{13}C)glycine (**Scheme 5**).

Scheme 5. Synthesis of allylglycine synthons **10**, (^{13}C)**10** and **11**.
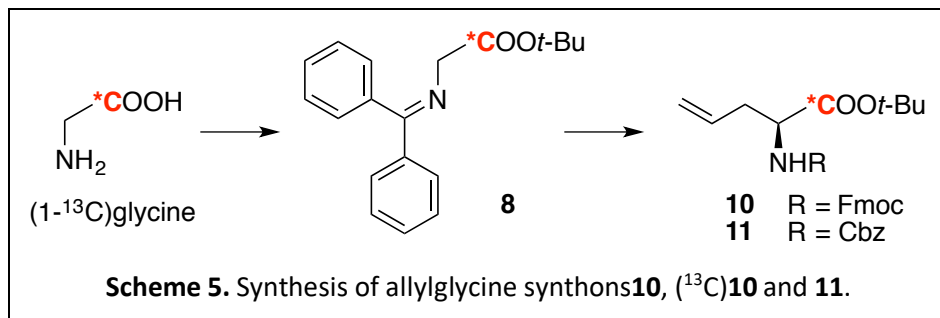
Cross-metathesis between these synthons led to the formation of four dehydro-*m*-A$_2$pm (**19**, (^{13}C)**19**, **24** and **28**). These compounds gave us access to four free *m*-A$_2$pm and five differentially protected *m*-A$_2$pm.

Scheme 6. Cross-metatheses.
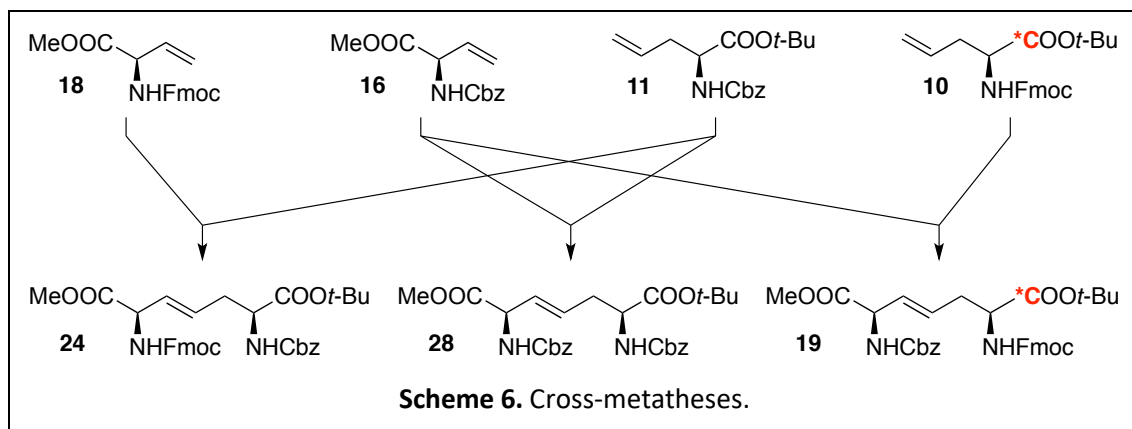
We highly optimized the preparation of natural *m*-A$_2$pm **30** in view of the total synthesis of selectively substituted (^{13}C)*m*-A$_2$pm (^{13}C)**30**. This 10 consecutive steps synthesis starting from commercial (1-^{13}C)glycine (^{13}C)**1** was completed with an overall 12% yield with a purity and a selectivity unreachable by enzymatic methods (**Scheme 7**).

Scheme 7. Total synthesis of (^{13}C)*m*-A$_2$pm (^{13}C)**30**.
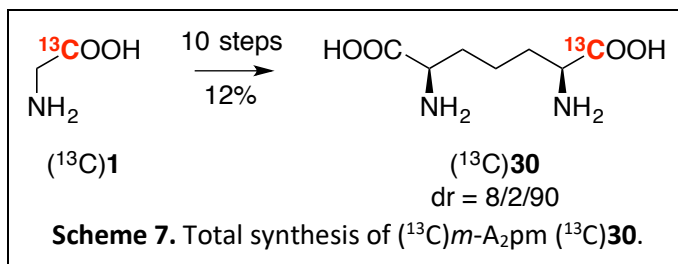
The key dehydro-*m*-A$_2$pm derivative **28** was deprotected and reduced into target molecules *m*-A$_2$pm **30** and (^{2}H$_2$)*m*-A$_2$pm (^{2}H$_2$)**30** without the need for any chromatographic purification (**Scheme 8**). The total synthesis of these two compounds required 6 steps for an overall 21% yield.

After some optimization to ensure compatibility with tritium imperatives, we were able to synthesize 239 mCi of tritiated *m*-A$_2$pm [^{3}H]**30** with a high specific activity (30.2 Ci/mmol) and a 95% radiochemical purity. This compound has been missing from the biochemist toolbox for the last few years. The quantity synthesized during this work will fulfill needs of tritiated *m*-A$_2$pm for years to come and we have some more precursor ready for future productions. We are glad to report that two laboratories have already expressed their interest in this compound (**Scheme 8**).

Scheme 8. Synthesis of *meso*-diaminopimelic acids **30**, (^{2}H$_2$)**30**, [^{3}H]**30**.
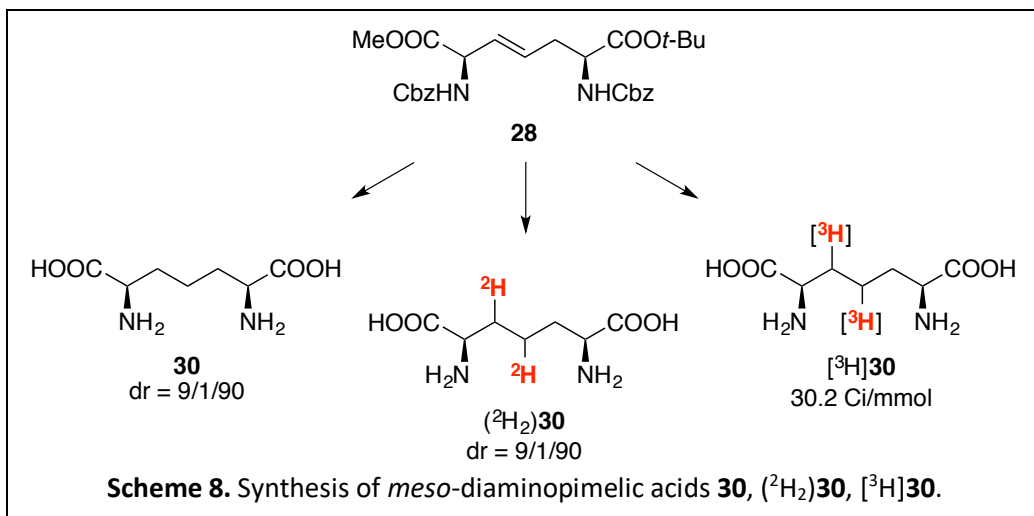
The versatility induced by our choice of a cross-metathesis key step allowed us to synthesize five differentially protected *m*-A$_2$pm (**22**, (^{2}H$_2$)**22**, **23**, (^{2}H$_2$)**23** and **27**, **Scheme 9**) from dehydro-*m*-A$_2$pm **19** and **24** in view of their introduction in solid-phase peptide synthesis.

Scheme 9. Protected *m*-A$_2$pm (**22**, (^{2}H$_2$)**22**, **23**, (^{2}H$_2$)**23** and **27**
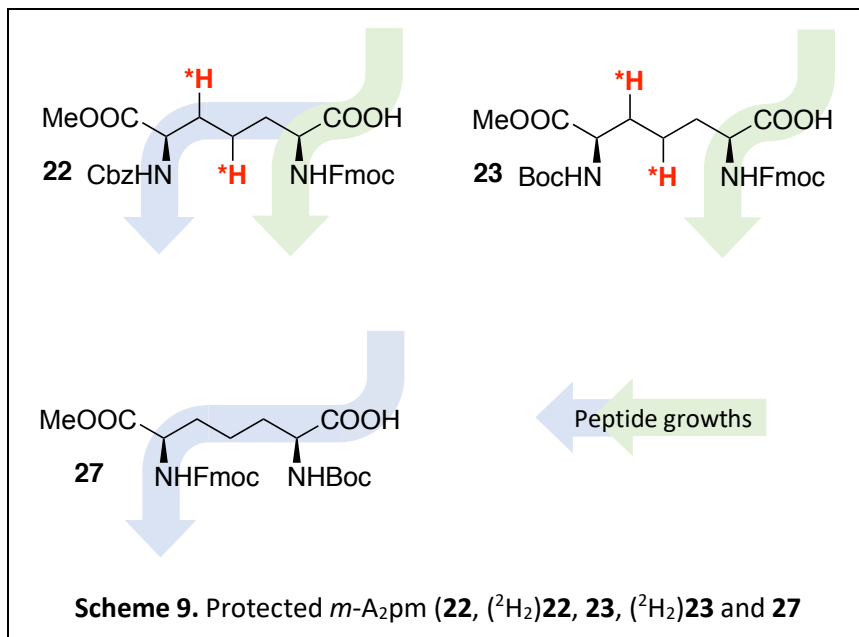
These compounds offer a platform for the preparation of peptides including *m*-A$_2$pm substituted in different positions. Four of these were successfully introduced in peptides which remain to be totally deprotected. The preparation of peptidoglycan fragments containing a trisubstituted *m*-A$_2$pm residue remains possible but a deeper investigation over protecting groups choice still has to be done.

Once deprotected, the target peptides will be used as chromatography or mass spectrometry references (in the case of deuterated peptides) for the study of β-lactamase induction phenomenon in penicillin resistant bacteria (**PEP2**) and as substrate for enzymatic and crystallography studies of penicillin-binding proteins involved in the peptidoglycan metabolism (**PEP1** and **PEP3**). All these compounds are currently unreachable via peptidoglycan digestion and their chemical synthesis will open new opportunities for the study of the human innate immune system.

Chapter V

References

1. Campbell NA, Reece JB, Urry LA, et al. *Campbell Biology*. Pearson; 2014.
2. Dougherty TJ, Pucci MJ. *Antibiotic Discovery and Development*.; 2014. doi:10.1007/978-1-4614-1400-1
3. Fleming A. On the antibacterial action of cultures of a penicillium, with special reference to their use in the isolation of B. influenzae. *Br J Exp Pathol*. 1929;10(3):226-236. doi:10.1093/clinids/2.1.129
4. Zifan A. Structure and contents of a typical gram-positive bacterial cell. https://en.wikipedia.org/wiki/Bacteria#/media/File:Prokaryote_cell.svg. Published 2015.
5. Prescott LM, Klein PH. *Microbiology*. 5th ed.; 2002.
6. Holtje J V. Growth of the stress-bearing and shape-maintaining murein sacculus of Escherichia coli. *Microbiol Mol Biol Rev*. 1998;62(1):181-203.
7. Vollmer W, Blanot D, De Pedro MA. Peptidoglycan structure and architecture. *FEMS Microbiol Rev*. 2008;32(2):149-167. doi:10.1111/j.1574-6976.2007.00094.x
8. Mengin-Lecreulx D, Lemaitre B. Structure and metabolism of peptidoglycan and molecular requirements allowing its detection by the Drosophila innate immune system. *J Endotoxin Res*. 2005;11(2):105-111. doi:10.1179/096805105X35233
9. Lazar K, Walker S. Substrate analogues to study cell-wall biosynthesis and its inhibition. *Curr Opin Chem Biol*. 2002;6(6):786-793. doi:10.1016/S1367-5931(02)00355-1
10. Heijenoort J van. Recent advances in the formation of the bacterial peptidoglycan monomer unit (1985 to 2000). *Nat Prod Rep*. 2001;18(5):503-519. doi:10.1039/a804532a
11. Heijenoort J van. Biosynthesis of bacterial peptidoglycan. In: *Microbial Glycobiology*. ; 2010:287-304.
12. Chung BC, Zhao J, Gillespie RA, et al. Crystal Structure of MraY, an Essential Membrane Enzyme for Bacterial Cell Wall Synthesis. *Science*. 2013;341(August):1012-1016.
13. Mohammadi T, Van Dam V, Sijbrandi R, et al. Identification of FtsW as a transporter of lipid-linked cell wall precursors across the membrane. *EMBO J*. 2011;30(8):1425-1432. doi:10.1038/emboj.2011.61
14. Sham L-T, Butler EK, Lebar MD, Kahne D, Bernhardt TG, Ruiz N. MurJ is the flippase of lipid-linked precursors for peptidoglycan biogenesis. *Science*. 2014;345(6193):220-222. doi:10.1109/TMI.2012.2196707.Separate
15. Heijenoort J v. Formation of the glycan chains in the synthesis of bacterial peptidoglycan. *Glycobiology*. 2001;11(3):25R-36R. doi:10.1093/glycob/11.3.25R
16. Zapun A, Contreras-Martel C, Vernet T. Penicillin-binding proteins and β-lactam resistance. *FEMS Microbiol Rev*. 2008;32:361-385. doi:10.1111/j.1574-6976.2007.00095.x

17. Sauvage E, Kerff F, Terrak M, Ayala JA, Charlier P. The penicillin-binding proteins: Structure and role in peptidoglycan biosynthesis. *FEMS Microbiol Rev*. 2008;32(2):234-258. doi:10.1111/j.1574-6976.2008.00105.x

18. González-Leiza SM, de Pedro MA, Ayala JA. Amph, a bifunctional DD-endopeptidase and DD-carboxypeptidase of Escherichia coli. *J Bacteriol*. 2011;193(24):6887-6894. doi:10.1128/JB.05764-11

19. Atrih A, Bacher G, Allmaier G, Williamson MP, Foster SJ. Analysis of Peptidoglycan Structure from Vegetative Cells of. *J Bacteriol*. 1999;181(13):3956-3966.

20. Patti GJ, Sung JK, Schaefer J. Characterization of the peptidoglycan of vancomycin-susceptible Enterococcus faecium. *Biochemistry*. 2008;47(32):8378-8385. doi:10.1021/bi8008032

21. Reith J, Mayer C. Peptidoglycan turnover and recycling in Gram-Positive bacteria. *Appl Microbiol Biotechnol*. 2011;92(1):1-11. doi:10.1007/s00253-011-3486-x

22. Goodell EW, Schwarz U. Release of cell wall peptides into culture medium by exponentially growing Escherichia coli. *J Bacteriol*. 1985;162(1):391-397.

23. Johnson JW, Fisher JF, Mobashery S. Bacterial cell-wall recycling. *Ann N Y Acad Sci*. 2013;1277(1):54-75. doi:10.1111/j.1749-6632.2012.06813.x

24. Vollmer W, Joris B, Charlier P, Foster S. Bacterial peptidoglycan (murein) hydrolases. *FEMS Microbiol Rev*. 2008;32(2):259-286. doi:10.1111/j.1574-6976.2007.00099.x

25. Borisova M, Gaupp R, Duckworth A, et al. Peptidoglycan recycling in gram-positive bacteria is crucial for survival in stationary phase. *MBio*. 2016;7(5):1-10. doi:10.1128/mBio.00923-16

26. Keestra-Gounder AM, Tsolis RM. NOD1 and NOD2: Beyond Peptidoglycan Sensing. *Trends Immunol*. 2017;xx:1-10. doi:10.1016/j.it.2017.07.004

27. Wolf AJ, Underhill DM. Peptidoglycan recognition by the innate immune system. *Nat Rev Immunol*. 2018. doi:10.1038/nri.2017.136

28. Hysi P, Kabesch M, Moffatt MF, et al. NOD1 variation, immunoglobulin E and asthma. *Hum Mol Genet*. 2005;14(7):935-941. doi:10.1093/hmg/ddi087

29. Hugot JP, Chamaillard M, Zouali H, et al. Association of NOD2 leucine-rich repeat variants with susceptibility to Crohn's disease. *Nature*. 2001;411(6837):599-603. doi:10.1038/35079107

30. Ogura Y, Bonen DK, Inohara N, et al. A frameshift mutation in NOD2 associated with susceptibility to Crohn's disease. *Nature*. 2001;411(6837):603-606. doi:10.1038/35079114

31. Kohanski MA, Dwyer DJ, Collins JJ. How antibiotics kill bacteria: From targets to networks. *Nat Rev Microbiol*. 2010;8(6):423-435. doi:10.1038/nrmicro2333

32. Bugg TDH, Braddick D, Dowson CG, Roper DI. Bacterial cell wall assembly: Still an attractive antibacterial target. *Trends Biotechnol*. 2011;29(4):167-173. doi:10.1016/j.tibtech.2010.12.006

33. Ventola CL. The antibiotic resistance crisis: part 1: causes and threats. *P T A peer-reviewed J Formul Manag*. 2015;40(4):277-283. doi:Article

34. Alanis AJ. Resistance to antibiotics: Are we in the post-antibiotic era? *Arch Med Res*. 2005;36(6):697-705. doi:10.1016/j.arcmed.2005.06.009

35. Falagas ME, Bliziotis IA. Pandrug-resistant Gram-negative bacteria: the dawn of the post-antibiotic era? *Int J Antimicrob Agents*. 2007;29(6):630-636. doi:10.1016/j.ijantimicag.2006.12.012

36. Domínguez-Gil T, Molina R, Alcorlo M, Hermoso JA. Renew or die: The molecular mechanisms of peptidoglycan recycling and antibiotic resistance in Gram-negative pathogens. *Drug Resist Updat*. 2016;28:91-104. doi:10.1016/j.drup.2016.07.002

37. Yılmaz, Özcengiz G. Antibiotics: Pharmacokinetics, toxicity, resistance and multidrug efflux pumps. *Biochem Pharmacol*. 2017;133:43-62. doi:10.1016/j.bcp.2016.10.005

38. Abraham EP, Chain E. An Enzyme from Bacteria able to Destroy Penicillin. *Nature*. 1940;146(3713):837-837. doi:10.1038/146837a0

39. Amoroso A, Boudet J, Berzigotti S, et al. A peptidoglycan fragment triggers β-lactam resistance in Bacillus licheniformis. *PLoS Pathog*. 2012;8(3). doi:10.1371/journal.ppat.1002571

40. Finlayson AJ, Simpson FJ. The conversion of 2,6-diaminopimelic acid-1,7-C14 to lysine 1-C14. 1961;39:1551.

41. Hanus J, Veres K. The synthesis of specifically 14C-labelled 2,6-diaminopimelic acid and its higher homologues. *J Labelled Compd*. 1970;6(2):143-149. doi:10.1002/jlcr.2590060205

42. Hanus J, Veres K. Preparation of tritium labelled D,L-2,6-diaminopimelic acid. *J Labelled Compd*. 1971;7(4):425-430. doi:10.1002/jlcr.2590070406

43. Tanizawa K, Yoshimura T, Asada Y, Sawada S, Misono H, Soda K. Stereochemistry of Proton Abstraction Catalyzed by Lysine and Ornithine w-Aminotransferases. *Biochemistry*. 1982;21(5):1104-1108.

44. Kelland JG, Palcic MM, Pickard MA, Vederas JC. Stereochemistry of Lysine Formation by meso-Diaminopimelate Decarboxylase from Wheat Germ: Use of 1H-13C NMR Shift Correlation To Detect Stereospecific Deuterium Labeling. *Biochemistry*. 1985;24:3263-3267.

45. Roth P, Hädener A, Tamm C. Further Studies on the Biosynthesis of Tabtoxin (Wildfire Toxin): Incorporation of [2,3-13C2]Pyruvate into the Beta-Lactam Moiety. *Helv Chim Acta*. 1990;73:476-482.

46. Schott D, Rousseau B, Beaucourt JP, Lellouche JP, Pichat L. Préparation de l'acide méso diamino-2,6 heptane-dioique-1,7-[3H-3,4,5] (méso-diamino pimélique-[3H-3,4,5]). *J Label Compd Radiopharm*. 1985;22(2):127-133.

47. Roten C-AH, Pagni P, Margot P, Touri F, Karamata D. Specific Labeling of Diaminopimelate: A Radioassy for the Determination of the Peptidoglycan Cross-Linking Index. *Anal Biochem*. 1994;223:208-211.

48. Jurgens AR. Asymmetric synthesis of differentially protected meso-2,6-diaminopimelic acid. *Tetrahedron Lett*. 1992;33(33):4727-4730.

49. Garner P, Park JM. The Synthesis and Configurational Stability of Differentially Protected β-Hydroxy-α-amino Aldehydes. *J Org Chem*. 1987;52(12):2361-2364. doi:10.1021/jo00388a004

50. Chen PT, Lin CK, Tsai CJ, et al. Expeditious synthesis of enantiopure, orthogonally protected bis-α-amino acids (OPBAAs) and their use in a study of Nod1 stimulation. *Chem Asian J*. 2015;10(2):474-482. doi:10.1002/asia.201403173

51. Holcomb RC, Schow S, Powell D. An symmetric synthesis of diffrentially protected meso-2,6-diaminopimelic acid. *Tetrahedron Lett*. 1994;35(38):7005-7008.

52. Wang W, Xiong C, Yang J, Hruby VJ. An Efficient Synthesis of (2S,6S)- and meso-Diaminopimelic Acids via Asymmetric Hydrogenation. *Synthesis*. 2002:94-98.

53. Hernández N, Martín VS. General stereoselective synthesis of chemically differentiated α-diamino acids: Synthesis of 2,6-diaminopimelic and 2,7-diaminosuberic acids. *J Org Chem*. 2001;66(14):4934-4938. doi:10.1021/jo0155714

54. Katsuki T, Martin VS. Asymmetric Epoxidation of Allylic Alcohols: the Katsuki-Sharpless Epoxidation Reaction. *Org React*. 1996:1-299. doi:10.1002/0471264180.or048.01

55. Kawasaki A, Karasudani Y, Otsuka Y, et al. Synthesis of diaminopimelic acid containing peptidoglycan fragments and tracheal cytotoxin (TCT) and investigation of their biological functions. *Chem Eur J*. 2008;14(33):10318-10330. doi:10.1002/chem.200801121

56. Blakemore PR, Cole WJ, Kocieński PJ, Morley A. A Stereoselective Synthesis of *trans* -1,2-Disubstituted Alkenes Based on the Condensation of Aldehydes with Metallated 1-Phenyl-1 *H* -tetrazol-5-yl Sulfones. *Synlett*. 1998;1998(1):26-28. doi:10.1055/s-1998-1570

57. Del Valle JR, Goodman M. An efficient RCM-based synthesis of orthogonally protected meso-DAP and FK565. *J Org Chem*. 2004;69(25):8946-8948. doi:10.1021/jo0485738

58. Saito Y, Yoshimura Y, Wakamatsu H, Takahata H. A facile synthesis of fully protected meso-diaminopimelic acid (DAP) and its application to the preparation of lipophilic N-Acyl iE-DAP. *Molecules*. 2013;18(1):1162-1173. doi:10.3390/molecules18011162

59. Chowdhury AR, Boons GJ. The synthesis of diaminopimelic acid containing peptidoglycan fragments using metathesis cross coupling. *Tetrahedron Lett*. 2005;46(10):1675-1678. doi:10.1016/j.tetlet.2005.01.062

60. Paradisi F, Porzi G, Sandri S. A new stereocontrolled synthesis of uncommon tripeptides derived from 2,6-diaminopimelic acid (2,6-DAP). *Tetrahedron Asymmetry*. 2001;12(23):3319-3324. doi:10.1016/S0957-4166(02)00002-2

61.   Kubasch N, Schmidt RR. Synthesis of muramyl peptides containing meso-diaminopimelic acid. *Eur J Org Chem*. 2002:2710-2726. doi:10.1002/1099-0690(200208)2002:16<2710::AID-EJOC2710>3.0.CO;2-8

62.   Kumar S, Chowdhury AR, Ember B, et al. Selective recognition of synthetic lysine and meso-diaminopimelic acid-type peptidoglycan fragments by human peptidoglycan recognition proteins 1α and S. *J Biol Chem*. 2005;280(44):37005-37012. doi:10.1074/jbc.M506385200

63.   Teller N. Synthèse et évaluation biologique de dérivés de l'acide meso-diaminopimélique. 2009.

64.   Mercier F, Zervosen A, Teller N, et al. 1,6-AnhMurNAc derivatives for assay development of amidase AmiD. *Bioorganic Med Chem*. 2010;18(21):7422-7431. doi:10.1016/j.bmc.2010.09.010

65.   Simon JF, Lamborelle N, Zervosen A, Lemaire C, Joris B, Luxen A. Development of solid-supported methodology for the preparation of peptidoglycan fragments containing (2S,6R)-diaminopimelic acid. *Tetrahedron Lett*. 2015;57(14):1572-1575. doi:10.1016/j.tetlet.2016.02.098

66.   Maruoka K, Ooi T. Enantioselective amino acid synthesis by chiral phase-transfer catalysis. *Chem Rev*. 2003;103(8):3013-3028. doi:10.1021/cr020020e

67.   O'Donnell MJ, Boniece JM, Earp SE. The synthesis of amino acids by phase-transfer reactions. *Tetrahedron Lett*. 1978;19(30):2641-2644. doi:10.1016/S0040-4039(01)91563-1

68.   O'Donnell MJ, Bennett WD, Bruder WA, et al. Acidities of Glycine Schiff Bases and Alkylation of Their Conjugate Bases. *J Am Chem Soc*. 1988;110(25):8520-8525. doi:10.1021/ja00233a031

69.   Neises B, Steglich W. Simple Method for the Esterification of Carboxylic Acids. *Angew Chemie*. 1978;90(7):556-557.

70.   Ressel H-J. Process for the preparation of a benzophenone glycine imine alkyl ester derivative. 2008.

71.   Antoni G, Langström B. Synthesis of racemic [3-11C]-labelled alanine, 2-aminobutyric acid, norvaline, norleucine, leuncine and phenylalanine and preparation of L-[3-11C]alanine and L-[3-11C]phenylalanine. *J Label Compd Radiopharm*. 1987;24(2):125-143.

72.   Siebum AHG, Woo WS, Lugtenburg J. Preparation and Characterization of [5-13C]-(2S,4R)-Leucine and [4-13C]-(2S,3S)-Valine– Establishing Synthetic Schemes to Prepare Any Site-Directed Isotopomer ofL-Leucine,L-Isoleucine andL-Valine. *European J Org Chem*. 2003;2003(23):4664-4678. doi:10.1002/ejoc.200300410

73.   Denoël T, Zervosen A, Lemaire C, et al. Enantioselective synthesis of α-benzylated lanthionines and related tripeptides for biological incorporation into E. coli peptidoglycan. *Org Biomol Chem*. 2014;12(48):9853-9863. doi:10.1039/C4OB01476F

74. Libert LC, Franci X, Plenevaux AR, et al. Production at the Curie level of no-carrier-added 6-18F-fluoro-L-dopa. *J Nucl Med*. 2013;54(7):1154-1161. doi:10.2967/jnumed.112.112284

75. Lemaire C, Libert L, Franci X, et al. Automated production at the curie level of no-carrier-added 6-[18 F]fluoro-l-dopa and 2-[18 F]fluoro-l-tyrosine on a FASTlab synthesizer. *J Label Compd Radiopharm*. 2015;58(7):281-290. doi:10.1002/jlcr.3291

76. Becker G, Bahri MA, Michel A, et al. Comparative assessment of 6-[18F]fluoro-L-m-tyrosine and 6-[18F]fluoro-L-dopa to evaluate dopaminergic presynaptic integrity in a Parkinson's disease rat model. *J Neurochem*. 2017;141(4):626-635. doi:10.1111/jnc.14016

77. Lygo B, Wainwright PG. Phase-transfer catalysed asymmetric epoxidation of enones using N- anthracenylmethyl-substituted cinchona alkaloids. *Tetrahedron*. 1999;55(20):6289-6300. doi:10.1016/S0040-4020(99)00205-7

78. Baldwin JE, Haber SB, Hoskins C, Kruse LI. Synthesis of beta,gamma-unsaturated amino acids. *J Org Chem*. 1977;42(7):1239-1241. doi:10.1021/jo00427a031

79. Afzali-Ardakani A, Rapoport H. L-Vinylglycine. *J Org Chem*. 1980;45(9):4817-4820. doi:10.1021/jo01312a002

80. Meffre P, Goffic F Le, Vo-Quang L, Vo-Quang Y. N-(Benzyloxycarbonyl)-L-Vinylglycine Methyl Ester from L-Methionine Methyl Ester Hydrochloride. *Synth Commun*. 1989;19(20):3457-3468. doi:10.1080/00397918908052755

81. Griesbeck AG, Hirt J. A photochemical route to vinylglycine and a vinylglycine dipeptide. *Liebigs Ann*. 1995;1995(11):1957-1961. doi:10.1002/jlac.1995199511275

82. Lumbroso A, Coeffard V, Le Grognec E, Beaudet I, Quintard JP. An efficient and scalable synthesis of N-(benzyloxycarbonyl)- and N-(methyloxycarbonyl)-(S)-vinylglycinol. *Tetrahedron Lett*. 2010;51(24):3226-3228. doi:10.1016/j.tetlet.2010.04.059

83. Beaulieu PL, Duceppe JS, Johnson C. Synthesis of Chiral Vinylglycines. *J Org Chem*. 1991;56(13):4196-4204. doi:10.1021/jo00013a023

84. Rose NGW, Blaskovich MA, Wong A, Lajoie GA. Synthesis of enantiomerically enriched beta,gama-unsaturated-alpha-amino acids. 2001;57.

85. Pellicciari R, Natalini B, Marinozzi M. L-vinylglycine from L-homoserine. *Synth Commun*. 1988;18(14):1715-1722. doi:10.1080/00397918808081334

86. Berkowitz DB, Smith MK. A convenient synthesis of L-α-vinylglycine from L-homoserine lactone. *Synthesis*. 1996:39-41.

87. Patel SK, Long TE. Preparation of vinylglycines by thermolysis of homocysteine sulfoxides. *Tetrahedron Lett*. 2009;50(36):5067-5070. doi:10.1016/j.tetlet.2009.06.082

88. Mulzer J, Angermann A, Schubert B, Seilz C. A General and Practical Synthesis of (R)-Phthalimido Aldehydes and D-a-Amino Acids from D-Mannitol. *J Org Chem*. 1986;51(26):5294-5299. doi:10.1021/jo00376a046

89.   Badorrey R, Cativiela C, Díaz-de-Villegas MD, Gálvez JA. A convenient Synthesis of L-alpha-Vinylglycine from D-Mannitol. *Synthesis*. 1997:747-749.

90.   Chandrasekhar S, Raza A, Takhi M. Synthesis of unusual amino acids : N - (tert -butoxycarbonyl) - L -vinyl glycine and. *Tetrahedron Asymmetry*. 2002;13(20212):423-428.

91.   Wipf P, Wenjing X, Hongyong K, Takahashi H. Zirconocene-catalyzed epoxy ester - ortho ester rearrangement: A new method for the protection of polyfunctionalized carboxylic acids and the asymmetric synthesis of ortho esters. *Tetrahedron*. 1997;53(48):16575-16596. doi:10.1016/S0040-4020(97)01038-7

92.   Hanessian S, Sahoo SP. A Novel and Efficent Synthesis of L-Vinylglycine. *Tetrahedron Lett*. 1984;25(14):1425-1428.

93.   Barton DHR, Crich D, Hervé Y, Potier P, Thierry J. The free radical chemistry of carboxylic esters of 2-selenopyridine-N-oxide: a convenient synthesis of (L)-vinylglycine. *Tetrahedron*. 1985;41(19):4347-4357. doi:10.1016/S0040-4020(01)97206-0

94.   Krol WJ, Mao S shan, Steele DL, Townsend CA. Stereochemical Correlation of Proclavaminic Acid and Syntheses of erythro- and threo-L-β-Hydroxyornithine from an Improved Vinylglycine Synthon. *J Org Chem*. 1991;56(2):728-731. doi:10.1021/jo00002a045

95.   Lamborelle N, Simon JF, Luxen A, Monbaliu JM. Continuous-flow thermolysis for the preparation of vinylglycine derivatives. 2015:11602-11606. doi:10.1039/c5ob02036k

96.   Lee TR, Whitesides GM. Isotopic Exchange in the Platinum-Catalyzed Reductions of Olefins in Protic Solvents. *J Am Chem Soc*. 1991;113(7):2568-2576. doi:10.1021/ja00007a035

97.   McKerrow J, Vagg S, McKinney T, et al. A simple HPLC method for analysing diaminopimelic acid diastereomers in cell walls of Gram-positive bacteria. *Lett Appl Microbiol*. 2000;30(3):178-182. doi:10.1046/j.1472-765x.2000.00675.x

98.   Bhushan R, Brückner H. Marfey's reagent for chiral amino acid analysis: A review. *Amino Acids*. 2004;27(3-4):231-247. doi:10.1007/s00726-004-0118-0

99.   Takahashi Y, Iwai Y, Tomoda H, Nimura N, Omura S. Optical resolution of 2,6-diaminopimelic acid stereoisomers by high performance liquid chromatography for the chromatography of actinomycete strains. *J Gen Appl Microbiol*. 1989;35:27-32.

100.   Zanol M, Gastaldo L. High-performance liquid chromatographic separation of the 3 stereoisomers of diaminopimelic acid in hydrolysed bacterial cells. *J Chromatogr*. 1991;536:211-216.

101. Nagasawa T, Ling JR, Onodera R. Chiral high-performance liquid chromatographic separation of the three stereoisomers of 2,6-diaminopimelic acid without derivatisation. *J Chromatogr A*. 1993;653(2):336-340. doi:10.1016/0021-9673(93)83192-U

102. Carolyn W K, Blanchard JS. Chemical mechanism of Haemophilus influenzae diaminopimelate epimerase. *Biochemistry*. 1999;38(14):4416-4422. doi:10.1021/bi982911f

103. Merrifield RB. Solid Phase Peptide Synthesis. I. The Synthesis of. *J Am Chem Soc*. 1963;85(14):2149. doi:10.1021/ja00897a025

Chapter VI

Supplementary data

Content

*For more information about the synthesis of vinylglycine synthons via continuous-flow thermolysis, please refer to the publication attached in **chapter VII**.*

General Methods

All chemicals and reagents were purchased from commercial suppliers. All solvents used were HPLC grade.

HPLC chain used during this work consists of pump (Waters 600) and a UV detector (Waters PDA 996). Analytical HPLC analyses were performed on a Waters Xterra RP18 column (150 x 4.6 mm, 3.5 μm).

The semi-preparative HPLC chain consists of a pump (Waters 600) and an UV detector (Waters PDA 996). HPLC separations were performed on a Waters Xterra semi-preparative column (250 x 10 mm, 10 μm).

HPLC used at the CEA for the synthesis of tritiated m-A$_2$pm [^{3}H]**30** consists of a pump and sample manager (Waters Alliance 2655), a UV detector (Waters PDA 996), a counter (Berthold) and a mass spectrometry module (Waters Micromass ZQ). Analytical HPLC analyses were performed on a ThermoFisher HyPURITY C18 column (250 x 4.6 mm, 5 μm). Total activity of [^{3}H]**30** was measured on a liquid scintillation counter (Perkin Elmer TriCarb 2910TR).

UPLC-MS analyses were performed on a Waters Acquity UPLC coupled to a tandem quadrupole mass detectore equipped with an electrospray ionization source. Separation of compounds were performed on a Waters BEH C18 column (50 x 2.1 mm, 1.7 μm).

NMR spectra were recorded on Bruker instruments (400 and 700 MHz) at 25 °C. Chemical shifts δ are given in ppm. Multiplicities are abbreviated as follow: s = singlet, d = doublet, t = triplet, q = quadruplet, br = broad. Coupling constants J are given in Hz. Spectra were recorded solutions with CDCl$_3$ (δ_H = 7.26 ppm, δ_C = 77.16 ppm), MeOD (δ_H = 3.31 ppm, δ_C = 49.00 ppm), DMSO (δ_H = 2.50 ppm, δ_C = 39.52 ppm) or D$_2$O (δ_H = 4.79 ppm) as solvent.

¹³COOH

NHCbz

(¹³C)2
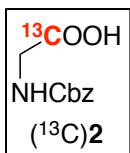
A solution of (1-¹³C)glycine (¹³C)**1** (5.1 g, 67.28 mmol, 1.0 equiv.) and NaOH (2M in H₂O, 33.6 mL, 67.28 mmol, 1.0 equiv.) was cooled in an ice bath. A solution of Cbz-Cl (14.4 mL, 100.90 mmol, 1.5 equiv.) in toluene (10.8 mL) and a solution a NaOH (4M in H₂O, 25.2 mL, 100.90 mmol, 1.5 equiv.) was added dropwise to the stirring mixture. Temperature was maintained to 0 °C for an hour and then ice was not renewed. After 1 night, phases were separated and the aqueous layer was washed diethyl ether (3x20 mL). The aqueous solution was then cooled down to 0 °C and acidified to pH = 1 using aqueous NaHSO₄ (10% wt). White solid (¹³C)**2** was filtered, washed with cold water and finally dried under vacuum (13.56 g, 96%). No further purification was needed. ¹H NMR (250 MHz, DMSO-d₆) δ 12.57 (s, 1H, COOH), 7.54 (t, $^{3}J_{HH}$ = 5.8Hz, 1H, NH), 7.34 (m, 5H, PhCHs), 5.03 (s, 2H, OCH₂Ph), 3.66 (dd, $^{2}J_{HC}$ = $^{3}J_{HH}$ = 5.8Hz, 2H, CH₂). ¹³C NMR (62.5 MHz, DMSO-d₆) δ 172.02 (¹³C=O), 156.95 (C=O), 137.46 (PhC), 128.79, 128.25, 128.16 (PhCHs), 65.91 (OCH₂Ph), 43.56 (d, $^{1}J_{CC}$ = 58.8 Hz, CH₂). ESI-MS (ES+): m/z: 167 [M+H–CO₂]⁺, 211 [M+H]⁺. m.p. = 119-121 °C.

¹³COOt-Bu

NHCbz

(¹³C)3
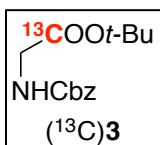
DCC (10.80 g, 52.33 mmol, 1.1 equiv.) was added to a solution of (¹³C)**2** (10 g, 47.57 mmol, 1.0 equiv.) in a mixture of CH₂Cl₂ (120 mL) and t-BuOH (13,56 mL, 143 mmol, 3.0 equiv.) and cooled down to 0 °C. Then, a solution of DMAP (0.58 g, 4.76 mmol, 0.1 equiv.) in CH₂Cl₂ (40 mL) was added dropwise to the stirring medium maintained to 0 °C for 15 minutes. After 36 hours, DCU was filtered and the filtrate was washed successively with KHSO₄ (5%, 2x50 mL), H₂O (50 mL), NaHCO₃ (sat., 50 mL) and brine (50 mL). Solvents were evaporated under vacuum and the resulting oil was dissolved using cold diethyl ether (150 mL) to precipitate residual DCU. DCU was filtered and washed with cold diethyl ether. Solutions were combined and solvents were evaporated under vacuum. Several cycles were necessary to completely eliminate DCU and to obtain a limpid oil. Flash chromatography (hexanes/AcOEt 1:1) gave (¹³C)**3** as a yellow oil (11.72 g, 93%). ¹H NMR (250MHz, CDCl₃) δ 7.35 (m, 5H, PhCHs), 5.03 (s, 2H, OCH₂Ph), 3.87 (dd,

$^2J_{HC} = {}^3J_{HH} = 5.8Hz$, 2H, CH$_2$), 1.47 (s, 9H, C(CH$_3$)$_3$). ^{13}C NMR (62.5 MHz, CDCl$_3$) δ 169.04 (^{13}C=O), 156.20 (C=O), 136.33 (PhCs), 128.49, 128.12, 128.07 (PhCHs), 82.20 (d, $^2J_{CC}$ = 3Hz, C(CH$_3$)$_3$), 66.95 (OCH$_2$Ph), 43.41 (d, $^1J_{CC}$ = 61.1 Hz, CH$_2$), 28.01 (C(CH$_3$)$_3$). ESI-MS (ES+): m/z: 267 [M+H]$^+$.
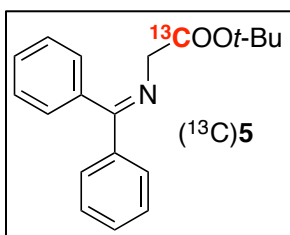
(^{13}C)**3** (8.92 g, 33.48 mmol, 1.0 equiv.) was dissolved in MeOH (50 mL). Pd/C (10% wt, dry, 0.15 g) was added to the medium and the suspension was stirred under pressure of H$_2$ (5 bar). HCl (0.97M in MeOH, 0.95 eq, 32.9 mL) was added to the medium in 5 times. After 6 hours, catalyst was removed by centrifugation. Solvent was eliminated under vacuum to afford (^{13}C)**4** chlorhydrate as a yellow oil. This crude oil was dissolved in CH$_2$Cl$_2$ (50 mL) and anhydrous MgSO$_4$ was added. Benzophenone imine (5.51 mL, 33.48 mmol, 1.0 equiv.) was added to the stirring suspension. Salts were filtered and solvent replaced by diethyl ether. This solution was washed with H$_2$O (2x50 mL) and dried over MgSO$_4$. Solvent was removed to afford (^{13}C)**5** as an off white solid (9.32 g, 94% over 2 steps). ^{1}H NMR (250 MHz, CDCl$_3$) δ 7.46 (m, 10H, PhCHs), 4.12 (d, $^2J_{CH}$ = 7.1 Hz, 2H, CH$_2$), 1.47 (s, 9H, C(CH$_3$)$_3$). ^{13}C NMR (62.5 MHz, CDCl$_3$) δ 170.69 (Ph$_2$C=N), 169.82 (^{13}C=O), 139.38, 136.17 (PhCs), 130.33, 128.73, 128.59, 128.00, 127.71 (PhCHs), 81.02 (d, $^2J_{CC}$ = 3Hz, C(CH$_3$)$_3$), 56.26 (d, $^1J_{CC}$ = 63Hz, CH$_2$), 28.09 (C(CH$_3$)$_3$). ESI-MS (ES+): m/z: 241 [M+2H–*t*-Bu]$^+$, 297 [M+H]$^+$.
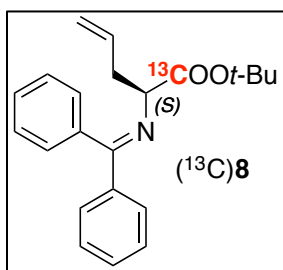
Catalyst **7b** (1.93 g, 3.15 mmol, 0.1 equiv.) was dissolved in CH$_2$Cl$_2$ (25 mL). Toluene (250 mL) was added to the solution. (^{13}C)**5** (9.32 g, 31.37 mmol, 1.0 equiv.) was then dissolved in this mixture. KOH (50% in H$_2$O, 150 mL) was added and the resulting biphasic system was stirred vigorously and cooled down to -20 °C. Allylbromide (13.64 mL, 5.0 equiv.) was added dropwise to the system. After one night, H$_2$O (400 mL) was added to the system and

layers were separated. Aqueous phase was extracted with diethyl ether (3x150 mL). The combined organic layers were washed with brine until pH lowered to 7. Solvents were evaporated and the resulting crude oil was dissolved in a minimum amount of CH_2Cl_2. Catalyst **7b** was recovered by precipitation and filtration using diethyl ether. The filtrate was then dried over $MgSO_4$ and evaporated to afford (^{13}C)**8** as a yellow oil (10.02 g, 95%). ^{1}H NMR (400 MHz, CDCl$_3$) δ 7.46 (m, 10H, PhCHs), 5.76 (ddt, $^3J_{HH, trans}$ = 17.5 Hz, $^3J_{HH, cis}$ = 10.2 Hz, $^3J_{HH}$ = 7.2 Hz, 1H, CH$_2$-C<u>H</u>=CH$_2$), 5.10 (d, $^3J_{HH, trans}$ = 17.5 Hz, 1H, CH$_2$-CH=C<u>H</u>$_2$), 5.04 (ddt, $^3J_{HH, cis}$ = 10.2 Hz, 1H, CH$_2$-CH=C<u>H</u>$_2$), 4.04 (m, 1H, CH$_\alpha$), 2.67 (m, 2H, C<u>H</u>$_2$-CH=CH$_2$), 1.47 (s, 9H, C(CH$_3$)$_3$). ^{13}C NMR (100 MHz, CDCl$_3$) δ 174.41 (Ph$_2$C=N), 170.89 (^{13}C=O), 139.74, 136.68 (PhCs), 134.74 (CH$_2$-<u>C</u>H=CH$_2$), 130.18, 128.82, 128.52, 128.40, 127.96 (PhCHs), 117.27 (CH$_2$-CH=<u>C</u>H$_2$), 81.02 (d, $^2J_{CC}$ = 3.2 Hz, <u>C</u>(CH$_3$)$_3$), 65.82 (d, $^1J_{CC}$ = 61 Hz, CH$_\alpha$), 38.17 (d, $^2J_{CC}$ = 1.6 Hz, <u>C</u>H$_2$-CH=CH$_2$), 28.07 (C(<u>C</u>H$_3$)$_3$). ESI-MS (ES+): m/z: 337 [M+H]$^+$.

(^{13}C)**10** NHFmoc
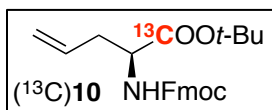
(^{13}C)**8** (6.72 g, 20 mmol, 1.0 equiv.) was dissolved in THF (30 mL) and hydrolyzed using citric acid (10% wt. in H$_2$O, 60 mL, 30 mmol, 1.5 equiv.) in 2 hours. The medium was washed with diethyl ether and then pH was brought to 12 using NaOH (4M). Aqueous phase was extracted with CH$_2$Cl$_2$. Solvent was then removed under vacuum to give (^{13}C)**9**. This crude oil (2.28 g, 13.2 mmol, 1.0 equiv.) was dissolved in a mixture of THF and H$_2$O (4:1, 30 mL). Fmoc-OSu (4.36 g, 12.9 mmol, 0.98 equiv.) was added to the solution. After one night, HPLC analysis showed complete disappearance of Fmoc-OSu. The medium was extracted with diethyl ether (3x50 mL). Combined organic phases were washed with KHSO$_4$ (50 mL) and brine (50 mL) and dried over MgSO$_4$. Removal of the solvent afforded (^{13})**10** as a clear yellow oil (5.13 g, 65% over 2 steps). ^{1}H NMR (400 MHz, CDCl$_3$) δ 7.79 (d, $^3J_{HH}$ = 7.5 Hz, 2H, FmocCH), 7.63 (d, $^3J_{HH}$ = 7.4 Hz, 2H, FmocCH), 7.43 (t, $^3J_{HH}$ = 7.3 Hz, 2H, FmocCH), 7.34 (t, $^3J_{HH}$ = 7.5 Hz, 2H, FmocCH), 5.75 (ddt, $^3J_{HH, trans}$ = 14.1 Hz, $^3J_{HH, cis}$ = 9.6 Hz, $^3J_{HH}$ = 7.2 Hz, 1H, CH$_2$-C<u>H</u>=CH$_2$), 5.41 (d, 8.1 Hz, 1H, NH), 4.40 (m, 3H, CH$_\alpha$ and FmocCH$_2$), 4.26 (t, $^3J_{HH}$ = 7.1 Hz, 1H, FmocCH), 2.57 (m, 2H, C<u>H</u>$_2$-CH=CH$_2$), 1.51 (s,

9H, C(CH$_3$)$_3$). ^{13}C NMR (100 MHz, CDCl$_3$) δ 170.82 (^{13}C=O), 155.67 (C=O), 143.96, 141.31 (FmocCs), 132.23 (CH$_2$-CH=CH$_2$), 127.70, 127.06, 125.17, 119.99 (FmocCHs), 119.11 (CH$_2$-CH=CH$_2$), 82.31 (d, $^2J_{CC}$ = 3 Hz, C(CH$_3$)$_3$), 66.99 (FmocCH$_2$), 53.62 (d, $^1J_{CC}$ = 60.3 Hz, CH$_\alpha$), 47.20 (FmocCH), 37.04 (CH$_2$-CH=CH$_2$), 28.06 (C(CH$_3$)$_3$). ESI-MS (ES+): m/z: 395 [M+H]$^+$.
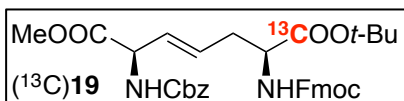
A degassed solution of (1-^{13}C)(S)-FmocNH-AG-Ot-Bu (^{13}C)**10** (2.43 g, 6.17 mmol, 1.0 equiv.) and of (R)-CbzNH-VG-OMe **16** (3.07 g, 12.34 mmol, 2.0 equiv.) in CH$_2$Cl$_2$ (100 mL) was brought to reflux under N$_2$ atmosphere. A degassed solution of Grubbs' second-generation catalyst (1.05 g, 1.24 mmol, 0.2 equiv.) in CH$_2$Cl$_2$ (20 mL) was added to the flask through a cannula in 4 times over 4 hours. After 6 hours of reaction, CH$_2$Cl$_2$ was removed under vacuum. The resulting crude oil was purified over a silica gel column to give (^{13}C)**19** as a light brown oil (2.51 g, 66%). ^{1}H NMR (400 MHz, CDCl$_3$) δ 7.78 (d, $^3J_{HH}$ = 7.5 Hz, 2H, FmocCH), 7.63 (d, $^3J_{HH}$ = 7.5 Hz, 2H, FmocCH), 7.38 (m, 9H, FmocCHs and CbzCHs), 5.74 (m, 1H, CH$_2$-CH=CH), 5.64 (m, 1H, CH$_2$-CH=CH), 5.14 (m, 2H, CbzCH$_2$), 4.92 (t, $^3J_{HH}$ = 6.8 Hz, 1H, CH$_\alpha$(R)), 4.41 (d, 7.2 Hz, 2H, FmocCH$_2$), 4.38 (m, 1H, CH$_\alpha$(S)), 4.24 (t, $^3J_{HH}$ = 7.0 Hz, 1H, FmocCH), 3.73 (s, 3H, COOCH$_3$), 2.59 (m, 2H, CH$_2$-CH=CH), 1.48 (s, 9H, C(CH$_3$)$_3$). ^{13}C NMR (100 MHz, CDCl$_3$) δ 170.42 (^{13}C=O, COOCH$_3$), 155.68 (CbzC=O), 155.50 (FmocC=O), 143.90, 143.84, 141.31 (FmocCs), 136.15 (CbzC), 128.54, 128.45, 128.22, 128.16, 127.72, 127.09, 125.16, 125.12, 120.00, 119.98 (aromatic and olefinic CHs), 82.48 (d, $^2J_{CC}$ = 2.9 Hz, C(CH$_3$)$_3$), 67.16 (FmocCH$_2$), 67.00 (CbzCH$_2$), 55.45 (CH$_\alpha$(R)), 53.6 (d, $^1J_{CC}$ = 60.3 Hz, CH$_\alpha$(S)), 52.73 (COOCH$_3$), 47.19 (FmocCH), 35.44 (CH$_2$-CH=CH), 28.02 (C(CH$_3$)$_3$). ESI-MS (ES+): m/z: 616 [M+H]$^+$, 560 [M+2H-t-Bu]$^+$, 516 [M+2H–t-Bu–CO$_2$]$^+$.
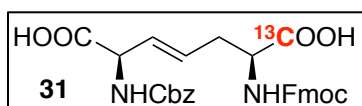
Cross metathesis product (^{13}C)**19** (200 mg, 0.325 mmol, 1.0 equiv.) was dissolved in a refluxing mixture of 1,4-dioxane (10 mL) and HCl (2M in H$_2$O, 4.8 mL, 9.7 mmol, 30 equiv.) for

4 hours. Medium was then extracted with CH_2Cl_2 (3x20 mL). Organic phase was washed once with brine (20 mL) and then dried over $MgSO_4$. Evaporation of solvents under vacuum yield **31** as a light brown oil (153 mg, 86%). ESI-MS (ES+): m/z: 546 $[M+H]^+$, 502 $[M+H-CO_2]^+$.
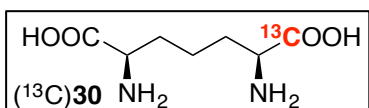
Pd black (25 mg) was added to a solution of **31** (124 mg, 0.23 mmol, 1.0 equiv.) in a mixture of THF and H_2O (1:4, 20 mL). This suspension was stirred under pressure of H_2 (5 bar) overnight. THF was removed under vacuum and the remaining suspension was washed with diethyl ether (2x10 mL). 10 mL of fresh THF were added to the suspension and reduction was extended for 24 hours. Catalyst was then filtrated and washed with H_2O and THF. THF was evaporated from the filtrate under vacuum and the resulting solution was washed with diethyl ether. The remaining aqueous solution was lyophilized to afford $(^{13}C)m$-A_2pm (^{13}C)**30** as a white solid (18 mg, 41%). ^{1}H NMR (400 MHz, D_2O) δ 3.97 (m, 2H, C$\underline{H}_\alpha$s), 2.01-1.81 (m, 4H, C$\underline{H}_2$-CH_2-C$\underline{H}_2$), 1.65-1.35 (m, 2H, CH_2-C$\underline{H}_2$-CH_2). ^{13}C NMR (100 MHz, D_2O) δ 172.06 (C=Os), 52.66 (d, $^1J_{CC}$ = 57 Hz, $\underline{C}H_\alpha(S)$-^{13}COOH), 52.68 ($CH_\alpha(R)$), 29.29 ($\underline{C}H_2$-CH_2-$\underline{C}H_2$), 20.27 (CH_2-$\underline{C}H_2$-CH_2). ESI-HRMS (ES+): calcd for $C_6{}^{13}CH_{14}N_2O_4$: 191.0987 $[M]^+$; found: 191.1035.
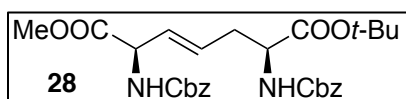
A degassed solution of (*S*)-CbzNH-AG-O*t*-Bu **11** (1.0 g, 3.27 mmol, 1.0 equiv.) and of (*R*)-CbzNH-VG-OMe **16** (1.63 g, 6.54 mmol, 2.0 equiv.) in CH_2Cl_2 (30 mL) was brought to reflux under N_2 atmosphere. A degassed solution of Grubbs' second-generation catalyst (278 mg, 0.33 mmol, 0.1 equiv.) in CH_2Cl_2 (10 mL) was added to the flask through a cannula. After 3 hours of reaction, CH_2Cl_2 was removed under vacuum. The resulting crude oil was purified by column chromatography (silica, petroleum ether (60-95)/EtOAc 7:3) to give **28** as a light brown oil (686 mg, 40%). ^{1}H NMR (400 MHz, $CDCl_3$) δ 7.42-7.29 (m, 10H, CbzCHs), 5.71 (dt, $^3J_{HH}$ = 14.5 Hz, 6.9 Hz, 1H, CH=C$\underline{H}$-CH_2), 5.61 (dd, $^3J_{HH}$ = 15.5 Hz, 5.7 Hz, 1H, C$\underline{H}$=CH-CH_2), 5.48 (d, $^3J_{HH}$ = 7.7 Hz, 1H, NH(*R*)),

5.38 (d, $^3J_{HH}$ = 7.7 Hz, 1H, NH(S)), 5.12 (m, 4H, CbzC$\underline{H}_2$s), 4.89 (t, $^3J_{HH}$ = 6.9 Hz, 1H, C$\underline{H}_\alpha$(R)), 4.89 (m, 1H, C$\underline{H}_\alpha$(S)), 3.74 (s, 3H, COOC$\underline{H}_3$), 2.65-2.42 (m, 2H, CH=CH-C$\underline{H}_2$), 1.46 (s, 9H, C(C$\underline{H}_3$)$_3$). ^{13}C NMR (100 MHz, CDCl$_3$) δ 170.89, 170.34, 155.63, 155.45 (CbzC=Os), 136.29, 136.14 (CbzCs), 128.52, 128.43, 128.20, 128.16, 128.12 (CbzCHs and $\underline{C}$H=$\underline{C}$H), 82.40 ($\underline{C}$(CH$_3$)$_3$), 67.13, 66.93 (CbzCH$_2$s), 55.41 (CH$_\alpha$(R)), 53.63 (CH$_\alpha$(S)), 52.72 (COO$\underline{C}$H$_3$), 35.41 (CH=CH-$\underline{C}$H$_2$), 27.97 (C($\underline{C}$H$_3$)$_3$).

29 HOOC / COOH NHCbz NHCbz
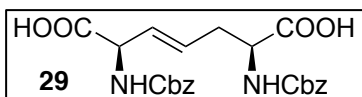
Compound **28** (686 mg, 1.30 mmol, 1.0 equiv.) was dissolved in a refluxing mixture of 1,4-dioxane (40 mL) and HCl (2M in H$_2$O, 19.5 mL, 39.1 mmol, 30 equiv.) for 4 hours. Medium was then extracted with CH$_2$Cl$_2$ (3x20 mL). Organic phase was washed once with brine (20 mL) and then dried over MgSO$_4$. Evaporation of solvents under vacuum yield **29** as a colorless oil (594 mg, 100%). ^{1}H NMR (700 MHz, DMSO-d$_6$) δ 12.72 (br, 2H, COOHs), 7.76 (d, $^3J_{HH}$ = 8.2 Hz, 1H, NH(R)), 7.54 (d, $^3J_{HH}$ = 8.2 Hz, 1H, NH(S)), 7.40-7.28 (m, 10H, CbzCHs), 5.72 (dt, $^3J_{HH}$ = 14.3 Hz, 7.0 Hz, 1H, CH=C$\underline{H}$-CH$_2$), 5.64 (dd, $^3J_{HH}$ = 15.5 Hz, 6.4 Hz, 1H, C$\underline{H}$=CH-CH$_2$), 5.04 (m, 4H, CbzCH$_2$s), 4.55 (t, $^3J_{HH}$ = 7.2 Hz, 1H, CH$_\alpha$(R)), 4.02 (m, 1H, CH$_\alpha$(S)), 2.42 (m, 2H, CH=CH-C$\underline{H}_2$). ^{13}C NMR (175 MHz, DMSO-d$_6$) δ 173.53 (CH$_\alpha$(S)-$\underline{C}$OOH), 172.53 (CH$_\alpha$(R)-$\underline{C}$OOH), 156.52, 156.28 (CbzC=Os), 137.40, 137.39 (CbzCs), 129.22 (CH=$\underline{C}$H-CH$_2$), 128.28, 128.26, 128.21, 128.17 (CbzCHs), 127.72 ($\underline{C}$H=CH-CH$_2$), 65.98, 65.92 (CbzCH$_2$s), 56.13 (CH$_\alpha$(R)), 54.08 (CH$_\alpha$(S)), 34.05 (CH=CH-$\underline{C}$H$_2$). ESI-MS (ES+): m/z: 913 [2M+H]$^+$, 457 [M+H]$^+$, 413 [M+H–CO$_2$]$^+$.

HOOC / COOH ^{2}**H** H$_2$N ^{2}**H** NH$_2$ (^{2}H$_2$)**30**
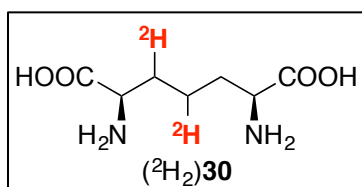
Compound **29** (20 mg, 44 μmol, 1 equiv.) was dissolved in 1 mL of THF. Addition of 4 mL of D$_2$O to the medium provoked partial precipitation of **29**. Pd black (2 mg) was added to the medium and the stirring suspension was introduced in an autoclave

under 5 bars of pressure of D_2 for two hours. Filtration of the catalyst and lyophilisation afforded $(^2H_2)$**30** as a white solid (8.5 mg, 100%). ^1H NMR (400 MHz, D_2O) δ 3.66 (m, 2H, C<u>H</u>$_\alpha$s), 1.89-1.74 (m, 3H, C<u>H</u>D-CHD-C<u>H</u>$_2$), 1.49-1.31 (m, 1H, CHD-C<u>H</u>D-CH$_2$). ^{13}C NMR (100 MHz, D_2O) δ 174.53 (C=Os), 54.45, 54.38 (CH$_\alpha$s), 30.04 (CHD-CHD-<u>C</u>H$_2$), 29.72 (t, $^1J_{CD}$ = 20 Hz, <u>C</u>HD-CHD-CH$_2$), 20.24 (t, $^1J_{CD}$ = 20 Hz, CHD-<u>C</u>HD-CH$_2$). ESI-HRMS (ES+): calcd for $C_7H_{12}D_2N_2O_4$: 192.1079 [M]$^+$; found: 192.1168.
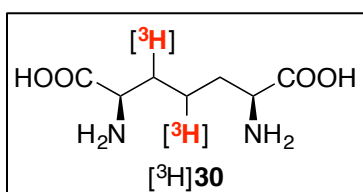
A stirrer, Pd black (1 mg), H_2O (0.6 mL) and a solution of **29** (5 mg, 11 μmol in 0.15 mL of THF) were successively introduced in a 5 mL Fischer-Porter tube (FP). Next steps were all performed in a hypobaric glovebox. Once the FP attached to the tritium reduction apparatus, medium was stirred for a minute and then frozen in liquid nitrogen for 5 minutes. Level of liquid nitrogen was carefully maintained at the air/solution interface height. Once completely frozen, vacuum was made in the system before introduction of tritium gas (P_{frozen} = 0.860 bar) from uranium bed 1. The medium was then brought back to rt and pressure rose to 1.06 bar. FP tube was isolated from the system and a strong stirring was applied for 24 hours. Medium was then frozen again so contaminated tritium gas could be trapped by uranium bed 2. FP was then disconnected from the system and its content was filtered on syringe. Filter was washed with water (2x1 mL). Solvents were eliminated under vacuum. Residue was taken up in methanol (20 mL) and concentrated to dryness under vacuum two times to eliminate labile tritium atoms. White solid residue [^3H]**30** was dissolved in 140 mL of EtOH/H_2O 1:1 (~2 mCi/mL) for conservation in a 250 mL round-bottom flask.
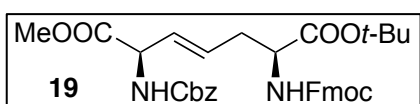
A degassed solution of (*S*)-FmocNH-AG-O*t*-Bu **10** (693 mg, 1.76 mmol, 1.0 equiv.) and of (*R*)-CbzNH-VG-OMe **16** (1.32 g, 5.28 mmol, 3.0 equiv.) in CH_2Cl_2 (25 mL) was brought to

reflux under N$_2$ atmosphere. A degassed solution of Grubbs' second-generation catalyst (299 mg, 0.35 mmol, 0.2 equiv.) in CH$_2$Cl$_2$ (10 mL) was added to the flask through a cannula in 3 times over 3 hours. 1 hour after the last addition of catalyst, CH$_2$Cl$_2$ was removed under vacuum. The resulting crude oil was purified over a silica gel column to give **19** as a light brown oil (844 mg, 78%). ^{1}H NMR (400 MHz, CDCl$_3$) δ 7.78 (d, $^3J_{HH}$ = 7.5 Hz, 2H, FmocCH), 7.63 (d, $^3J_{HH}$ = 7.5 Hz, 2H, FmocCH), 7.38 (m, 9H, FmocCHs and PhCHs), 5.74 (m, 1H, CH$_2$-C<u>H</u>=CH), 5.64 (m, 1H, CH$_2$-CH=C<u>H</u>), 5.52, 5.46 (NHs), 5.14 (m, 2H, CbzCH$_2$), 4.92 (t, $^3J_{HH}$ = 6.8 Hz, 1H, CH$_\alpha$(*R*)), 4.41 (d, 7.2 Hz, 2H, FmocCH$_2$), 4.38 (m, 1H, CH$_\alpha$(*S*)), 4.24 (t, $^3J_{HH}$ = 7.0 Hz, 1H, FmocCH), 3.73 (s, 3H, COOCH$_3$), 2.59 (m, 2H, C<u>H</u>$_2$-CH=CH), 1.48 (s, 9H, C(CH$_3$)$_3$). ^{13}C NMR (100 MHz, CDCl$_3$) δ 170.91 (<u>C</u>OOCH$_3$), 170.41 (<u>C</u>OOC(CH$_3$)$_3$), 155.65 (CbzC=O), 155.48 (FmocC=O), 143.90, 143.83, 141.30 (FmocCs), 136.13 (CbzC), 128.54, 128.45, 128.23, 128.16, 127.72, 127.09, 125.16, 125.13, 120.00, 119.98 (aromatic and olefinic CHs), 82.48 (<u>C</u>(CH$_3$)$_3$), 67.15 (FmocCH$_2$), 66.99 (CbzCH$_2$), 55.45 (CH$_\alpha$(*R*)), 53.60 (CH$_\alpha$(*S*)), 52.73 (COO<u>C</u>H$_3$), 47.19 (FmocCH), 35.43 (<u>C</u>H$_2$-CH=CH), 28.01 (C(<u>C</u>H$_3$)$_3$). ESI-MS (ES+): m/z: 615 [M+H]$^+$, 559 [M+2H–*t*-Bu]$^+$, 515 [M+2H–*t*-Bu–CO$_2$]$^+$.
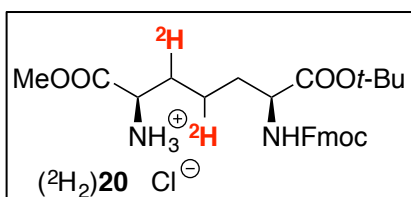
Dehydro-*m*-A$_2$pm derivative **19** (223 mg, 0.36 mmol, 1.0 equiv.) was dissolved in a mixture of D$_2$O (1 mL) and THF (5 mL). Aqueous DCl was added to the medium to lower pH down to 1. 5 mg of Pd/C (10% wt) were added as catalyst. This solution was inserted in an autoclave and a pressure of D$_2$ was applied (1 atm). After one night of reduction, UPLC-MS analysis confirmed cleavage of the Cbz carbamate and full reduction of the alkene function. A partial cleavage of *t*-Bu ester was also observed. Solvents were removed under vacuum to afford crude (^{2}H$_2$)**20**. ESI-MS (ES+): m/z: 485 [M+H]$^+$, 429 [M+2H–*t*-Bu]$^+$.

MeOOC — COOH
²H
H₃N⁺ —O⁻ ²H NHFmoc
(²H₂)**21** TFA⁻
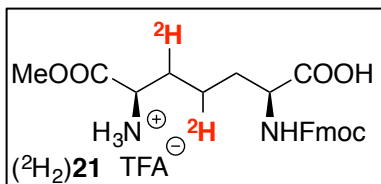
Crude (²H₂)**20** was then dissolved in 2 mL of TFA for 15 minutes to fully cleave the remaining *t*-Bu ester. Addition of 50 mL of diethyl ether provoked precipitation of (²H₂)**21** as a white solid (183 mg, 93%, 2 steps). ESI-MS (ES+): m/z: 429 [M+H]⁺.

MeOOC — COOH
²H
CbzHN ²H NHFmoc
(²H₂)**22**
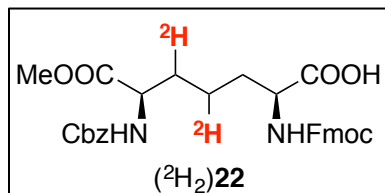
Salt (²H₂)**21** (183 mg, 0.34 mmol, 1.0 equiv.) was dissolved in a mixture of THF (10 mL) and H₂O (5 mL). A solution of Cbz-Cl (73 mg, 0.43 mmol, 1.0 equiv.) in THF (1 mL) was added dropwise to this stirring medium. An aqueous solution of NaHCO₃ (5 % wt) was added to this mixture to maintain a neutral pH. An additional 0.1 equiv. of Cbz in THF was required to achieve complete conversion of (²H₂)**21** into (²H₂)**22**. After 2 hours of reaction, THF was evaporated and the residue was treated with 5 mL of aqueous KHSO₄ (10% wt) and extracted with diethyl ether trice. Reassembled organic phases were then washed brine and dried over anhydrous MgSO₄. Evaporation of solvent afforded (²H₂)**22** as a pale-yellow oil (118 mg, 49%). UPLC-MS confirmed structure of this compound before its direct introduction in SPPS. ESI-MS (ES+): 563 [M+H]⁺, 519 [M+H–CO₂]⁺.

MeOOC — COOH
²H
BocHN ²H NHFmoc
(²H₂)**23**
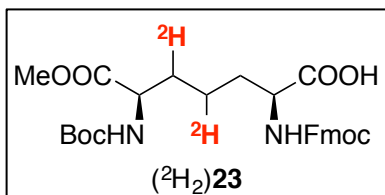
Salt (²H₂)**21** (200 mg, 0.37 mmol, 1.0 equiv.) was dissolved in THF (20 mL). An aqueous solution of NaHCO₃ (5 % wt, 620 mg, 1.0 equiv.) was added dropwise under stirring. A solution of Boc₂O (81 mg, 0.37 mmol, 1.0 equiv.) in THF (10 mL) was added dropwise to the medium. After one night of reaction, THF was evaporated under vacuum and replaced with CH₂Cl₂ (50 mL). This organic solution was washed with aqueous KHSO₄ (5% wt, 25 mL) and brine (25 mL). Evaporation of CH₂Cl₂ afforded (²H₂)**23** as a yellow oil (191 mg, 98%).

UPLC-MS confirmed structure of this compound before its direct introduction in SPPS. ESI-MS (ES+): m/z: 529 [M+H]$^+$, 473 [M+2H–t-Bu]$^+$, 429 [M+2H–Boc]$^+$.
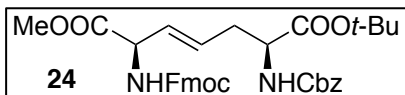
A degassed solution of (*S*)-CbzNH-AG-Ot-Bu **11** (1.0 g, 3.27 mmol, 1.0 equiv.) and of (*R*)-FmocNH-VG-OMe **18** (2.21 g, 6.55 mmol, 2.0 equiv.) in CH$_2$Cl$_2$ (50 mL) was brought to reflux under N$_2$ atmosphere. A degassed solution of Grubbs' second-generation catalyst (555 mg, 0.65 mmol, 0.2 equiv.) in CH$_2$Cl$_2$ (20 mL) was added to the flask through a cannula 2 mol% at a time over 5 hours. 1 hour after the last addition of catalyst, CH$_2$Cl$_2$ was removed under vacuum. Crude oil obtained after evaporation of solvents was purified over a silica gel column to give **24** as a colorless oil (1.0 g, 50%). ^{1}H NMR (400 MHz, CDCl$_3$) δ 7.79 (d, $^3J_{HH}$ = 7.5 Hz, 2H, FmocCH), 7.63 (d, $^3J_{HH}$ = 7.1 Hz, 2H, FmocCH), 7.42 (t, $^3J_{HH}$ = 7.4 Hz, 2H, FmocCHs), 7.35 (m, 7H, FmocCHs and CbzCHs), 5.55 (d, $^3J_{HH}$ = 7.4 Hz, 1H, NH(*R*)), 5.40 (d, $^3J_{HH}$ = 7.5 Hz, 1H, NH(*S*)), 5.72 (m, 1H, CH$_2$-C<u>H</u>=CH), 5.65 (m, 1H, CH$_2$-CH=C<u>H</u>), 5.13 (m, 2H, CbzCH$_2$), 4.90 (t, $^3J_{HH}$ = 6.2 Hz, 1H, CH$_α$(*R*)), 4.42 (m, 2H, FmocCH$_2$), 4.36 (m, 1H, CH$_α$(*S*)), 4.25 (t, $^3J_{HH}$ = 7.0 Hz, 1H, FmocCH), 3.75 (s, 3H, COOCH$_3$), 2.57 (m, 2H, C<u>H</u>$_2$-CH=CH), 1.47 (s, 9H, C(CH$_3$)$_3$). ^{13}C NMR (100 MHz, CDCl$_3$) δ 170.95(<u>C</u>OOCH$_3$), 170.36 (<u>C</u>OOC(CH$_3$)$_3$), 155.67 (CbzC=O), 155.51 (FmocC=O), 141.31, 141.30 (FmocCs), 136.3 (CbzC), 128.53, 128.39, 128.28, 128.18, 128.13, 127.73, 127.09, 125.12, 120.00, 119.99 (aromatic and olefinic CHs), 82.41 (<u>C</u>(CH$_3$)$_3$), 67.19 (FmocCH$_2$), 66.95 (CbzCH$_2$), 55.41 (CH$_α$(*R*)), 53.67 (CH$_α$(*S*)), 52.77 (COO<u>C</u>H$_3$), 47.15 (FmocCH), 35.46 (<u>C</u>H$_2$-CH=CH), 27.99 (C(<u>C</u>H$_3$)$_3$). ESI-MS (ES+): m/z: 615 [M+H]$^+$, 559 [M+2H–t-Bu]$^+$, 515[M+2H–t-Bu–CO$_2$]$^+$.
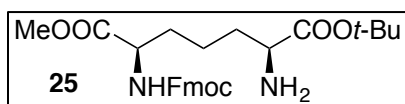
Dehydro-*m*-A$_2$pm derivative **24** (1.0 g, 1.63 mmol, 1.0 equiv.) was dissolved in 75 mL of THF. Pd/C (10% wt, dry, 0.10 g) was added to the medium and the suspension was stirred under pressure of H$_2$ (5 bar) for 72h. UPLC-

MS analysis confirmed complete conversion of **24** and identification of **25** (ESI-MS (ES+): m/z: 483 [M+H]$^+$, 427 [M+2H–*t*-Bu]$^+$).
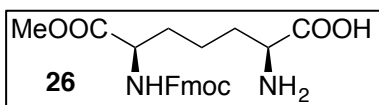
After filtration of the catalyst and evaporation of the solvent, crude **25** was treated with 10 mL of a TFA/CH$_2$Cl$_2$ (1:1) solution. Cleavage of the *tert*-butyl ester was monitored by HPLC. After one hour, HPLC analysis showed complete disappearance of **25**. TFA was removed by multiple cycles of dissolution/evaporation in CH$_2$Cl$_2$ to afford crude **26**.

MeOOC ⌢⌢⌢⌢ COOH
26 NHFmoc NH$_2$
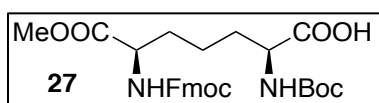
Crude **26** was dissolved in 50 mL of a solution of Et$_3$N in CH$_2$Cl$_2$ (0.45 mL, 3.25 mmol, 2.0 equiv.). A solution of Boc$_2$O (0.45 mL, 1.95 mmol, 1.2 equiv.) in CH$_2$Cl$_2$ (20 mL) was added to the medium. A third equivalent of base was added after 30 min of reaction. One hour later, HPLC analysis showed complete conversion of **26** to **27**. Medium was quenched with aqueous KHSO$_4$ (5% wt, 25 mL) and phases were separated. Aqueous phase was extracted with CH$_2$Cl$_2$ (2x25 mL). Rassembled organic phases were washed with brine (50 mL) and dried over anh. MgSO$_4$. Filtration and evaporation of solvents under vacuum yielded **27** as a light brown oil (819 mg, 95% over 3 steps) ^{1}H NMR (400 MHz, CDCl$_3$) δ 7.68 (d, $^3J_{HH}$ = 7.5 Hz, 2H, FmocCH), 7.52 (d, $^3J_{HH}$ = 7.4 Hz, 2H, FmocCH), 7.32 (t, $^3J_{HH}$ = 7.5 Hz, 2H, FmocCH), 7.24 (t, $^3J_{HH}$ = 7.4 Hz, 2H, FmocCH), 5.60 (d, $^3J_{HH}$ = 8.3 Hz, 1H, NH(*S*)), 5.25 (d, $^3J_{HH}$ = 7.8 Hz, 1H, NH(*R*)), 4.47 (m, 2H, FmocCH$_2$), 4.45 (m, 1H, CH$_\alpha$(*S*)), 4.39 (m, 1H, CH$_\alpha$(*R*)), 4.30 (t, $^3J_{HH}$ = 7.1 Hz, 1H, FmocCH), 3.83 (s, 3H, COOCH$_3$), 1.97 (m, 2H, CH$_\alpha$(*R*)-C$\underline{H}_2$), 1.78 (m, 2H, CH$_\alpha$(*S*)-C$\underline{H}_2$), 1.57 (m, 2H, CH$_2$-C$\underline{H}_2$-CH$_2$), 1.52 (s, 9H, Boc). ^{13}C NMR (100 MHz, CDCl$_3$) δ 175.89 (COOH), 172.88 ($\underline{C}$OOCH$_3$), 156 (FmocC=O & BocC=O), 143.92, 143.79, 141,36 (FmocCs), 127.78, 127.16, 125.19, 120.04 (FmocCHs), 80.45 (BocC), 67.13 (FmocCH$_2$), 53.57 (CH$_\alpha$(*S*)), 52.94 (CH$_\alpha$(*R*)), 52.50 (COOCH$_3$), 47.19 (FmocCH), 32.02($\underline{C}$H$_2$-CH$_2$-$\underline{C}$H$_2$) 28.45 (BocCH$_3$), 21.14 (CH$_2$-$\underline{C}$H$_2$-CH$_2$).

MeOOC ⌢⌢⌢⌢ COOH
27 NHFmoc NHBoc
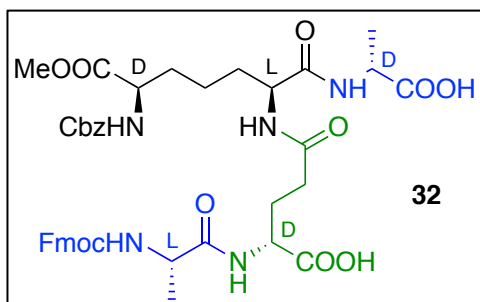
D-Ala-*m*-A$_2$pm-γ-D-Glu-L-Ala-Wang resin was synthesized from FmocNH-D-Ala-Wang resin (50 mg, 0.045 mmol, 1.0 equiv.), differentially protected (^{2}H$_2$)*m*-A$_2$pm **22** (51 mg, 0.09 mmol, 2.0 equiv.), FmocNH-D-Glu(OH)-O*t*-Bu (77 mg, 0.18 mmol, 4.0 equiv) and FmocNH-L-Ala-Wang (56 mg, 0.18 mmol, 4.0 equiv) via a Biotage Initiator+ Alstra synthesizer. First, resin was swelled with DMF for 20 min at 70 °C. Deprotection-coupling cycles were done at rt with piperidine (20% in DMF, 45 equiv.) and activation with HBTU (285 μL, 0.6 mol/L in DMF, 0.17 mmol, 3.8 equiv.) and NMM (900 μL, 0.4 mol/L in DMF, 0.36 mmol, 8.0 equiv.). Resin was filtered and rinsed with CH$_2$Cl$_2$ prior to cleavage with TFA/CH$_2$Cl$_2$ 1:1. Solvents were evaporated and crude product was purified over semi-preparative HPLC (CH$_3$CN/H$_2$O/TFA 40:60:0.1) giving **32** as a white solid (6.1 mg, 16%). ^{1}H NMR (700 MHz, MeOD) δ 7.81 (d, $^3J_{HH}$ = 7.8 Hz, 2H, FmocCHs), 7.69 (d, $^3J_{HH}$ = 7.7 Hz, 2H, FmocCHs), 7.41 (t, $^3J_{HH}$ = 7.5 Hz, 2H, FmocCHs), 7.37-7.27 (m, 7H, FmocCHs & CbzCHs), 5.08 (m, 2H, CbzCH$_2$), 4.42 (m, 3H, FmocCH$_2$ & CH$_\alpha$(S)$_{A2pm}$), 4.40 (q, $^3J_{HH}$ = 7.3 Hz, 1H, CH$_{\alpha Ala1}$), 4.31 (m, 1H, CH$_{\alpha Glu}$), 4.25 (t, $^3J_{HH}$ = 6.9 Hz, 1H, FmocCH), 4.18 (q, $^3J_{HH}$ = 7.3 Hz, 1H, CH$_{\alpha Ala2}$), 4.17 (m, 1H, CH$_\alpha$(R)$_{A2pm}$), 3.70 (s, 3H, COOCH$_3$), 2.30 (m, 3H, CH$_{2\beta Glu}$ & CH$_{2\gamma Glu}$), 1.90 (m, 1H, CH$_{2\beta Glu}$), 1.86-1.62 (m, 4H, CH$_{2\beta A2pm}$s), 1.56-1.35 (m, 2H, CH$_{2\gamma A2pm}$), 1.40 (d, $^3J_{HH}$ = 7.3 Hz, 3H, CH$_{3Ala1}$), 1.37 (d, $^3J_{HH}$ = 7.3 Hz, 3H, CH$_{3Ala2}$). ESI-MS (ES+): m/z: 832 [M+H]$^+$.
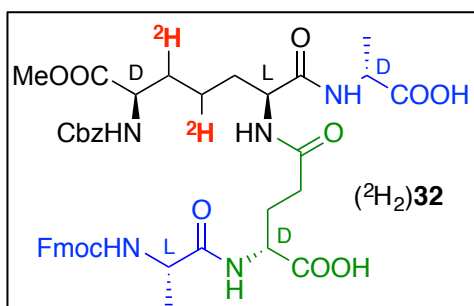
Same procedure was applied for the synthesis of (^{2}H$_2$)**32** (4.9 mg, 13%). ^{1}H NMR (700 MHz, MeOD) δ 7.81 (d, $^3J_{HH}$ = 7.6 Hz, 2H, FmocCHs), 7.69 (dd, $^3J_{HH}$ = 7.8, 3.5 Hz, 2H, FmocCHs), 7.41 (t, $^3J_{HH}$ = 7.4 Hz, 2H, FmocCHs), 7.37-7.27 (m, 7H, FmocCHs & CbzCHs), 5.08 (m, 2H, CbzCH$_2$), 4.41 (m, 3H, FmocCH$_2$ & CH$_\alpha$(S)$_{A2pm}$), 4.40 (q, $^3J_{HH}$ = 7.3

Hz, 1H, CH$_{\alpha Ala1}$), 4.31 (m, 1H, CH$_{\alpha Glu}$), 4.25 (t, $^3J_{HH}$ = 6.9 Hz, 1H, FmocCH), 4.18 (q, $^3J_{HH}$ = 7.2 Hz, 1H, CH$_{\alpha Ala2}$), 4.16 (d, $^3J_{HH}$ = 6.0 Hz, 1H, CH$_\alpha(R)_{A2pm}$), 3.70 (s, 3H, COOCH$_3$), 2.30 (m, 3H, CH$_{2\beta Glu}$ & CH$_{2\gamma Glu}$), 1.90 (m, 1H, CH$_{2\beta Glu}$), 1.85-1.61 (m, 4H, CH$_{2\beta A2pm}$s), 1.51-1.35 (m, 2H, CH$_{2\gamma A2pm}$), 1.40 (d, $^3J_{HH}$ = 7.3 Hz, 3H, CH$_{3Ala1}$), 1.37 (d, $^3J_{HH}$ = 7.2 Hz, 3H, CH$_{3Ala2}$). ESI-MS (ES+): m/z: 834 [M+H]$^+$.
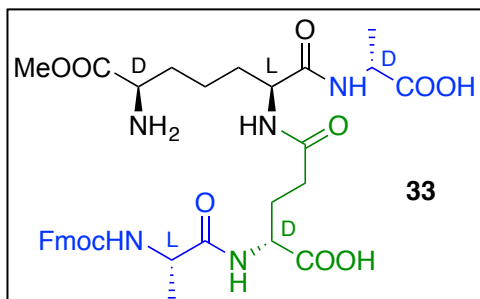
D-Ala-*m*-A$_2$pm-γ-D-Glu-L-Ala-Wang resin was synthesized from FmocNH-D-Ala-Wang resin (100 mg, 0.09 mmol, 1.0 equiv.), differentially protected (^{2}H$_2$)*m*-A$_2$pm **23** (190 mg, 0.36 mmol, 4.0 equiv.), FmocNH-D-Glu(OH)-O*t*-Bu (77 mg, 0.18 mmol, 4.0 equiv) and FmocNH-L-Ala-Wang (56 mg, 0.18 mmol, 4.0 equiv) via a Biotage Initiator+ Alstra synthesizer. First, resin was swelled with DMF for 20 min at 70 °C. Deprotection-coupling cycles were done at rt with piperidine (20% in DMF, 45 equiv.) and activation with HBTU (285 μL, 0.6 mol/L in DMF, 0.17 mmol, 3.8 equiv.) and NMM (900 μL, 0.4 mol/L in DMF, 0.36 mmol, 8.0 equiv.). Resin was filtered and rinsed with CH$_2$Cl$_2$ prior to cleavage with TFA. Solvents were evaporated and crude product was purified over semi-preparative HPLC (CH$_3$CN/H$_2$O/TFA 25:75:0.1) giving **33** as a white solid (13.9 mg, 15%). ^{1}H NMR (700 MHz, D$_2$O) δ 7.81 (d, $^3J_{HH}$ = 7.8 Hz, 2H, FmocCHs), 7.60 (m, 2H, FmocCHs), 7.40 (t, $^3J_{HH}$ = 7.5 Hz, 2H, FmocCHs), 7.32 (m, 2H, FmocCHs), 4.43 (m, 2H, FmocCH$_2$), 4.23 (m, 3H, FmocCH, CH$_{\alpha Glu}$, CH$_{\alpha Ala1}$), 4.05 (t, $^3J_{HH}$ = 7.2 Hz, 1H, CH$_\alpha(S)_{A2pm}$), 3.95 (q, $^3J_{HH}$ = 7.3 Hz, 1H, CH$_{\alpha Ala2}$), 3.93 (t, $^3J_{HH}$ = 6.6 Hz, 1H, CH$_\alpha(R)_{A2pm}$), 3.70 (s, 3H, COOCH$_3$), 2.19 (m, 2H, CH$_{2\gamma Glu}$), 2.10, 1.82 (m, 2H, CH$_{2\beta Glu}$), 1.80, 1.73 (m, 1H, CH$_\alpha(R)$-C$\underline{H}$D$_{\beta A2pm}$), 1.61, 1.51 (m, 2H, C$\underline{H}_2{}_{\beta A2pm}$-CH$_\alpha(S)$), 1.29 (m, 1H, CHD$_{\gamma A2pm}$), 1.28 (d, $^3J_{HH}$ = 7.3 Hz, 3H, CH$_{3Ala1}$), 1.23 (d, $^3J_{HH}$ = 7.3 Hz, 3H, CH$_{3Ala2}$). ESI-MS (ES+): m/z: 698 [M+H]$^+$.
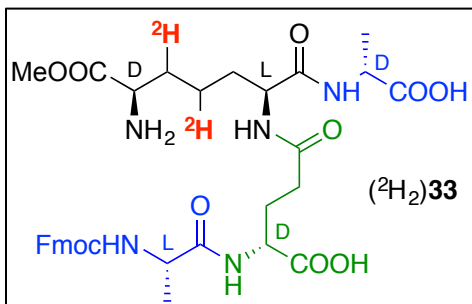
Same procedure was applied for the synthesis of (^{2}H$_2$)**33** (3.1 mg, 4%). ^{1}H NMR (700 MHz, D$_2$O) δ 7.78 (d, $^3J_{HH}$ = 7.7 Hz, 2H, FmocCHs), 7.58 (m, 2H, FmocCHs), 7.38 (t, $^3J_{HH}$ = 6.8 Hz, 2H, FmocCHs), 7.30 (m, 2H, FmocCHs), 4.40 (m, 2H, FmocCH$_2$), 4.22 (m, 3H, FmocCH, CH$_{\alpha Glu}$, CH$_{\alpha Ala1}$), 4.05 (t, $^3J_{HH}$ = 7.1 Hz, 1H, CH$_\alpha$(S)$_{A2pm}$), 3.95 (q, $^3J_{HH}$ = 7.2 Hz, 1H, CH$_{\alpha Ala2}$), 3.92 (d, $^3J_{HH}$ = 6.6 Hz, 1H, CH$_\alpha$(R)$_{A2pm}$), 3.70 (s, 3H, COOCH$_3$), 2.18 (m, 2H, CH$_{2\gamma Glu}$), 2.10, 1.82 (m, 2H, CH$_{2\beta Glu}$), 1.77, 1.71 (m, 1H, CH$_\alpha$(R)-C$\underline{H}$D$_{\beta A2pm}$), 1.60, 1.50 (m, 2H, C$\underline{H}_{2\beta A2pm}$-CH$_\alpha$(S)), 1.27 (1H, CHD$_{\gamma A2pm}$), 1.27 (d, $^3J_{HH}$ = 7.3 Hz, 3H, CH$_{3Ala1}$), 1.23 (d, $^3J_{HH}$ = 7.3 Hz, 3H, CH$_{3Ala2}$). ESI-MS (ES+): m/z: 701 [M+H]$^+$.
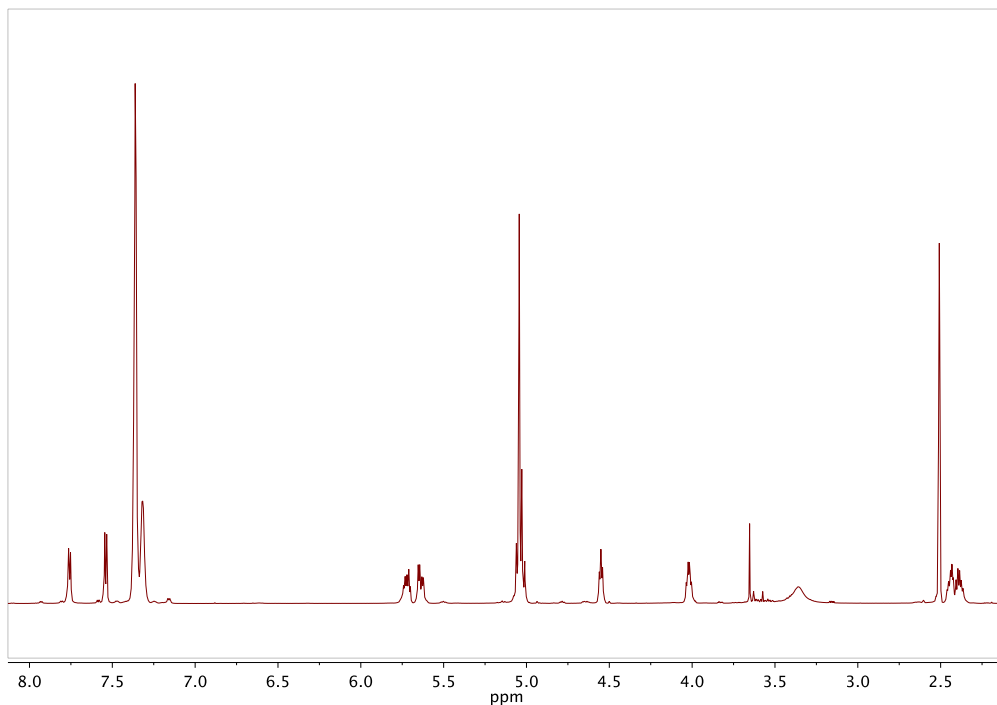
Figure 1. ^{1}H NMR spectrum of **29** in DMSO (700 MHz, 25 °C).
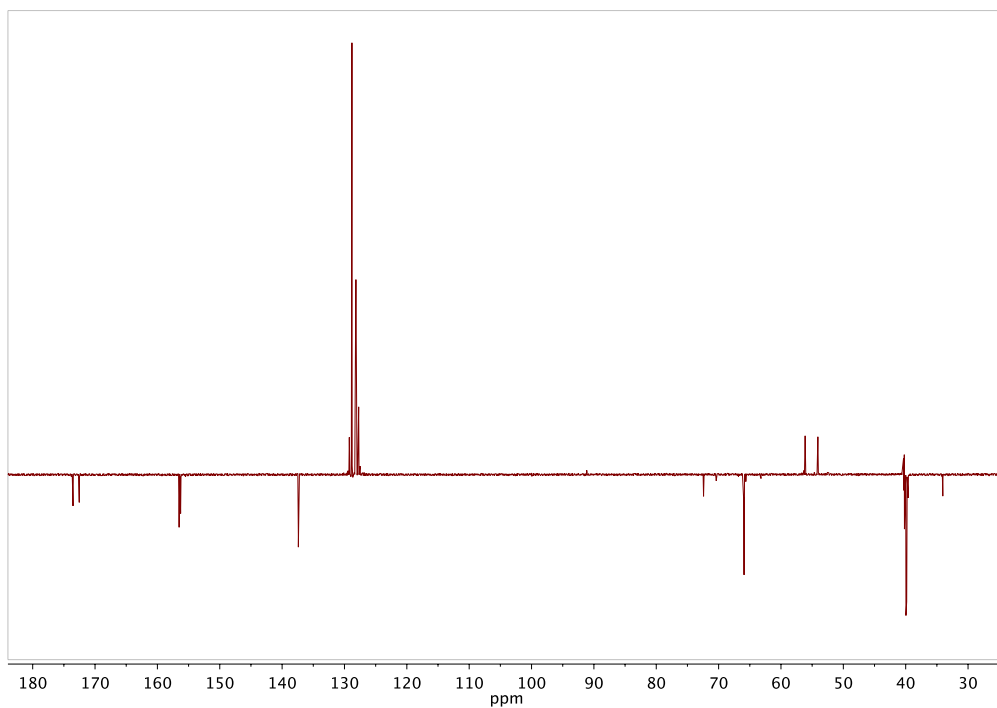
Figure 2. ^{13}C-APT NMR spectrum of **29** in DMSO (175 MHz, 25 °C).
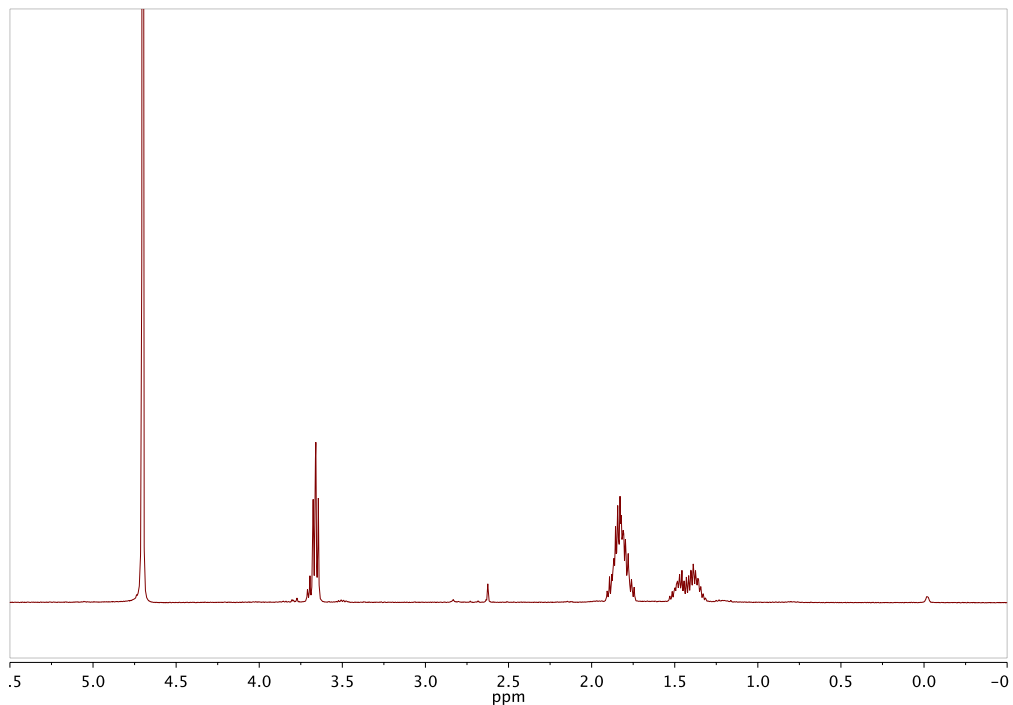
Figure 3. ^{1}H NMR spectrum of **30** in D$_2$O (400 MHz, 25 °C).
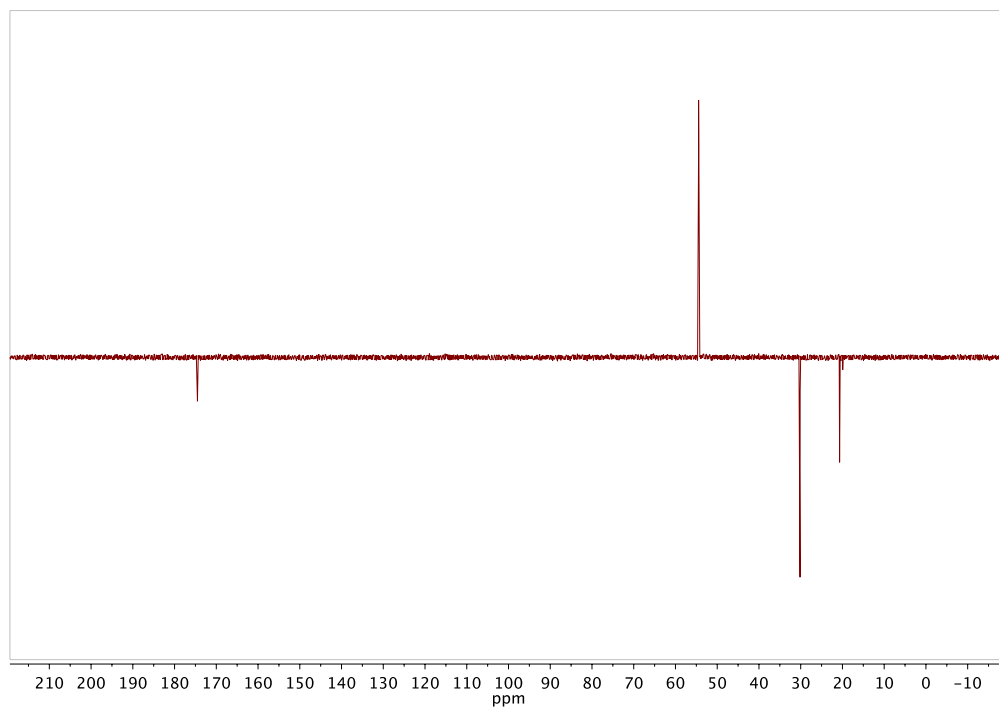
Figure 4. ^{13}C-APT NMR spectrum of **30** in D$_2$O (100 MHz, 25 °C).
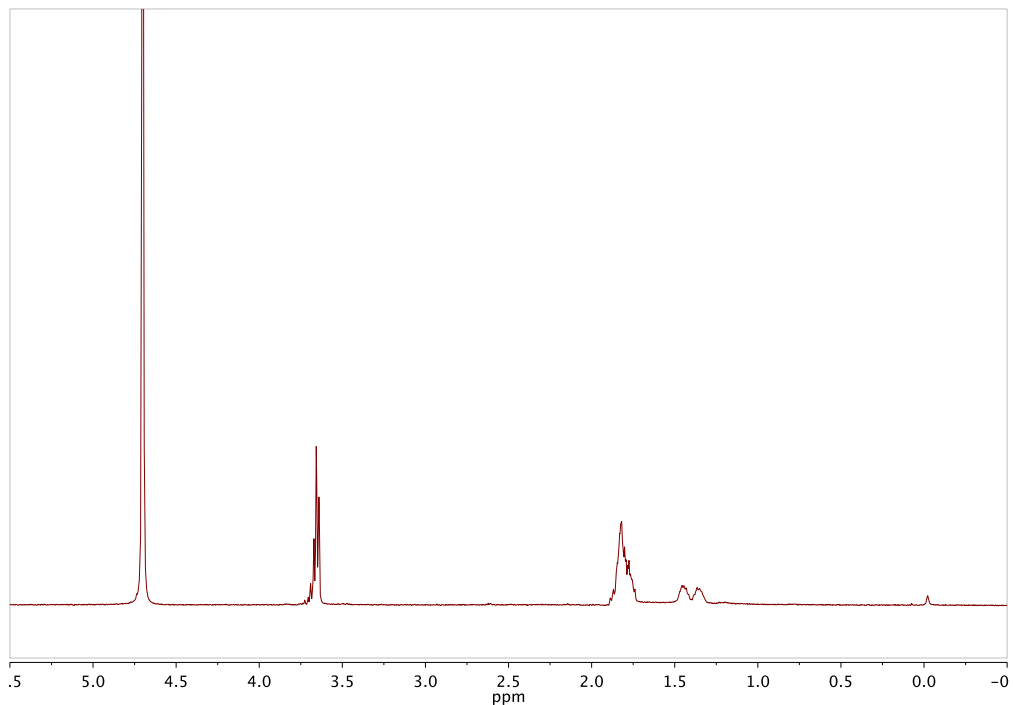
Figure 5. ^{1}H NMR spectrum of (^{2}H$_2$)**30** in D$_2$O (400 MHz, 25 °C).
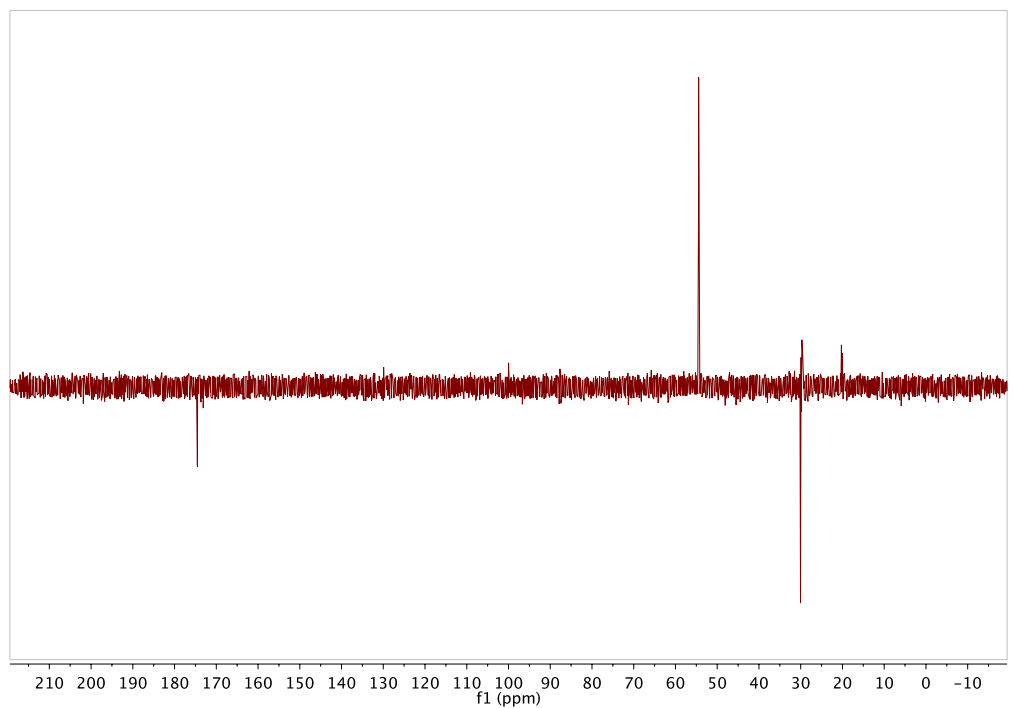
Figure 6. ^{13}C-APT NMR spectrum of (^{2}H$_2$)**30** in D$_2$O (100 MHz, 25 °C).
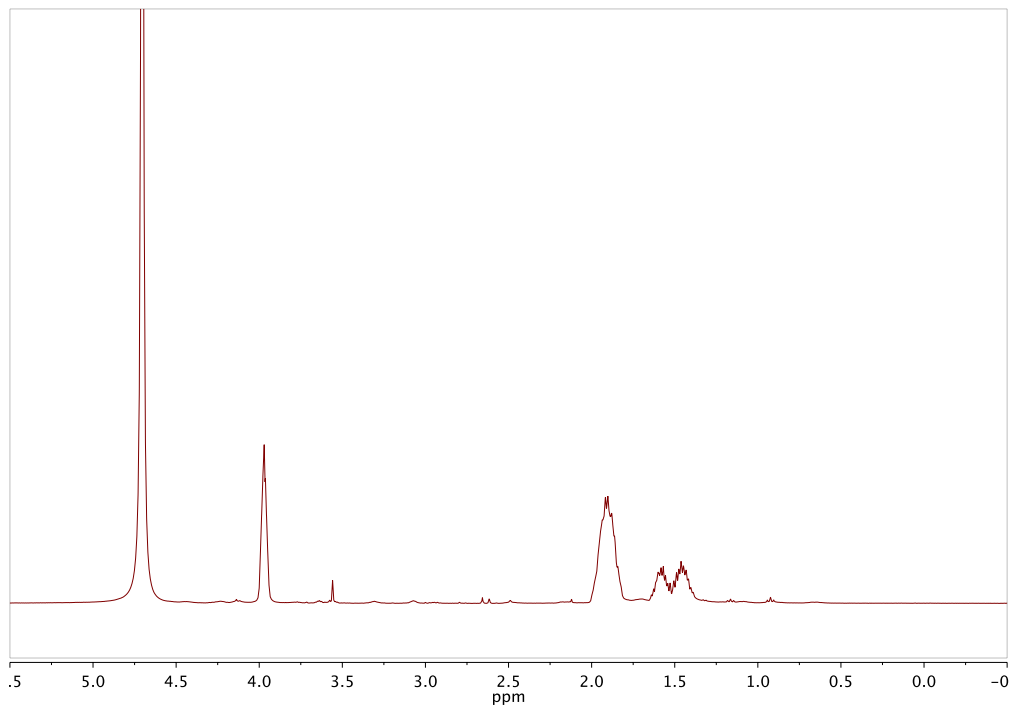
Figure 7. ^{1}H NMR spectrum of (^{13}C)**30** in D$_2$O (400 MHz, 25 °C).
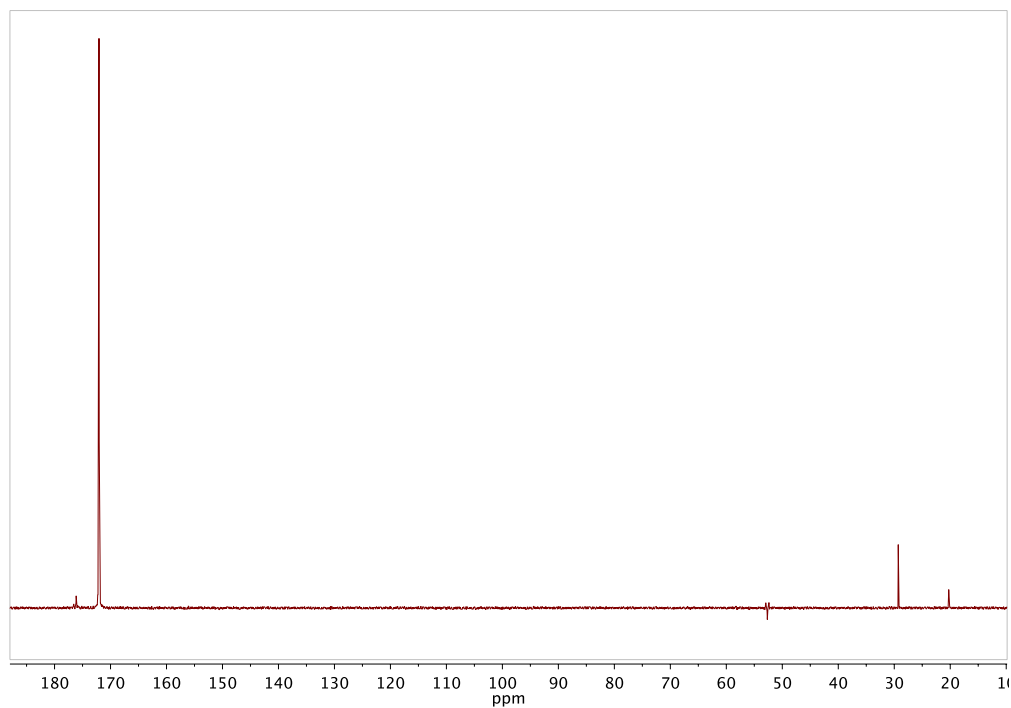
Figure 8. ^{13}C-APT NMR spectrum of (^{13}C)**30** in D$_2$O (100 MHz, 25 °C).
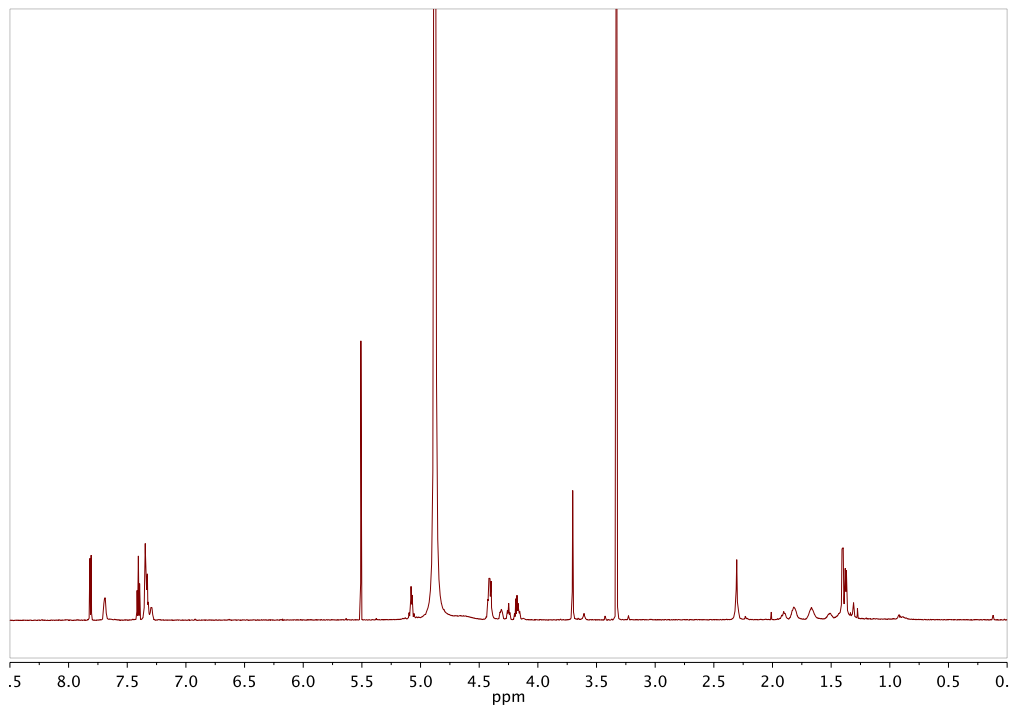
Figure 9. ^{1}H NMR spectrum of **32** in D_2O (700 MHz, 25 °C).
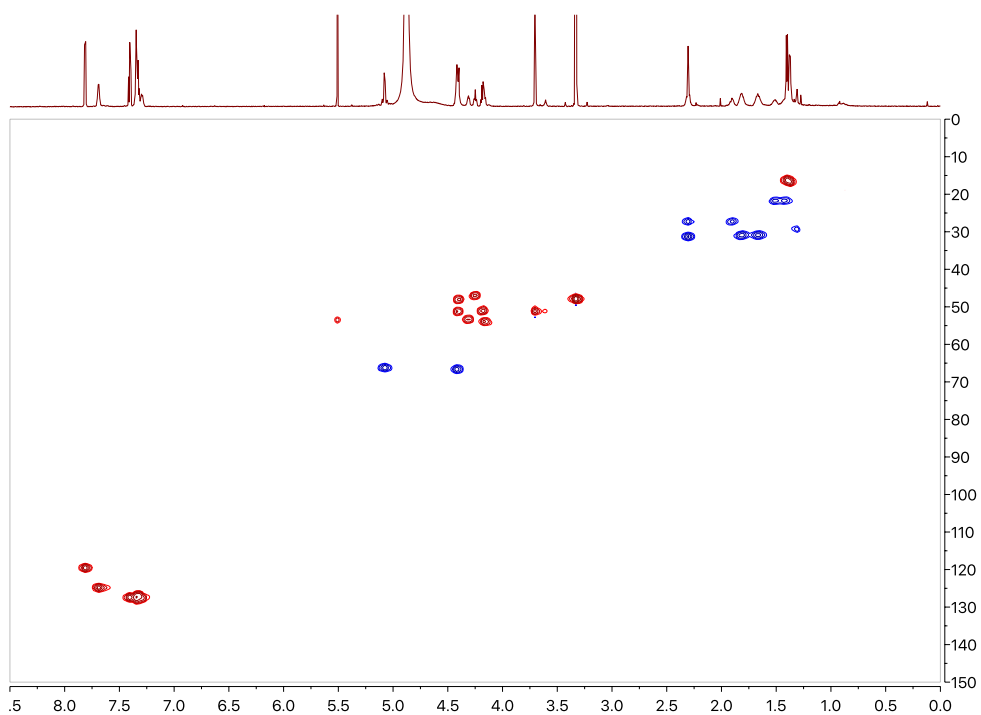
Figure 10. HSQC spectrum of **32** in D_2O (25 °C).

115
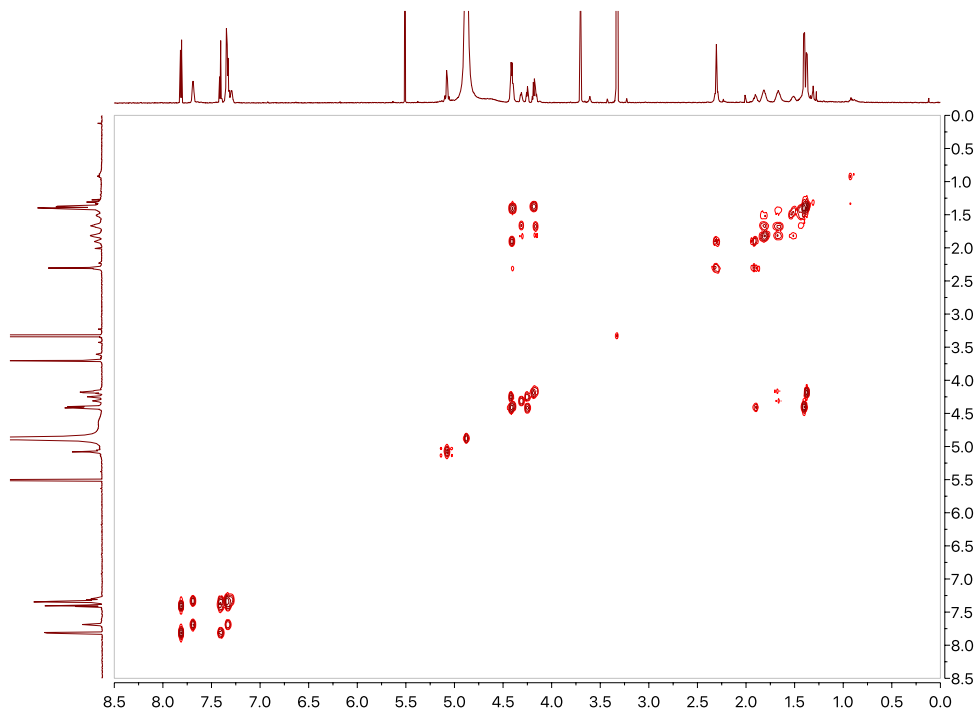
Figure 11. COSY spectrum of **32** in D₂O (25 °C).
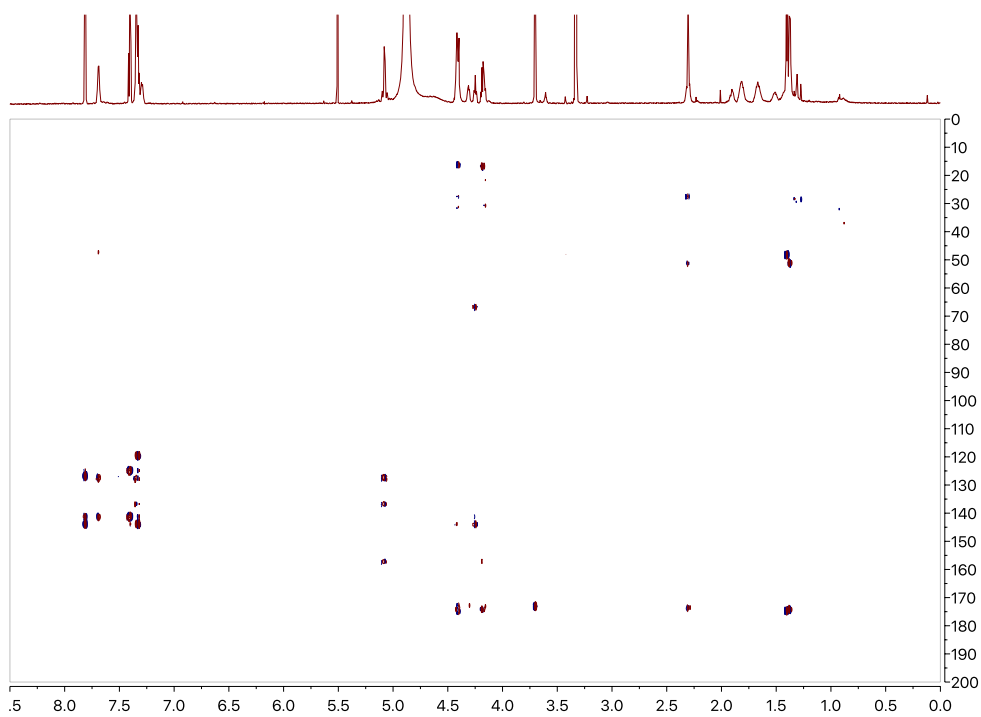
Figure 12. HMBC spectrum of **32** in D₂O (25 °C).
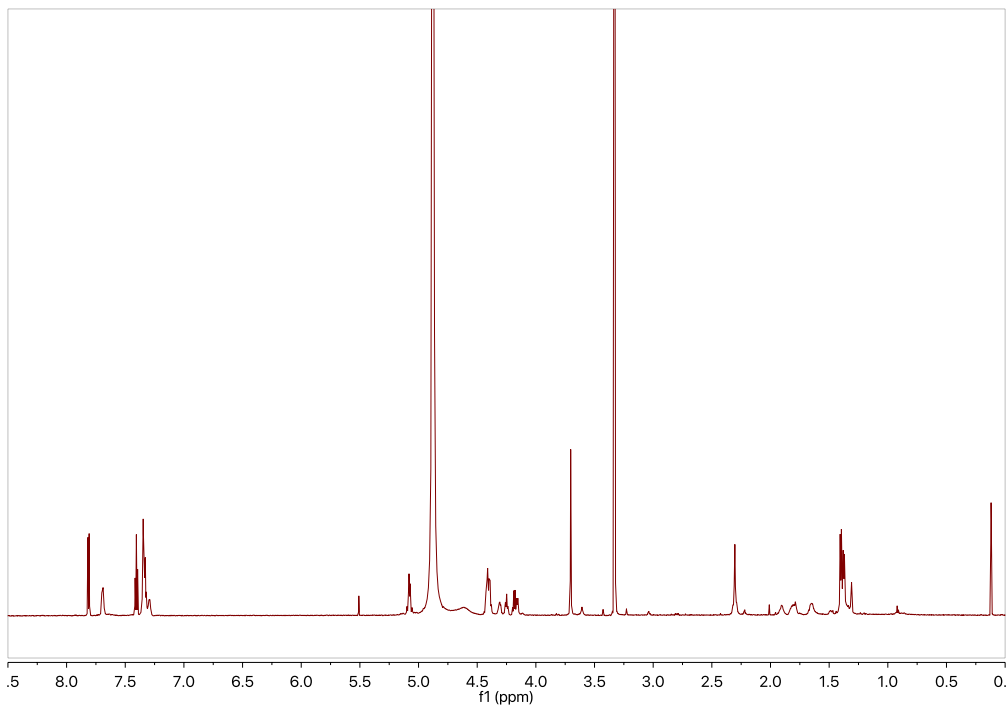
Figure 13. ^{1}H NMR spectrum of (^{2}H$_2$)**32** in D$_2$O (700 MHz, 25 °C).
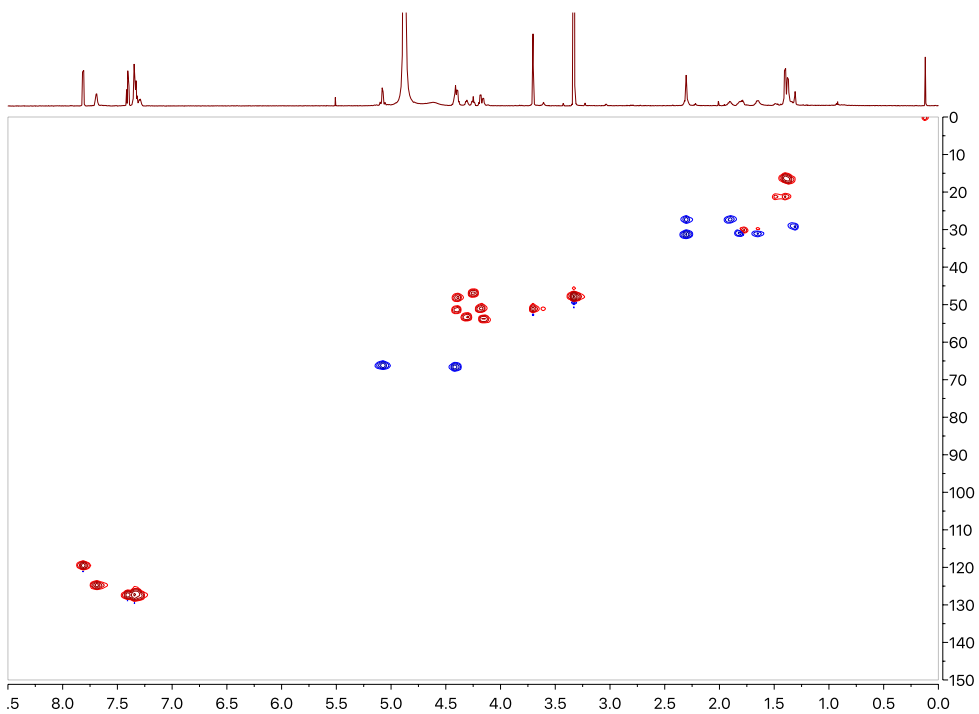
Figure 14. HSQC spectrum of (^{2}H$_2$)**32** in D$_2$O (25 °C).
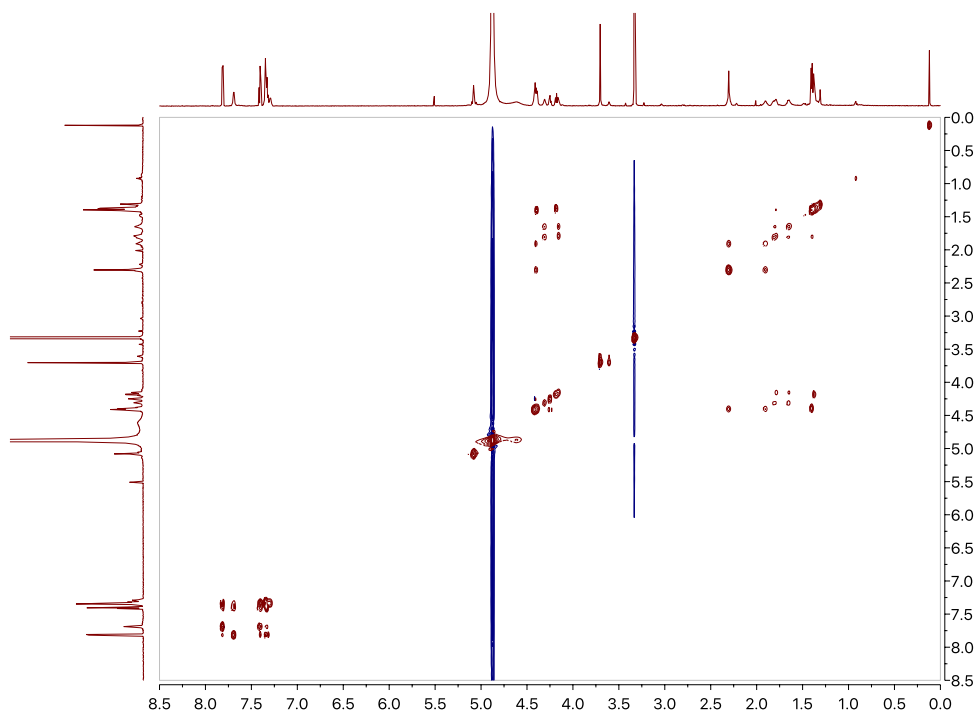
Figure 15. COSY spectrum of (^{2}H$_2$)**32** in D$_2$O (25 °C).
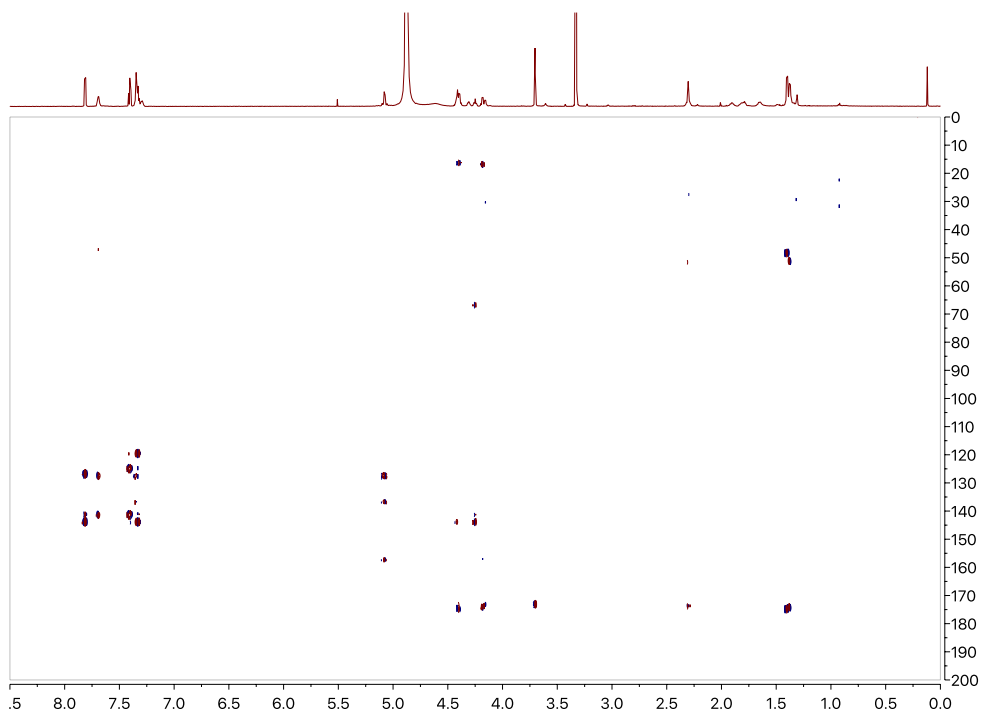
Figure 16. HMBC spectrum of (^{2}H$_2$)**32** in D$_2$O (25 °C).
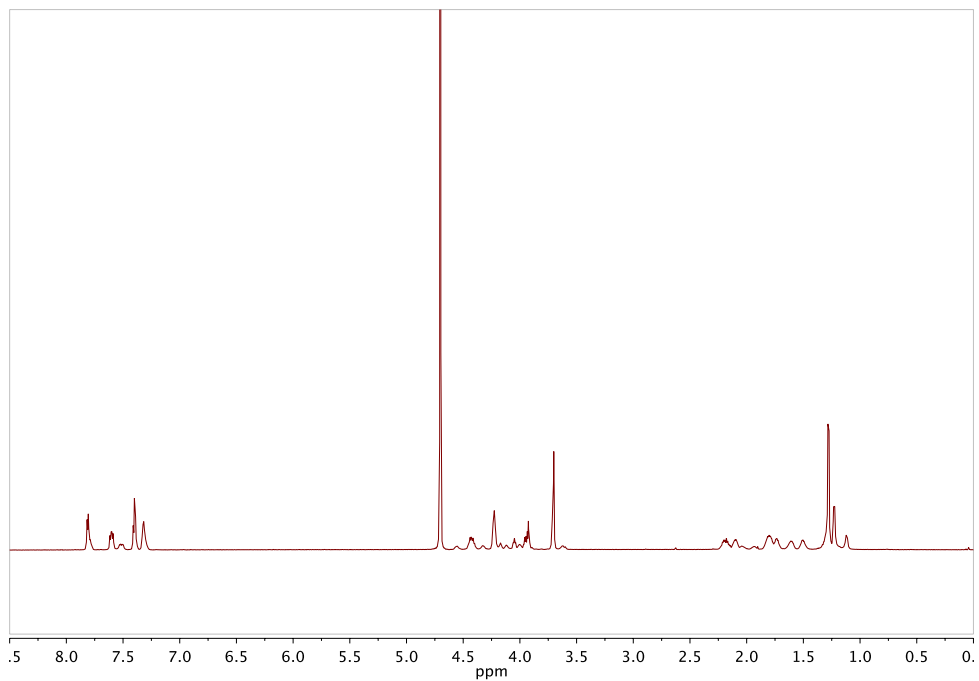
Figure 17. ^{1}H NMR spectrum of **33** in D$_2$O (700 MHz, 25 °C).
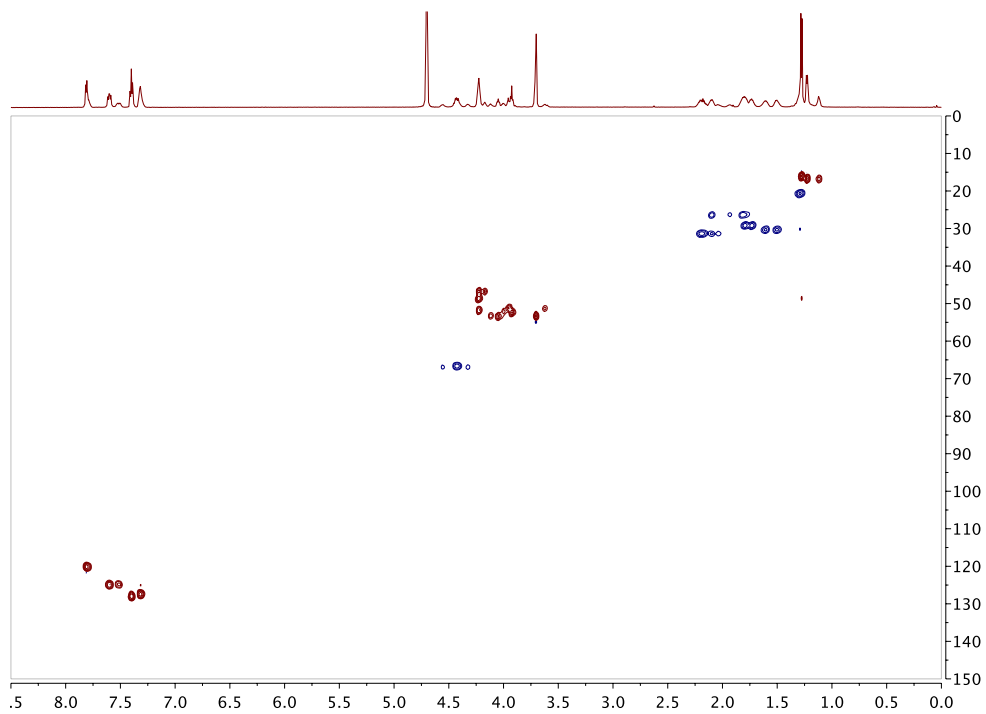
Figure 18. HSQC spectrum of **33** in D$_2$O (25 °C).

119
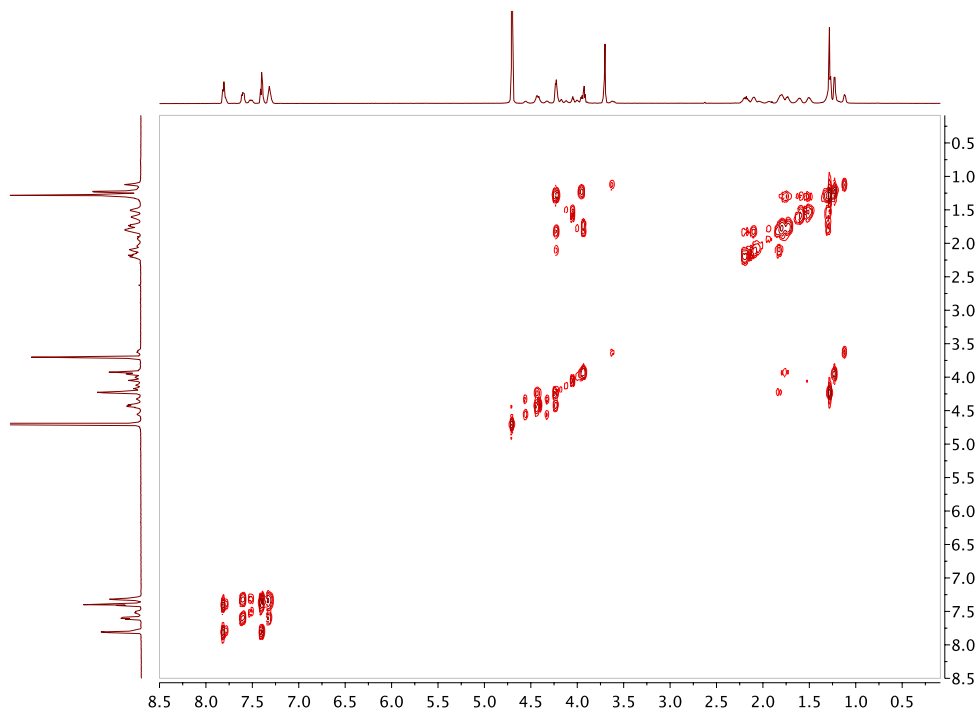
Figure 19. COSY spectrum of **33** in D$_2$O (25 °C).
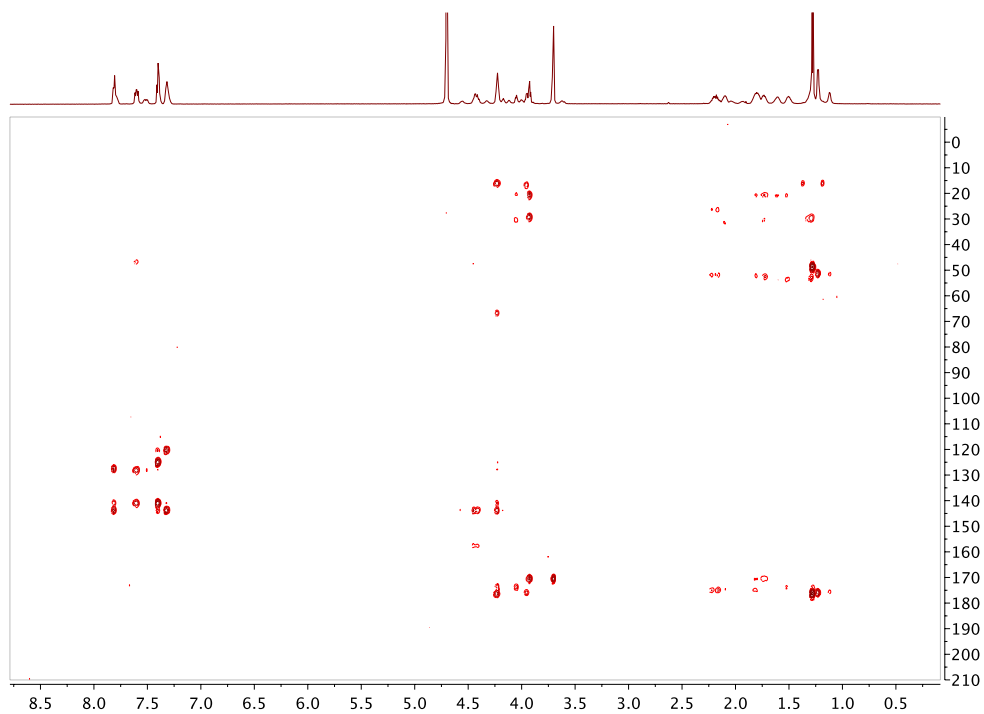
Figure 20. HMBC spectrum of **33** in D$_2$O (25 °C).
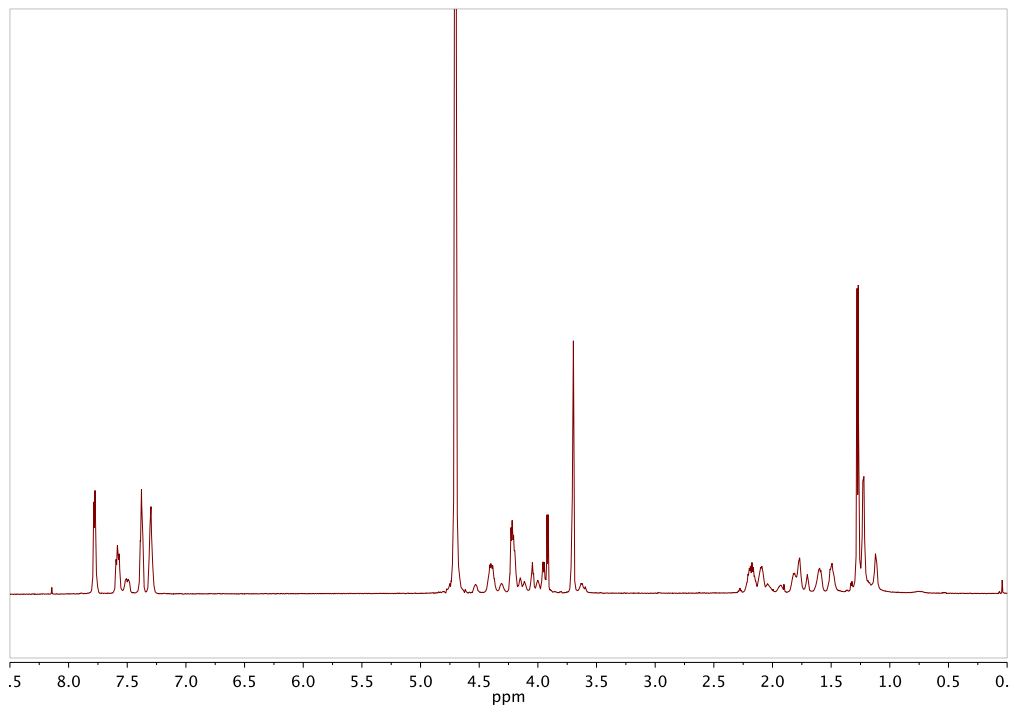
Figure 21. ^{1}H NMR spectrum of (^{2}H$_2$)**33** in D$_2$O (700 MHz, 25 °C).
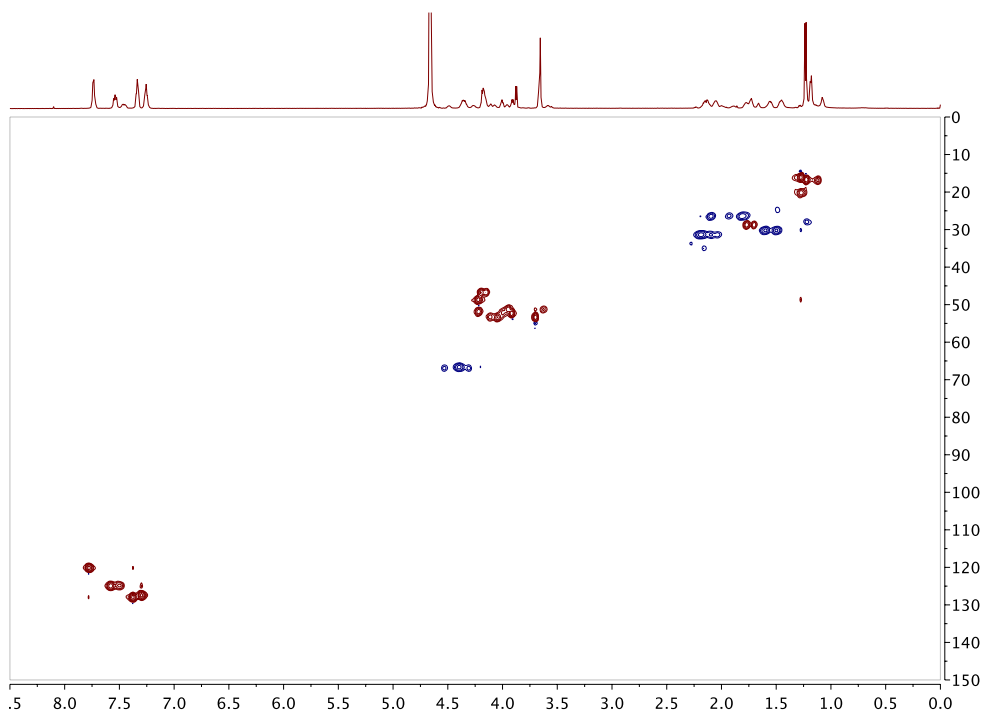
Figure 22. HSQC spectrum of (^{2}H$_2$)**33** in D$_2$O (25 °C).
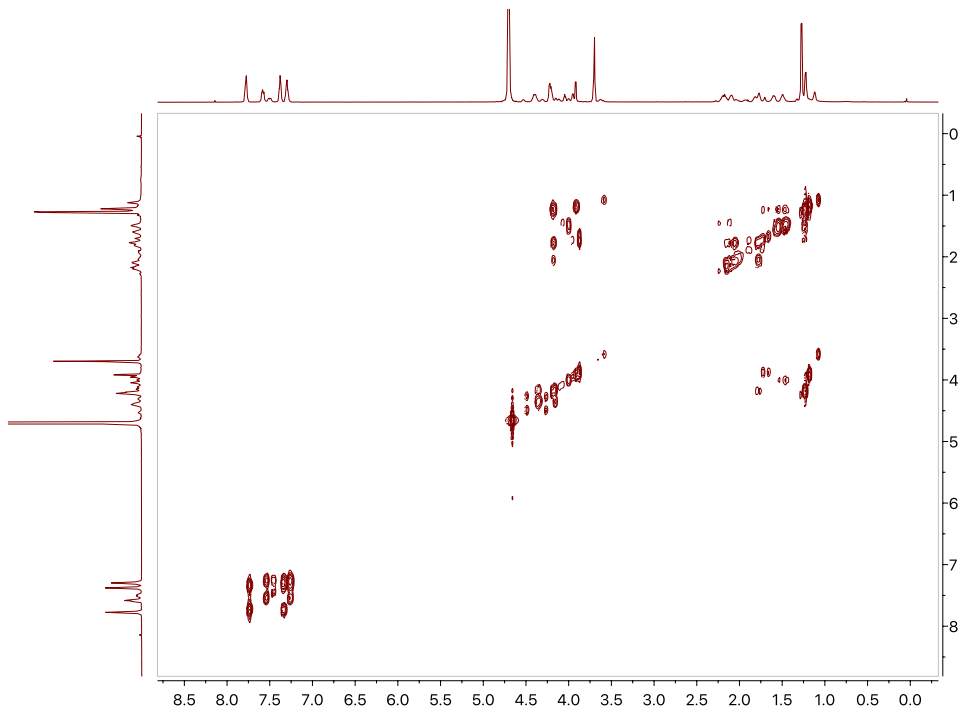
Figure 23. COSY spectrum of (^{2}H$_2$)**33** in D$_2$O (25 °C).
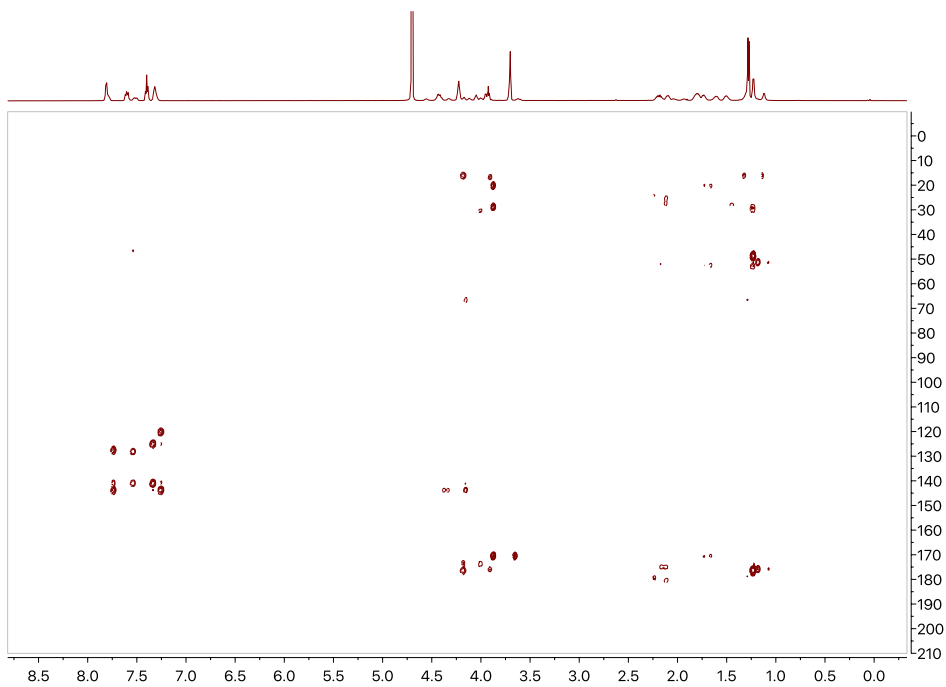
Figure 24. HMBC spectrum of (^{2}H$_2$)**33** in D$_2$O (25 °C).

Chapter VII

Article

COMMUNICATION

Continuous-flow thermolysis for the preparation of vinylglycine derivatives†

Nicolas Lamborelle,[a,b] Justine F. Simon,[b] André Luxen[b] and
Jean-Christophe M. Monbaliu*[a]

Syn sulfoxide elimination was carried out under continuous-flow conditions in a mesofluidic thermolysis reactor. The design of the reactor enabled accurate control of reaction time and conditions, affording a convenient scale-independent procedure for the production of *N,C*-protected vinylglycine derivatives. Thermolysis at 270 °C under 1000 psi of pressure in superheated toluene enabled typical daily outputs ranging from 11 to 46 g per day with excellent selectivities and ee (>97%). The various competitive reaction pathways were studied and rationalized according to a computational study.

Introduction

Vinylglycine (VG) is the simplest but the most widely studied natural non-proteinogenic β,γ-unsaturated amino acid.[1] D-VG is produced by the mushroom *Rhodophyllus nidorosus*, while L-VG is a common metabolite or mechanistic intermediate produced in a variety of pyridoxal phosphate enzymatic processes.[1] VG displays a wide range of biological activities such as transaminase inhibition and antibacterial properties.[1] Consequently, VG and its derivatives have attracted considerable attention from synthetic chemists. A plethora of synthetic strategies to produce VG have flourished since 1977[2] starting from methionine,[3] serine,[4] homoserine,[5] homocysteine,[6] mannitol,[7] xylose,[8] aspartic acid,[9] glutamic acid,[10] or other building blocks.[11] Either stereoselective or racemic strategies, possibly followed by enzymatic resolution, have been reported and reviewed.[1,3d,6] VG and derivatives have also found utility as chiral building blocks for accessing diverse and complex molecular architectures.[1,12]

Among the wide variety of strategies developed for the synthesis of VG derivatives, the most straightforward one involves

[a]*Center for Integrated Technology and Organic Synthesis, Department of Chemistry, University of Liège, 4000 Liège, Belgium. E-mail: jc.monbaliu@ulg.ac.be*
[b]*Cyclotron Research Centre, University of Liège, 4000 Liège, Belgium*
†Electronic supplementary information (ESI) available: Typical procedure for continuous-flow thermolysis, experimental and computational details. See DOI: 10.1039/c5ob02036k

the thermolysis of methionine sulfoxide (MetO) derivatives. This strategy, however, usually requires high temperatures and vacuum, and is hampered by extensive isomerization and degradation. Quintard *et al.* reported a scalable process for the large-scale thermolysis of sulfoxides derived from *N*-Cbz-L-methionine methyl ester in batch.[3d] They reproduced the original procedure reported by Rapoport in a Kugelrhor distillation apparatus,[3a] but faced significant amounts of dehydrobutyrine isomers among other side products; after optimization, the thermolysis was performed in batch in refluxing mesitylene. Typically, 48 h were required to process 16.5 g of *N*-Cbz-L-methionine sulfoxide methyl ester (77%). The control of the temperature and the reaction time are paramount for achieving high conversion and selectivity for this reaction, but other parameters have also a significant impact on the reaction outcome such as additives and solvent nature.[3a,b,d,6] Long *et al.* studied the impact of the nature of the sulfoxide on the thermolysis step by considering various alkyl and aryl homocysteine sulfoxides. The 2-nitrophenyl analog underwent *syn* elimination in refluxing toluene for 18 h.[6] Longer reaction times, or higher boiling point solvents increased the isomerisation of vinylglycine towards its dehydrobutyrine isomers. Despite promising results, this method suffers from long reaction time and requires less common homocysteine derivatives.

Continuous-flow chemical processing, *i.e.* chemical processes carried out in continuous-flow micro- and mesostructured reactors (μFRs), has emerged over the last decade as an economically viable alternative to batch reactors for a wide variety of synthetic applications.[13] They enable the continuous production of commodity and specialty chemicals according to a more reliable, reproducible, efficient and flexible manufacturing strategy.[14] μFRs offer a wide range of advantages for performing organic transformations, even under intensified[15] or extreme conditions (temperature, pressure):[16] precise control over local temperature conditions, fast mixing, inherent safety and homogeneity of the production are amongst the most important.[17]

In this work, we report a scale-independent continuous-flow process for the stereoselective thermolysis of MetO

derivatives. The *syn* sulfoxide elimination required less than 2 min to reach 99% conversion in a mesofluidic continuous-flow device at 270 °C under 1000 psi of pressure (69 bar), using superheated toluene and in the presence of a methyl-sulfenic acid scavenger. The procedure conveniently sustains the production of up to 46 g per day of VG derivatives, and is compatible with a variety of *N,C*-protecting groups. We also provide a computational rationalization of the competitive reaction pathways leading to the formation of the main impurities, *i.e.* the *E,Z*-dehydrobutyrine isomers.

Results and discussion

N,C-Protected L- or D-methionine derivatives were prepared from commercial L- or D-methionine, and then oxidized towards the corresponding MetO derivatives **1a–g** using NaIO$_4$ according to literature procedures.[3a,b,d,6] Common protecting groups were selected for this library of MetO derivatives: Cbz (L-,D-**1a** and L-**1e**), Boc (L-**1b**), Fmoc (L-**1c** and L-**1f**), NBOC (L-**1d** and L-**1g**) and methyl (**1a–d**) or benzyl (**1e–g**) esters for N- and C-termini protection, respectively (Scheme 1).

Flash thermolysis was carried out in a mesofluidic device consisting of a temperature-regulated oven embedded with a SS coil reactor (OD 1/16″, ID 500 μm, V_{int} = 1.7 mL) (Scheme 1). The reactor setup enabled fast reaction parameters screening, *i.e.* temperature and residence time. The pressure was set at 1000 psi (69 bar) to enable superheated conditions inside the reactor. The reactor effluent was cooled to 10 °C, collected and then analyzed (off-line HPLC). The operational parameters were optimized on compound L-**1a** (feed concentration 10 g L^{-1}). Various solvents were tested, but the best results were obtained from experiments carried out in toluene;[6] besides, toluene eased downstream purification (see below).

The impact of both the temperature and the residence time (ranging from 34 s to 1.7 min) inside the thermolysis reactor are summarized in Fig. 1 (entries 1–3, 10–12, 19–21). Higher temperatures and longer residence times increased the conversion of compound L-**1a** (calculated on the residual amount of L-**1a** in the crude mixture). The conversion with a 5 mL min^{-1} flow rate was 46, 86 and 98% at 250, 270 and 290 °C, respectively, while with a 1 mL min^{-1} flow rate, the conversion
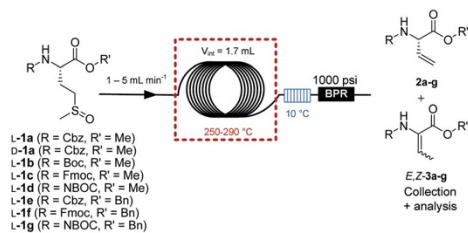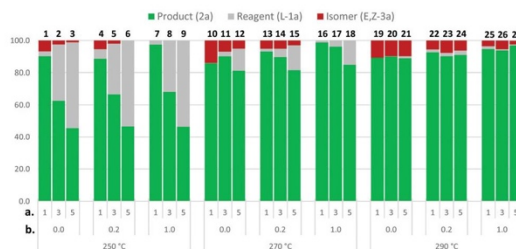
Fig. 1 Composition of the crude reactor effluents (HPLC values, %) and optimization of the continuous-flow thermolysis on MetO derivative L-**1a**. ((a) flow rates, mL min^{-1}; (b) equiv. DMAD).

increased to 97, 99 and >99% at 250, 270 and 290 °C, respectively (entries 1–3, 10–12 and 19–21). The product ratio (**2a**/*E,Z*-**3a**) was also significantly affected by the temperature and the residence time. At 250 and 270 °C, a larger amount of *E,Z*-**3a** was observed at longer residence times, and this amount increased with the temperature as well (entries 1–3 and 10–12). Such observations are consistent with previous literature reports.[3a,b,d,6]

At 290 °C, the effect of the temperature on the appearance of *E,Z*-**3a** dominated the effect of the residence time (Fig. 1, entries 19–21). Since the *E,Z*-dehydrobutyrine isomers are difficult to separate from vinylglycine, their formation is still problematic.[6] Based on this preliminary study, an acceptable compromise between good conversion and low *E,Z*-**3a** contamination required 270 °C, 5 mL min^{-1} flow rate and 34 s residence time (Fig. 1, entry 12), in which case the daily productivity of VG derivative reached 46 g per day.

Preliminary tests for accessing larger scales of VG derivatives ruled out a scaling-out approach.[13] The thermolysis of L-**1a** in a larger internal-diameter continuous-flow reactor led to a significant decrease of the conversion, most likely as a consequence of the appearance of temperature gradients across the section of the reactor.

A liquid–liquid extraction and separation module (Fig. 2) was implemented after the reactor to eliminate the residual sulfoxide L-**1a** in the aqueous waste, while redirecting the organic stream for further purification. Attempts to remove the *E,Z*-**3a** isomers using an in-line cartridge filled with supported scavengers such as silica-adsorbed cysteamine failed, leading
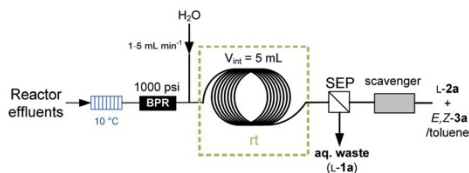

Scheme 1 Continuous-flow thermolysis of methionine derivatives **1a–g**.

Fig. 2 In-line purification with an extraction/separation module.

This journal is © The Royal Society of Chemistry 2015

Org. Biomol. Chem., 2015, **13**, 11602–11606 | **11603**

to increased amounts of E,Z-**3a** by base-catalyzed isomerization of vinylglycine **2a**.[18]

In order to improve the efficiency of the thermolysis and to get a complete picture of the competitive reaction pathways, a computational study was undertaken. Computations were performed at the B3LYP/6-31+G* level of theory to rationalize the formation of dehydrobutyrine isomers E,Z-**3**, and the corresponding results are presented in Fig. 3. The initial thermolysis from a model MetO derivative **1** to vinylglycine derivative **2** proceeds with an activation barrier of 25.2 kcal mol^{-1}, and is an endothermic reaction (ΔH° = 6.6 kcal mol^{-1}). The direct isomerization of compound **2** towards dehydrobutyrine derivatives E,Z-**3** through a thermal [1,3]-shift has a high activation barrier (69.4 kcal mol^{-1}), and is an exothermic reaction (ΔH° = −6.5 kcal mol^{-1}). The high activation barrier can be correlated with the increased amount of dehydrobutyrine isomers at higher temperatures.[3a,b,d,6] However, the natural by-product of the reaction, *i.e.* methylsulfenic acid (MeSOH), and its confined presence with vinylglycine triggers a much more favorable pathway towards dehydrobutyrine isomers. This competitive route proceeds through the formation of Markovnikov adduct **4** (ΔG^{TS} = 22.0 kcal mol^{-1}), which then undergoes thermolysis towards dehydrobutyrine derivatives E,Z-**3** (ΔG^{TS} = 17.8 kcal mol^{-1}). These results emphasize that in a confined system or without proper quench to suppress methylsulfenic acid, a more favorable competitive reaction path takes place and eventually leads to significant contamination with dehydrobutyrine isomers. Last, the epimerization from L- to D-vinylglycine proceeds under these conditions through a [1,3]-shift with a very high activation barrier (see ESI†). This is to be correlated with the low epimerization observed under these conditions.

From these results, we expected that proper *in situ* quenching of methylsulfenic acid would suppress the formation of Markovnikov adduct **4**, and hence its thermolysis towards E,Z-**3**. A variety of sulfenic acid scavengers have been previously reported,[3b,6,19] but few are compatible with a development in a continuous-flow mesofluidic thermolysis reactor. Dimethyl acetylenedicarboxylate (DMAD) attracted our attention since it is a strong electrophile with a good tolerance to high temperatures, and it was successfully used in the past for quenching
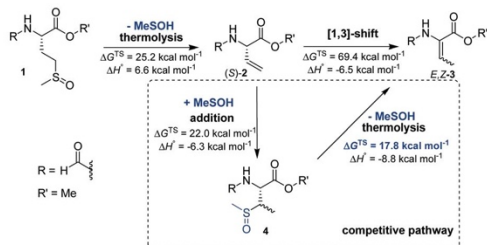
Table 1 Thermolysis of MetO derivatives L-**1b−g** [a]

	Residual **1b–g** (%)	**2b–g** (%)	E,Z-**3a–g** (%)
1b[b]		Decomposition	
1c[b]	2	98	—
1d[c]	2	98	—
1e[b]	1	99	—
1f[b]	2	98	—
1g[b]	3	97	—

[a] HPLC conversion. [b] 10 g L^{-1} feed solution. [c] 5 g L^{-1} feed solution.

sulfenic acids.[19] The results of the thermolysis of L-**1a** in the presence of substoichiometric (0.2 equiv.) or stoichiometric amounts of DMAD are presented in Fig. 1 (entries 4–9, 13–18, 22–27). The experiments at 250 and 270 °C showed that 1 equivalent of DMAD suppressed the formation of the dehydrobutyrine isomers at the shortest residence times (Fig. 1, entries 9 and 18). At 290 °C, up to 5.5% dehydrobutyrine isomers were still present in the crude mixture, despite the presence of DMAD. These results suggest that at higher temperatures, the competitive thermal [1,3]-isomerization is most likely the predominant pathway leading to the formation of the dehydrobutyrine isomers, while at lower temperatures (270 °C), the predominant isomerization pathway involves methylsulfenic acid.

With the in-line quench of methylsulfenic acid, the best conditions for the thermolysis of L-**1a** required 270 °C, 1 mL min^{-1} flow rate and 1.7 min residence time (Fig. 1, entry 16) with 99% conversion.[20] The remaining traces of L-**1a** could be efficiently removed using the in-line extraction/separation module described in Fig. 2, or by chromatography on silica gel. The Michael adduct from the mono-addition of methylsulfenic acid on DMAD could be easily removed from the crude vinylglycine samples by chromatography on silica gel. The enantiomeric excess was determined by HPLC and was consistently >97%. Similar results were observed in the D-series.

Next, we transposed the optimized conditions for the thermolysis of substrates **1b–g** (Table 1). The thermolysis of substrate L-**1b** failed and led to complete decomposition, as expected from the literature results.[12o] As summarized in Table 1, the thermolysis of derivatives **1c–1g** proceeded with excellent selectivity. The residual sulfoxide (1–3%) was removed by liquid–liquid extraction with water (see Fig. 2).

Conclusions

In summary, we have developed a convenient, scale-independent and highly-selective procedure for the continuous-flow preparation of VG derivatives using superheated toluene. The successful development of this continuous-flow process relied on a computational rationalization of the various competitive reaction pathways. The competitive formation of dehydrobutyrine derivatives was suppressed with the *in situ* quenching

Fig. 3 Competitive reaction pathways computed at the B3LYP/6-31+G* level of theory.

11604 | *Org. Biomol. Chem.*, 2015, **13**, 11602–11606

This journal is © The Royal Society of Chemistry 2015

of the thermolysis by-product methylsulfenic acid. The implementation of an in-line liquid–liquid membrane separator enabled the integration of downstream purification.

Acknowledgements

Notes and references

1 D. B. Berkowitz, B. D. Charette, K. R. Karukurichi and J. M. McFadden, *Tetrahedron: Asymmetry*, 2006, **17**, 869–882.
2 J. E. Baldwin, S. B. Haber, C. Hoskins and L. I. Kruse, *J. Org. Chem.*, 1977, **42**, 1239–1241.
3 (a) A. Afzali-Ardakani and H. Rapoport, *J. Org. Chem.*, 1980, **45**, 4817–4820; (b) P. Meffre, L. Vo-Quang, Y. Vo-Quang and F. Le Goffic, *Synth. Commun.*, 1989, **19**, 3457–3468; (c) A. G. Griesbeck and J. Hirt, *Liebigs Ann.*, 1995, 1957–1961; (d) A. Lumbroso, V. Coeffard, E. Le Grognec, I. Beaudet and J. P. Quintard, *Tetrahedron Lett.*, 2010, **51**, 3226–3228.
4 (a) P. L. Beaulieu, J.-S. Duceppe and C. Johnson, *J. Org. Chem.*, 1991, **56**, 4196–4204; (b) N. G. W. Rose, M. A. Blaskovich, A. Wong and G. A. Lajoie, *Tetrahedron*, 2001, **57**, 1497–1507.
5 (a) R. Pellicciari, B. Natalini and M. Marinozzi, *Synth. Commun.*, 1988, **18**, 1715–1721; (b) D. B. Berkowitz and M. K. Smith, *Synthesis*, 1996, 39–41.
6 S. K. Patel and T. E. Long, *Tetrahedron Lett.*, 2009, **50**, 5067–5070.
7 (a) J. Mulzer, A. Angermann, B. Schubert and C. Seilz, *J. Org. Chem.*, 1986, **51**, 5294–5299; (b) R. Badorrey, C. Cativiela, M. D. Díaz-de-Villegas and J. A. Gálvez, *Synthesis*, 1997, 747–749.
8 S. Chandrasekhar, A. Raza and M. Takhi, *Tetrahedron: Asymmetry*, 2002, **13**, 423–428.
9 P. Wipf, W. Xu, H. Kim and H. Takahashi, *Tetrahedron*, 1997, **53**, 16575–16596.
10 (a) S. Hanessian and S. P. Sahoo, *Tetrahedron Lett.*, 1984, **25**, 1425–1428; (b) D. H. R. Barton, D. Crich, Y. Hervé, P. Potier and J. Thierry, *Tetrahedron*, 1985, **41**, 4347–4357; (c) W. J. Krol, S.-S. Mao, D. L. Steele and C. A. Townsend, *J. Org. Chem.*, 1991, **56**, 728–731.
11 (a) P. F. Hudrlik and A. K. Kulkarni, *J. Am. Chem. Soc.*, 1981, **103**, 6251–6253; (b) U. Schöllkopf, J. Nozulak and U. Groth, *Tetrahedron*, 1984, **40**, 1409–1417; (c) D. M. Vyas, Y. Chiang and T. W. Doyle, *J. Org. Chem.*, 1984, **49**,

2037–2039; (d) W. J. Greenlee, *J. Org. Chem.*, 1984, **49**, 2632–2634; (e) A. L. Castelhano, S. Horne, R. Billedeau and A. Krantz, *Tetrahedron Lett.*, 1986, **27**, 2435–2438; (f) S. Sewada, T. Nakayama, N. Esaki, H. Tanaka, K. Soda and R. K. Hill, *J. Org. Chem.*, 1986, **51**, 3384–3386; (g) A. L. Castelhano, S. Horne, G. J. Taylor, R. Billedeau and A. Krantz, *Tetrahedron*, 1988, **44**, 5451–5466; (h) R. W. Williams and W. Zhai, *Tetrahedron*, 1988, **44**, 5425–5430; (i) T. Hayashi, A. Yamamoto and Y. Ito, *Tetrahedron Lett.*, 1988, **29**, 99–102; (j) L. Duhamel, P. Duhamel, S. Fouquay, J. J. Eddine, O. Peschard, J.-C. Plaquevent, A. Ravard, R. Solliard, J.-Y. Valnot and H. Vincens, *Tetrahedron*, 1988, **44**, 5495–5506; (k) K. O. Hallinan, D. H. G. Crout and W. Errington, *J. Chem. Soc., Perkin Trans. 1*, 1994, 3537–3543; (l) B. M. Trost, R. C. Bunt, R. C. Lemoine and T. L. Calkins, *J. Am. Chem. Soc.*, 2000, **122**, 5968–5976; (m) G. Delle Monache, D. Misiti, P. Salvatore and G. Zappia, *Chirality*, 2000, **12**, 143–148; (n) H. Acherki, C. Alvarez-Ibarra, G. García-Navazo, E. Gómez-Sánchez and M. L. Quiroga-Feijóo, *Tetrahedron: Asymmetry*, 2004, **15**, 3419–3426; (o) D. B. Berkowitz and G. Maiti, *Org. Lett.*, 2004, **6**, 2661–2664; (p) F. Palacios, J. Vicario and D. Aparicio, *J. Org. Chem.*, 2006, **71**, 7690–7696.
12 (a) N. Tokutake, J. Hiratake, M. Katoh, T. Irie, H. Kato and J. Oda, *Bioorg. Med. Chem.*, 1998, **6**, 1935–1953; (b) D. B. Berkowitz, J. M. McFadden and M. K. Sloss, *J. Org. Chem.*, 2000, **65**, 2907–2918; (c) D. B. Berkowitz, E. Chisowa and J. M. McFadden, *Tetrahedron*, 2001, **57**, 6329–6343; (d) D. M. Bartley and J. K. Coward, *J. Org. Chem.*, 2005, **70**, 6757–6774; (e) E. G. Nolen, A. J. Kurish, J. M. Potter, L. A. Donahue and M. D. Orlando, *Org. Lett.*, 2005, **7**, 3383–3386; (f) F. W. Schmidtmann, T. E. Benedum and G. J. McGarvey, *Tetrahedron Lett.*, 2005, **46**, 4677–4681; (g) A. R. Chowdhury and G. J. Boons, *Tetrahedron Lett.*, 2005, **46**, 1675–1678; (h) H. M. E. Duggan, P. B. Hitchcock and D. W. Young, *Org. Biomol. Chem.*, 2005, **3**, 2287–2295; (i) J. Kaiser, S. S. Kinderman, B. C. J. van Esseveldt, F. L. van Delft, H. E. Schoemaker, R. H. Blaauw and F. P. J. T. Rutjes, *Org. Biomol. Chem.*, 2005, **3**, 3435–3467; (j) C. Nájera and J. M. Sansano, *Org. Biomol. Chem.*, 2009, **7**, 4567–4581; (k) Y. Goto, K. Iwasaki, K. Torikai, H. Murakami and H. Suga, *Chem. Commun.*, 2009, 3419–3421; (l) Ž. Jakopin, M. Gobec, J. Kodela, T. Hazdovac, I. Mlinarič-Raščan and M. Sollner Dolenc, *Eur. J. Med. Chem.*, 2013, **69**, 232–243; (m) M. D. Lebar, T. J. Lupoli, H. Tsukamoto, J. M. May, S. Walker and D. Kahne, *J. Am. Chem. Soc.*, 2013, **135**, 4632–4635; (n) M. D. Lebar, J. M. May, A. J. Meeske, S. A. Leiman, T. J. Lupoli, H. Tsukamoto, R. Losick, D. Z. Rudner, S. Walker and D. Kahne, *J. Am. Chem. Soc.*, 2014, **136**, 10874–10877; (o) A. K. Ghosh and K. Lv, *Eur. J. Org. Chem.*, 2014, 6761–6768; (p) B. Commare, D. Rigault, I. A. Lemasson, P. Deschamps, A. Tomas, P. Roussel, I. Brabet, C. Goudet, J.-P. Pin, F. R. Leroux, F. Colobert and F. C. Acher, *Org. Biomol. Chem.*, 2015, **13**, 1106–1112.

This journal is © The Royal Society of Chemistry 2015

Org. Biomol. Chem., 2015, **13**, 11602–11606 | **11605**

13 *Micro Reaction Technology in Organic Synthesis*, ed. C. Wiles and P. Watts, CRC Press Taylor and Francis Group, Boca Raton Fl., 2011.

14 (*a*) D. R. Snead and T. F. Jamison, *Chem. Sci.*, 2013, **4**, 2822–2827; (*b*) D. R. Snead and T. F. Jamison, *Angew. Chem., Int. Ed.*, 2015, **54**, 983–987.

15 V. Hessel, D. Kralisch, N. Kockmann, T. Noël and Q. Wang, *ChemSusChem*, 2013, **6**, 746–789.

16 Representative examples of continuous-flow processes under extreme temperature/pressure conditions: (*a*) B. Gutmann, J.-P. Roduit, D. Roberge and C. O. Kappe, *Angew. Chem., Int. Ed.*, 2010, **49**, 7101–7105; (*b*) T. N. Glasnov and C. O. Kappe, *Chem. – Eur. J.*, 2011, **17**, 11956–11968; (*c*) M. Damm, B. Gutmann and C. O. Kappe, *ChemSusChem*, 2013, **6**, 978–982; (*d*) B. Reichart, G. Tekautz and C. O. Kappe, *Org. Process Res. Dev.*, 2013, **17**, 152–157.

17 (*a*) R. L. Hartman, J. P. McMullen and K. F. Jensen, *Angew. Chem., Int. Ed.*, 2011, **50**, 7502–7519; (*b*) K. S. Elvira, X. Casadevall i Solvas, R. C. R. Wootton and A. J. DeMello, *Nat. Chem.*, 2013, **5**, 905–915.

18 Y. Zhu, M. D. Gieselman, H. Zhou, O. Averin and W. A. van der Donk, *Org. Biomol. Chem.*, 2003, **1**, 3304–3315.

19 (*a*) S. Menichetti, M. C. Aversa, P. Bonaccorsi, G. Lamanna and A. Moraru, *J. Sulfur Chem.*, 2006, **27**, 393–400; (*b*) M. C. Aversa, A. Barattucci, P. Bonaccorsi, P. Giannetto and S. S. Agata, *Curr. Org. Chem.*, 2007, **11**, 1034–1052; (*c*) V. Gupta and K. S. Carroll, *Biochim. Biophys. Acta*, 2014, **1840**, 847–875.

20 Typical procedure: a feed solution of L-**1a** (10 g L^{-1}) and DMAD (1.0 equiv.) was prepared in toluene, and conveyed to the thermolysis reactor (T = 270 °C, back pressure P = 1000 psi) *via* a HPLC pump set at 1 mL min^{-1}, with a 1.7 min residence time in the thermolysis reactor. The reactor effluents were directed to a waste tank until the reactor reached steady state. After 5 min, the reactor effluents were collected and sampled every 10 min for analysis (HPLC). Continuous liquid–liquid extraction: the reactor effluent was cooled down to 10 °C and mixed with a stream of water (1 mL min^{-1}) and directed to an extraction/separation module consisting of a tubular PFA reactor (5 mL internal volume, 1/8″ o.d.) and a continuous-flow liquid–liquid membrane separator (Zaiput Flow Technologies®). The aqueous stream was connected to a waste tank, and the organic (toluene) stream was collected and analyzed.

11606 | *Org. Biomol. Chem.*, 2015, **13**, 11602–11606

This journal is © The Royal Society of Chemistry 2015

Continuous-Flow Thermolysis for the

Preparation of Vinylglycine Derivatives

Nicolas Lamborelle,[a,b] Justine F. Simon,[b] André Luxen[b] and

Jean-Christophe M. Monbaliu[a,*]

[a.] *Center for Integrated Technology and Organic Synthesis, Department of Chemistry, University of Liège, 4000 Liège, Belgium*
[b.] *Cyclotron Research Centre, University of Liège, 4000 Liège, Belgium*
E-mail: jc.monbaliu@ulg.ac.be

Supporting Information

Contents

1.   Experimental section

Compounds **1a-c** and **1e-g** were synthesized according to reported procedures. [S1] The preparation and characterization of compounds L-**1d** and **L-2d** are described hereafter.

1.1   Continuous-flow setup

1.1.1   Pumps

FLOM HPLC pumps (Intelligent Pump AI 12 Series) were selected for handling the feed solutions of compounds **1a-g** and the extraction solvent (water).

1.1.2   Connectors, ferrules and tubing

PFA/PEEK tubing, and PEEK/ETFE connectors and ferrules were utilized for the sections of the reactor exposed to low temperature and pressure (feed inlets, extraction module). SS tubing, connectors and ferrules were utilized for the sections of the reactor exposed to high temperature and pressure (Table S1).

Table S1. Tubing, Junctions, Nuts and Ferules

Equipment	Material	Specifications
Tubing	High-purity PFA tubing	1/16'' i.d., 1/8" o.d.
	PEEK tubing	1/32" i.d., 1/16" o.d.
	SS tubing	500 µm i.d., 1/16" o.d.
Mixers	Upchurch Scientific Tee, natural PEEK	1/4-28 thread for 1/8" o.d. tubing, 0.05" (1.25 mm) thru hole
Nuts	Upchurch Scientific Super Flangeless Nuts, natural PEEK	1/4-28 thread for 1/8" o.d. tubing; 1/4-28 thread for 1/16" o.d. tubing
	Upchurch Scientific fingertight Nuts, natural PEEK	10/32 thread for 1/16" o.d. tubing
	SS Valco internal nut	For 1/16" o.d. tubing
Ferrules	Upchurch Scientific Super Flangeless Ferrules, yellow ETFE	1/8" and 1/16" o.d. tubing
	Valco Type 303 stainless ferrules	For 1/16" o.d. tubing
Unions	SS Valco internal unions	1/16'' standard with 0.15 mm bore

1.1.3 Back pressure regulators

Upchurch Scientific back pressure regulators (BPRs) were utilized. 250 PSI BPRs were inserted after the pressure transducer of the HPLC pumps to ensure steady pump operation. A 1000 PSI BPR was inserted after the thermolysis reactor to sustain superheated conditions.

1.1.4 Membrane separator

A continuous-flow liquid-liquid membrane separator (Zaiput Flow Technologies®) with a PTFE membrane (0.5 μm pores) was utilized after the extraction loop.

1.2 HPLC method

HPLC analyses were performed on a Waters setup (Alliance 2695 system, Empower software) with a 996 PDA UV detector (190 – 400 nm) using a X-Terra® RP18 column (150 x 4.6 mm, 3.5 μm) with a 70:30 mixture acetonitrile/H_2O containing 0.1% TFA. Conversions were measured at 210 nm.

1.3 General procedure for the preparation of L-1d

1.3.1 NBOC-L-methionine

$C_{13}H_{16}N_2O_6S$
Mol. Wt.: 328.34

To a solution of L-methionine (2.98 g, 20 mmol, 1.0 equiv.) in 20 mL of $NaOH_{aq}$ (1 M, 1.0 equiv.) were added dropwise a solution of 2-nitrobenzyl chloroformate [S2] (6.47 g, 30 mmol, 1.5 equiv.) in toluene (30 mL) and 30 mL of $NaOH_{aq}$ (1 M, 1.5 equiv.) at 0 °C under vigorous stirring. After 12 h of reaction at room temperature, the organic phase was discarded and the aqueous phase was washed with diethyl ether (3x 50 mL). The pH of the aqueous phase was then adjusted to 1 with aqueous $KHSO_4$ (10% wt.), and the title compound was extracted with dichloromethane (3x 50 mL). The combined dichloromethane fractions were then dried over $MgSO_4$, filtered and evaporated under reduced pressure to afford a yellow oil (5.39 g, yield = 82%).

^{1}H NMR (400 MHz, CDCl$_3$) δ: 8.20 (br s, 1H), 8.08 (dd, J = 8.2, 0.8 Hz, 1H), 7.71-7.52 (m, 2H), 7.51-7.41 (m, 1H), 5.66 (d, J = 8.2 Hz, 1H), 5.54 (s, 2H), 4.56-4.45 (m, 1H), 2.66-2.50 (m, 2H), 2.28-2.13 (m, 1H), 2.10 (s, 3H), 2.06-1.95 (m, 1H).
^{13}C NMR (100.6 MHz, CDCl$_3$) δ: 176.8, 156.0, 147.6, 134.2, 132.9, 129.0, 125.4, 64.2, 53.4, 31.6, 30.3, 15.7.
ESI HRMS m/z $C_{13}H_{17}O_6N_2S$ [M+H]: calcd 329.08018. Found 329.08020.

1.3.2 2-Nitrobenzyl (S)-1-(methoxycarbonyl)-3-(methylthio)propylcarbamate (NBOC-L-methionine methyl ester)

C$_{14}$H$_{18}$N$_2$O$_6$S
Mol. Wt.: 342.37
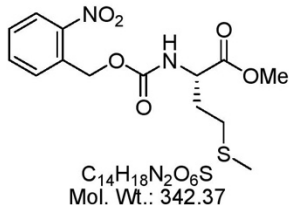
NBOC-L-methionine (5.23 g, 15.93 mmol, 1.0 equiv.) was mixed with trimethylsilyl chloride (6.92 g, 63.71 mmol, 4 equiv.) at 0 °C. Methanol (100 mL) was added in one portion, and to the mixture was stirred for 12 h at room temperature. The volatile compounds were removed under reduced pressure to afford essentially pure NBOC-L-methionine methyl ester as a yellow oil (5.38 g, yield = 99%). No further purification was needed.

^{1}H NMR (400 MHz, CDCl$_3$) δ: 8.09 (dd, J = 8.2, 0.9 Hz, 1H), 7.67-7.56 (m, 2H), 7.50-7.43 (m, 1H), 5.55 (d, J = 9.0 Hz, 1H), 5.52 (s, 2H), 4.50 (dt, J = 7.8, 4.9 Hz, 1H), 3.75 (s, 3H), 2.54 (t, J = 7.3 Hz, 2H), 2.23-2.12 (m, 1H), 2.08 (s, 3H), 2.04-1.93 (m, 1H).

^{13}C NMR (100.6 MHz, CDCl$_3$) δ: 172.7, 155.7, 147.6, 134.1, 133.2, 129.1, 129.0, 125.4, 64.0, 53.6, 53.0, 32.1, 30.2, 15.8.

ESI HRMS m/z C$_{14}$H$_{19}$O$_6$N$_2$S [M+H]: calcd 343.09583. Found 329.09623

1.3.3 2-Nitrobenzyl (S)-1-(methoxycarbonyl)-3-methylsulfinyl) propylcarbamate (L-**1d**)

C$_{14}$H$_{18}$N$_2$O$_7$S
Mol. Wt.: 358.37
L-**1d**
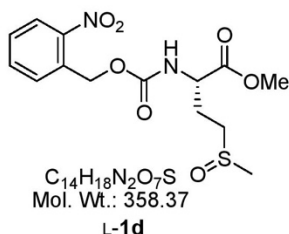
To a solution of NBOC-L-methionine methyl ester (5.21 g, 15.22 mmol, 1.0 equiv.) in methanol (125 mL) was added an aqueous solution of NaIO$_4$ (15.22 mmol, 1 equiv. in 25 mL H$_2$O) dropwise at room temperature under vigorous stirring. After 12 h, the salts were filtered off, and the solvent was evaporated under reduced pressure. The remaining aqueous solution was extracted with dichloromethane (3x 50 mL). The combined organic phases were then washed with brine, dried over MgSO$_4$, filtered and concentrated under reduced pressure to afford the title compound as a yellow oil (5.04 g, yield = 92%). No further purification was needed.

^{1}H NMR (400 MHz, CDCl$_3$) δ: (mixture of diasteromers) 8.09 (d, J = 8.1 Hz, 1H), 7.69-7.55 (m, 2H), 7.52-7.45 (m, 1H), 6.03-5.87 (two d, J = 7.5 Hz, 1H), 5.57-5.43 (m, 2H), 4.50 (dq, J = 8.5, 8.4, 4.6 Hz, 1H), 3.78 (s, 3H), 2.92-2.76 (m, 2H), 2.65-2,60 (two s, 3H), 2.49-2.36 (m, 1H), 2.28-2.12 (m, 1H).

^{13}C NMR (100.6 MHz, CDCl$_3$) δ: (mixture of diasteromers) 172.0 (171.9), 155.8 (155.9), 147.6 (147.5), 134.1, 133.1 (133.0), 129.1 (129.0), 129.0 (128.9), 125.3 (125.2), 64.0 (63.9), 53.5, 53.1 (53.0), 50.5 (50.4), 38.9 (38.8), 26.2 (25.9).

ESI HRMS m/z C$_{14}$H$_{19}$O$_7$N$_2$S [M+H]: calcd 329.09075. Found 329.09072.

1.4   Preparation and characterization of L-2d
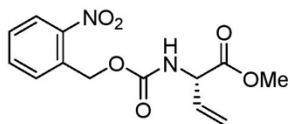
C$_{13}$H$_{14}$N$_2$O$_6$
Mol. Wt.: 294.26
L-**2d**

A feed solution of L-**1d** (5 g L^{-1}, 0.375 g, 1.05 mmol, 1.0 equiv.) and DMAD (0.1487 g, 1.05 mmol, 1.0 equiv.) was prepared in toluene, and conveyed to the thermolysis reactor (T = 270 °C, back pressure P = 1000 psi) via a HPLC pump set at 1 mL min^{-1}, with a 1.7 min residence time in the thermolysis reactor. The reactor effluents were directed to a waste tank until the reactor reached steady state. After 5 min, the reactor effluents were collected and sampled every 10 min for quality control. Toluene was then evaporated and the resulting oil purified on silica gel column (petroleum ether/EtOAc 70:30, Rf = 0.45). 2-Nitrobenzyl (S)-1-(methoxycarbonyl)allylcarbamate (L-**2d**) was isolated as a yellow oil (74% after purification).

^{1}H NMR (400 MHz, CDCl$_3$) δ: 8.10 (d, J = 8.6 Hz, 1H), 7.71-7.60 (m, 2H), 7.52-7.47 (m, 1H), 5.94 (ddd, J = 17.1, 10.3, 5.5 Hz, 1H), 5.66 (br d, J = 7.3 Hz, 1H), 5.57 (s, 2H), 5.41 (dd, J = 17.1, 1.5 Hz, 1H), 5.32 (dd, J = 10.3, 1.4 Hz, 1H), 4.99-4.92 (m, 1H), 3.80 (s, 3H).
^{13}C NMR (100.6 MHz, CDCl$_3$) δ: 171.1, 155.3, 147.6, 134.1, 133.2, 132.4, 128.9, 125.3, 118.3, 63.9, 56.4, 53.1.
ESI HRMS m/z C$_{13}$H$_{15}$O$_6$N$_2$ [M+H]: calcd 295.09246. Found 295.09257.

1.5 Copy of representative NMR spectra
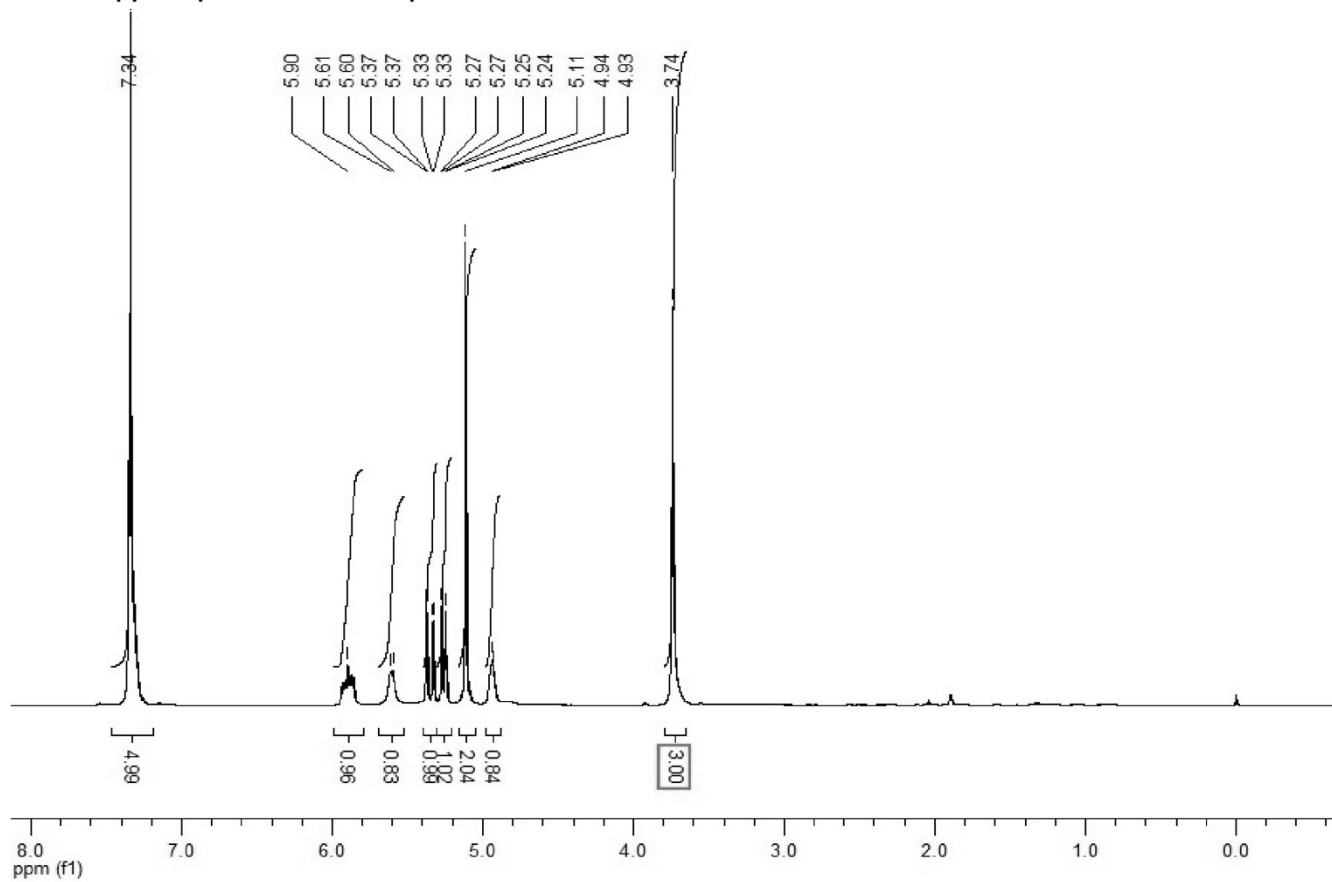
Figure S1. ¹H NMR of L-*N*-Cbz-vinylglycine methyl ester (L-**2a**)
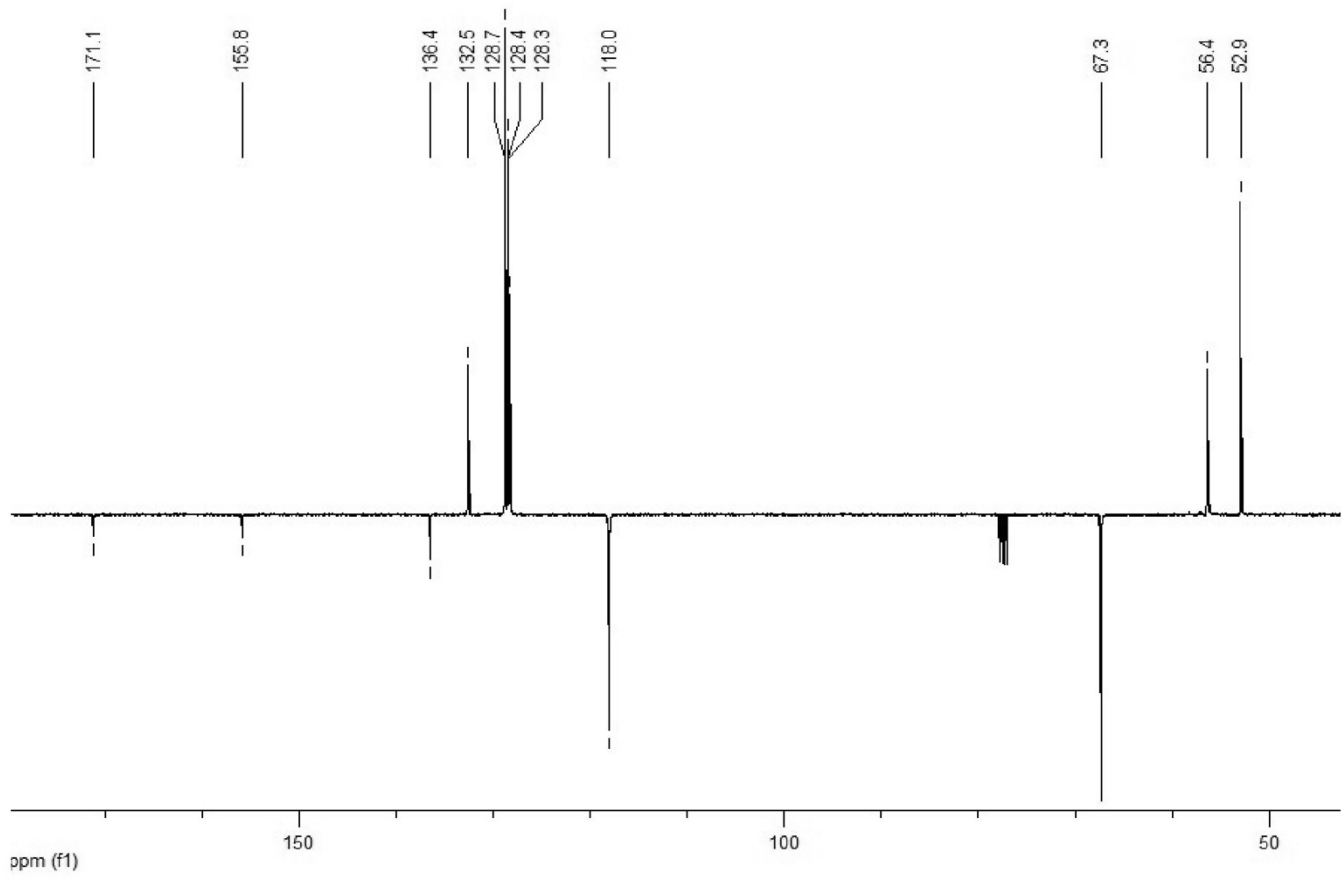
Figure S2. ^{13}C NMR of L-*N*-Cbz-vinylglycine methyl ester (L-**2a**)
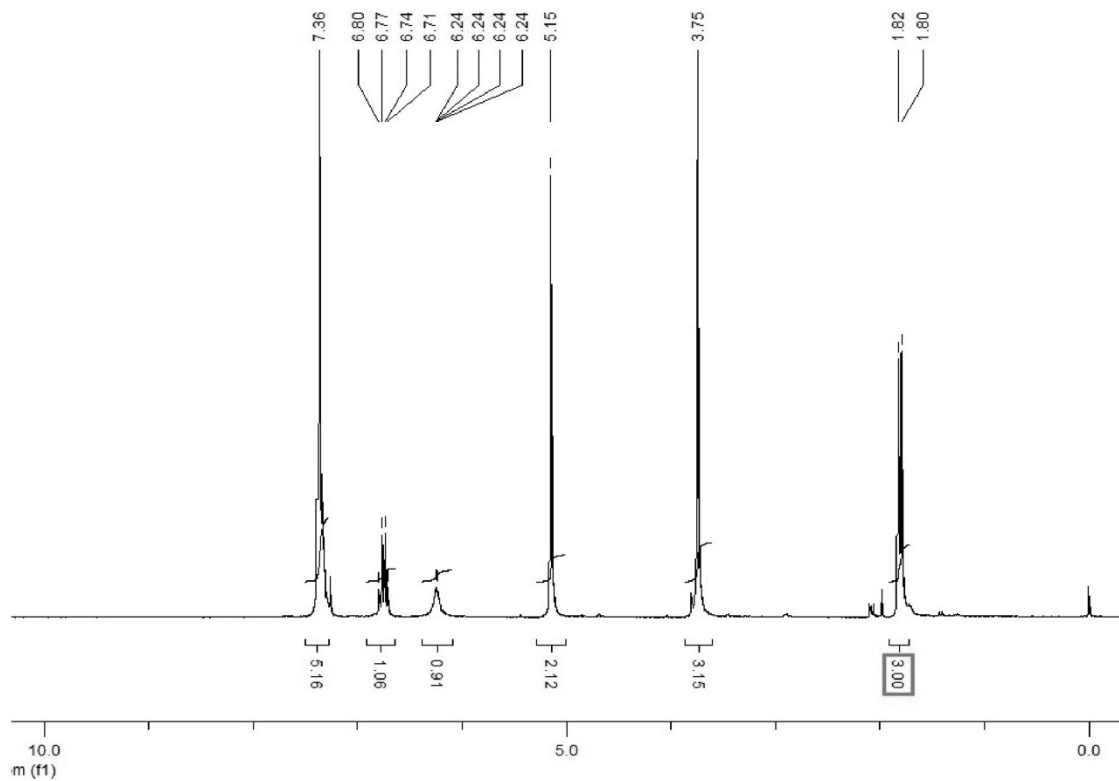
Figure S3. ^{1}H NMR of dehydrobutyrin derivative *E,Z*-**3a**
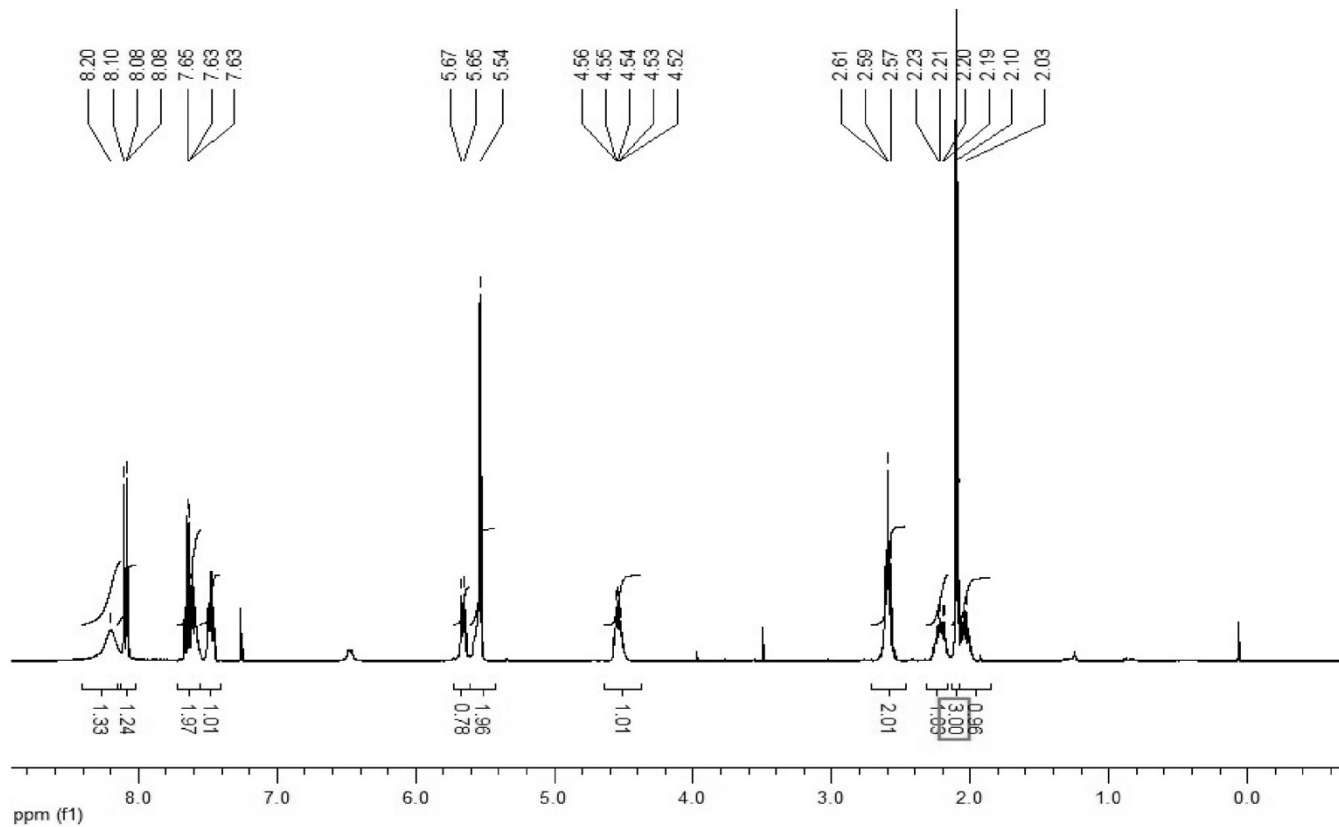
Figure S4. ^{1}H NMR of NBOC-L-methionine

176.8
156.0
147.6
134.2
132.9
129.0
125.4
64.2
53.4
31.6
30.3
15.7

150   100   50

ppm (f1)
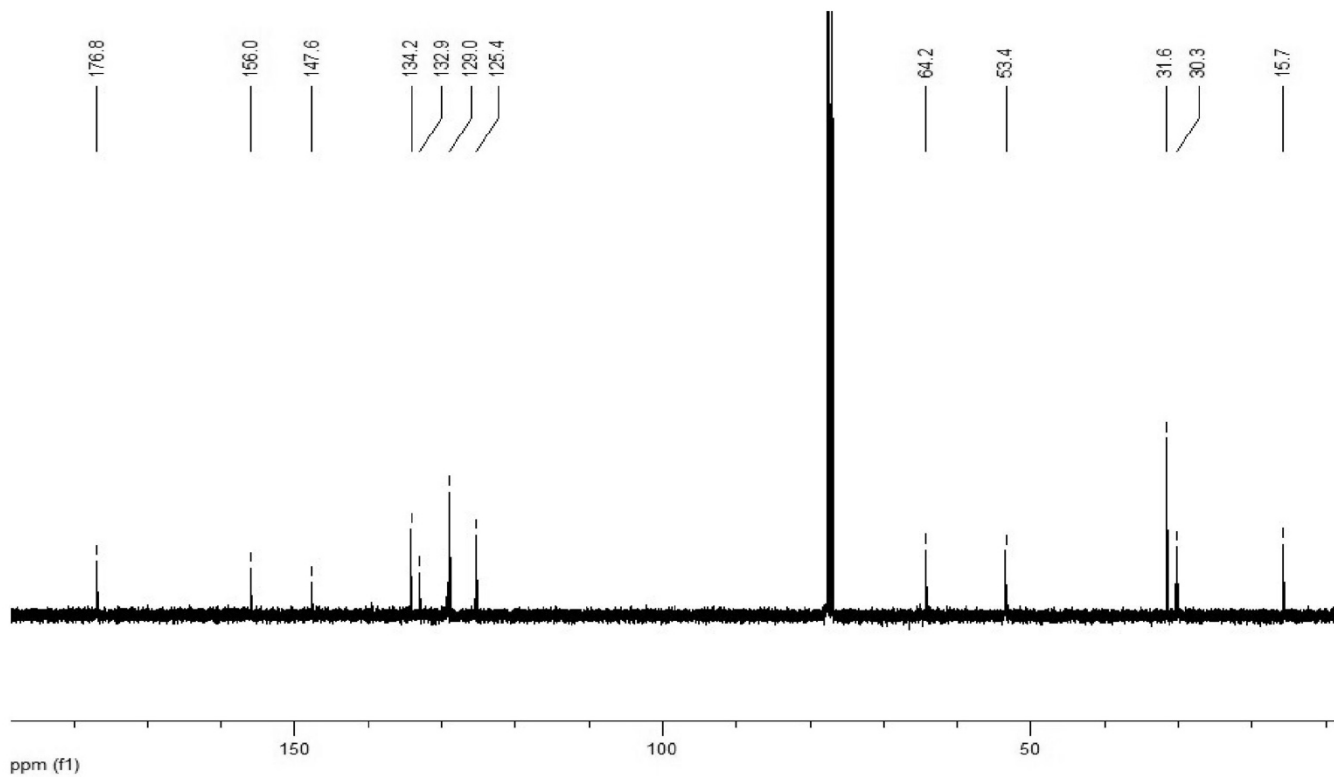
Figure S5. ^{13}C NMR of NBOC-L-methionine
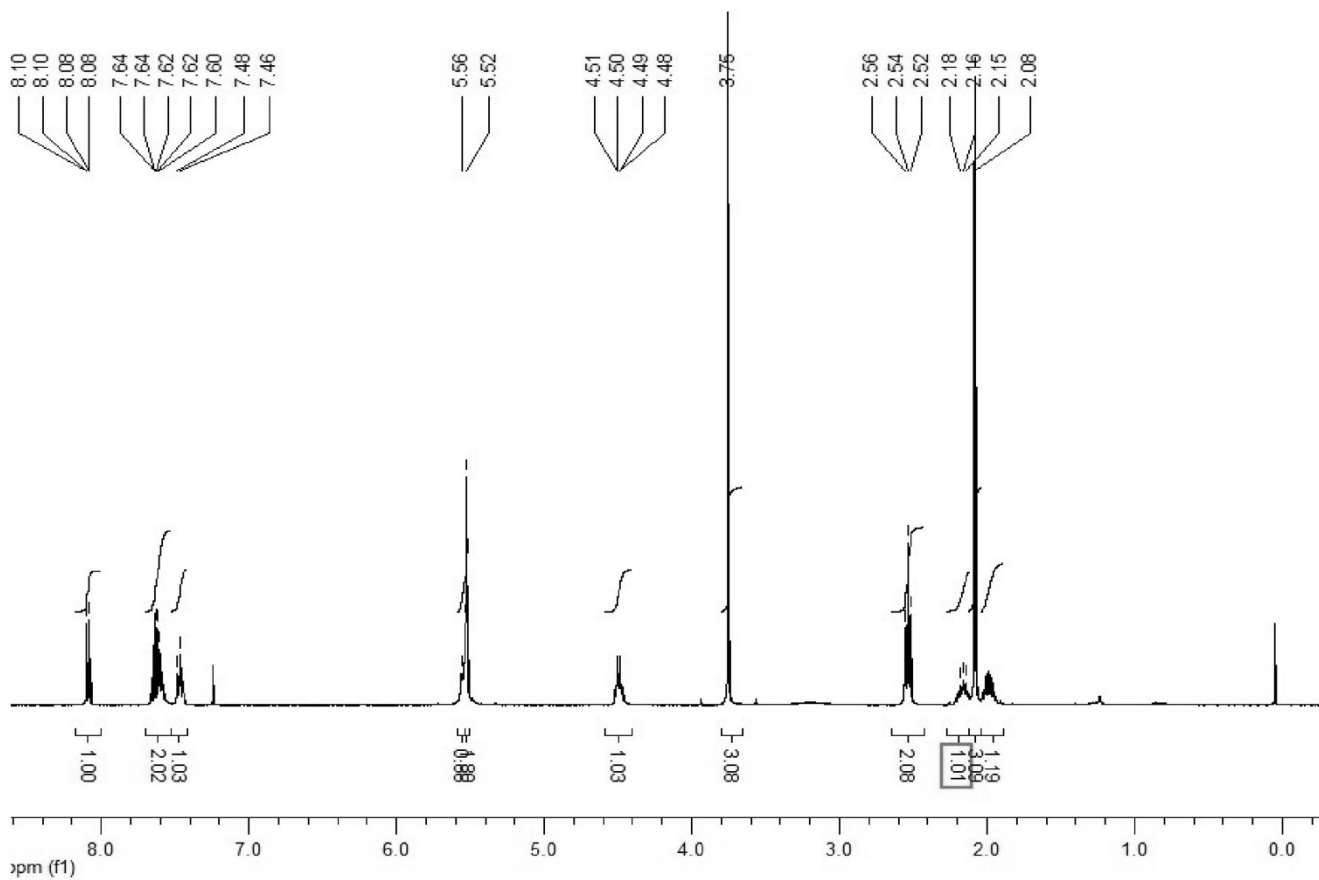
Figure S6. ^{1}H NMR of NBOC-L-methionine methyl ester

172.7
155.7
147.6
134.1
133.2
129.0
129.0
125.4
64.0
53.6
53.0
32.1
30.2
15.8

150   100   50

ppm (f1)
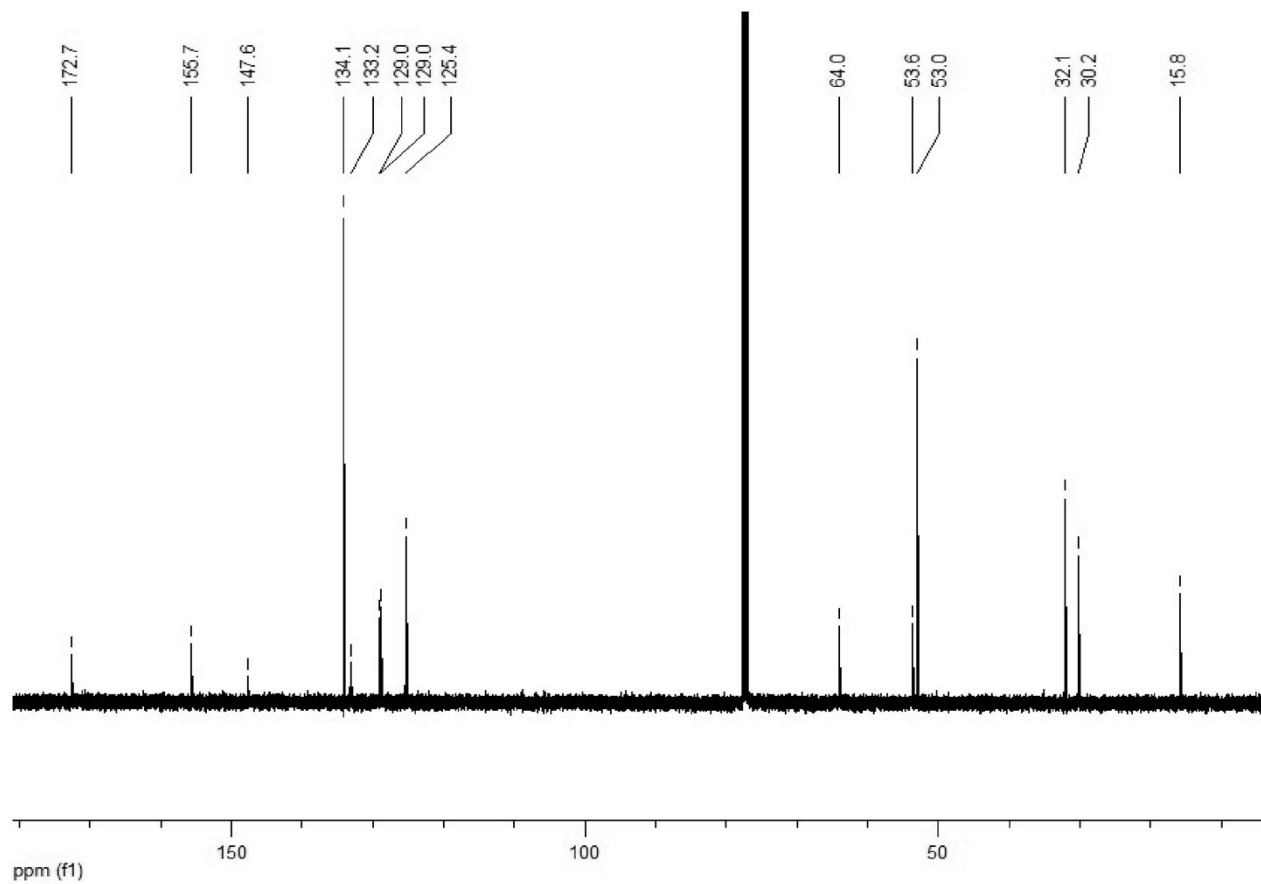
Figure S7. ^{13}C NMR of NBOC-L-methionine methyl ester
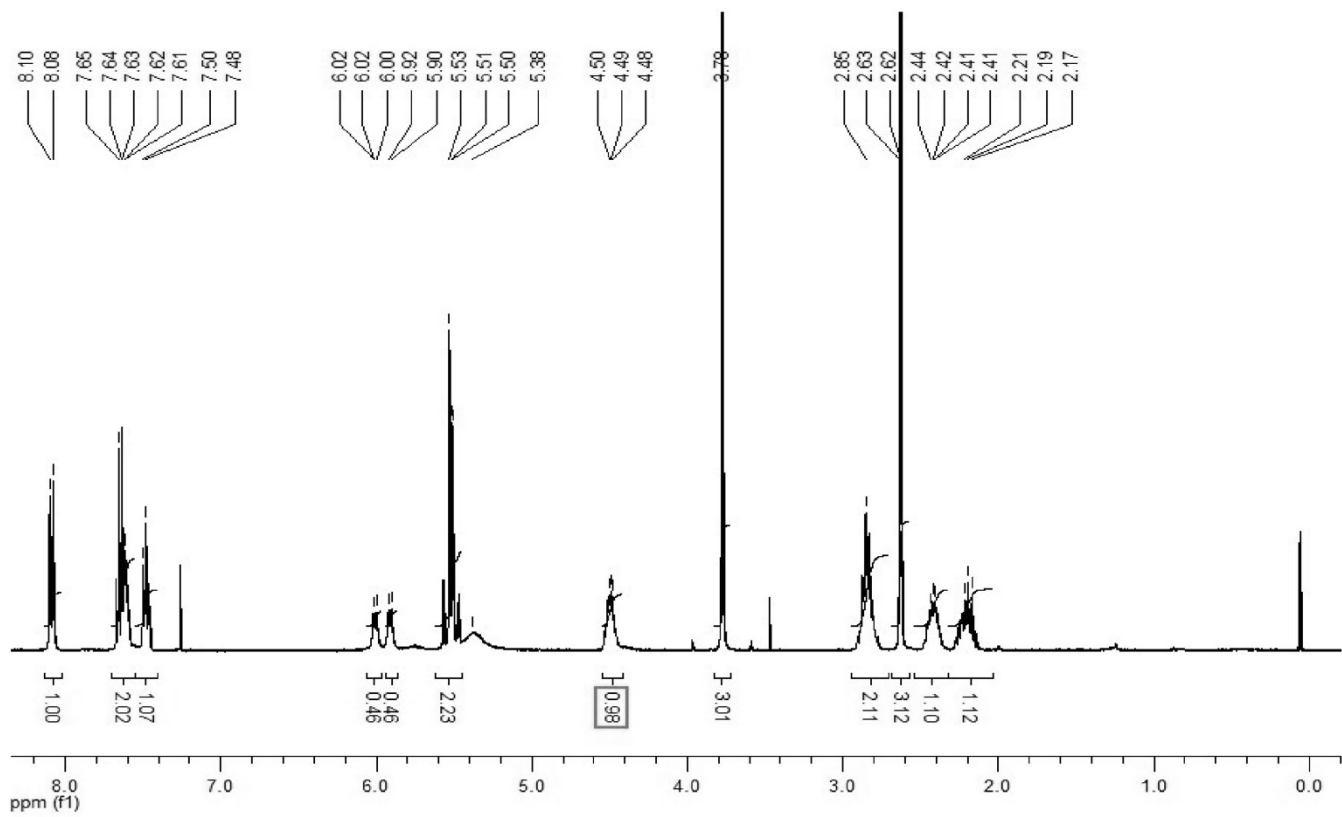
Figure S8. ^{1}H NMR of 2-nitrobenzyl (*S*)-1-(methoxycarbonyl)-3-methylsulfinyl) propylcarbamate (L-1d)
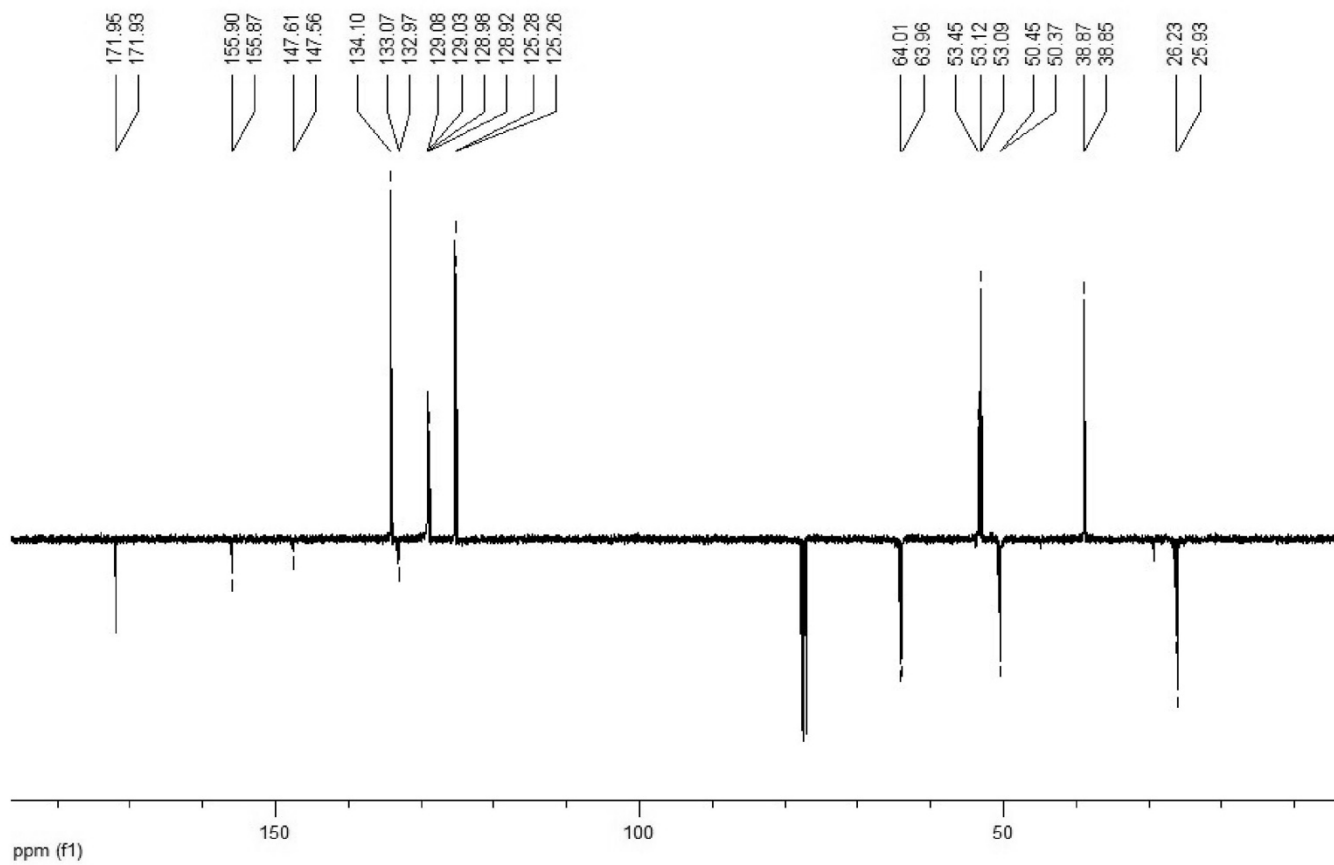
Figure S9. ^{13}C NMR of 2-nitrobenzyl (*S*)-1-(methoxycarbonyl)-3-methylsulfinyl) propylcarbamate (L-1d)
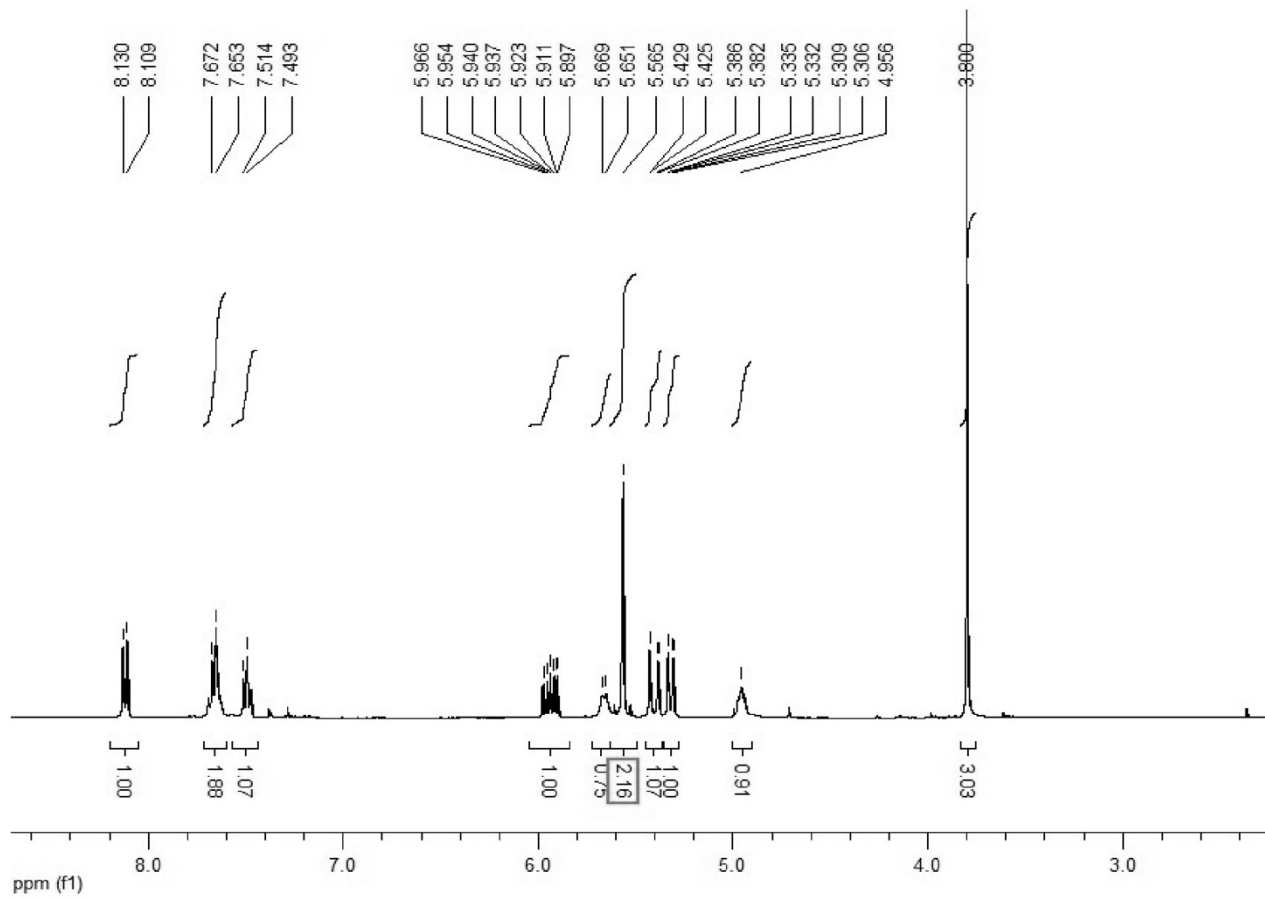
Figure S10. ^{1}H NMR of **L-2d**
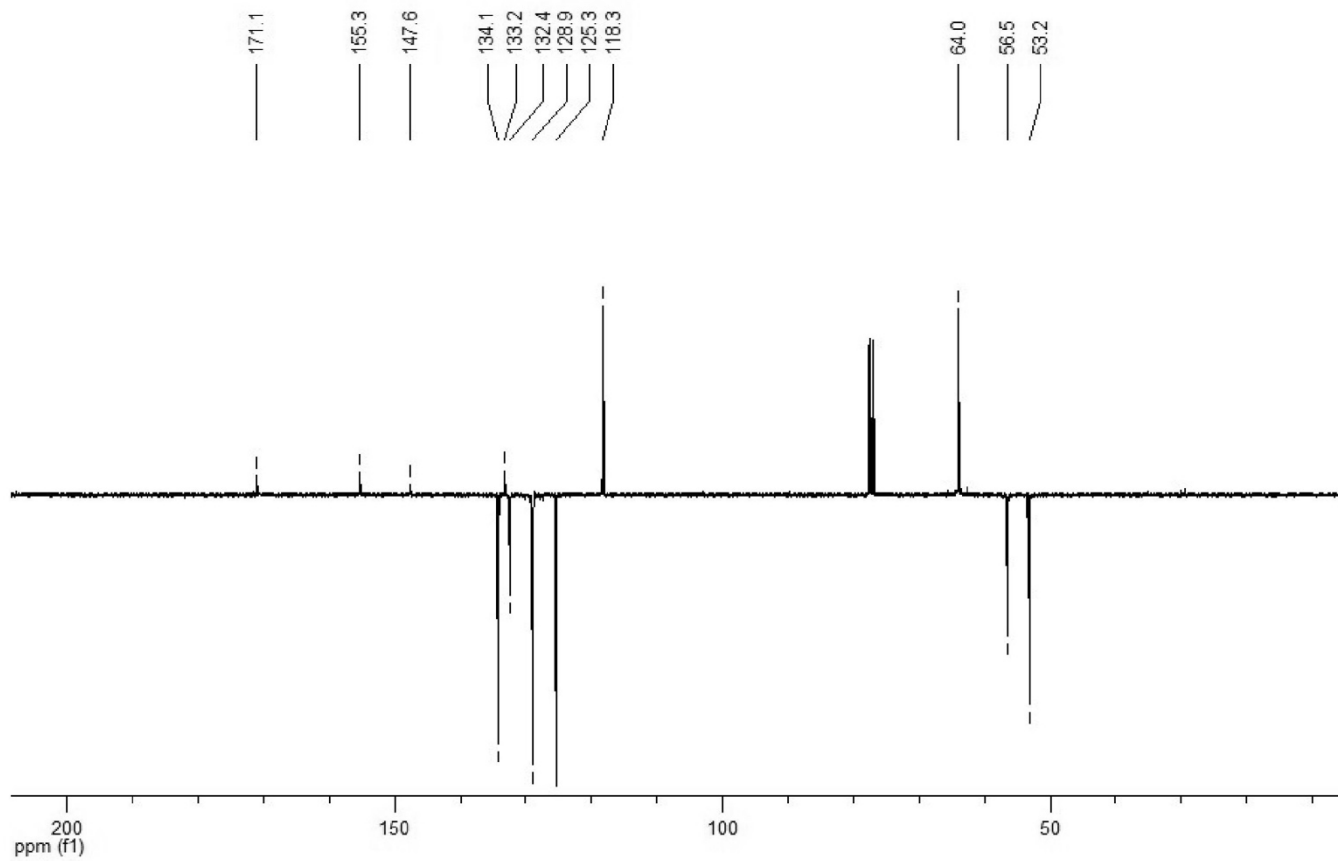
Figure S11. ^{13}C NMR of L-2d

2.   Computational section

2.1   Generalities

Quantum chemical calculations were performed using the Gaussian 09 package of programs (Revision A.02). [S3] DFT computations were carried out using the B3LYP hybrid functional employing the 6-31+G* basis set with 5 pure d functions. Gradient techniques using internal coordinates with very tight optimization convergence criteria (each component of the first energy derivative below 2.0 10-6 Hartree/Bohr or radian) were used for both geometry optimization and computation of vibrational properties. The transitions states were localized using the Newton-Raphson algorithm, and the nature of the stationary points was determined by analysis of the Hessian. The activation and reaction energies were calculated from the thermochemical output (298.150 Kelvin, 1 atm) computed for the reagents, transition states and products, using standard thermochemistry as implemented in Gaussian 09. Intrinsic reaction coordinate (IRC) calculations were performed in the gas phase on the neutral pathway to localize the nearest local minima on the reactant and product sides of the reaction coordinate. [S4]
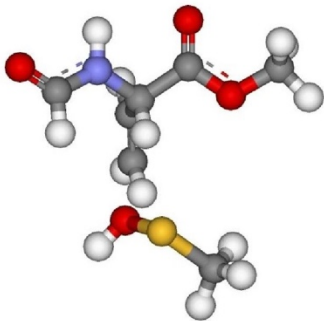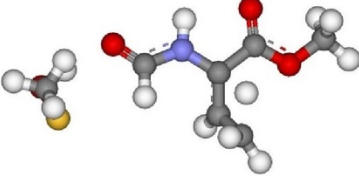
2.2   Cartesian coordinates and absolute energies for all intermediates and transitions states
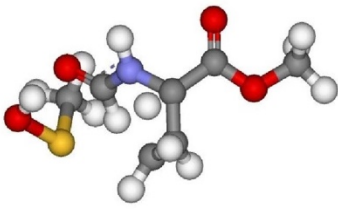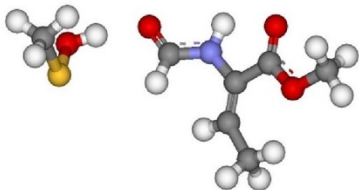
Thermolysis				
1			**B3LYP/6-31+G***	
26			H = -1028.168178 Hartree	
scf done: -1028.391158			G = -1028.231570 Hartree	
C	0.000000	0.000000	0.000000	
C	0.000000	0.000000	1.535234	
N	1.380469	0.000000	-0.461631	
C	-0.771294	-1.237175	-0.507096	
O	0.404904	-0.921424	2.214026	
O	-0.505249	1.146676	2.032340	
C	-0.485752	1.282915	3.471638	
C	1.991175	1.050471	-1.070361	
O	3.166832	1.076998	-1.397182	
C	-2.247142	-1.199096	-0.098322	
S	-3.072514	-2.757169	-0.687775	
O	-2.935444	-2.770987	-2.201007	
C	-4.805676	-2.299033	-0.295708	
H	-0.466667	0.917381	-0.367017	
H	-1.084494	0.493772	3.933869	
H	0.540469	1.223685	3.841592	
H	-0.913763	2.264759	3.673023	
H	1.961257	-0.803826	-0.239539	
H	1.304643	1.899018	-1.254168	
H	-0.694334	-1.274918	-1.598141	
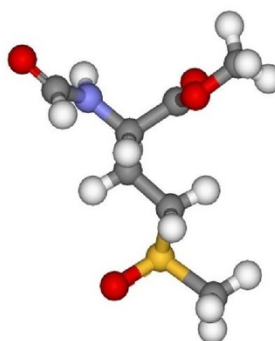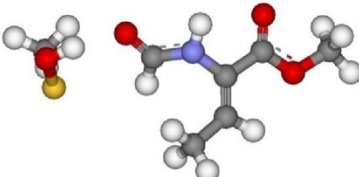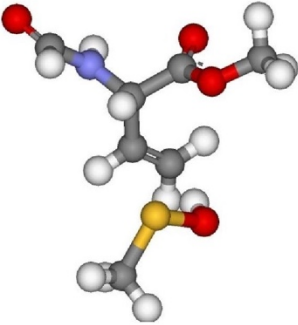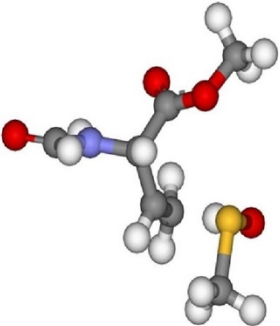
H	-0.288286	-2.138565	-0.108774	
H	-2.773322	-0.371161	-0.588950	
H	-2.379873	-1.118512	0.986491	
H	-5.118907	-1.403381	-0.843467	
H	-4.880168	-2.144491	0.785668	
H	-5.424545	-3.150253	-0.591100	
TS$^{1\text{-}2}$				**B3LYP/6-31+G***
26				H = -1028.129262 Hartree
scf done: -1028.346687				G = -1028.191445 Hartree
S	0.000000	0.000000	0.000000	
O	0.000000	0.000000	1.590381	
C	2.420839	0.000000	0.113783	
C	2.552045	0.039488	1.517710	
H	1.210405	0.073968	1.836968	
C	-0.226976	1.760626	-0.433954	
C	3.031321	-1.210753	2.279047	
C	4.534245	-1.396739	2.058558	
O	5.392028	-0.914027	2.769939	
O	4.788199	-2.120312	0.953066	
C	6.180946	-2.283547	0.608621	
N	2.796691	-1.133198	3.710584	
C	1.731031	-1.684212	4.359050	
O	1.546051	-1.620176	5.564946	
H	2.559897	-0.929730	-0.431247	
H	2.568129	0.899488	-0.478224	
H	2.902065	0.977925	1.954815	
H	0.525902	2.376173	0.066065	
H	-1.226982	2.079902	-0.129444	
H	-0.126015	1.853153	-1.521326	
H	2.511472	-2.090122	1.883620	
H	6.712977	-2.786217	1.419918	
H	6.183616	-2.894614	-0.293961	
H	6.639443	-1.309227	0.420586	
H	3.496323	-0.661123	4.276484	
H	1.033492	-2.207531	3.678478	
2+MeSOH				**B3LYP/6-31+G***
26				H = -1028.157584 Hartree
scf done: -1028.378958				G = -1028.229573 Hartree
C	0.000000	0.000000	0.000000	
C	0.000000	0.000000	1.336049	
C	1.258373	0.000000	2.191977	
N	1.159670	-0.910412	3.321934	
C	1.745669	-2.142071	3.381523	
O	1.666287	-2.894595	4.341854	
C	1.484253	1.418483	2.730370	
O	2.223057	2.155198	1.887974	
C	2.427559	3.535077	2.261476	
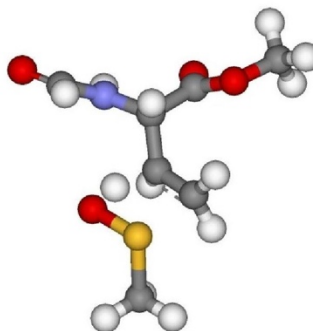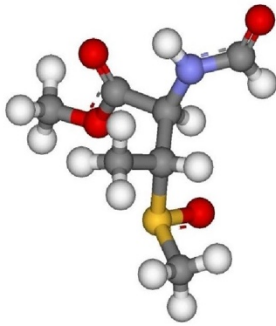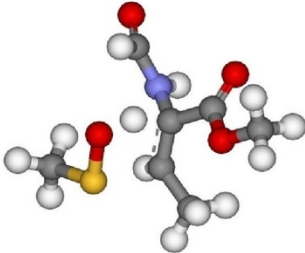
O	1.016030	1.826053	3.774192
O	2.287998	-2.439967	-0.151950
S	3.101865	-3.870424	-0.604112
C	3.558349	-3.457150	-2.313711
H	2.114297	-0.287813	1.575513
H	1.467091	4.052524	2.327899
H	2.941179	3.592345	3.224253
H	3.042474	3.958139	1.467368
H	0.670642	-0.583736	4.150859
H	2.302555	-2.399614	2.463344
H	-0.936407	0.013859	1.893459
H	0.926502	-0.000420	-0.570813
H	-0.929179	0.017079	-0.564201
H	2.681488	-3.369592	-2.962451
H	4.179938	-4.289142	-2.666938
H	4.148125	-2.536589	-2.343195
H	1.334199	-2.571769	-0.296808

Thermal isomerization from 1

TS[2-E3]			B3LYP/6-31+G*

26			H = -514.208849 Hartree
scf done: -1028.274511			G = -514.256691 Hartree

C	0.000000	0.000000	0.000000
C	0.000000	0.000000	1.401536
C	1.370868	0.000000	1.819324
H	1.465036	0.093003	0.283948
C	2.186986	1.266175	1.850365
O	3.214278	1.335126	2.506135
O	1.673253	2.294991	1.158874
C	2.467145	3.498576	1.149474
N	1.800367	-0.865450	2.849653
C	1.349185	-2.139573	3.022103
O	1.741032	-2.878809	3.921628
O	0.473073	-5.383037	4.019786
S	0.282983	-5.740686	2.381659
C	1.785612	-6.718146	2.064163
H	0.407317	-0.868269	-0.522016
H	-0.767908	0.513857	-0.587620
H	-0.859039	0.084214	2.067153
H	2.597147	3.876068	2.166647
H	3.446630	3.305047	0.704130
H	1.900349	4.205646	0.543676
H	2.586556	-0.560282	3.422180
H	0.598906	-2.457260	2.282052
H	2.691779	-6.114360	2.173422
H	1.712575	-7.075387	1.029526
H	1.825570	-7.579169	2.737813
H	0.958773	-4.526205	4.078825

TS²⁻ᶻ³	B3LYP/6-31+G*
26	H = -514.187170 Hartree
scf done: -1028.274511	G = -514.236153 Hartree

C	0.000000	0.000000	0.000000
C	0.000000	0.000000	1.401536
C	1.370868	0.000000	1.819324
H	1.465036	0.093003	0.283948
C	2.186986	1.266175	1.850365
O	3.214278	1.335126	2.506135
O	1.673253	2.294991	1.158874
C	2.467145	3.498576	1.149474
N	1.800367	-0.865450	2.849653
C	1.349185	-2.139573	3.022103
O	1.741032	-2.878809	3.921628
O	0.473073	-5.383037	4.019786
S	0.282983	-5.740686	2.381659
C	1.785612	-6.718146	2.064163
H	0.407317	-0.868269	-0.522016
H	-0.767908	0.513857	-0.587620
H	-0.859039	0.084214	2.067153
H	2.597147	3.876068	2.166647
H	3.446630	3.305047	0.704130
H	1.900349	4.205646	0.543676
H	2.586556	-0.560282	3.422180
H	0.598906	-2.457260	2.282052
H	2.691779	-6.114360	2.173422
H	1.712575	-7.075387	1.029526
H	1.825570	-7.579169	2.737813
H	0.958773	-4.526205	4.078825

E-3 (kinetic product)	B3LYP/6-31+G*
26	H = -514.327097 Hartree
scf done: -1028.400179	G = -514.377310 Hartree

C	0.000000	0.000000	0.000000
C	0.000000	0.000000	1.351177
C	1.136246	0.000000	2.327613
C	1.158068	-0.181701	-0.932467
O	0.992238	-0.371978	-2.126174
O	2.368099	-0.146327	-0.353536
C	3.491858	-0.361245	-1.235275
N	-1.208046	0.109515	-0.735734
C	-2.271288	0.892820	-0.415039
O	-3.288864	0.964654	-1.102174
H	-4.696810	1.944070	-0.482484
O	-5.359906	2.524878	-0.038174
S	-4.502613	3.709196	0.803870
C	-4.384527	5.015690	-0.458545
H	-0.984785	0.010177	1.817438
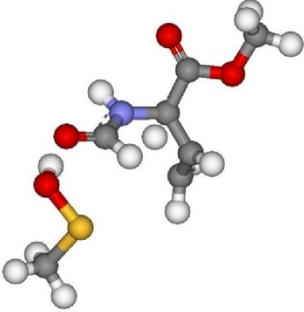
H	2.115975	-0.033031	1.856037	
H	1.036642	-0.857147	3.007638	
H	1.078900	0.899169	2.957389	
H	3.514935	0.408111	-2.010673	
H	3.422676	-1.347336	-1.700858	
H	4.371402	-0.294112	-0.595094	
H	-1.204574	-0.293061	-1.669945	
H	-2.150581	1.473391	0.511720	
H	-3.781691	4.696750	-1.314405	
H	-3.899971	5.873217	0.024414	
H	-5.383533	5.310401	-0.793094	

Z-3 (thermodynamic product)				B3LYP/6-31+G*
26				H = -514.330892 Hartree
scf done: -1028.403950				G = -514.380197 Hartree
C	0.000000	0.000000	0.000000	
C	0.000000	0.000000	1.348616	
C	1.186998	0.000000	2.263825	
C	-1.246327	-0.177338	-0.806632	
O	-1.223411	-0.341166	-2.015131	
O	-2.373091	-0.169525	-0.074713	
C	-3.599124	-0.378230	-0.805348	
N	1.146853	0.093005	-0.820998	
C	2.186555	0.955312	-0.648848	
O	3.121513	1.047588	-1.441231	
O	5.244451	2.678692	-0.595729	
S	4.443893	3.793473	0.385470	
C	4.128138	5.137574	-0.801132	
H	-0.978492	-0.023779	1.818602	
H	2.103577	-0.326771	1.762810	
H	0.999263	-0.668993	3.112016	
H	1.373348	0.996966	2.687401	
H	-3.584162	-1.353941	-1.297553	
H	-3.730794	0.406260	-1.554697	
H	-4.388655	-0.334277	-0.055224	
H	1.077150	-0.341803	-1.738676	
H	2.124882	1.576038	0.255816	
H	4.559098	2.080906	-0.978710	
H	3.677020	5.958131	-0.229680	
H	3.437618	4.826900	-1.591232	
H	5.068958	5.482202	-1.240209	

Addition of MeSOH on 2 towards intermediate 4 (competitive path)				
Van Der Waals complex				B3LYP/6-31+G*
26				H = -1028.156397 Hartree
scf done: -1028.378927				G = -1028.225862 Hartree
C	0.000000	0.000000	0.000000	
C	0.000000	0.000000	1.521554	
C	1.073127	0.000000	2.320304	

C	1.401531	0.234785	-0.576879
O	2.203829	-0.647632	-0.799340
O	1.628764	1.542351	-0.773665
C	2.936911	1.901885	-1.270067
N	-0.554654	-1.243993	-0.507264
C	-1.664615	-1.332309	-1.298450
O	-2.099445	-2.368559	-1.772305
O	0.364239	3.384800	2.159283
S	-1.151347	3.600736	1.428798
C	-2.224936	3.654477	2.896147
H	-0.649988	0.814704	-0.338450
H	-0.999873	-0.042826	1.952003
H	2.090360	0.010166	1.935515
H	0.963710	-0.038186	3.401072
H	2.924006	2.988613	-1.345777
H	3.709203	1.569798	-0.571719
H	3.105463	1.442600	-2.247217
H	-0.017679	-2.095056	-0.367217
H	-2.152513	-0.351750	-1.462969
H	0.561349	2.427367	2.148485
H	-1.903443	4.450447	3.573691
H	-2.245867	2.695871	3.423425
H	-3.232825	3.883077	2.528760

TS$^{2-4(exo)}$	B3LYP/6-31+G*

26
scf done: -1028.346554

H = -1028.129237 Hartree
G = -1028.190739 Hartree

S	0.000000	0.000000	0.000000
O	0.000000	0.000000	1.587859
C	2.480151	0.000000	0.138871
C	2.554291	-0.140947	1.540476
H	1.240526	-0.079448	1.847185
C	-0.199403	-1.766309	-0.429548
C	2.859784	1.282448	-0.603336
C	2.552040	2.536509	0.224136
O	1.310418	2.984544	-0.006341
O	3.333199	3.036357	1.007031
C	0.875850	4.109325	0.791103
N	4.277178	1.261463	-0.935578
C	4.776025	1.133766	-2.198907
O	5.962754	1.116079	-2.481977
H	2.953886	0.692059	2.120400
H	2.826934	-1.124517	1.925055
H	2.580330	-0.882960	-0.489713
H	-0.126453	-1.859182	-1.519307
H	0.578499	-2.368067	0.049152
H	-1.183746	-2.107554	-0.098202
H	2.301019	1.339473	-1.541985

H	-0.139816	4.319057	0.457282	
H	0.888214	3.841618	1.850227	
H	1.530469	4.966845	0.618030	
H	4.943794	1.396054	-0.180766	
H	3.981808	1.042052	-2.965996	

TS$^{2\text{-}4(\text{endo})}$				**B3LYP/6-31+G***
26				H = -1028.123654 Hartree
scf done: -1028.341098				G = -1028.184912 Hartree
S	0.000000	0.000000	0.000000	
O	0.000000	0.000000	1.583078	
C	2.549543	0.000000	0.171476	
C	2.558964	-0.021484	1.585851	
H	1.282572	0.060128	1.855342	
C	-0.413990	1.721716	-0.459215	
C	3.086135	1.146554	-0.695310	
C	3.541571	2.346233	0.148674	
O	4.684653	2.525265	0.508761	
O	2.515576	3.156967	0.455949	
C	2.829623	4.296316	1.290220	
N	4.214963	0.686197	-1.487861	
C	4.189326	0.504564	-2.840562	
O	5.138850	0.138655	-3.512516	
H	2.777694	-0.985040	2.051211	
H	3.005717	0.824009	2.110451	
H	2.561621	-0.943368	-0.366661	
H	0.323389	2.423945	-0.065087	
H	-1.406848	1.955904	-0.065388	
H	-0.440260	1.773580	-1.554007	
H	2.319044	1.491000	-1.396664	
H	1.883823	4.819656	1.427779	
H	3.231013	3.960135	2.249101	
H	3.560874	4.935106	0.789602	
H	5.107979	0.568838	-1.017278	
H	3.197186	0.722062	-3.283612	

4				**B3LYP/6-31+G***
26				H = -1028.166464 Hartree
scf done: -1028.390053				G = -1028.228373 Hartree
C	0.000000	0.000000	0.000000	
C	0.000000	0.000000	1.560560	
C	1.387109	0.000000	2.201738	
S	-1.055185	1.439274	2.161498	
O	-2.345819	1.358518	1.357993	
C	-1.447842	0.740341	3.814095	
C	1.002335	1.003061	-0.576386	
O	2.059302	0.694379	-1.088718	
O	0.578987	2.262807	-0.408937	
C	1.455043	3.307739	-0.885998	

N	0.312364	-1.314324	-0.527836
C	-0.624808	-2.215757	-0.946791
O	-0.367047	-3.301491	-1.441441
H	-1.008473	0.287642	-0.319089
H	-0.561034	-0.895560	1.851167
H	1.916367	0.945452	2.035426
H	1.333131	-0.173270	3.281013
H	1.996374	-0.804591	1.774082
H	-1.935710	-0.231518	3.692018
H	-0.542302	0.657965	4.422267
H	-2.141765	1.442477	4.283461
H	2.419127	3.256003	-0.373818
H	0.939358	4.238968	-0.653896
H	1.606910	3.204314	-1.963061
H	1.282826	-1.516766	-0.751259
H	-1.662733	-1.867565	-0.783887

Sulfoxide elimination from intermediate 4 (competitive path)

TS^4_^{E3}	B3LYP/6-31+G*

26
scf done: -1028.353361

H = -1028.135718 Hartree
G = -1028.195829 Hartree

S	0.000000	0.000000	0.000000
O	0.000000	0.000000	1.591567
C	2.272114	0.000000	-0.023503
C	2.536567	0.208579	1.382799
H	1.171881	0.079839	1.811844
C	-0.279695	1.749499	-0.442779
C	2.608737	-1.250250	-0.806337
C	3.226650	-0.818854	2.228786
O	4.035490	-0.556765	3.098402
O	2.806408	-2.081557	1.968411
C	3.377971	-3.113349	2.795333
N	2.898796	1.569308	1.709035
C	2.420069	2.249622	2.798868
O	2.864691	3.317346	3.188817
H	2.388880	0.914470	-0.605755
H	2.218222	-2.156694	-0.342443
H	2.218585	-1.174952	-1.827089
H	3.700519	-1.357719	-0.873439
H	-1.298135	2.026729	-0.159181
H	0.442048	2.388010	0.071869
H	-0.162938	1.841658	-1.528550
H	4.464575	-3.140716	2.678426
H	3.132207	-2.936108	3.845566
H	2.928000	-4.043573	2.446556
H	3.788774	1.925845	1.367864
H	1.558016	1.751751	3.278387

TS^4_^{Z3}	B3LYP/6-31+G*

26	H = –1028.140015 Hartree
scf done: –1028.356940	G = –1028.199963 Hartree

26			
S	0.000000	0.000000	0.000000
O	0.000000	0.000000	1.591567
C	2.272114	0.000000	-0.023517
C	2.536573	0.208585	1.382785
H	1.171880	0.079829	1.811854
C	-0.240140	-1.757093	-0.435044
C	2.618188	1.047852	-1.055187
C	3.163639	-0.911229	2.154347
O	3.888328	-0.770041	3.119328
O	2.792016	-2.135113	1.682535
C	3.306055	-3.263319	2.415494
N	2.962589	1.522602	1.776364
C	2.459131	2.210270	2.850033
O	2.942970	3.241278	3.288155
H	2.399390	-1.026315	-0.358760
H	0.466052	-2.373871	0.125993
H	-1.267120	-2.044655	-0.196469
H	-0.070574	-1.863333	-1.512623
H	2.167112	0.814937	-2.025997
H	3.708342	1.077308	-1.199190
H	2.297380	2.046881	-0.748026
H	4.398975	-3.267253	2.394487
H	2.965342	-3.229632	3.453597
H	2.908617	-4.143562	1.908355
H	3.873216	1.855675	1.468357
H	1.544991	1.753211	3.269119

Thermal epimerization

TS$^{E3\_epi2}$	B3LYP/6-31+G*

26	H = –1028.058105 Hartree
scf done: –1028.274451	G = –1028.125125 Hartree

26			
C	0.000000	0.000000	0.000000
C	0.000000	0.000000	1.401514
C	1.370729	0.000000	1.819480
H	1.464886	-0.092686	0.284130
C	2.187453	-1.265790	1.850190
O	3.214201	-1.334667	2.506733
O	1.674947	-2.294354	1.157340
C	2.470830	-3.496630	1.145794
N	1.800457	0.865950	2.849381
C	1.343378	2.137537	3.025274
O	1.735435	2.878195	3.923621
H	0.407449	0.867960	-0.522476
H	-0.767673	-0.514147	-0.587704
H	-0.859351	-0.083434	2.066802
H	2.601308	-3.875880	2.162259

H	3.450059	-3.300589	0.701012	
H	1.905338	-4.203466	0.538501	
H	2.592250	0.564500	3.416167	
H	0.581324	2.448994	2.294611	
O	0.674860	5.480283	3.877819	
S	-0.890087	5.194144	3.315726	
C	-1.796182	5.021290	4.885343	
H	1.120718	4.604084	3.960895	
H	-1.470251	4.139369	5.445415	
H	-1.670316	5.920180	5.496030	
H	-2.855713	4.911188	4.623172	

TS$^{Z3\_epi2}$				B3LYP/6-31+G*
26				H = -1028.036952 Hartree
scf done: -1028.253123				G = -1028.104035 Hartree
C	0.000000	0.000000	0.000000	
C	0.000000	0.000000	1.406632	
C	1.393209	0.000000	1.801490	
H	1.417963	0.020503	0.286984	
C	1.933588	-0.952388	2.824040	
O	3.056480	-0.903670	3.290625	
O	1.037318	-1.922977	3.103202	
C	1.459244	-2.917337	4.058070	
N	2.077224	1.270347	1.822307	
C	1.521406	2.444560	2.214792	
O	2.128306	3.514591	2.221926	
H	0.357044	-0.912045	-0.486798	
H	-0.757043	0.514120	-0.603494	
H	-0.866611	0.012459	2.067215	
H	1.700246	-2.446448	5.014658	
H	2.338281	-3.447973	3.683189	
H	0.611970	-3.595245	4.161876	
H	3.073712	1.287680	1.626445	
H	0.464309	2.362739	2.511809	
O	0.684847	5.683106	3.246511	
S	-0.873085	5.362498	2.686084	
C	-0.876900	6.292533	1.120908	
H	-0.166042	5.875033	0.401118	
H	-1.892336	6.213944	0.713146	
H	-0.646538	7.345803	1.306364	
H	1.275881	4.972440	2.898467	

epi2				B3LYP/6-31+G*
26				H = -1028.166507 Hartree
scf done: -1028.389281				G = -1028.235243 Hartree
C	0.000000	0.000000	0.000000	
C	0.000000	0.000000	1.520018	
C	1.106473	0.000000	2.266709	
C	-0.584135	1.322097	-0.509116	

O	-1.756337	1.480022	-0.784837
O	0.349661	2.280340	-0.571001
C	-0.109574	3.593259	-0.961233
N	-0.799356	-1.082163	-0.559587
C	-0.347199	-2.354234	-0.743252
O	-1.025076	-3.281095	-1.159356
O	0.280184	-5.754886	-1.252636
S	1.843441	-5.308913	-1.701163
C	1.740721	-5.458492	-3.512763
H	1.030975	-0.081085	-0.359404
H	-0.986839	-0.018724	1.981992
H	1.057212	-0.013191	3.352172
H	2.099900	0.012471	1.822064
H	0.780931	4.221226	-0.952738
H	-0.550845	3.555702	-1.960135
H	-0.850981	3.959077	-0.246506
H	-1.774739	-0.886931	-0.769066
H	0.722655	-2.473389	-0.484900
H	-0.265315	-4.931895	-1.225262
H	1.046094	-4.728471	-3.939725
H	1.436901	-6.471724	-3.791865
H	2.749227	-5.267077	-3.899854
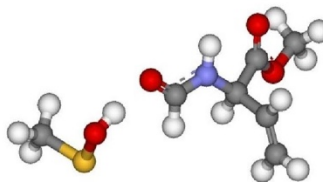
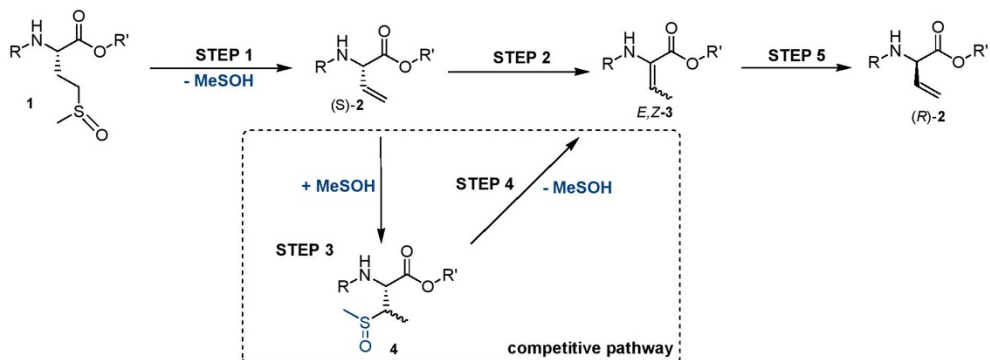## 2.3   Summary of relevant thermochemistry data

Figure S12. Overview of the competitive pathways for the thermolysis of **1**

Table S2. Summary of relevant thermochemistry data (see Figure S9)

Activation/reaction parameters (kcal mol^{-1})	Step 1	Step 2	Step 3	Step 4	Step 5
$\Delta G^{\neq}$	25.2	69.4	22.0	17.8	75.4
$\Delta H^{\neq}$	24.4	68.0	17.0	16.6	74.5
$\Delta G°$	1.3	-6.3	-1.6	-12.4	6.3
$\Delta H°$	6.6	-6.5	-6.3	-8.8	6.5

3 References

[S1] (*a*) A. K. Ghosh and K. Lv, *Eur. J. Org. Chem*., 2014, 6761–6768 and references therein; (*b*) M. Nakajima, B. Watanabe, L. Han, B. I. Shimizu, K. Wada, K. Fukuyama, H. Suzuki and J. Hiratake, *Bioorganic Med. Chem.*, 2014, **22**, 1176–1194; (*c*) Y. Yasuno, M. Hamada, T. Yamada, T. Shinada and Y. Ohfune, *European J. Org. Chem.*, 2013, **2013**, 1884–1888. (*d*) F. Sicherl, T. Cupido and F. Albericio, *Chem. Commun.*, 2010, **46**, 1266–1268; (*e*) D. J. St-Cyr, A. G. Jamieson and W. D. Lubell, *Org. Lett.*, 2010, **12**, 1652–1655; (*f*) Y. Saito, H. Ouchi and H. Takahata, *Tetrahedron*, 2006, **62**, 11599–11607.

[S2] L.-C. Hu, Y. Yonamine, S.-H. Lee, W. E. van der Veer, and K. J. Shea, *J. Am. Chem. Soc.* 2012, **134**, 11072-11075.

[S3] Gaussian 09. Revision A.02, M. J. Frisch, G. W. Trucks, H. B. Schlegel, G. E. Scuseria, M. A. Robb, J. R. Cheeseman, G. Scalmani, V. Barone, B. Mennucci, G. A. Petersson, H. Nakatsuji, M. Caricato, X. Li, H. P. Hratchian, A. F. Izmaylov, J. Bloino, G. Zheng, J. L. Sonnenberg, M. Hada, M. Ehara, K. Toyota, R. Fukuda, J. Hasegawa, M. Ishida, T. Nakajima, Y. Honda, O. Kitao, H. Nakai, T. Vreven, J. A. Montgomery, Jr., J. E. Peralta, F. Ogliaro, M. Bearpark, J. J. Heyd, E. Brothers, K. N. Kudin, V. N. Staroverov, R. Kobayashi, J. Normand, K. Raghavachari, A. Rendell, J. C. Burant, S. S. Iyengar, J. Tomasi, M. Cossi, N. Rega, J. M. Millam, M. Klene, J. E. Knox, J. B. Cross, V. Bakken, C. Adamo, J. Jaramillo, R. Gomperts, R. E. Stratmann, O. Yazyev, A. J. Austin, R. Cammi, C. Pomelli, J. W. Ochterski, R. L. Martin, K. Morokuma, V. G. Zakrzewski, G. A. Voth, P. Salvador, J. J. Dannenberg, S. Dapprich, A. D. Daniels, O. Farkas, J. B. Foresman, J. V. Ortiz, J. Cioslowski, and D. J. Fox, Gaussian, Inc., Wallingford CT, 2009.

[S4] (*a*) K. Fukui, *Acc. Chem. Res.* 1981, **14**, 363-68; (*b*) H. P. Hratchian and H. B. Schlegel, in *Theory and Applications of Computational Chemistry: The First 40 Years*, (Eds. C. E. Dykstra, G. Frenking, K. S. Kim, and G. Scuseria), Elsevier, Amsterdam, 2005, 195-249.